


2013

Simulating Land Use Land Cover Change Using Data Mining and Machine Learning Algorithms

Amin Tayyebi
Purdue University

Follow this and additional works at: https://docs.lib.purdue.edu/open_access_dissertations

 Part of the [Civil Engineering Commons](#), [Computer Sciences Commons](#), and the [Urban Studies and Planning Commons](#)

Recommended Citation

Tayyebi, Amin, "Simulating Land Use Land Cover Change Using Data Mining and Machine Learning Algorithms" (2013). *Open Access Dissertations*. 1.

https://docs.lib.purdue.edu/open_access_dissertations/1

This document has been made available through Purdue e-Pubs, a service of the Purdue University Libraries. Please contact epubs@purdue.edu for additional information.

**PURDUE UNIVERSITY
GRADUATE SCHOOL
Thesis/Dissertation Acceptance**

This is to certify that the thesis/dissertation prepared

By Amin Tayyebi

Entitled

Simulating land use land cover change using data mining and machine learning algorithms

For the degree of Doctor of Philosophy

Is approved by the final examining committee:

Bryan C. Pijanowski

Chair

Jeffrey D. Holland

Guofan Shao

Songlin Fei

To the best of my knowledge and as understood by the student in the *Research Integrity and Copyright Disclaimer (Graduate School Form 20)*, this thesis/dissertation adheres to the provisions of Purdue University's "Policy on Integrity in Research" and the use of copyrighted material.

Approved by Major Professor(s): Bryan C. Pijanowski

Approved by: Robert K. Swihart

Head of the Graduate Program

02/25/2013

Date

SIMULATING LAND USE LAND COVER CHANGE USING DATA MINING
AND MACHINE LEARNING ALGORITHMS

A Dissertation
Submitted to the Faculty
of
Purdue University
by
Amin Tayyebi

In Partial Fulfillment of the
Requirements for the Degree
of
Doctor of Philosophy

May 2013
Purdue University
West Lafayette, Indiana

“The price of success is hard work, dedication to the job at hand, and the determination that whether we win or lose, we have applied the best of ourselves to the task at hand”

Vince Lombardi

“I really owe everything to my parents and their devotion and drive to see to it that their children had the education which led to the opportunities that they never were able to have”

George J. Mitchell

ACKNOWLEDGMENTS

I would like to say warm thanks to Prof. Bryan C. Pijanowski who helped me during last 4 years as a co-chair of my master program and as a chair of my PhD program. His flexibility, patience and remarkable contribution for high quality work were encouraging for me to complete my PhD promptly. I am also very thankful to the other members of my dissertation committee: Prof. Jeffrey Holland, Prof. Guofan Shao and Prof. Songlin Fei, for their academic support. I would also like to thank the United States Geological Survey (USGS) and National Science Foundation (NSF) which provided funds to support a research assistantship that supported the two years of my PhD. I would also like to say thanks to each of my lab-mates, Dr. Burak Pekin, Jarrod Doucette, James Plourde, Sarah Dumyahn, Luis Villanueva, Kim Robinson, NahNah Kim and Maryam Ghadiri, for the encouragement they provided. My special gratitude is also extended to Kelly Garret who has answered to every single question I asked her about the Graduate School.

It is an honor for me to be a contributing member of the land use land cover change (LUCC) community. I would like to give special thanks to the LUCC scientists who gave me encouragement (Prof. Micheal Batty; Prof. Bryan C. Pijanowski; Prof. Keith Clarke; Prof. Robert G. Pontius; Prof. Peter Verburg; Prof Tom Veldkamp; Prof.

Xia Li; Prof. Anthony Gar-On Yeh; Prof. John D. Landis; Prof. Danielle J. Marceau; Prof. Jie Shan; Prof. Peter Deadman; Prof. Zhiyong Hu) and other scientists (Prof. Billie L. Turner; Prof. Eric Lambin; Prof. Dan Brown, Prof. Erle Ellis; Dr. Thomas Albright; Prof. Thomas Saaty; Prof. Kevin Gurney; Dr. Robert Kennedy; Prof. Helen Briassoulis; Prof. Eric Koomen) who assess the impact of LUCC on other fields (e.g. climate, biodiversity, hydrology, pollution and so on). I asked each of them to make a video approximately 5 minutes in length where they discuss LUCC modeling and what they have contributing to our understanding of the impacts of land use change on the environment. So, I would like give a special “thanks” to those that contributed to the online video archive.

TABLE OF CONTENTS

	Page
LIST OF TABLES	ix
LIST OF FIGURES	xi
ABBREVIATIONS	xiv
ABSTRACT	xvi
CHAPTER 1: LAND CHANGE SCIENCE: A BRIEF INTRODUCTION	1
1.1 Introduction.....	1
1.2 Research objectives and structure of the dissertation	4
1.3 References.....	7
CHAPTER 2: LAND CHANGE SCIENCE THROUGH THE LENS OF THE LAND TRANSFORMATION MODEL (LTM)	9
2.1 Introduction.....	9
2.2 LTM as a case-study LUCC Model.....	10
2.3 LTM used in land-climate interaction studies	14
2.4 LTM in land-hydrologic dynamic studies.....	15
2.5 Organismal responses to LUCC.....	18
2.6 Joint LUCC and climate change effect on biodiversity	19
2.7 LTM and planning decisions	20
2.8 Quantifying error propagation in coupled models containing the LTM.....	21
2.9 Conclusion	23
2.10 References.....	24
CHAPTER 3: A SUMMARY OF LAND USE LAND COVER CHANGE MODELS ..	31
3.1 Introduction.....	31
3.2 Calibration, validation and null models	32
3.3 Cellular automata models	34
3.3.1 Cellular automata overview	34
3.3.2 Slope, land use, exclusion, urban, transportation, and hill shading (SLEUTH).....	35
3.3.3 Geo-simulation.....	37
3.3.4 Vector based CA (VEC-GCA).....	38
3.4 Weighted-map models	39
3.4.1 Multi criteria evaluation (MCE)	39
3.4.2 Geomod.....	40
3.5 Regression based models	42
3.5.1 Logistic regression overview	42
3.5.2 Conversion of land use and its effects (CLUE)	43
3.6 Agent based models (ABMs).....	44
3.7 Machine learning	45

	Page
3.7.1 Artificial neural networks (ANNs)	45
3.7.2 Support vector machines (SVMs)	46
3.7.3 Genetic algorithms (GAs)	47
3.8 Data mining	47
3.8.1 Classification and regression tree (CART)	48
3.8.2 Multiple adaptive regression splines (MARS)	48
3.9 Hybrid models of CA	49
3.9.1 CA-MCE	49
3.9.2 CA-SVM	50
3.9.3 CA-GA	50
3.9.4 CA-ANN	51
3.10 Urban growth boundary models (UGBMs)	52
3.10.1 ANN UGBM	52
3.11 Rule based UGBMs	52
3.11.1 Distance dependent model (DDM)	53
3.11.2 Distance independent model (DIM)	53
3.12 Conclusion	54
3.13 References	64
CHAPTER 4: USING CART, MARS AND ANNS TO MODEL LAND USE LAND COVER CHANGE: APPLICATION OF DATA MINING TOOLS TO THREE DIVERSE AREAS IN THE USA AND AFRICA UNDERGOING LAND TRANSFORMATION	70
4.1 Introduction	70
4.1.1 Literature review on LTM, CART and MARS	73
4.1.2 Objectives and structure of chapter	75
4.2 Methods	77
4.2.1 Global parametric model (LTM)	77
4.2.2 Local non-parametric models (CART and MARS)	78
4.2.3 Validation metrics	83
4.3 Study areas and model building	86
4.4 Results	87
4.4.1 CART	87
4.4.2 MARS	89
4.4.3 LTM	92
4.4.4 Ranking variables in CART and MARS	93
4.4.5 Terminal node in CART	93
4.4.6 Calibration of three models using cross tabulation matrices and ROC values	94
4.4.7 Comparison of LTM, CART and MARS simulations using cross tabulation matrix	95
4.5 Discussion	96
4.6 Conclusion	99
4.7 References	100

	Page
CHAPTER 5: SIMULATING MULTIPLE LAND USE CLASSES USING THE ARTIFICIAL NEURAL NETWORK-BASED LAND TRANSFORMATION MODEL AND TWO NONLINEAR DATA MINING TOOLS.....	130
5.1 Introduction.....	130
5.1.1 Nonlinear modeling tools.....	131
5.1.2 Multiple classification (MC) problem	132
5.1.3 Land use land cover change models and multiple classifications (MC)	135
5.2 Methods.....	138
5.2.1 LTM-MC as a GPM.....	138
5.2.2 CART and MARS as multiple classification LNPMs	140
5.2.3 Adapted rules to remove conflicts in MC.....	144
5.2.4 Calibration and validation runs.....	145
5.3. Study areas, data preparation and model building	147
5.3.1 Study areas	147
5.3.2 Data preparation.....	148
5.3.3 Model building.....	148
5.4 Results and discussion	149
5.4.1 CART.....	149
5.4.2 MARS training.....	151
5.4.3 LTM-MC training.....	152
5.4.4 Variable rankings in CART and MARS	152
5.4.5 Terminal node in CART	153
5.4.6 Validation of three models using PCM and ROC.....	153
5.5 Discussion.....	154
5.6 Conclusion	156
5.7 References.....	158
CHAPTER 6: AN URBAN GROWTH BOUNDARY MODEL USING NEURAL NETWORKS, GIS AND RADIAL PARAMETERIZATION: AN APPLICATION TO TEHRAN, IRAN.....	182
6.1 Introduction.....	182
6.1.1 Literature Review on UGBs.....	184
6.1.2 Research questions and chapter structure	187
6.2 Materials and methods	188
6.2.1 Background on artificial neural networks.....	188
6.2.2 Urban growth boundary model	189
6.2.3 Study area and data sources	193
6.3 Parameterization of our UGBM for TMA	194
6.3.1 Base map development	194
6.3.2 Urban boundary delineation.....	195
6.3.3 Simulation.....	197
6.3.4 Calibration metrics.....	198
6.4 Results.....	199
6.4.1 Training of UGBM	199

	Page
6.4.2 Testing run and model validation	199
6.4.3 Prediction	200
6.5 Conclusion and discussion	201
6.6 References	205
CHAPTER 7: TWO RULE-BASED URBAN GROWTH BOUNDARY MODELS APPLIED TO THE TEHRAN METROPOLITAN AREA, IRAN	217
7.1 Introduction	217
7.1.1 Urban growth boundaries (UGBs)	217
7.1.2 Urban growth boundary models (UGBMs) versus urban growth models (UGMs)	220
7.1.3 Research question and chapter structure	221
7.2 Urban growth boundary models (UGBMs)	223
7.2.1 Application of null model to UGBMs	223
7.2.2 Rule-based simulation UGBMs	224
7.3 Implementation of UGBMs	229
7.3.1 Study area	230
7.3.2 Data preparation for null, DDM and DIM UGBM	230
7.4 Result and discussion	232
7.4.1 Null UGBM	232
7.4.2 Distance dependent method (DDM)	233
7.4.3 Distance independent method (DIM)	235
7.4.4 Comparison of DDM UGBM, DIM UGBM and null UGBM	236
7.5 Conclusion	238
7.6 References	241
CHAPTER 8: CONCLUSIONS AND FUTURE RESEARCH	262
8.1 Major conclusions of dissertation	262
8.2 Future directions	265
8.3 References	266
VITA	267

LIST OF TABLES

Table	Page
Table 4-1. Coding system employed here for the contingency table calculations used to compare simulated and reference LUCC map	122
Table 4-2: Spatial predictor variables in CLIP, SEWI and MRW	122
Table 4-3: Size of samples and resolution of data in CLIP, SEWI and MRW	122
Table 4-4: Competitor, split and improvement in CART	123
Table 4-5: Coefficients, variables and knots in MARS	125
Table 4-6: Ranking variables in CART and MARS	128
Table 4-7: ROC of CART, MARS and LTM obtained from the cross validation with the testing data	129
Table 5-1. A contingency table to compare simulated and reference land use maps	177
Table 5-2: Spatial predictor variables for SEWI and MRW	177
Table 5-3: Size of samples and resolution of data for SEWI and MRW	177
Table 5-4: Competitor, split and improvement for CART	178
Table 5-5: Coefficients, variables and knots in MARS	179
Table 5-6: Ranking variables in CART and MARS	181
Table 6-1: MSE of UGBMs with reduced-variable for the statistical analysis	216
Table 6-2: PAM values for different cardinal directions	216
Table 7-1: Reference area in 1988 and 2000 for the whole TMA and three regions of TMA	258
Table 7-2: Comparing the PAM quantity values of predicted urban boundaries using null UGBMs across the distances	258
Table 7-3: Predicted area of TMA using null UGBMs in 2012	258
Table 7-4: Best PAM quantity value for under and over estimate of DDM	258
Table 7-5: Range of change in PAM quantity values in multiple and whole region model	259
Table 7-6: Area of TMA for under and over DDM estimates in 2012 from the Whole and Multiple region Models	259
Table 7-7: ARCDT of regions 1, 2 and 3, and FARCDT for the whole TMA	259
Table 7-8: PAM quantity between the 2000 projection (using ARCDTs from each region and FARCDT) and the reference 2000 boundary for the whole TMA using DIM	260
Table 7-9: PAM quantity between the 2000 projection (using regional ARCDT values and FARCDT) to the reference area in 2000 for regions 1, 2 and 3 using DIM	260
Table 7-10: Predicted area of whole TMA using DIM	260
Table 7-11: Predicted area of individual TMA regions using DIM	261

Table	Page
Table 7-12: Comparing the PAM quantity and location values of rule-based simulation UGBMs versus Null UGBM.....	261

LIST OF FIGURES

Figure	Page
Figure 1-1: Land use science and sustainability	6
Figure 1-2: Dissertation structure	6
Figure 3-1: Calibration and validation across time and space	55
Figure 3-2: Classification of LUCC models	55
Figure 3-3: Cellular automata models.....	56
Figure 3-4: Structure of SLEUTH model	56
Figure 3-5: Components of Geo-Simulation model.....	57
Figure 3-6: Structure of Vector CA model	57
Figure 3-7: The process of MCE	57
Figure 3-8: Structure of the Geomod model	58
Figure 3-9: Conceptual view of CLUE model adopted from Veldkamp and Fresco, (1996)	58
Figure 3-10: Structure of agent based models	59
Figure 3-11: Structure of land transformation model	59
Figure 3-12: Structure of support vector machine model	60
Figure 3-13: Structure of genetic algorithm model.....	60
Figure 3-14: Structure of CART model	61
Figure 3-15: Structure of MARS model	61
Figure 3-16: Structure of SVM-CA model adopted from Yang et al. (2008).....	62
Figure 3-17: Structure of ANN-UGBM.....	62
Figure 3-18: Structure of DDM	63
Figure 3-19: Structure of DIM.....	63
Figure 4-1: Three study areas.....	108
Figure 4-2: Tree Navigator in CART.....	110
Figure 4-3: CART models for each study area	112
Figure 4-4: GCV across adding radial basis functions to MARS	113
Figure 4-5: R-square across adding radial Basis functions in MARS	113
Figure 4-6: ANOVA in MARS.....	115
Figure 4-7: BFs for significant drivers in CLIP, SEWI and MRW	117
Figure 4-8: Training run of LTM.....	117
Figure 4-9: Terminal node in CART	119
Figure 4-10: Reference agriculture change and error maps of three models in CLIP	120
Figure 4-11: PCM_N and PCM_P values for CART, MARS and LTM.....	121
Figure 4-12: Similarity values for LTM, CART and MARS simulations	121

Figure	Page
Figure 5-1: The idea of One-Versus-All (OVA) and All-Versus-All (AVA) procedures for MC.....	163
Figure 5-2: Model structure and coding scheme of LTM-MC	164
Figure 5-3: Coding scheme of LTM-MC, CART and MARS to model MC	165
Figure 5-4a: Simulated land use maps for three outputs (suitability map scale from 0 to 3) using MARS. Where in $N(i) = j$, i and j show the code and number of transition for each land use class, respectively	166
Figure 5-5: $k - fold$ cross validation procedure in SPM software.....	168
Figure 5-6: Study area in MRW and SEWI.....	168
Figure 5-7: Tree navigator in CART	170
Figure 5-8: Viewing the main splitter in CART	171
Figure 5-9: GCV and R-squared across number of radial basis functions in MARS.....	172
Figure 5-10: ANOVA in MARS.....	173
Figure 5-11: Training run of LTM-MC	174
Figure 5-12: Terminal node in CART (gray, red, yellow and green represent no-change, urban change, agriculture change and forest change, respectively).....	175
Figure 5-13: PCM and ROC for CART, MARS and LTM-MC.....	176
Figure 6-1: A typical architecture of feed-forward back propagation ANN.....	209
Figure 6-2: Conceptual model of UGBM	210
Figure 6-3: Image classification results for TMA in 1988 and 2000.....	211
Figure 6-4: Urban boundary of TMA for the years 1988 and 2000.....	212
Figure 6-5: Maps of the seven variables in 1988 used as input for ANN.....	213
Figure 6-6: Centre configuration used as output for training data collection in 2000, TMA centre location: $(x, y) = (534694.929, 3953534.460)$ meters	214
Figure 6-7: MSE value across training cycles	214
Figure 6-8: MSEs across training cycles for the drop one out predictor variable sensitivity analysis. Each curve is labelled with the predictor variable that is left out of the training	215
Figure 6-9: Illustration of the result of UGB predictions of TMA in 2012	215
Figure 7-1: Conceptual scheme of DDM.....	244
Figure 7-2: Conceptual scheme of DIM	245
Figure 7-3: Simulated under-estimate and over-estimated areas by UGBMs	246
Figure 7-4: Restrictions for urban boundary simulation.....	247
Figure 7-5: Location of three central points and corresponding regions of TMA in 1988 and 2000.....	248
Figure 7-6: Comparing predicted UB from Null UGBM in TMA with reference UB in 2000: (1) Reference UB of TMA in 1988; (2) Reference UB of TMA in 2000; (3) Under-estimate predicted UB of TMA using Null UGBM in 2000 including 700m buffer (Black color); (4) Over-estimate of predicted UB of TMA using Null UGBM in 2000 including 750m buffer (Green color).....	249

Figure	Page
Figure 7-7: The predicted change in UB of TMA from Null UGBM in 2012: (1) Reference UB of TMA in 1988; (2) Reference UB of TMA in 2000; (3) Under-estimate predicted UB of TMA using Null UGBM in 2012 including 700m buffer (Black Color); (4) Over-estimate of predicted UB of TMA using Null UGBM in 2012 including 750m buffer (Green Color)	250
Figure 7-8: Comparing predicted UB from DDM in TMA with reference UB in 2000: (1) Reference UB of TMA in 1988; (2) Reference UB of TMA in 2000; (3 and 4) Under-estimate and over-estimate of predicted UB of TMA using Multiple-region Model in 2000; (5 and 6) Under-estimate and over-estimate of predicted UB of TMA using Whole-region Model in 2000.....	252
Figure 7-9: The predicted change in UB of TMA from DDM in 2012: (1) Reference UB of TMA in 1988; (2) Reference UB of TMA in 2000; (3 and 4) Under-estimate and over-estimate of predicted UB of TMA using Multiple-region Model in 2012; (5 and 6) Under-estimate and over-estimate of predicted UB of TMA using Whole-region Model in 2012	254
Figure 7-10: Comparing predicted UB of TMA (from DIM) with reference UB in 2000: (1) UB of TMA in 1988; (2) UB of TMA in 2000; (3) Predicted UB of TMA with ARCDT1; (4) Predicted UB of TMA with ARCDT2; (5) Predicted UB of TMA with ARCDT3; (6) Predicted UB of TMA with FARCDT and (7) Predicted UB of TMA with best ARCDT for each region	256
Figure 7-11: UGB prediction of TMA with DIM in 2012: (1) UB of TMA in 1988; (2) UB of TMA in 2000; (3) Predicted UB of TMA with ARCDT1; (4) Predicted UB of TMA with ARCDT2; (5) Predicted UB of TMA with ARCDT3; (6) Predicted UB of TMA with FARCDT and (7) Predicted UB of TMA with best ARCDT for each region.	257

ABBREVIATIONS

ABM	Agent Base Model
ANN	Artificial Neural Network
AVA	All-Verses-All
BBS	Breeding Bird Survey
CA	Cellular Automata
CART	Classification And Regression Tree
CA-GA	Cellular Automata – Genetic Algorithm
CLIP	Climate Land Interaction Project
CLUE	Conversion of Land Use and its Effects
DDM	Distance Dependent Model
DEM	Digital Elevation Model
DIM	Distance Independent Model
ECOC	Error-Correcting Output-Coding
EPA	Environmental Protection Agency
ESRI	Environmental Systems Research Institute
FN	False Negative
FP	False Positive
GCV	Generalized Cross Validation
GIS	Geographical Information System
GPM	Global Parametric Model
HPC	High Performance Computing
IPCC	Intergovernmental Panel on Climate Change
KS	Kappa Statistic
LAI	Leaf Area Index
LNPM	Local Non-Parametric Model
LTM	Land Transformation Model
LUCC	Land Use Land Cover Change
LULC	Land Use Land Cover
MARS	Multivariate Adaptive Regression Spline
MC	Multiple Classification
MLP	Multi Layer Perceptron
MODIS	Moderate Resolution Imaging Spectroradiometer
MRW	Muskegon River Watershed
MSE	Mean Square Error
NLCD	National Land Cover Dataset
OVA	One-Verses-All

PAM	Percent Area Match
PCM	Percent Correct Match
PID	Principle Index Driver
RAMS	Regional Atmospheric Modelling System
RCDT	Rate of Change in Distance Over Time
ROC	Relative Operating Characteristic
RS	Remote Sensing
SEWI	Southeast Wisconsin
SF	Scale Factor
SLEUTH	Slope, Land use, Exclusion, Urban extent, Transportation, Hill shade
SNNS	Stuttgart Neural Network Simulator
SPM	Salford Predictive Modeler
SVM	Support Vector Machine
TMA	Tehran Metropolitan Area
TN	True Negative
TP	True Positive
UGBM	Urban Growth Boundary Model
USGS	United States Geological Survey
UTM	Universal Transverse Mercator
Vec-GCA	Vector-based Cellular Automata
VFC	Vegetative Fractional Cover
XML	Extensible Markup Language

ABSTRACT

Tayyebi, Amin. Ph.D., Purdue University, May 2013. Simulating land use land cover change using data mining and machine learning algorithms. Major Professor: Bryan C. Pijanowski.

The objectives of this dissertation are to: (1) review the breadth and depth of land use land cover (LUCC) issues that are being addressed by the land change science community by discussing how an existing model, Purdue's Land Transformation Model (LTM), has been used to better understand these very important issues; (2) summarize the current state-of-the-art in LUCC modeling in an attempt to provide a context for the advances in LUCC modeling presented here; (3) use a variety of statistical, data mining and machine learning algorithms to model single LUCC transitions in diverse regions of the world (e.g. United States and Africa) in order to determine which tools are most effective in modeling common LUCC patterns that are nonlinear; (4) develop new techniques for modeling multiple class (MC) transitions at the same time using existing LUCC models as these models are rare and in great demand; (5) reconfigure the existing LTM for urban growth boundary (UGB) simulation because UGB modeling has been ignored by the LUCC modeling community, and (6) compare two rule based models for urban growth boundary simulation for use in UGB land use planning.

The review of LTM applications during the last decade indicates that a model like the LTM has addressed a majority of land change science issues although it has not explicitly been used to study terrestrial biodiversity issues. The review of the existing

LUCC models indicates that there is no unique typology to differentiate between LUCC model structures and no models exist for UGB. Simulations designed to compare multiple models show that ANN-based LTM results are similar to Multivariate Adaptive Regression Spline (MARS)-based models and both ANN and MARS-based models outperform Classification and Regression Tree (CART)-based models for modeling single LULC transition; however, for modeling MC, an ANN-based LTM-MC is similar in goodness of fit to CART and both models outperform MARS in different regions of the world. In simulations across three regions (two in United States and one in Africa), the LTM had better goodness of fit measures while the outcome of CART and MARS were more interpretable and understandable than the ANN-based LTM. Modeling MC LUCC require the examination of several class separation rules and is thus more complicated than single LULC transition modeling; more research is clearly needed in this area. One of the greatest challenges identified with MC modeling is evaluating error distributions and map accuracies for multiple classes. A modified ANN-based LTM and a simple rule based UGBM outperformed a null model in all cardinal directions. For UGBM model to be useful for planning, other factors need to be considered including a separate routine that would determine urban quantity over time.

CHAPTER 1: LAND CHANGE SCIENCE: A BRIEF INTRODUCTION

1.1 Introduction

Land use land cover change (LUCC) has been recognized as a significant driver of environmental change at all important spatial and temporal scales (Turner et al. 1995). LUCC is known to influence and disrupt large-scale climate dynamics (Pielke 2001, 2005; Feddema et al. 2005; Pijanowski et al. 2011), biogeochemical cycles (Verchot et al. 1999; Tang et al. 2005a), the hydrologic cycle (Foley et al. 2005), and biodiversity patterns (Dale et al. 1994). Research that examines these issues across spatial-temporal scales using a multi-disciplinary approach is termed land change science (Figure 1-1).

Land change scientists recognize several facets of the land surface that alter ecosystem dynamics; the first is land cover, which refers to the physical cover of the earth surface (e.g. water, vegetation and man-made features) and the second, land use, defined as all human activities on the land (Turner, 1995). A third is the level of intensity. For example, agricultural growth has occurred simultaneously with some degree of intensification, making characterization of land use cover a multi-dimensional phenomenon (Armesto et al. 2009). Agricultural intensification usually results in more chemical inputs and modifications to the hydrologic cycle.

At a global scale, extensive conversion of native vegetation (forests and grasslands) to agriculture to produce food for society has occurred over the last ten millennia although rates of change in the last century have been unprecedented (Armesto et al. 2009). Recently, the human species crossed an important threshold as more than half of us now live in cities. The urban footprint now doubles every 30 years. At this rate, urban land use should approach 10% of the land surface by 2070.

Conversions of land use can be multiple if followed over a long time period. For example, some recovery of forests from shrublands and abandoned agricultural land to natural areas (Brown, 2005; Carmona et al. 2010; Diaz et al. 2011) is a common pattern in many developed countries. Local land use changes are often as a result of global factors. Shifts of agriculture are often due to the globalization of the food production system. Thus, land use cover change can be complex and the need to understand the drivers of these changes at multiple spatial-temporal scales are among some of the most pressing needs currently in environmental science research.

One of the most pressing global environmental change issues is climate change but its causes are not solely due to the burning of fossil fuels. We now recognize that a significant amount of climate change, up to half, is due to land use change (IPCC, 2007; Pielke, 2005). LUCC, especially urban and agriculture growth, is known to have a direct impact on climate change patterns by increasing surface temperature along with indirect effects via the emission of greenhouse gases through burning of vegetation during clearing (Cai et al. 2003; Kalnay and Cai, 2003).

The loss of many natural areas, such as forests, has numerous ramifications to the environment and human well-being. Decision makers, natural resource managers, and

policy makers are interested in preserving forest ecosystems for the conservation of biodiversity (Kirschbaum, 2000), supporting wood products (Wernick et al. 2007), reducing emissions (via a global program called REDD, or reducing emissions from deforestation and degradation) and decreasing impacts to the water cycle (Ray et al. 2010, Peng et al. 2002). People in the world are today more dependent upon forest resources for meeting essential needs than ever before (e.g. oxygen and food; FAO, 2009, Pijanowski et al. 2010).

Representing land use digitally is often accomplished using GIS maps. LULC data can belong either to a single LULC category (e.g. categorical representation of land cover) (Loveland et al. 1999) or consist of continuous biophysical variables (e.g. continuous representation of LULC such as leaf area index) (DeFries et al. 1995). LULC conversion is a complete replacement of one LULC category by another one (e.g. urban gain, deforestation or agricultural loss). The categorical representation of LULC classes has the advantages to characterize LULC conversions easily although in many cases, land cover modifications are gradual processes that influence the land cover character without changing its classification. Agricultural intensification is such an example of land cover modification that increases food production (Tilman, 1999). Land cover modification detection requires LULC representations, which vary gradually across space and time.

LULC conversions are known to be associated with the occurrence of land uses in the local neighborhood. When modeling LUCC, especially in the context of urban change, it is useful to include neighborhood interactions as a driving factor (Verburg et al. 2003). Lambin et al. (2003), in a very well cited paper, were able to show that urbanization, agriculture intensification, deforestation along with a still unmeasured land

cover change are highly autocorrelated at a local scale (Lambin et al. 2003). Thus it is not surprising that many LUCC models have local interactions, quantified through the use of GIS, in their algorithms.

Some LULC conversions may be considered essentially irreversible; once converted they remain in that land use for extended periods of time or their conversion to another use is extremely difficult. Examples include urbanization, wetland destruction and desertification from climate change. Many LULC conversions are reversible; for example, conversion of a natural area to forest could lead to its abandonment, which would then revert back to a natural state if left alone (Kumar et al. 2012). The amount of time between these transitions is thus likely a factor of both human activities (e.g. economics of land production) and environmental processes (e.g. successional patterns). Thus, in terms of sustainability, some land use cover changes are of more concern than are others.

1.2 Research Objectives and Structure of the Dissertation

The structure and objectives of this dissertation are as follows (Figure 1-2). Chapter 2 discusses the lessons learned in using LTM to address global environmental change issues during the last decade of developing LTM. Chapter 3 summarizes the existing LUCC models that have been used to simulate and predict LUCC. The characteristics of LUCC models have been summarized in more detail. The review of LUCC models helps to provide a practical framework as a literature review.

In chapter 4, one global parametric LUCC model, the ANN-based LTM was compared with two local non-parametric models, a CART and MARS, for binary LUCC

modeling. The ANN-based LTM, developed to simulate spatial patterns of LUCC over time, currently simulates only a single land use transition at a time. In chapter 5, the current model structure and coding scheme of the LTM was modified for MC, and compared with two statistical models, one based on CART and another MARS, that simulate MC. We explored the benefits and challenges of model structure and coding scheme for three data mining approaches for MC. Finally, potential rules were proposed to solve the conflict problem in MC.

Urban growth boundaries models (UGBMs) are land use planning tools that limit urban expansion. These models are being implemented by planning agencies. Thus, there is a need to create models that can simulate changes in urban boundaries. In chapter 6, an UGBM which utilizes ANN, GIS and remote sensing was developed to simulate the complex geometry of the urban boundary. Raster-based predictive variables are used as inputs to the ANNs parameterized using vector routines. ANNs were used to train predictor variables of urban boundary geometry. Similarly, in chapter 7, two rule-based spatial-temporal models, one which employs a distance dependent modeling (DDM) approach and the other a distance independent modeling (DIM) approach, were presented to simulate UGBs. These rule-based UGBMs use azimuth and distance values, vector-based predictive variables, directed from central points within the urban area, to simulate UGB change.

Chapter 8 summarizes the conclusions from the previous chapters and future research in LUCC modeling is presented particularly for the LTM. This chapter also discusses the lessons learned in using the LTM in this dissertation and the use of scenarios to explore future and past landscapes.

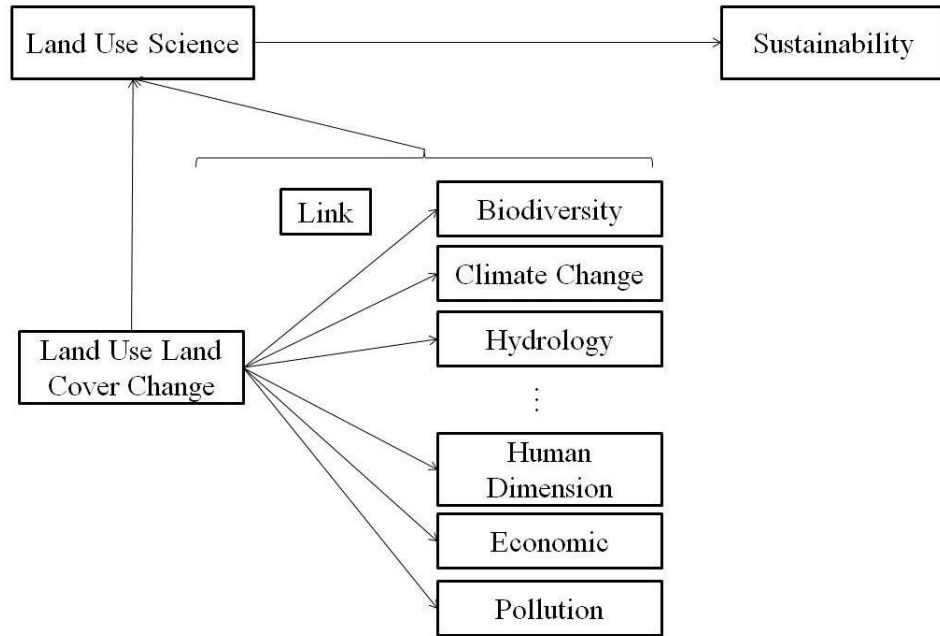


Figure 1-1: Land use science and sustainability

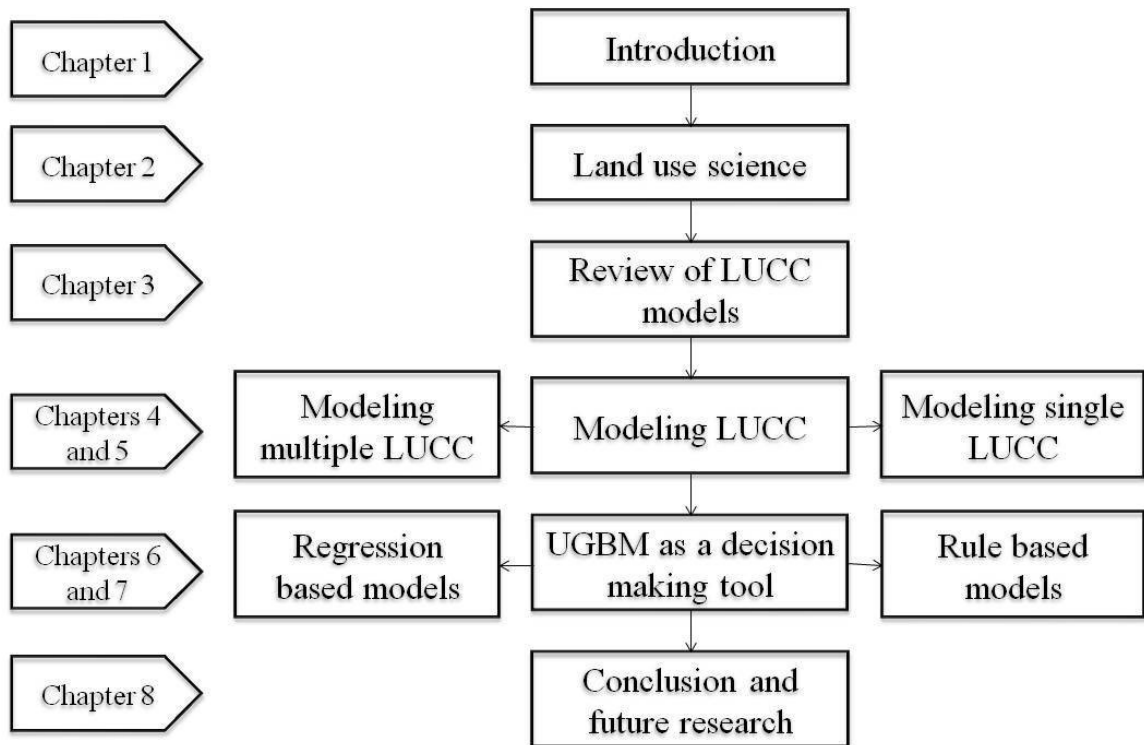


Figure 1-2: Dissertation structure

1.3 References

- Armesto, J. J., Smith-Ramírez, C., Carmona, M. R., Celis-Diez, J. L., Díaz, I. A., Gaxiola, A., Gutiérrez, A. G., Nuñez-Avila, M. C., Pérez, C. A., Rozzi, R. (2009). Old-growth temperate rainforests of South America: Conservation, plant–animal interactions, and baseline biogeochemical processes. Pages 367–390 in Wirth C, Gleixner G, Heiman M, eds. *Old-Growth Forests*. Springer.
- Brown, D. G., Pijanowski, B. C., & Duh, J. D. (2000). Modeling the relationships between land-use and land-cover on private lands in the Upper Midwest, USA. *Journal of Environmental Management*, 59, 247–263.
- Cai, Z., S. Sawamoto, C. Li, G. Kang., J. Boonjawat., A. Mosier., and R. Wassmann. (2003). Field validation of the DNDC model for greenhouse gas emissions in East Asian cropping systems. *Global Biogeochem. Cycles* 17(4).
- Carmona, A., Nahuelhual, L., Echeverría, C., Báez, A. (2010). Linking farming systems to landscape change: an empirical and spatially explicit study in southern Chile. *Agriculture Ecosystem Environment*. 139, 40–50.
- Dale, V. H., Offerman, H., Pearson, S., and O’Neill, R. V. (1994). Effects of Forest Fragmentation on Neotropical Fauna, *Conservation Biology*, 8, 1027-1036.
- DeFries, R. S., Field, C. B., Fung, I., Justice, C. O., Los, S. (1995). Mapping the land surface for global atmosphere-biosphere models: toward continuous distributions of vegetation’s functional properties.
- Diaz, G. I., Nahuelhual, L., Echeverría, C., Marín, S. (2011). Drivers of land abandonment in Southern Chile and implications for landscape planning. *Landscape and Urban Planning*, 99, 207-217.
- FAO. (2009). Seed security for food security in the light of climate change and soaring food prices: challenges and opportunities. Rome, FAO. (available at <ftp://ftp.fao.org/docrep/fao/meeting/016/k4275e.pdf>).
- Feddema, J. J., Oleson, K. W., Bonan, G. B., Mearns, L. O., Buja, L. E., Meehl, G. A., and Washington, W. M. (2005). The Importance of Land-Cover Change in Simulating Future Climates. *Science*, 310, 1674-1678.
- Foley, J. A., DeFries, R., Asner, G. P., Barford, C., Bonan, G., Carpenter., S. R., Chapin, F. S., Coe, M. T., Daily, G. C., Gibbs, H. K., Helkowski, J. H., Holloway, T., Howard, E. A., Kucharik, C. J., Monfreda, C., Patz, J. A., Prentice, I. C., Ramankutty, N., and Snyder, P. K. (2005). Global Consequences of Land Use, *Science*, 309, 570–574.
- IPCC. (2007) Climate change 2007: the physical science basis. Contribution of working group I to the fourth assessment report of the intergovernmental panel on climate change. In: Solomon, S., Qin, D., Manning, M., Chen, Z., Marquis, M., Averyt, K. B., Tignor, M., Miller, H. L. (eds). Cambridge University Press, Cambridge; New York, 996 p.
- Kalnay, E., Cai, M. (2003). Impacts of urbanization and land-use change on climate, *Nature*, 423, 528-531.
- Kirschbaum, M. U. F. (2000). Forest growth and species distribution in a changing climate. *Tree Physiology*, 20, 309-322.

- Lambin, E. F., Geist, H. J., Lepers, E. (2003). Dynamics of land-use and land-cover change in tropical regions. *Annu. Rev. Environ. Resour.* 28:205-41.
- Loveland, T. R., Zhu, Z., Ohlen, D. O., Brown, J. F., Reed, B. C., Yang, L. M. (1999). An analysis of the IGBP global land-cover characterization process. *Photogramm. Eng. Remote Sens.* 65(9):1021–32.
- Peng, Y., U. Lohmann, R. Leaitch, C. Banic, and M. Couture, (2002). The cloud albedocloud droplet effective radius relationship for clean and polluted clouds from RACE and FIRE. *ACE. J. Geophys. Res.*, 107 (D11).
- Pielke, Sr., R. A. (2001). Earth System Modeling - An Integrated Assessment Tool for Environmental Studies, in *Present and Future of Modeling Global Environmental Change: Toward Integrated Modeling*, eds. T. Matsuno and H. Kida, Tokyo: Terra Scientific, 311–337.
- Pielke, Sr., R. A. (2005). Land Use and Climate Change, *Science*, 310, 1625–1626. View related paper by Feddema et al. 2005: The importance of land-cover change in simulating future climates., 310, 1674–1678.
- Pijanowski, B., L. Iverson, C. Drew, H. Bulley, J. Rhemtulla, M. Wimberly, A. Bartsch and J. Peng. (2010). Addressing the Interplay of Poverty and the Ecology of Landscapes: A Grand Challenge Topic for Landscape Ecologists? *Landscape Ecology*. doi:10.1007/s10980-009-892 9415-z.
- Pijanowski, B., N. Moore, D. Mauree and D. Niyogi. (2011). Evaluating error propagation in coupled land-atmosphere models. *Earth Interactions*. 15:1-15.
- Ray, D. K., Duckles, J. M., B. C. Pijanowski. (2010). The Impact of Future Land Use Scenarios on Runoff Volumes in the Muskegon River Watershed. *Environmental Management*. DOI 10.1007/s00267-010-9533-z.
- Tang, Z., B. Engel, K. Lim, B. Pijanowski and J. Harbor. (2005a). Minimizing the impact of urbanization on long-term runoff. *Journal of the Water Resources Association*. 41(6): 1347-1359.
- Tilman, D. (1999). Global environmental impacts of agricultural expansion: the need for sustainable and efficient practices. *Proc. Natl. Acad. Sci. USA* 96(11): 5995-6000.
- Turner, B. L., D. Skole, S. Sanderson, G. Fischer, L. Fresco, and R. Leemans. (1995). Land-use and land-cover change science/research plan. IGBP report no. 35 and HDP report no. 7.
- Verchot, L. V., Davidson, E. A., Cattanio, J. H., Ackerman, I. L., Erickson, H. E., and Keller, M. (1999). Land Use Change and Biogeochemical Controls of Nitrogen Oxide Emissions From Soils in Eastern Amazonia. *Global Biogeochemical Cycles*, 13, 31-46.
- Wernick, I. K. (2007). *Global Warming and the Industrial System*, International Relations and Security Network (ISN), Zurich, Switzerland. See <http://www.isn.ethz.ch/pubs/ph/details.cfm?lng=en&id=30366>.

CHAPTER 2: LAND CHANGE SCIENCE THROUGH THE LENS OF THE LAND TRANSFORMATION MODEL (LTM)

2.1 Introduction

In the 1990s, there were few land use cover change models as many researchers in the 1970s and 1980s abandoned land use change modeling for a lack of sufficient tools and data (cf. Lee's famous *Requiem for Land Use Change Models* published in 1973). A 1996 USGS workshop at the EROS data center brought together nine land change modelers in an attempt to revive the field. Modelers present discussed the current state and future of LUCC modeling. The Land Transformation Model (LTM) at that time was it is infancy, a model incorporated within a GIS, with limited data, and it, among several other models, was showcased at the meeting. In 2002, the first journal article describing its current form, which couples an artificial neural network (ANN) and GIS, was published in *Computers, Environment and Urban Systems* (CEUS), the de facto journal for publishing new urban change models. To date, it is the fourth highest cited paper in the history of the journal (1986 – present). It now is among dozens of land change models used to study a variety of global environmental change issues.

Over a decade of model development and experiment has gone into the model, and the LTM has been now applied to forecast LUCC patterns in a variety of places around the world, such as all lower 48 states in the USA, central Europe, East Africa and Asia. Forecasts are often linked to climate, hydrologic or biological models where the coupled models are used to examine how what-if land use change scenarios impact the environment and/or economics. The LTM has been engineered to run “back-wards” in order to examine environmental impacts of historical land use changes or the effects of land use legacies on slow environmental processes, such as groundwater transport through watersheds.

Here, we discuss the lessons learned in using the model to address global environmental change issues. These lessons learned include: (1) how the model should be properly coupled to other models; (2) the ways that the model should be interpreted given errors that occur in simulations; (3) the use of scenarios to explore futures and pasts; and (4) the heuristic value of a model like the LTM.

2.2 LTM as a case-study LUCC Model

Most LUCC models determine suitability of change and rates of change (quantity of change for a land use class) using separate modules. The LTM, which couples GIS with ANNs to forecast LUCC, is able to use a variety of social, political, economical and environmental factors (Pijanowski et al. 2002a). ANNs learn LUCC patterns using GIS to develop the relationship between dependent and independent drivers, and assess the predictive ability of the model.

Research on ANNs in other fields proved that ANNs can generalize patterns well (Skapura, 1999). To test this concept for LUCC modeling, LTM was executed for two places in the US to test whether the network file developed for one area is transferable across another region. Four accuracy assessment metrics were used that quantified how well the models performed using hard-classed contingency tables, probability distributions and spatial patterns (Pijanowski et al. 2005). LTM was trained and tested using data from the same area (called the non-swap case) and then compared against simulations designed to train for data in one area and then tested on the other data (called swap case). For the non-swap simulations, LTM performed well in both regions; however, the swap simulations yielded variable results; one swap simulation performed as well as the non-swap but transferability was not strong in the other swap case.

Understanding LUCC in diverse regions contributes toward our understanding of LUCC changes across space and time. LTM urban change simulations were compared in two diverse regions, one in the USA and the other in Albania, (Pijanowski et al. 2006) using eight calibration metrics (four location-based metrics and four spatial metrics) to quantify model accuracy. Location-based metrics show that LTM perform better in Albania because urbanization occurred in clumped patterns in Albania while urbanization occurred in patchy arrangements in the USA. Patch metrics are more useful where urbanization is fragmented; especially for application where LULC patches are important for planning, policy and management. In addition, results show that more training cycles did not necessarily yield a better accuracy for patch metrics (Pijanowski et al. 2006).

ANNs developed in other fields have been found to outperform similarly parameterized statistical models, such as those using logistic regression. LTM was

trained for prediction of urban and forest areas at a county level (Thekkudan, 2008). The LTM was tested using percent correct match (PCM) and relative operating characteristic (ROC). Both accuracy metrics showed that LTM performs better than a logistic regression model. Although LTM performed well at predicting fringe development at urbanized areas, it performed poorly in tests at forests. Similarly, Tayyebi et al. (2010) compared logistic regression with LTM to simulate urban change pattern. Results show that LTM performs better than logistic regression for urban change simulation. Calibration of both models was performed using area under the ROC curve and the kappa statistic (Pijanowski et al. 2009).

The ANN-based, global parametric LTM has also been compared with two local non-parametric models, one CART and the other MARS, parameterized with identical data from three different areas of the world, one undergoing extensive agricultural expansion (East Africa), another where forests are re-growing (western Michigan, USA), and a third where urbanization is prominent (Milwaukee Metropolitan Area, USA). Independent training and testing data were used to calibrate and validate each model, respectively. Although all approaches obtained similar accuracies, the ANN-LTM provided a slightly better goodness-of-fit than MARS and CART across testing data for all three study sites (Tayyebi and Pijanowski, in review). Details of these simulations are provided in Chapter 4.

The ANN-based LTM currently simulates a single LULC transition at a time. LUCC models that can simulate multiple LULC classes are rare. The current model structure and coding scheme of the LTM has been modified to compare it with other two local non-parametric models (CART and MARS) for multiple LUCC modeling (Tayyebi

and Pijanowski, in review). Potential rules were also suggested to solve the confliction prediction in multiple classes simulation. Results show that the new coding scheme and model structure of LTM was accurate, stable and straightforward to implement. The ANN-based LTM and CART outperformed MARS and LTM was slightly better than CART. Details of these simulations are provided in Chapter 5.

Scaling up a LUCC simulation often requires re-engineering the model so that it may handle larger datasets. To address research needs at continental scale, we redesigned LTM in the HEMA lab for running at continental scales with fine (30 m) resolution using a new architecture that employs a windows-based High Performance Compute (HPC) cluster (Pijanowski et al. in revision). This new version of LTM (called LTM-HPC) has a new architecture which uses HPC to handle large data sets in terms of size and quantity of files and integrate tools that are executed using different scripting languages (e.g. SQL, Python and C#). When developing meso-scale modules within LUCC models, it is first necessary to determine what spatial units are most appropriate to incorporate into the model at the meso-scale. We were able to compared meso-scale LTMs with three null models that lack meso-scale drivers. Results show that introducing meso-scale modules into large-scale LTM simulations significantly increased model accuracy (Tayyebi et al. 2012).

It has been shown that by 2001, 33% of the land covers were anthropogenic in the conterminous US (Rittenhouse et al. 2010). Many studies have explored interactions between LUCC patterns and species diversity (White et al. 1997). Topography remains a significant constraining factor on LUCC patterns, allowing some areas to persist in forest cover regardless of development pressures (Wear and Bolstad, 1998). Topography has a

strong influence on forest change. Areas at lower elevation are more likely to remain in non-forest or to have experienced more recent losses of forest (Turner et al. 1994).

2.3 LTM Used in Land-Climate Interaction Studies

LUCC can impact climate in a variety of ways. The replacement of productive soil and vegetation with urban materials, such as concrete, asphalt, and buildings, affects the albedo and runoff characteristics of the land surface, thus significantly impacting the land-atmosphere energy exchange. LUCC reduces carbon sequestration rates to soil and aboveground vegetation (Houghton et al. 1985). Local evapotranspiration to the water cycle is one direct impact of LUCC on climate (Eltahir and Bras, 1996). A variety of LUCC and climate change impacts on ecosystem dynamics have been studied using the LTM coupled to other models and spatial databases. In a land-climate study, a multi-modeling system was developed (Wiley et al. 2010) to evaluate the individual and combined impacts of LUCC and climate to the freshwater fish habitat suitability in the Midwest USA. Comparisons of two scenarios with and without the climate change illustrate the impacts of climate on rivers. Simulations of the multi-models showed that water temperature has a significant influence on species distributions and fish diversity was more sensitive to climate change than to LUCC.

Fluxes of energy and water at the land-atmosphere are a function of land surface characteristics. In another land-climate set of simulations (Moore et al. 2010), leaf area index (LAI) and vegetative fractional cover (VFC), which were derived moderate resolution imaging spectroradiometer (MODIS), were coupled to the LTM and the Regional Atmospheric Modelling System (RAMS) to assess the effect of land surface

characteristics on precipitation and land surface temperature. The remotely sensed data products of LAI and VFC were modeled using spline. This research (Moore et al. 2010) concluded that MODIS products were superior to generalized routines in RAMS as land surface temperature simulations improved fit to observed data. The ability to properly characterize precipitation patterns were not improved using these methods.

Understanding the interaction between LUCC and climate needs more efforts. To address this concern, a multi-methodological framework was developed to quantify these interactions (Olson et al. 2007). LUCC simulation models (all including the LTM) were combined with social science techniques like semi-structured interviews, household surveys and spatial analysis of LUCC to enhance our understanding of these complex processes. These results have been integrated into climate adaptation stories that have been provided to the governments of developing countries in Africa, such as Kenya, Uganda and Tanzania (Olson et al. 2007). To assess the urbanization effects on the water and energy cycle, U.S. Geological Survey (USGS) stream flow data (such as flow distribution, daily variation in stream flow, and frequency of high-flow events) were analyzed (Yang et al. 2010). Results showed that urban intensity has a significant effect on hydrologic metrics. Temperature in the urban region increased greatly because of the reduced albedo, increased volumetric heat capacity, and thermal conductivity of the urban land use type (Yang et al. 2010).

2.4 LTM in Land-Hydrologic Dynamic Studies

LUCC influences the hydrology of watersheds across a variety of spatial and temporal scales (Tang et al. 2005a; Tang et al. 2005b). LTM used to explore the impact

of future urban sprawl and non-sprawl trends (Pijanowski et al. 2002b) on the hydrological cycle. Population density used to discriminate between sprawl and non-sprawl patterns. Results show that hydrological change (e.g. nitrogen) resulted in a significant loss of agricultural and forest along the streams. Agricultural activities (such as pesticide and fertilizer in soil and water, livestock manure; Widory et al. 2004) and urbanization trends, are considered the primary anthropogenic source of nitrogen contamination in hydrologic ecosystems (Howarth, 2004). Amount of run-off in groundwater from chemical substances (e.g. nitrate and phosphates) and sediment has consequences for both human diseases and deaths, and ecosystem health such as biodiversity loss (Rabalais et al. 2002).

The biogeochemistry of surface and groundwater are related to LUCC. Groundwater age needs to be accurately quantifying the temporally varying impacts of LUCC on water quality. Temporal analysis on stream chemistry can be an important factor for managing LUCC in regional watersheds (Wayland et al. 2002). Results show that the impacts of near surface groundwater flow during storm events represent a significant source of anthropogenic solutes to a watershed. Land use management reduce solute loading to a watershed might not result in water quality improvements (Wayland et al. 2002). Groundwater is sensitive to chemical alteration, the extent of which may vary depending on LUCC within recharge areas.

LUCC can significantly alter hydrologic dynamics. LTM simulation has been used to explore the consequence of urbanization on amount of runoff in hydrology cycle (Tang et al. 2005a). Results show that urbanization can slightly or considerably increase the amount of runoff, depending on the rate of urban change. In addition, urbanization

slightly increases nutrient losses in runoff, but significantly increases losses of heavy metals in runoff. Results of this research can be used to raise decision makers' awareness of urban sprawl impacts. While concern about disorganized urbanization in cities increases, smart growth has been suggested as an alternative to protect water resource and minimize the amount of runoff resulting from urbanization (Tang et al. 2005b). One of the major direct environmental impacts caused by the conversion of open spaces to urban and suburban areas is the degradation of water quality (USEPA, 2001). The impact of urbanization on water resources is reflected in terms of increasing the runoff rate, decreasing infiltration, altering ground water recharge patterns (Moscrip and Montgomery, 1997) and degradation of water quality in streams and ground water (USGS, 1999). The future scenario of LTM was used to select best type of LULC placements for non-sprawl and sprawl scenarios, which reduce runoff (Tang et al. 2005b). The magnitude that runoff can be minimized depends on LULC types, soil properties, and the urbanization level of a watershed.

Historical LUCC maps were created using a back-cast LUCC model (Pijanowski et al. 2007). Two spatial-temporal models, a back-cast LUCC model and a groundwater flow model, were coupled (Pijanowski et al. 2007) to develop "land-use legacy maps." The difference between a land-use legacy map, created from maps of past land use and groundwater travel times, and a current land-use map was quantified. These map differences can affect watershed planning and management decisions at a variety of spatial and temporal scales. Results show that land-use legacy maps provide a more accurate representation of the linkage between LULC and current water quality compared to the current land-use map (Pijanowski et al. 2007).

In another hydrological study, the relative impact of LUCC patterns (e.g. simulated by LTM) and projected future climate change on hydrologic processes was examined (Mishra et al. 2010). Results suggest that the land surface water and energy balance can be affected by LUCC and climate change. The runoff was increased annually, while evapotranspiration was reduced due to forest-to-cropland and forest-to-urban conversion. Radiation was decreased considerably due to forest-to-cropland conversion (e.g. albedo). Agricultural and urban areas increase runoff compared to a landscape that is in its natural state (NRC, 2007). Future LUCC scenarios for forest regrowth and urbanization rates were developed using the LTM (Ray et al. 2010). Results show that controlling urbanization rate can reduce runoff; reforestation can abate some of the runoff effects from urban growth (Ray et al. 2010).

2.5 Organismal Responses to LUCC

Understanding the impacts of LUCC on biodiversity is important in landscape ecology (Dale et al. 2000). LUCC alter the spatial pattern of habitats often resulting in habitat loss and fragmentation (Turner et al. 1994). Species diversity is defined as species richness (the number of species present in an area) and less often as species diversity, the number of species weighted by their abundance (Rittenhouse et al. 2010). Biodiversity is highly affected by LUCC (e.g. loss of forest species within deforested areas) or when undisturbed lands become more intense (e.g. agriculture, livestock grazing). The habitat suitability is impacted by existing habitat fragmenting into smaller pieces (e.g. habitat fragmentation). Smaller habitat areas generally support fewer species, and fragmentation can cause local and even global extinction. Rittenhouse et al. (2012) integrated National

Land Cover Data (NLCD) and American Breeding Bird Survey (BBS) data to assess LUCC affect on species diversity (e.g. bird diversity) in the conterminous USA. Results show that the natural land cover conversion to anthropogenic was significantly associated with bird species richness and abundance. In particular, grassland and shrub-land loss has the most significant loss bird species richness and abundance.

2.6 Joint LUCC and Climate Change effect on Biodiversity

Biodiversity loss results from a variety of factors including hydrology, climate change and fragmentation. The risk of heat waves increase with global warming that changes mean temperature and precipitation. Heat waves, consecutive days with higher than average temperatures, have increased mortality among species (Albright et al. 2011). Indicators of heat waves derived from MODIS land surface temperature and interpolated air temperature data were compared with each other to identify their associations with avian community composition (Albright et al. 2011). Results show that MODIS land surface temperature indices were more predictive and abundance and species richness declined due to heat waves (Albright et al. 2011).

Climate changes are expected to produce more heat waves and droughts. Drought increases the risk of higher mortality, lower habitat quality, reduced reproductive effort, and can decrease abundance and species richness. Heat waves can also stress species by increasing water requirements, reducing reproduction and survival, resulting in lower species richness (Albright et al. 2010a and 2010b). Results show that large changes related to extreme weather events occurring in both breeding and post-fledging periods (Albright et al. 2010b). Jointly, rather than individually occurring heat waves and

droughts were more predictive of abundance changes (Albright et al. 2010b). These results indicate that avian responses to weather extremes change based on the traits, timing, and geography.

Hurricanes, which are the direct consequence of climate change, can alter forests and affect avian communities. These changes affect food availability (e.g. fruit, flowers, seeds, and insects), and alter local avian species richness and abundance. Detection of hurricane-disturbed and non-disturbed areas is possible through using satellite imagery. Results show a decrease in community similarity in the first post-hurricane breeding season (Rittenhouse et al. 2010). Hurricane has significant effect on abundance for species that breed in urban and woodland habitats and greater declines for woodland species than grassland or urban species due to forest loss (Rittenhouse et al. 2010).

2.7 LTM and Planning Decisions

Spatial and temporal analysis for rates and patterns of change in the Upper Great Lake States at five spatial levels (global, regional, zonal, landscape, and patch) and two temporal rates (referred to as first and second order) of change showed considerable amounts of urban gain, agriculture loss, and either gained or lost forest (Pijanowski and Robinson, 2011). The amount of LULC fragmentation varied over time across 5 km buffer zones but increased substantially over the study periods. Urbanization and fragmentation are characteristics of LUCC across the region (Pijanowski and Robinson, 2011).

Urban and sub-urban regions started to experience scattered development near cities. Such development patterns heavily burden local governments with high financial

costs which they must provide services. The purpose of designating non-urban planned districts is the conservation of environmentally sensitive areas and to protect rural landscapes. An urban growth boundary model (UGBM) which utilizes ANN and GIS was developed to simulate the complex geometry of the urban boundary (Tayyebi et al. 2011a). ANN-UGBM distinguishes land that is designated urban, to be used for housing, industry and commerce, from non-urban land is to be used for activities such as conservation, agriculture, resource development and suitable community infrastructure like airports, water supply and sewage treatment facilities that require large areas of open land. This study is provided in more detail in Chapter 6. Two rule-based spatial-temporal models, one which employs a Distance Dependent Method (DDM) and the other a Distance Independent Method (DIM), were proposed to simulate UGBs (Tayyebi et al. 2011b). Percent Area Match (PAM) quantity and location goodness of fit metrics are used to assess the agreement between simulated and observed urban boundaries. Results indicate that rule-based UGBMs have a better goodness of fit compared to a null UGBM using PAM quantity and location goodness of fit metrics (Tayyebi et al. 2011b). This study is provided in more detail in Chapter 7.

2.8 Quantifying Error Propagation in Coupled Models containing the LTM

LUCC (e.g. crop yield) and greenhouse gases impact food production. Regional Atmospheric Modeling System (RAMS) is a regional climate model used to compare the effects of projected future greenhouse gases and future LUCC on spatial variability of crop yields in Africa (Moore et al. 2011). Results suggest that climate change and LUCC

have highly heterogeneous influence on yield changes. This study confirms that LUCC is the main factor in assessing food production risk.

Coupling back-cast LUCC (Ray and Pijanowski, 2010) and groundwater models (Pijanowski et al. 2007) can be used to create a map (called legacy map) to quantify the contribution of land uses to the groundwater signal arriving at streams. The uncertainty in groundwater models and back-cast LTM affect the outcome of the coupled model and their reliability to natural resource and land use planning (Ray et al. 2012). A multi-metric score was proposed to evaluate the application uncertainty of the land use legacy maps for planning. Results indicate that managers can benefit from using maps as planning tools despite a wide range of evaluated uncertainties.

A joint study between land-climate (Pijanowski et al. 2011) quantified the errors generated by the LTM through climate as simulated by RAMS. Results indicate that errors in LUCC models do not appear to propagate onto the regional climate simulation for the long term simulation. Rainy and dry seasons exhibited greater and less precipitation in LTM-RAMS simulations, respectively. Small errors from a LUCC model can amplify if LUCC model and RAMS are used to forecast into the future.

Having knowledge about uncertainty in LUCC maps give more confidence to urban planners in their decisions. In an error study in LUCC modeling (Tayyebi et al. in review), the framework of Walker et al. (2003) was used to address the importance of assessing various dimensions of uncertainty (data uncertainty, model parameter uncertainty and model outcome uncertainty) through ANN and LR urban change simulation. Results show that the error in output data is more significant than error in

input data and data uncertainty is more significant than model parameter uncertainty in LUCC models.

2.9 Conclusion

This chapter reviews the various applications of LTM as a LUCC model over the last decade across the globe. LTM, works independently of user by randomizing variable weights, may currently be an appropriate option for management and urban planning. There are three weaknesses of LTM. ANNs may not converge to a global optimal solution. ANNs have over-fitting problem. ANNs are ‘black-box’ and it is difficult to explain their behavior (Roiger and Geatz, 2003). The first two problems have been solved by adding hidden layers and numer of nodes; however, it is still mysterious to explain how ANNs make decisions through their layers.

2.10 References

- Albright, T. P., A. M. Pidgeon., C. D. Rittenhouse., M. K. Clayton., C. H. Flather., P. D. Culbert., B. D. Wardlow., and V. C. Radeloff. (2010a). Effects of drought on avian community structure, *Global Change Biology* 16:2158-2170.
- Albright, T. P., A. M. Pidgeon., C. D. Rittenhouse., M. K. Clayton., C. H. Flather., P. D. Culbert., B. D. Wardlow., and V. C. Radeloff. (2010b). Combined effects of heat waves and droughts on avian communities across the conterminous United States, *Ecosphere*, 1(5)art11.
- Albright, T. P., A. M. Pidgeon, C. D. Rittenhouse, M. K. Clayton, C. H. Flather, P. D. Culbert, & V. C. Radeloff, (2011). Heat waves measured with MODIS land surface temperature data predict changes in avian community structure, *Remote Sensing of Environment*, 115(1)245-254.
- Armesto, J. J., Smith-Ramírez, C., Carmona, M. R., Celis-Diez, J. L., Díaz, I. A., Gaxiola, A., Gutiérrez, A. G., Nuñez-Avila, M. C., Pérez, C. A., Rozzi, R.. (2009). Old-growth temperate rainforests of South America: Conservation, plant–animal interactions, and baseline biogeochemical processes. Pages 367–390 in Wirth C, Gleixner G, Heiman M, eds. *Old-Growth Forests*. Springer.
- Brown, D. G., Pijanowski, B. C., & Duh, J. D. (2000). Modeling the relationships between land-use and land-cover on private lands in the Upper Midwest, USA. *Journal of Environmental Management*, 59, 247–263.
- Cai, Z., S. Sawamoto, C. Li, G. Kang, J. Boonjawat, A. Mosier, and R. Wassmann. (2003). Field validation of the DNDC model for greenhouse gas emissions in East Asian cropping systems. *Global Biogeochem. Cycles* 17(4), doi:10.1029/2003GB002046.
- Carmona, A., Nahuelhual, L., Echeverría, C., Báez, A., (2010). Linking farming systems to landscape change: an empirical and spatially explicit study in southern Chile. *Agr. Ecosyst. Environ.* 139, 40–50.
- Culbert, P. D., V. C. Radeloff, V. St-Louis, C. H. Flather, C. D. Rittenhouse, T. P. Albright, & A. M. Pidgeon, (2012). Modeling broad-scale patterns of avian species richness across the Midwestern United States with measures of satellite image texture, *Remote Sensing of Environment*, 118:140-150.
- Dale, V. H., Offerman, H., Pearson, S., and O’Neill, R.V. (1994), Effects of Forest Fragmentation on Neotropical Fauna, *Conservation Biology*, 8, 1027–1036.
- Dale, V. H., Brown, S., Haeuber, R., Hobbs, N. T., Huntly, N., Naiman, R. J. (2000). Ecological principles and guidelines for managing the use of land. *Ecological Applications* 10: 639-670.
- DeFries, R. S., Field, C. B., Fung, I., Justice, C. O., Los, S., (1995). Mapping the land surface for global atmosphere-biosphere models: toward continuous distributions of vegetation’s functional properties.
- Diaz, G. I., Nahuelhual, L., Echeverría, C., Marín, S. (2011). Drivers of land abandonment in Southern Chile and implications for landscape planning. *Landscape and Urban Planning* 99 (2011) 207–217.
- Eltahir, E. A. B., Bras, R. L. (1996). Precipitation recycling. *Rev. Geophys.* 34:367-78.

- Euskirchen, E. S., McGuire, A. D., Kicklighter, D. W., Zhuang, Q., Clein, J. S., Dargaville, R. J., Dye, D. G., Kimball, J. S., McDonald, K. C., Melillo, J. M., Romanovsky, V. E., Smith, N. V. (2006). Importance of recent shifts in soil thermal dynamics on growing season length, productivity and carbon sequestration in terrestrial high-latitude ecosystems. *Glob Chang Biol* 12(4):731–750. doi:10.1111/j.1365-2486.2006.01113.x.
- FAO. (2009). Seed security for food security in the light of climate change and soaring food prices: challenges and opportunities. Rome, FAO. (available at <ftp://ftp.fao.org/docrep/fao/meeting/016/k4275e.pdf>).
- Feddema, J. J., Oleson, K. W., Bonan, G. B., Mearns, L. O., Buja, L. E., Meehl, G. A., and Washington, W. M. (2005). The Importance of Land-Cover Change in Simulating Future Climates. *Science*, 310, 1674–1678.
- Field, C. B., Lobell, D. B., Peters, H. A., Chiariello, N. R. (2007). Feedbacks of terrestrial ecosystems to climate change. *Ann Rev Environ Res* 32. doi:10.1146/annurev.energy.1132.053006.141119.
- Foley, J. A., DeFries, R., Asner, G. P., Barford, C., Bonan, G., Carpenter, S. R., Chapin, F. S., Coe, M. T., Daily, G. C., Gibbs, H. K., Helkowski, J. H., Holloway, T., Howard, E. A., Kucharik, C. J., Monfreda, C., Patz, J. A., Prentice, I. C., Ramankutty, N., and Snyder, P. K. (2005). Global Consequences of Land Use, *Science*, 309, 570–574.
- Fuchs, R., (1996). Global change system for analysis, research and training (START). Proceedings of Land Use and Cover Change (LUCC) Open Science Meeting, Amersterdam, The Netherlands.
- Geist, H. J., Lambin, E. F. (2002). Proximate causes and underlying driving forces of tropical deforestation. *BioScience* 52(2): 143-50.
- GLP (2005). Science Plan and Implementation Strategy, IGBP Report No. 53/IHDP Report No. 19, IGBP Secretariat, Stockholm. 64 pp.
- Houghton, R. A., Boone, R. D., Melillo, J. M., Palm, C. A., Myers, N. (1985). Net flux of carbon dioxide from tropical forest in 1980. *Nature* 316:617–20.
- Howarth, R.W. (2004). Human acceleration of the nitrogen cycle: drivers, consequences, and steps toward solutions. *Water Science and Technology* 49: 7-13.
- IPCC. (2007) Climate change 2007: the physical science basis. Contribution of working group I to the fourth assessment report of the intergovernmental panel on climate change. In: Solomon S, Qin D, Manning M, Chen Z, Marquis M, Averyt KB, Tignor M, Miller HL (eds). Cambridge University Press, Cambridge; New York, 996 p.
- Kalnay, E., Cai, M., (2003). Impacts of urbanization and land-use change on climate, *Nature*, 423, 528-531.
- Kirschbaum, M. U. F. (2000). Forest growth and species distribution in a changing climate. *Tree Physiology* 20, 309-322.
- Kostmayer, P. H., (1989). The American landscape in the 21st century, *Congressional Record*, 135, 18 May, p. 9963.
- Lambin, E. F., Geist, H. J., Lepers, E. (2003). Dynamics of land-use and land-cover change in tropical regions. *Annu. Rev. Environ. Resour.* 28:205-41.
- Loveland, T. R., Zhu, Z., Ohlen, D. O., Brown, J. F., Reed, B. C., Yang, L. M. (1999). An analysis of the IGBP global land-cover characterization process. *Photogramm. Eng. Remote Sens.* 65(9):1021–32.

- Mishra, V., K. Cherkauer, D. Niyogi, L. Ming, B. Pijanowski, D. Ray and L. Bowling. (2010). Regional scale assessment of land use/land cover and climatic changes on surface hydrologic processes. *International Journal of Climatology* 30:2025-2044.
- Moore, N., N. Torbick, B. Lofgren, J. Wang, B. Pijanowski, J. Andresen, D. Kim, and J. Olson. (2010). Adapting MODIS-derived LAI and fractional cover into the Regional Atmospheric Modeling System (RAMS) in East Africa. *International Journal of Climatology*. 30(3):1954-1969.
- Moore, N., G. Alargawamy, B. Pijanowski, P. Thornton, B. Lofgren, J. Olson, J. Andresen, P. Yanda, and J. Qi. (2011). East African food security as influenced by future climate change and land use change at local to regional scales. *Climatic Change*. DOI: 10.1007/s10584-011-0116-7.
- Nair, P. K. R. (1993). *An introduction to agroforestry*. Dordrecht, Netherlands, Kluwer Academic Publishers.
- NRC, (2005). *Radiative Forcing of Climate Change: Expanding the Concept and Addressing Uncertainties*. National Research Council, 208 pp.
- NCR, (2007). *Earth Science and Applications from Space: National Imperatives for the Next Decade and Beyond*. National Research Council, 456 pp.
- Olson, J. M., G. Alargawamy, J. Andresen, D. Campbell, A. Davis, J. Ge, M. Huebner, B. Lofgren, D. Lusch, N. Moore, B. Pijanowski, J. Qi, P. Thornton, N. Torbick, J. Wang. (2008). Integrating diverse methods to understand climate-land interactions in East Africa. *Geoforum* 39: 898–911.
- Peng, Y., U. Lohmann, R. Leaitch, C. Banic, and M. Couture, (2002). The cloud albedocloud droplet effective radius relationship for clean and polluted clouds from RACE and FIRE.ACE. *J. Geophys. Res.*, 107 (D11).
- Pielke, Sr., R. A. (2001). *Earth System Modeling - An Integrated Assessment Tool for Environmental Studies*, in *Present and Future of Modeling Global Environmental Change: Toward Integrated Modeling*, eds. T. Matsuno and H. Kida, Tokyo: Terra Scientific, 311–337.
- Pielke, Sr., R. A. (2005). *Land Use and Climate Change*, *Science*, 310, 1625–1626. View related paper by Feddema et al. 2005: The importance of land-cover change in simulating future climates., 310, 1674–1678.
- Pijanowski, B. C., Daniel G. Brown, Bradley A. Shellito, Gaurav A. Manik. (2002a). Using neural networks and GIS to forecast land use changes: a Land Transformation Model. *Computers, Environment and Urban Systems*. 26, 553–575.
- Pijanowski, B. C., Shellito, B., Pithadia, S., Alexandridis, K. (2002b). Forecasting and assessing the impact of urban sprawl in coastal watersheds along eastern Lake Michigan. *Lakes & Reservoirs: Research and Management* 2002 7: 271–285.
- Pijanowski B. C., Pithadia S., Shellito B. A., Alexandridis, K. (2005). Calibrating a neural network based urban change model for two metropolitan areas of Upper Midwest of the United States. *International Journal of Geographical Information Science*. 19:197–215.
- Pijanowski, B. C., K. Alexandridis and D. Mueller. (2006). Modeling urbanization patterns in two diverse regions of the world. *Journal of land use science*. (1): 83-108.

- Pijanowski, B., D. K. Ray, A. D. Kendall, J. M. Duckles, and D. W. Hyndman. (2007). Using back-cast land-use change and groundwater travel time models to generate land-use legacy maps for watershed management. *Ecology 884 and Society* 12 (2):25.
- Pijanowski, B. C., Tayyebi, A., Delavar, M. R., and Yazdanpanah, M. J. (2009). Urban expansion simulation using geographic information systems and artificial neural networks. *International Journal of Environmental Research*, 3(4), 493-502.
- Pijanowski, B., L. Iverson, C. Drew, H. Bulley, J. Rhemtulla, M. Wimberly, A. Bartsch and J. Peng. (2010). Addressing the Interplay of Poverty and the Ecology of Landscapes: A Grand Challenge Topic for Landscape Ecologists? *Landscape Ecology*. doi:10.1007/s10980-009-892 9415-z.
- Pijanowski, B. C., and K. D. Robinson. (2011). Rates and patterns of land use change in the Upper Great Lakes States, USA: A framework for spatial-temporal analysis. *Landscape and Urban Planning* 102, 102-116.
- Pijanowski, B., N. Moore, D. Mauree and D. Niyogi. (2011). Evaluating error propagation in coupled land-atmosphere models. *Earth Interactions*. 15:1-15.
- Pijanowski, B. C., Tayyebi, A., Doucette J., Braun, D., Pekin B. K., Plourde J. D. (In review). Simulating urban growth at a national scale and with a fine resolution: Configuring the GIS bases Land Transformation Model to run in a High Performance Computing environment. *Journal of Environmental Modeling & Software*.
- Rabalais, N.N., R.E Turner, and W.J. Wiseman, Jr. (2002). Gulf of Mexico hypoxia, a.k.a. "the dead zone." *Annual Review of Ecology and Systematics* 33: 235-263.
- Ray, D. K., and B. C. Pijanowski, (2010). A back-cast land use change model to generate past land use maps: application and validation at the Muskegon river watershed of Michigan, USA, *journal of land use science*, 5: 1, 1-29.
- Ray, D. K., Duckles, J. M., B. C. Pijanowski. (2010). The Impact of Future Land Use Scenarios on Runoff Volumes in the Muskegon River Watershed. *Environmental Management*. DOI 10.1007/s00267-010-9533-z.
- Ray, D. K., Pijanowski, B. C., Kendall, A. D., Hyndman, D. W. (2012). Coupling land use and groundwater models to map land use legacies: Assessment of model uncertainties relevant to land use planning. *Applied Geography* 34 (2012) 356-370.
- Rittenhouse, C. D., A. M. Pidgeon, T. P. Albright, P. D. Culbert, M. K. Clayton, C. H. Flather, C. Q. Huang, J. G. Masek, & V. C. Radeloff, (2010). Avifauna response to hurricanes: Regional changes in community similarity, *Global Change Biology*, 16:905-917.
- Rittenhouse, C. D., A. M. Pidgeon, T. P. Albright, P. D. Culbert, M. K. Clayton, C. H. Flather, J. G. Masek, and V. C. Radeloff. (2012). Land Cover Change and Avian Diversity in the conterminous United States, *Conservation Biology*. DOI: 10.1111/j.1523-1739.2012.01867.x.
- Sala, O. E., Chapin, F. S., Armesto, J. J., Berlow, E., Bloomfield, J. (2000). Biodiversity - global biodiversity scenarios for the year 2100. *Science* 287:1770-74.
- Skapura, D. (1996). *Building neural networks* (New York: ACM Press).
- Soja, A. J., Tchebakova, N. M., French, N. H. F., Flannigan, M. D., Shugart, H. H., Stocks, B. J., Sukhinin, A. I., Parfenova, E. I., Chapin, F. S., Stackhouse, P. W. (2007) Climate-induced boreal forest change: predictions versus current observations. *Glob Planet Change* 56:274-296.

- Sturm, M., Racine, C., Tape, K. (2001) Climate change: increasing shrub abundance in the Arctic. *Nature* 411:546–547.
- Tang, Z., B. Engel, K. Lim, B. C. Pijanowski, and J. Harbor. (2005a). Minimizing the impact of urbanization on long-term runoff. *Journal of the Water Resources Association*. 41(6): 1347-1359.
- Tang, Z., B. A. Engel, B. C. Pijanowski, and K. J. Lim. (2005b). Forecasting Land Use Change and Its Environmental Impact at a Watershed Scale. *Journal of Environmental Management*. 76: 35-45.
- Taylor, C., Lambin, E. F., Stephenne, N., Harding, R., Essery, R. (2002). The influence of land-use change on climate in the Sahel. *J. Clim.* 15(24):3615-29.
- Tayyebi, A., Delavar, M. R., Pijanowski, B. C., Yazdanpanah, M. J. (2009a). Accuracy Assessment in Urban Expansion Model. *Spatial Data Quality, From Process to Decisions*, Edited by R. Devillers and H. Goodchild, Taylor and Francis, CRC Press, Canada, pp. 107-115.
- Tayyebi, A., Delavar, M. R., Pijanowski, B. C., Yazdanpanah, M. J. (2009b). Spatial variability of errors in Urban Expansion Model: Implications for error propagation. *Spatial Data Quality, From Process to Decisions*, Edited by R. Devillers and H. Goodchild, Taylor and Francis, CRC Press, Canada, pp. 134-135.
- Tayyebi, A., Delavar, M. R., Pijanowski, B. C., Yazdanpanah, M. J., Saedi, S. and Tayyebi, A. H. (2010). A Spatial Logistic Regression Model for Simulating Land Use Patterns, A Case Study of the Shiraz Metropolitan Area of Iran. *Advances in Earth Observation of Global Change*, Edited by Emilio Chuvieco, Jonathan Li and Xiaojun Yang. Springer press.
- Tayyebi, A., Pijanowski, B. C., Tayyebi, A. H. (2011a). An Urban Growth Boundary Model Using Neural Networks, GIS and Radial Parameterization: An Application to Tehran, Iran. *Landscape and Urban Planning*, 100, 35-44.
- Tayyebi, A., Pijanowski, B. C., Pekin, B. (2011b). Two rule-based urban growth boundary models applied to the Tehran metropolitan area, Iran. *Applied Geography*, 31(3), 908-918.
- Tayyebi, A. H., S. Homayouni, J. Shan, M. J. Yazdanpanah, B. C. Pijanowski and A. Tayyebi. (2011a). Uncertainty Framework in Land Use Change Models: An Application of Data, Model Parameter and Model Outcome Uncertainty in Land Transformation Model. 7th International Symposium on Spatial Data Quality. Coimbra, Portugal, October 12-14, 2011.
- Tayyebi, A. H., S. Homayouni, J. Shan, M. J. Yazdanpanah, B. C. Pijanowski and A. Tayyebi. (2011b). Multi-Scale Analysis Approach of Simulating Urban Growth Pattern using a Land Use Change Model. 7th International Symposium on Spatial Data Quality. Coimbra, Portugal, October 12-14, 2011.
- Tayyebi, A. H., S. Homayouni, J. Shan, M. J. Yazdanpanah, B. C. Pijanowski and A. Tayyebi. (2011c). Model Parameter Uncertainty Assessment in Land Transformation Model. 7th International Symposium on Spatial Data Quality. Coimbra, Portugal, October 12-14, 2011.
- Tayyebi, A., Pekin B. K., Pijanowski B. C., Plourde J. D., Doucette J., Braun, D. (2012). Hierarchical modeling of urban growth across the conterminous USA: A comparison of three modules of the Land Transformation Model. *Journal of Land Use Science*.

- Tayyebi, A. H., A. Tayyebi, and N. Khanna. (In review). Error propagation and uncertainty assessment in Land Use Change Models: Application of Artificial Neural Network and Spatial Logistic Regression. *Computers, Environment and Urban Systems*.
- Tayyebi, A., Pijanowski B. C. (In review). Using CART, MARS and ANNs to Model Land Use Land Cover Change: Application of Data Mining Tools to Three Diverse Areas in USA and Africa Undergoing Land Transformation. *Journal of Applied Soft Computing*.
- Tayyebi, A., Pijanowski B. C. (In review). Simulating Multiple Land Use Land Cover Change Classes using the Artificial Neural Network Model-based Land Transformation Model (LTM) and Two Data Mining Tools. *International Journal of GIS*.
- Thekkudan, T. F. (2008). Calibration of an Artificial Neural Network for Predicting Development in Montgomery County, Virginia: 1992-2001. Master Thesis, Department of Geography, Blacksburg, Virginia.
- Tilman, D. (1999). Global environmental impacts of agricultural expansion: the need for sustainable and efficient practices. *Proc. Natl. Acad. Sci. USA* 96(11): 5995-6000.
- Trimble, S. W., Crosson, P. (2000). Land use-US soil erosion rates: myth and reality. *Science* 289:248-50.
- Turner, B. L., D. Skole, S. Sanderson, G. Fischer, L. Fresco, and R. Leemans. (1995). Land-use and land-cover change science/research plan. IGBP report no. 35 and HDP report no. 7.
- Twarakavi, N. K. C., J. J. Kaluarachchi. (2006). Sustainability of ground water quality considering land use changes and public health risks. *Journal of Environmental Management* 81 (2006) 405–419.
- UN Food Agric. Organ. (2001). FAO Statistical Databases. <http://apps.fao.org>.
- Verchot, L. V., Davidson, E. A., Cattanio, J. H., Ackerman, I. L., Erickson, H. E., and Keller, M. (1999). Land Use Change and Biogeochemical Controls of Nitrogen Oxide Emissions From Soils in Eastern Amazonia. *Global Biogeochemical Cycles*, 13, 31-46.
- Walker, W. E., P. Harremoes, J. Rotmans, J. P. Van Der Sluijs, M. B. A. Van Asselt, P. Janssen, and M. P. Kraye Von Krauss. (2003). Defining uncertainty a conceptual basis for uncertainty management in model-based decision support. *Integrated assessment*, 4 (1), 5-17.
- Washington, C., B. Pijanowski, D. Campbell, J. Olson, J. Kinyamario, E. Irandu, J. Nganga, and P. Gicheru. (2010). Using a role-playing game to inform the development of land-use models for the study of a complex socio-ecological system. *Agricultural Systems*. doi: 10.1016/j.agsy.2009.10.002.
- Wayland, K. G., D. W. Hyndman, D. Boutt, B. C. Pijanowski and D. T. Long. (2002). Modelling the impact of historical land uses on surface-water quality using groundwater flow and solute-transport models. *Lakes & Reservoirs: Research and Management* 2002 7: 189-199.
- Wear, D. N., Turner, M. G. and Naiman, R. J. (1998). Institutional imprints on a developing forested landscape: implications for water quality. *Ecological Applications* 8: 619-630.

- Wear, D. N., and Bolstad, P. (1998). Land-use changes in Southern Appalachian landscapes: spatial analysis and forecast evaluation. *Ecosystems* 1: 575-594.
- Wernick, I. K. (2007). Global Warming and the Industrial System, International Relations and Security Network (ISN), Zurich, Switzerland. See <http://www.isn.ethz.ch/pubs/ph/details.cfm?lng=en&id=30366>.
- White, D., Minotti, P. G., Barczak, M. J., Sifneos, J. C., Freemark, K. E., Santelmann, M. V. (1997). Assessing risks to biodiversity from future landscape change. *Conservation Biology* 11: 349-360.
- Widory, D., W. Kloppmann, L. Chery, J. Bonnin, H. Rochdi, and J-L. Guinamant. (2004). Nitrate in groundwater: an isotopic multi-tracer approach. *Journal of Contaminant Hydrology* 72: 165-188.
- Willert, M. V., Windhorst, K., Techel, G. (2010). Modeling of forest growth and yield in Uganda, Final report, Kampala, Study Commissioned by SPGS, 2010.
- Wiley, M., D. Hyndman, B. C. Pijanowski, A. Kendall, C. Riseng, E. Rutherford, S. Cheng, M. Carlson, J. Tyler, R. Stevenson, P. Steen, P. Richards, P. Seelbach, and J. Koches. (2010). A Multi-modeling approach to evaluate impacts of global change on river ecosystems. *Hydrobiologia*. 657:243–262.
- Yang, G., Bowling, L. C., Cherkauer, K. A., Pijanowski, B. C., Niyogi, D. (2010). Hydroclimatic Response of Watersheds to Urban Intensity-An Observational and Modeling Based Analysis for the White River Basin, Indiana. *Journal of Hydrometeorology* 11(1): 122–138.
- Young, A. (1999). Is there really spare land? A critique of estimates of available cultivable land in developing countries. *Environ. Dev. Sustain.* 1:3–18.

CHAPTER 3: A SUMMARY OF LAND USE LAND COVER CHANGE MODELS

3.1 Introduction

Remarkable advancements in LUCC models have occurred over the last two decades. Models have been applied to study just about every kind of land use cover transition. These advances are made for four reasons: first, data are plentiful now for LULC at different time periods for nearly all areas of the world. Second, computers are faster and we can run complex models quickly while using numerous scenarios. Third, advances in statistical and data mining tools allow us to examine non-linear patterns in data well. Finally, many of these models have been integrated with GIS making managing data and model output possible.

Understanding human behavior is needed and this is currently at a poor level of understanding. We also need LUCC models that have adequate couplings and feedback loops and describe LULC within a system of components. This chapter summarizes LUCC models that are being used to simulate and predict LUCC. Models have been summarized with a brief description of their application. The characteristics of LUCC models have been explored in some depth what features distinguish them from other modeling techniques.

3.2 Calibration, Validation and Null Models

Scientists often do not compare the performance of LUCC models against that of a null model (Fielding and Bell, 1997; Pontius et al. 2004). It is important to compare the LUCC models to a null model to assess the additional predictive power, if any, that the model provides (Pontius et al. 2004). A null model is ‘a pattern-generating model that is based on randomization of ecological data or random sampling from a known or imagined distribution’ (Gotelli and Graves, 1996). Null models generate random values that are in the absence of a hypothesized mechanism or to deliberately exclude a mechanism being tested (Caswell, 1988; Gotelli and Graves, 1996).

Model development also needs to consider both calibration and validation. Calibration is the adjustment of input parameters to ensure the best goodness of fit between the model output and observed data. Validation, on the other hand, is demonstrating that the model is accurate within given the intended use of the model (Rykiel, 1996). There are two common ways available to separate calibration and validation run (Figure 3-1a and b) from each other (Pontius et al. 2004): 1) Time: Separation through time is the most common way has used for LUCC modeling. A subset of the entire dataset between time t_1 and t_2 is randomly selected to train the model (training run of calibration run) and then the entire information in time t_1 was used to simulate the change from t_1 to some subsequent point in time t_2 . Then, the simulated map of t_2 was compared to an actual map of t_2 (testing run of calibration run). Validation is accomplished by using the model to assess how well the model can predict a third time step (Pontius et al. 2004). The whole information in time t_2 use to predict the change from

t_2 to some subsequent point in time t_3 . The predicted map of t_3 is usually compared to an observed map of t_3 to assess the level of agreement between the two (validation run) and

2) Space: Separation through space is another common way. The model uses data from the first region to fit the parameters for the calibration run. Thus, a subset of the entire dataset from first region was randomly selected to train the model (training run of calibration run) and then the entire information from first region was used to simulate LUCC. Then, the simulated map is compared to an actual map for the first region (testing run of calibration run). The fitted model for the first region is applied to the entire information from second region to predict LUCC for validation run. Then, the simulated map is compared to an actual map for the second region. Most LUCC models use at least two time series maps for calibration (Veldkamp and Fresco, 1996).

LUCC patterns derived from historical data (Kok et al. 2001) usually do not replicate well in the future (Gibson et al. 2000) and are not transferable to other locations (Jenerette and Wu, 2001). Most also determine probability of change and rates of change (quantity of change for a land use class) using separate modules. From our perspective, there are several fundamental forms of LUCC models (Figure 3-2) (1) statistical (e.g. logistic regression) models; (2) machine learning (e.g. ANN, GA) models; (3) data mining (e.g. CART, MARS) models; (4) agent-based models; (5) process-based/life-cycle based models and (6) hybrid models. Many models are hybrids that combine viz, statistical and some form of process-based. LUCC models can be classified based on the sources of data using as input and output to calibrate the model: (1) using only raster data as input and output of the model (Pijanowski et al. 2002; Clarke et al. 1997) which is the most common case in LUCC models, (2) using combination of raster and vector data as

input and output of LUCC models (Tayyebi et al. 2011a) and (3) using only vector data as input and output of LUCC models; few such LUCC models are available (Tayyebi et al. 2011b; Moreno et al. 2009). Next section represents a brief overview of each LUCC model summarizing its structure and well known applications. Next section illustrates a brief overview of each LUCC models and urban growth boundary change models summarizing their structure and applications.

3.3 Cellular Automata Models

3.3.1 Cellular Automata Overview

The most common LUCC modeling approach that has been used so far is cellular automata (CA). Ulam and Von Neumann (1940) originally developed CA, which is a dynamic model, to simulate complex patterns (Von Neumann and Burks, 1966). CA, which can capture a wide variety of local behaviors and global patterns (Wolfram, 1984), include five basic components (Figure 3-3): (1) grid space which can be represented as a regular or irregular cells, (2) each cell has status which can change by the attributes of collection of cells in its neighbors, (3) transition rules that are used to classify the data, (4) a neighborhood that defines the extent of influence of the cells that are surrounding the central cell, (5) time step. The objective of CA calibration is to find the best combination of transition rules to model LUCC (Batty and Xie, 1994a and 1994b; Batty et al. 1999; Landis and Zhang, 1998). CA can deliberately articulate global patterns through local processes (Batty and Xie, 1994a and 1994b). CA has been used for simulating various spatial and temporal phenomena including LUCC (Almeida et al. 2003; Ménard and Marceau, 2007), urban change simulation (Batty et al. 1999; Dietzel

and Clarke, 2006; White et al. 2000), fire propagation (Yassemi et al. 2008) and species competition (Matsinos and Troumbis, 2002).

It is difficult to define the best combinations of transitions rules when there are many variables because LUCC patterns are complex (Batty and Xie, 1994a; White and Engelen, 1993; Li and Yeh 2000; Wu and Webster, 2000). The variations are due to the many possible ways of defining the transition rules. There are two common ways to perform CA calibration. Using statistical methods (e.g. LR), machine learning algorithms (e.g. ANN, SVM) or data mining approaches (e.g. CART, MARS), is the first way (which is known as hybrid model) to calibrate CA models (Wu, 2002). The second way, which is known as trial and error approaches, does not require using statistical methods; the simulation results from different combinations of parameters are compared (Clarke et al. 1997). White et al. (1997) propose an intuitive method using a trial and error approach to obtain a parameter matrix for urban simulation; however, this approach is very time consuming.

3.3.2 Slope, Land Use, Exclusion, Urban, Transportation, and Hill Shading (SLEUTH)

SLEUTH uses spatial and temporal data in two times or more to simulate urban gain in the future or urban loss in the past (Clarke et al. 1997; Clarke and Gaydos, 1998; Candau, 2002; Silva and Clarke, 2002; Yang and Lo, 2003; Jantz et al. 2003). SLEUTH, which is a dynamic model, was one of the first generation of LUCC models that use CA to simulate urbanization and was first applied to the San Francisco Bay area (Clarke et al. 1997). The original version of SLEUTH has been modified for a variety of applications. The lessons learned from applying SLEUTH to the entire world were recently discussed.

SLEUTH has been applied to major cities in US including Detroit, Chicago, New York, Washington, San Francisco and Albuquerque, and other countries such as Netherlands, Portugal and Australia.

SLEUTH uses four types of growth (Figure 3-4) to control urbanization patterns which include (Clarke et al. 1997) spontaneous, spreading center, edge and road-influenced growth. Four parameters associated with growth can take values ranging from 1 to 100 and are defined to characterize LUCC patterns. Spontaneous growth urbanizes the cells randomly and is used to determine dispersion coefficient. Based on spreading center growth, new urban cells occur around the cells that have urbanized through spontaneous growth. The breed coefficient is calculated based on spreading center growth. Edge growth uses neighborhood characteristic like CA to calculate the spread coefficient by taking into account the number of urban cells around the central cell. SLEUTH is quite flexible and the user can define the area of influence. Thus, it is expected that this rule urbanizes the cells in the vicinity of existing urban cells. Transportation systems (e.g. roads) influence urbanization by generating new spreading centers in the neighborhood of roads. Lastly, a road gravity coefficient defines the distance from roads is determined by road growth. SLEUTH enables the user to specify two exclusionary layers: (1) user can define the areas that are excluded from urbanization and (2) slope suitability constrains the urbanization according to the percentage slope at locations.

SLEUTH calibration receives the initial values for parameters from the user directly, and the model uses Monte Carlo as an iterative approach to check the combination of parameter sets. Monte Carlo finds the parameters across three iterative

steps (e.g. coarse, medium, and fine) to minimize the difference between the simulated and reference map. Several studies have been focused on SLEUTH calibration (Candau, 2002; Silva and Clarke, 2002; Jantz et al. 2003). Parameters and a suitability map are the output of the SLEUTH calibration run (Clarke and Gaydos, 1998). SLEUTH also uses a self-modification function for realistic simulation (Clarke et al. 1997), which changes the values of the coefficients as the model iterates. When the development rate exceeds/falls below a specified threshold, the coefficients are multiplied by a factor greater/less than one, simulating a development ‘boom’/‘bust’ cycle. Without self-modification, SLEUTH simulates a linear growth rate, producing the same number of new urban cells.

3.3.3 Geo-Simulation

Geo-simulation (Figure 3-5) is able to show urban systems in a more realistic manner than conventional approach (Holland, 1998). Geo-simulation operates with human, entities and spatial components to specify the spatial relationships (Fotheringham and O’Kelly, 1989). Geo-simulation uses spatial units, which can be partitioned in different ways and are modifiable, to represent urban systems (Openshaw, 1983). Geo-simulation defines the interactions by considering spatial objects’ behavior. The interactions of spatial units at higher levels are the results of behavior of urban objects at lower-level (bottom-up systems).

Temporal behavior of objects can occur as either synchronous (all objects change at the same time), or asynchronous (objects change in turn; Nagel et al. 1999). The possibility of asynchronous behavior is more than synchronous behavior. The sequence of objects’ changes can be completely random or logical. Geo-simulation has been

designed to control all kind of events. Realistic description of objects' behaviors makes this model unique. Geo-simulation uses CA model to define transition of objects' behavior. The characteristics of objects can change based on the rules that control their reaction to CA inputs. CA is potential to provide an efficient tool for representing the properties of objects: attributes, behaviors, relationships, environments, and time.

3.3.4 Vector Based CA (VEC-GCA)

CA outputs vary according to the cell size and the neighborhood. Jenerette and Wu (2001) found that CA is sensitive to detect LUCC patterns across spatial resolutions. Jantz and Goetz (2005) compared the SLEUTH model outputs across cell sizes. The results indicate that SLEUTH is sensitive to cell size for detecting LUCC patterns. Moving from raster to vector space was considered as a solution to overcome CA limitation in raster space. Using grid with irregular shape (e.g. Voronoi diagrams) rather than the regular grid (e.g. square or rectangular diagrams) was the initial work to minimize the scale sensitivity (Shi and Pang, 2000). Voronoi diagrams decompose the space to Voronoi polygons to chraterize the neighborhood of spatial object. Similar to the raster environment, the state of each spatial object change based on the neighbors attributes. Delaunay triangle is another common way of using irregular grid in CA (Semboloni, 2000). The neighborhood of each triangle is defined by its adjacent triangles. These approaches are limited in three ways: (1) the automatic polygon generation is quick in vector space (Tayyebi et al. 2012) but may not match to the real world objects, (2) the neighborhood definition is limited since it just depends on topology (White and

Engelen, 2000) and (3) irregular change in the shape and size of the objects is not permitted.

A new vector-based CA (Vec-GCA) model developed by Moreno and her students (Moreno et al. 2009; Moreno and Marceau, 2006; Moreno et al. 2008), allows showing real objects with irregular shape and changing the shape and size of the objects across time using variety of functions (Figure 3-6). This new topology is free of defining influence zone around each object; it uses the entire region to assess which objects influence others to generate a change of shape. Using vector data solves the problem of cell size dependency of CA model by using a dynamic neighborhood. Two objects are neighbors if their states are interested to change the state of each other. Binary matrix uses to describe the transitions, where the number of rows is the number of states of an object and the number of columns is the number of transitions in the model. In the matrix, the entry takes 0/1 when state is not/is favorable to transition. This model is not limited to the number of objects between two objects. The computation of Vec-GCA model is intensive due to variety of operations when an object changes shape. However, Vec-GCA eliminates the extensive computation time for sensitivity analysis of scale. Vec-GCA makes more realistic results than raster CA model (Marceau and Moreno, 2008; Moreno and Marceau, 2007).

3.4 Weighted-Map Models

3.4.1 Multi Criteria Evaluation (MCE)

Multi-criteria evaluation (MCE; Wu, 1998) selects spatial drivers and integrates them, Boolean overlay or weighted linear combination, to get at an appropriate evaluation

based on the given function (Eastman, 1997; Figure 3-7). MCE is able to reduce driver using PCA and then standardize the continuous driver to a proper numeric range. The weighted linear combination (WLC) generates suitability value for each grid cell by weighting and combining each driver maps. The suitability for LUCC was evaluated using series of independent parameters that influence LUCC. MCE can consider drivers such as proximity, accessibility and environmental protection. Eastman and Jiang (1996) suggested using ordered weighted average (OWA), which employ a wider range of decision. In contrast to WLC, OWA has two steps for weighting of drivers.

3.4.2 Geomod

Geomod is a raster-based LUCC model (Figure 3-8), which simulates the spatial pattern of LUCC backward and forwards in time (Pontius et al. 2001). IDRISI's Geomod has been used to predict LUCC at the continental scale (Africa, Asia and Latin America), at the country scale (Costa Rica and India), and at the local scale (India, Egypt, United States and several countries in Latin America). Pontius et al. (2001) gave the comprehensive description of Geomod that has been used to analyze the impact of deforestation (e.g. carbon offset) on climate change. The software needs to have a LULC map in initial time and number of changed cells between initial and subsequent time. The input files at the beginning time are the necessary files for running Geomod. This model determines the location of cells using four decision rules as one of the binary categories for the next time. If the number of change/non-change cells between initial and subsequent time steps increases, Geomod searches among non-change/change cells to select them as those most likely to be converted to change/non-change category in

subsequent time. A reference map of the region in subsequent time can be used to compare with Geomod simulation as a validation run. Geomod enables the user to define an exclusionary zone which shows areas that are excluded from analysis as well. Geomod can create its own suitability map using an IDRISI module such as MCE (Eastman et al. 1997) which combines a variety of spatial or temporal drivers or to use a suitability map that has already been created from other LUCC models (e.g. LTM, CLUE, SLEUTH) for LUCC simulation. Geomod develops the suitability map using a combination of drivers and the LULC map in the initial time that the user gives it. Each driver map must show a categorical variable (e.g. bin) before running the model; this is different from most of the other LUCC models that can use both categorical and continuous variables. The categories within variables are called bins. Geomod's suitability map has relatively high/low values at locations with attributes similar to the developed/non-developed area of the initial time.

Geomod use four decision rules to locate the changes in LULC maps (Figure 3-8). The first decision rule is mandatory; while other three decision rules can be either included or excluded based on the user experience. The first decision rule concerns persistence in the study area. Geomod simulates binary change, either from non-change to change or from change to non-change. The second decision rule allows simulating LUCC using any type of smaller regions nested in a larger region (e.g. political boundary; Tayyebi et al. 2012). For each smaller region, the user is responsible for giving the quantity of each category at the subsequent time. The new changes occur pseudo-randomly. The third decision rule is based on nearest neighbor principle like CA, whereby Geomod allows LUCC occur around the edge between change and non-change.

This rule simulates LUCC where the new change can grow out of previous change, and then the search is only limited to those cells within a small square window around any change cells. The user is responsible to define the width of the window which is called the neighborhood search. The fourth decision rule uses a suitability map, which shows the suitability for LUCC for each cell. Geomod simulates additional change by searching the region for the location of the non-changed cells that have the highest suitability. Geomod is not dynamic in the sense that the suitability map does not change over time. However, Geomod is dynamic in the sense that Geomod re-computes for each year the cells as candidates for change by re-computing which cells are on the edge between changed and non-changed using neighborhood constraint rule.

3.5 Regression Based Models

3.5.1 Logistic Regression Overview

The inputs of Logistic Regression (LR) are suitability values of predictor variables at time t_1 while the output is binary change between t_1 and t_2 . If the output of LR equals 1/0, it indicates change/non-change. The LR function is bounded between 0 and 1, of the form given by He and Lo (2007). LR output gives the LUCC likelihood for each cell as a function of the spatial predictor variables. Intercept and the coefficients need to be estimated as a fixed parameter and for each spatial predictor, respectively. The LR has a non-linear form but can be transformed into a linear form with the simple transformation (Tayyebi et al. 2010; Schneider and Pontius, 2001). Then, the coefficients of spatial predictor variables are estimated using the transformed function. Instead of fitting a LR with the suitability of LUCC in each cell as the outcome, the logarithm of the

odds is considered as the outcome. If a particular regression coefficient is zero, then the corresponding explanatory variable is not associated with the occurrence of the response.

3.5.2 Conversion of Land Use and its Effects (CLUE)

The Conversion of Land Use and its Effects modeling framework (CLUE) (Veldkamp and Fresco, 1996; Verburg et al. 1999) was originally developed to simulate LUCC and determine suitability of each cell with the dynamic simulation of competition between LULC classes. The second version of the model has been developed for regional application and has been called CLUE-S (Conversion of Land Use and its Effects at Small regional extent; Verburg et al. 2002; Verburg and Veldkamp, 2004). CLUE has been applied at the national scale for Ecuador, China and Java, Indonesia. The CLUE model includes two distinct modules, called a quantity module and an allocation module (Figure 3-9). The quantity module calculates the number of transitions for each LULC class; while the allocation module locates the given quantity of LUCC at different locations. The quantity module in CLUE is able to run different models ranging from simple to complex models. The results from the quantity module are a direct input for the allocation module.

CLUE model incorporates four major components: (1) Policy option highlights areas in the map where LULC changes are restricted or can imply stimulation arrangements for a certain land use on a location. CLUE uses a LULC conversion matrix to show the transitions that are prohibited by a certain policy, (2) Conversion settings and LULC transition sequences are two sets of parameters to characterize the LULC categories. The conversion settings related to the reversibility of LUCC ranging from 0

(easy conversion) to 1 (irreversible change). LULC transition sequences show conversion settings and temporal characteristics which can be defined using a conversion matrix, (3) LULC requirements control the simulation by defining the required change in LULC (LUCC quantity). The extrapolation of patterns in the historical LULC data into the near future is a common technique to calculate LULC requirements and (4) LULC conversions are expected to take place at locations with the highest suitability (LUCC location). A statistical approach (e.g. logistic regression) is usually used to quantify the relations between LUCC locations and a set of independent drivers. To run the model, it is minimally needed to have spatial data for at least one time; however, to allow model calibration and validation, it is necessary to have data of another time.

3.6 Agent Based Models (ABMs)

Different studies have shown that Agent-based models (ABMs) are useful for exploring LUCC processes (Parker et al. 2003; Verburg, 2006). ABMs have been used more particularly for simulating local scale LUCC due to the complex nature of LUCC (Acosta-Michlik and Espaldon, 2008) while their applications have been restricted more in planning and policy-making. ABMs computations are extensive; so these models usually incorporate empirical models for parameterization (Valbuena et al. 2008) or couple with other LUCC models affectively to make the simulation run faster (e.g. CA and Markov models; Parker et al. 2008).

ABMs simulate LUCC as a result of interaction among individual agents (e.g. decisions about policy, planning and management; Parker et al. 2003 and 2008). In a LUCC model (Figure 3-10), an agent can be a farmer of a village in a small extent or a

president of a country in a bigger scale. Agents are decision-making units in ABMs and they are acting autonomously in the environment. Agents need to share spatial space to interact with each other and respond to the environment. Rules are the outcome of the interaction between agents, and determine future behavior of actions. Agents' behavior can change from simple rules to complex decisions. Agents usually have unique characteristics (e.g. DNA in human body or finger print) that let them to be identified from other other (Figure 3-10). Agents change their behaviors to satisfy their desired goal by comparing the outcome of their behavior relative to its goals.

3.7 Machine Learning

Machine learning (ML) is a core of artificial intelligence. ML studies computer algorithms for learning to complete a task. The emphasis of ML is to devise learning algorithms that do the learning automatically without human assistance. ML researchers are familiar with most of statistical models.

3.7.1 Artificial Neural Networks (ANNs)

Many scholars have found that artificial neural networks (ANNs) can solve classification problems accurately. Land Transformation Model (LTM) uses the combination of spatial drivers (Pijanowski et al. 2002) that have an influence on LUCC. The parameters of LTM are determined by a training procedure of ANNs. ANNs consist of neurons (e.g. structure of human brains) within layers which simulate LUCC. The layers and neurons allow ANNs to learn like the human brain, especially non-linear patterns. LTM uses back-propagation learning algorithms and follows four sequential steps (Pijanowski et al. 2009; Figure 3-11): (1) creating spatial predictor variables, (2)

applying spatial (e.g. distance) and non-spatial (e.g. density) functions in GIS, (3) using ANNs to train LTM and (4) using population density to calculate the quantity of LUCC for future. LTM is designed to use the difference of mean square error (MSE) between two consecutive cycles (with 100 intervals) as the stopping criteria (Pijanowski et al. 2009). The resulting weights and biases of the ANN are then applied to the rest of input data that have not been used in training run to calculate the output values (continuous value between 0 and 1) for the testing run. Then, cells are ranked in the suitability map by sorting them according to their suitability values. Cells with high ranks are then selected and undergo changes to create the simulated map. The simulated map can then be compared to a reference map to calculate the accuracy of the model (Pijanowski et al. 2005 and 2006).

3.7.2 Support Vector Machines (SVMs)

Like ANN, Support Vector Machine (SVM) can be used as a machine learning algorithm to detect non-linear patterns in data. SVM projects data to a higher dimensional (which is called Hilbert space; Figure 3-12) to construct an optimal classifying hyperplane. In Hilbert space, SVMs can classify LUCC patterns linearly through using structural risk minimization and margin maximization (Vapnik, 1998). The function of the optimal separating hyperplane is developed using the kernel function and the support vectors. In contrast to ANN, SVMs provide a unique and global optimal hyperplane. SVM has been used in many applications, such as credit scoring (Baesens et al. 2003), financial time series prediction (Gestel et al. 2001), spam categorization (Drucker et al. 1999) and brain tumor classification (Lu et al. 1999).

3.7.3 Genetic Algorithms (GAs)

Genetic algorithms (GAs), originated from natural selection theory in biology, perform a search within the space to find the optimal solution (Holland, 1975; Goldberg, 1989). GA can estimate global minimum or maximum using the given fitness functions (Figure 3-13). GA calibration approach consists of the following steps (Shan et al. 2008): firstly, GA randomly generates the initial population of solutions and encoded to binary strings (encoding and initial population). Each string in encoded binary style corresponds to a solution; secondly, the GA then run for each string in the population until a year with reference LUCC map. A reference map is used to rank the initial solutions based on a fitness function (rank selection and elitism). This step is responsible to select the strings for the next generation. For rank selection, all strings are ordered based on their fitness function in ascending order (from minimum to maximum) and finally, the last step is (crossover and mutation) producing the next generation of solutions. Crossover operation produces next generation in each run that are expected to have same or better quality than their parents. Mutation prevents the solution from becoming lock on local minima. The training run of GA continues for a number of generations and the generation with the minimum fitness functions chooses as the final solution.

3.8 Data Mining

Data mining (DM) refers to the patterns or rules extraction from a large data. Data mining process involves identifying the problem, retrieving the needed data, and analyzing the data for making decisions (Berry and Linoff, 2004; Mitra et al. 2002). To avoid under-fitting, DM models run forward to add more complexity to the model by

adding nodes in CART or basis functions in MARS; however, in order to over-fitting, DM models run backward (e.g. pruning mechanism) to reduce model complexity by removing extra nodes in CART or basis functions in MARS (Tayyebi and Pijanowski, in review).

3.8.1 Classification and Regression Tree (CART)

Classification and Regression Tree (CART) is one of the common DM models that classify the data hierarchically (Figure 3-14). CART produces a model with a structure using a series of if-then-else rules (Breiman et al. 1984). CART is responsible for identifying the splits at each node to best divide the data (Tayyebi and Pijanowski, in review). The nodes in the tree are representative of each variable in CART. The location of the nodes at the hierarchical level shows the contribution of each variable. The nodes at the top/bottom have higher/lower contribution for modeling. Gini index uses an impurity function to find the best split (Breiman et al. 1984) between all unique values among predictors to fragment data. Gini makes more homogeneous subsets than the before node by choosing the better split to minimize the reduction in impurity.

3.8.2 Multiple Adaptive Regression Splines (MARS)

Multivariate adaptive regression splines (MARS), which is a regression model, could overcome some of the CART limitations. MARS generalizes the recursive partitioning approach with more flexibility and captures interactions (Friedman, 1991). MARS uses basis functions to find the relationship between the inputs and outputs (Figure 3-15). MARS splits the data into sub-regions using different knots, where the coefficients can change (Tayyebi and Pijanowski, in review), and fits the data in each

sub-region using a set of basis functions automatically (Friedman, 1991). Basis functions take two forms, one for the values on the left of the knot and one for the values on the right of knot.

3.9 Hybrid Models of CA

Many models are hybrids that combine viz, statistical and some form of process-based. The original CA has been significantly modified. CA calibrations run suppose to obtain a set of CA parameters. Extensive search is necessary within the space by comparing possible combinations of parameters. Using more variables with wider ranges in transition rules make the CA modeling more sophisticated. Computer search algorithms such as machine learning (e.g. ANN, SVM or GA) and data mining approaches (e.g. CART and MARS) can be coupled with CA to make the calibration run faster.

3.9.1 CA-MCE

CA transition rules have been defined using MCE method (MCE; Wu and Webster, 1998). ANN has been integrated into CA for deriving parameter (Li and Yeh, 2002); however, it is difficult to comprehend the meanings of these parameter because of the black-box nature of ANN. Interpreting the meanings of MCE weights is easy; a larger/smaller weight shows that the corresponding driver has a more/less contribution to the LUCC. Understanding these parameter values can provide useful information for urban planning since they can control urban struture.

3.9.2 CA-SVM

Transition rules define linear boundaries in CA to distinguish LULC classes; however, LUCC patterns are not usually linear and they are highly complex (Yang et al. 2008). Thus, it is essential to use a model which can find the non-linear boundaries for the transition rules (Yang et al. 2008). ANN used as a non-linear machine learning algorithm (Li and Yeh, 2002) to parametrize CA; however, the ANN training run may result in local rather than global optimization (Vapnik, 1998). To address this problem, Yang et al. (2008) used SVM to define transition rules in CA and improve the ability of CA in dealing with non-linear complexity. The decision function of the optimal hyperplane is used to form the transition rule for CA (Martens et al. 2007). The transition rule is detected by combining the output from SVM and other constraint information (Figure 3-16). The simulation of LUCC is iteratively running until certain conditions are satisfied (e.g. the quantity of LUCC simulated equals the amount of reference LUCC). The outcome of transition rule is LUCC probability map which is estimated based on the decision function (Ana et al. 2004).

3.9.3 CA-GA

GA has been coupled with CA to improve the time complexity in calibration run (Goldstein, 2003). GA has been suggested (Shan et al. 2008) to enhance the time efficiency of CA for LUCC simulation. It has been shown that coupling CA with GA can produce similar results to CA in a time effective manner and optimal rule values can be reached within the early generations of GA (Shan et al. 2008). The best CA parameters can be found using the goal function to produce the minimum error. A CA model has

been designed using multi-temporal satellite imagery and population density (Alkheder and Shan, 2006). GA was used to optimize the search algorithm for best transition rule. CA model is run for each string in the population. The reference map is used to rank the initial solutions based on the fitness function. The rank selection and elitism operations are first used to select the strings for the next generation. For rank selection, all strings are ordered based on their fitness function in ascending order.

3.9.4 CA-ANN

With emerging multiple LULC class simulation, CA model structure has become more sophisticated (Batty et al. 1999). Multiple LUCC simulation needs to deal with numerous complex spatial variables that may correlate with each other. Conventional CA has difficulties in handling complex variables and determining parameter values. A new method was developed (Li and Yeh, 2002) to simulate multiple LULC classes based on the integration of ANN and CA. This model uses ANN with multiple outputs to calculate the conversion suitabilities for multiple LULC classes. The neurons in input layer correspond to the input variables while the output layer consists of neurons corresponding to number of output LUCC classes. A stochastic disturbance is incorporated in ANN-CA to generate more realistic results (White and Engelen, 1993). The disturbance produces simulation results with fractal properties that are found in historical LUCC patterns. Each neuron in the output layer generates conversion suitability from the existing type to another type of LULC class. CA simulation involves more cycles to decide whether a cell is converted or not. User-defined threshold can be used to control the rate of conversion.

If the highest conversion suitability is less than the threshold value, the cell remains unchanged.

3.10 Urban Growth Boundary Models (UGBMs)

Globally, urban and sub-urban regions have experienced scattered development near cities. Such development patterns heavily burden local governments with high financial costs. Urban growth boundary models (UGBM) are a class of land change models that simulate urban boundary locations and configurations so development proceeds only within these designated zones (Tayyebi et al. 2011a and b). Several cities in the United States use urban growth boundaries (UGB), such as Portland and Oregon.

3.10.1 ANN UGBM

An UGBM which utilizes ANN and GIS is developed here to simulate the complex geometry (Figure 3-17) of the urban boundary (Tayyebi et al. 2011a). UGBM examines the relationship between predictor variables as inputs and the radial extent of the boundary at specified azimuths as outputs to simulate UGB. Percent area match (PAM) is used to evaluate the accuracy of the model for UGB simulation. The input drivers are in raster format while the output drivers are in vector format.

3.11 Rule Based UGBMs

Two rule-based spatial-temporal models, one which employs a distance dependent method (DDM) and the other a distance independent method (DIM), were used to simulate UGBs (Tayyebi et al. 2011b). Both models use azimuths and distances, vector-based predictive variables, directed from central points within the urban area, to simulate UGB change.

3.11.1 Distance Dependent Model (DDM)

The DDM approach uses the points on the urban boundary in initial time and a suitable prediction method to anticipate the urban boundary in any subsequent time (Tayyebi et al. 2011b; Figure 3-18). The suitable prediction method projects a new urban boundary by increasing distances by percentage increments across different azimuths. Central points in the city are defined visually based on different constraints and the distances from the central point to points on the urban boundary are computed for the different azimuths. Percent Area Match (PAM) quantity is used as a stop condition to simulate urban boundary change because the quantity of simulated area by UGBMs provides a better match for the quantity of area that is derived from the urban boundary in subsequent time periods, producing a better UGBM. There are different PAM quantities and locations for DDM which equal to the number of simulations that are repeated until a stop condition is satisfied.

3.11.2 Distance Independent Model (DIM)

DIM uses the change in distance between two boundaries, one in the initial time step and one in subsequent time step, across different azimuths, to predict the future urban boundary (Tayyebi et al. 2011b). DIM simulates the urban boundaries using data from two time periods and measure distances from central points to urban boundaries (Figure 3-19). DIM uses central points to indicate an azimuth for measuring the rate of change in distance between the two urban boundaries using a rate of change in distances over time (RCDT). The central points used to compute the distances and azimuths are the same across the two time periods. The RCDT is measured across different azimuths,

which is repeated for all points along the urban boundary so that each point on urban boundary has its own RCDT. RCDTs for all points on the urban boundary map are averaged giving an Average RCDT (ARCDT). A new urban boundary can be created using predicted distances from the urban boundary to central points calculated with ARCDTs from the region. There is one PAM quantity and location for DIM.

3.12 Conclusion

The current LUCC modeling research moves toward the use of hybrid models, researchers should compare the integration of LUCC models for LUCC simulations. It is necessary to have more studies to compare LUCC models with each other where they may help researchers to select the best method for solving classification problems. Each of the available models shows unique characteristics, which may be interesting in the context of LUCC. For example, CART is a simple model for interpretation while ANNs can help to structure the understanding of prediction. ANNs can provide a framework to inform the optimal design for urban planner and decision maker (Li and Yeh, 2002; Tayyebi et al. 2011a).

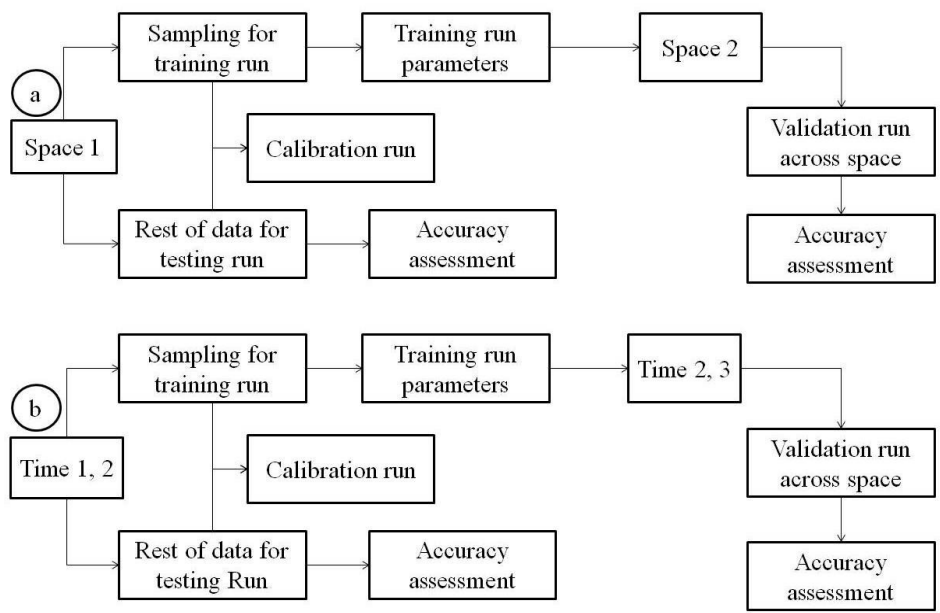


Figure 3-1: Calibration and validation across time and space

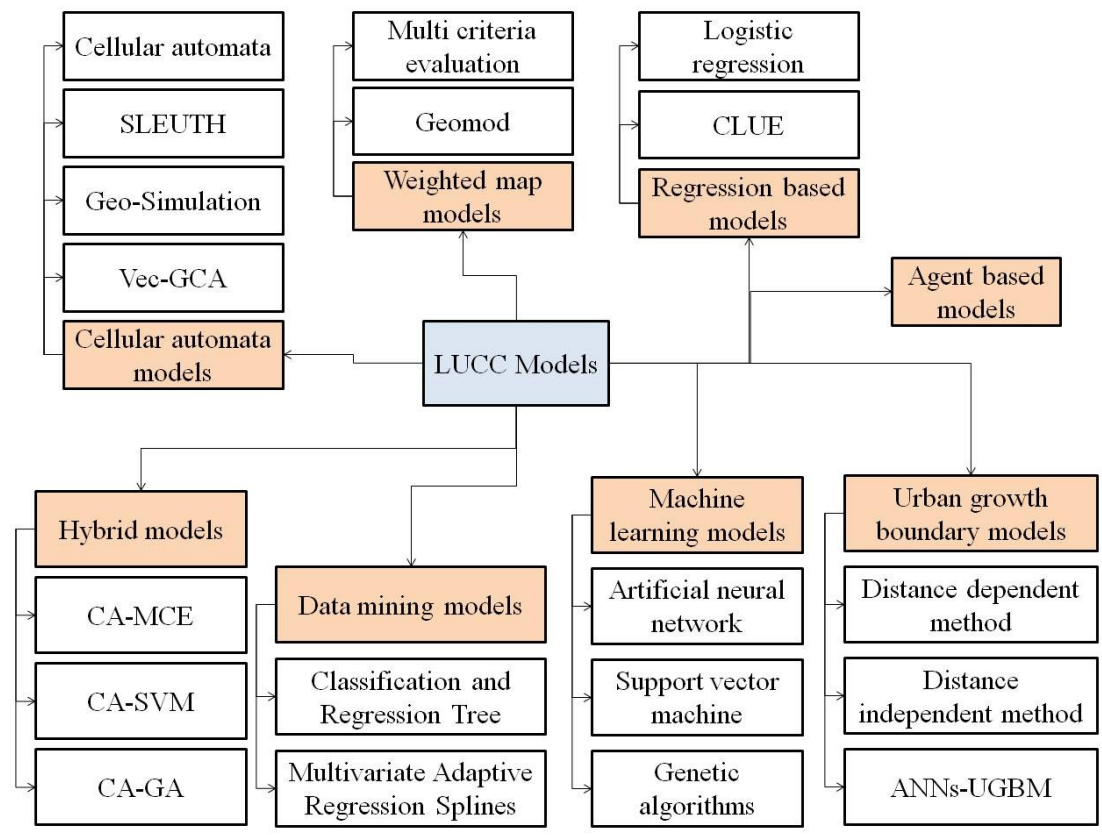


Figure 3-2: Classification of LUCC models

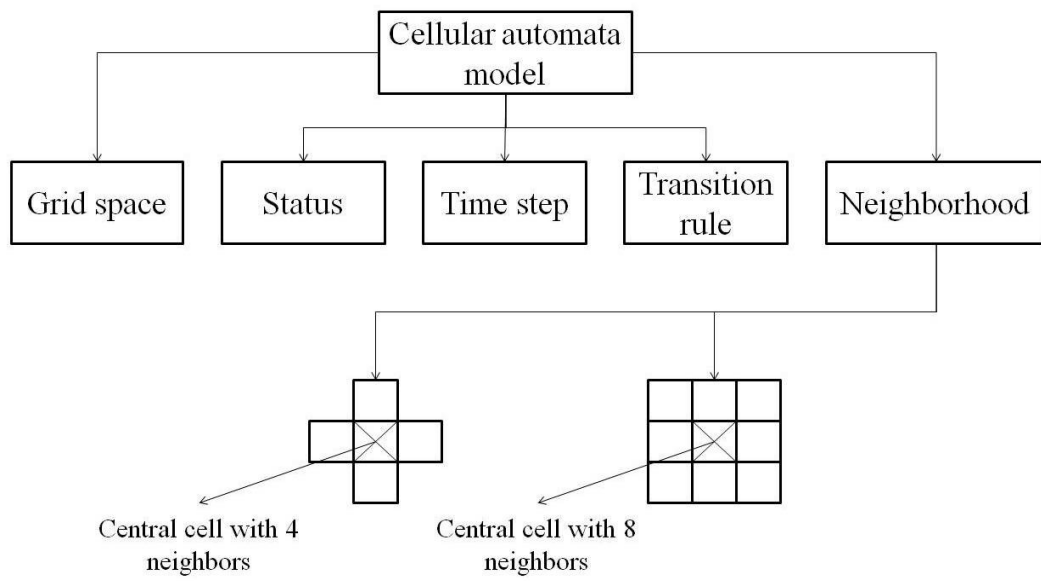


Figure 3-3: Cellular automata models

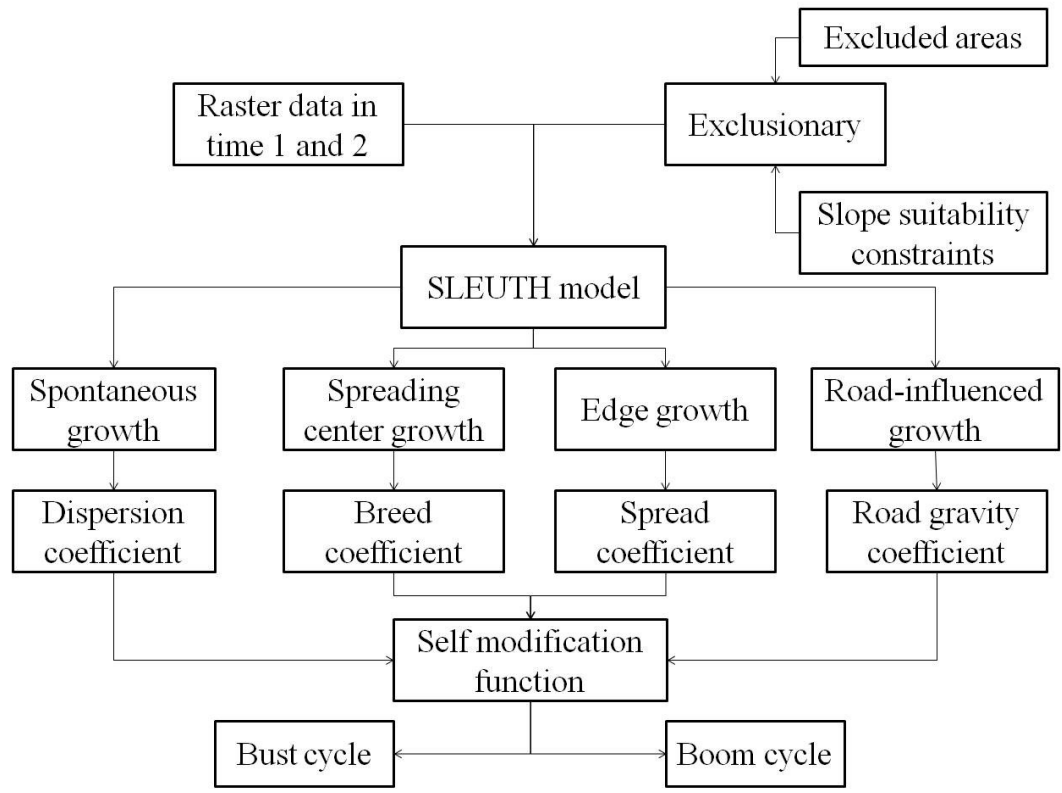


Figure 3-4: Structure of SLEUTH model

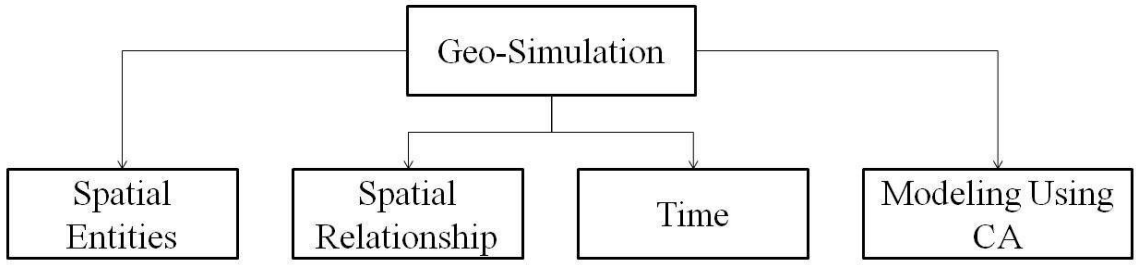


Figure 3-5: Components of Geo-Simulation model

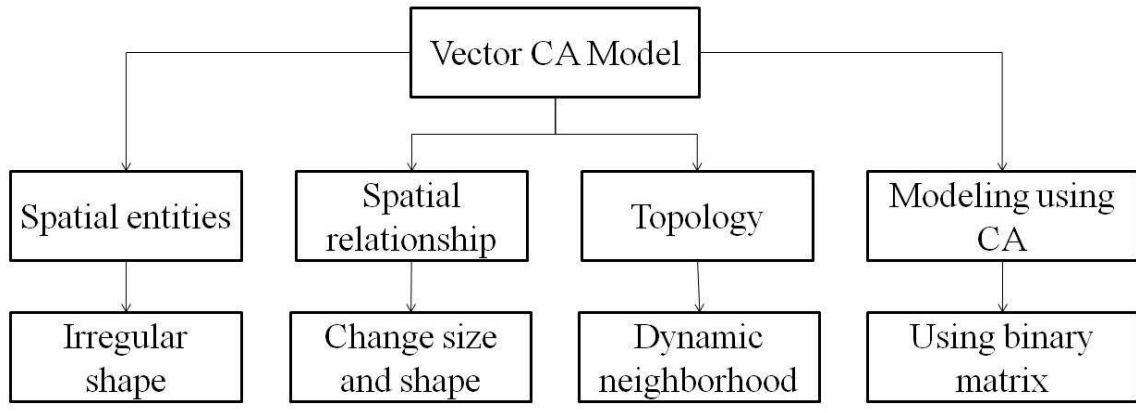


Figure 3-6: Structure of Vector CA model

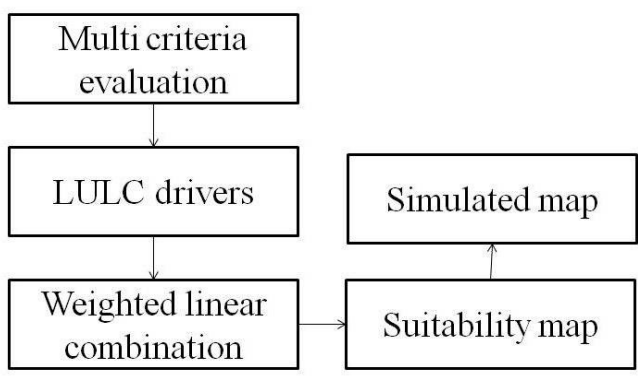


Figure 3-7: The process of MCE

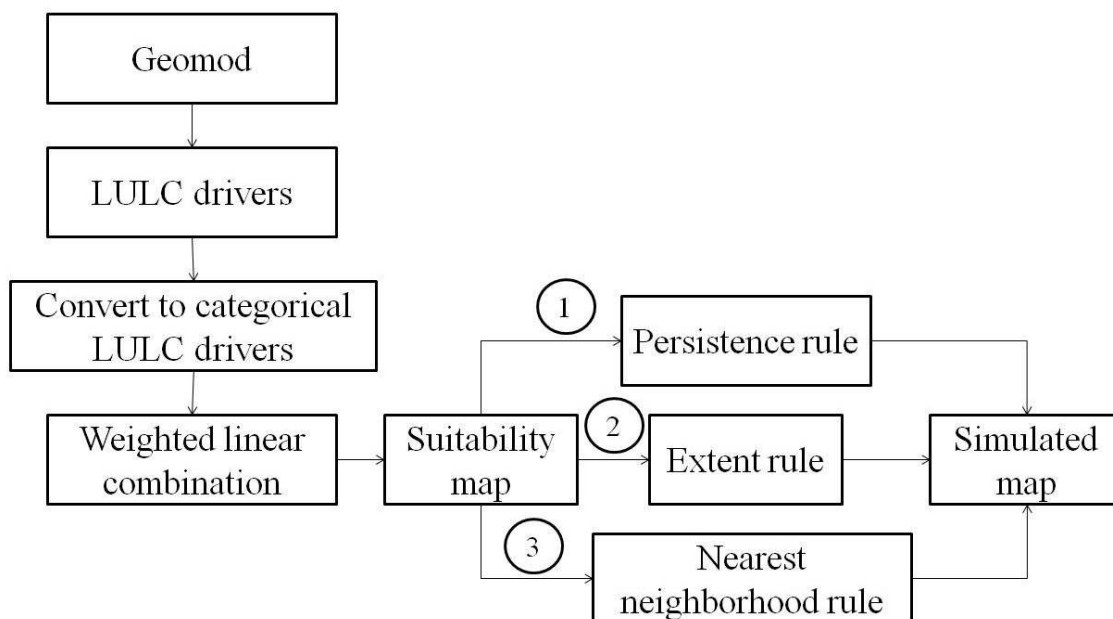


Figure 3-8: Structure of the Geomod model

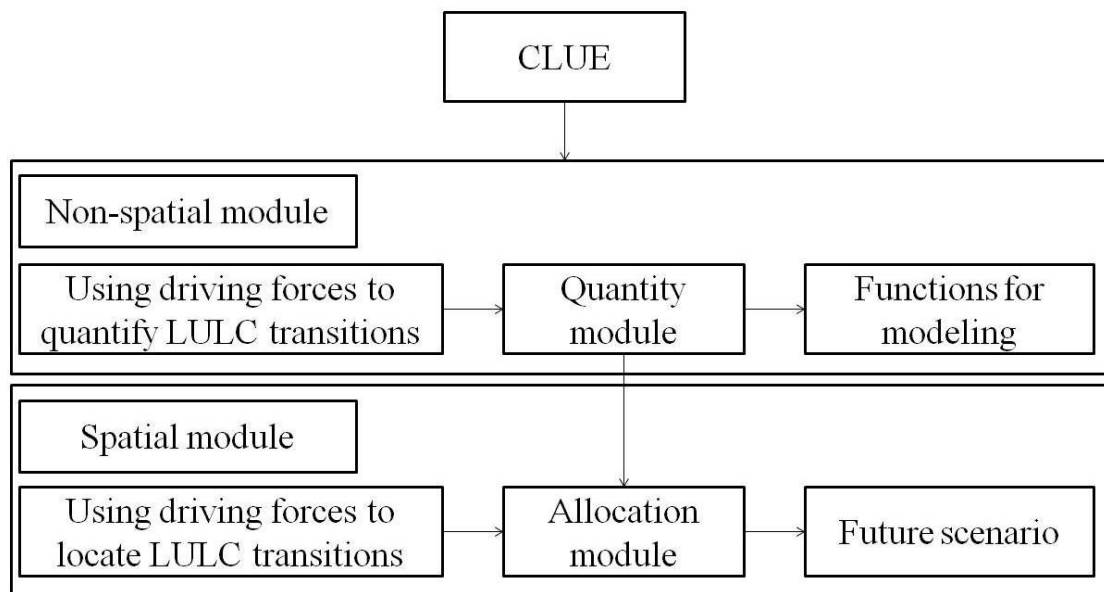


Figure 3-9: Conceptual view of CLUE model adopted from Veldkamp and Fresco, (1996)

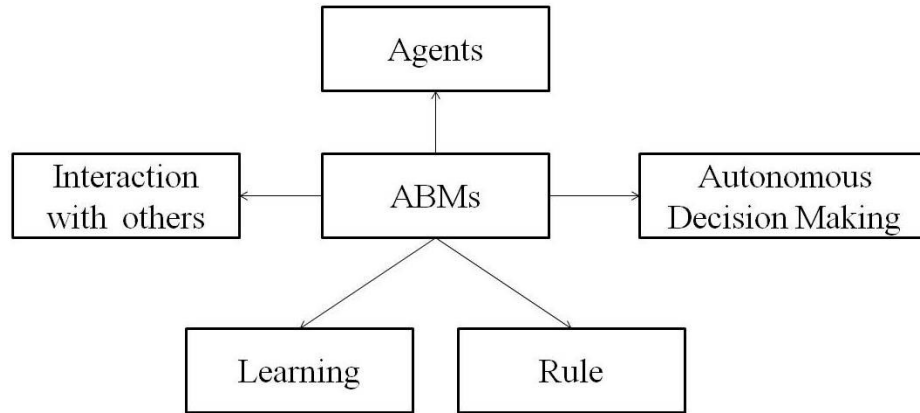


Figure 3-10: Structure of agent based models

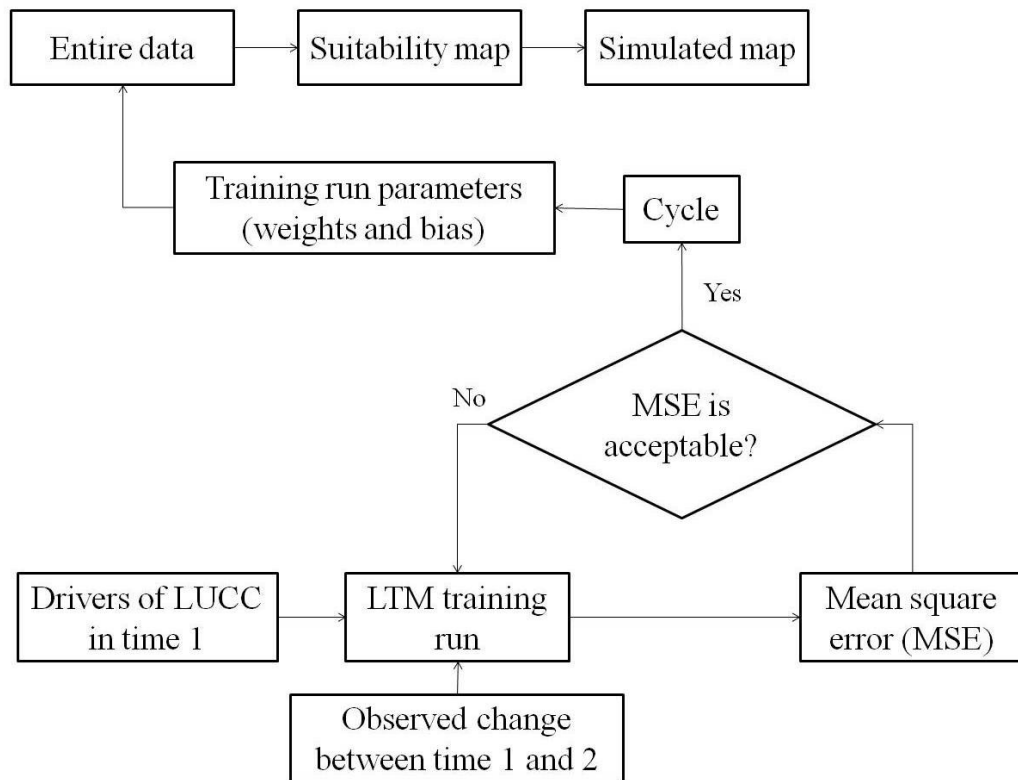


Figure 3-11: Structure of land transformation model

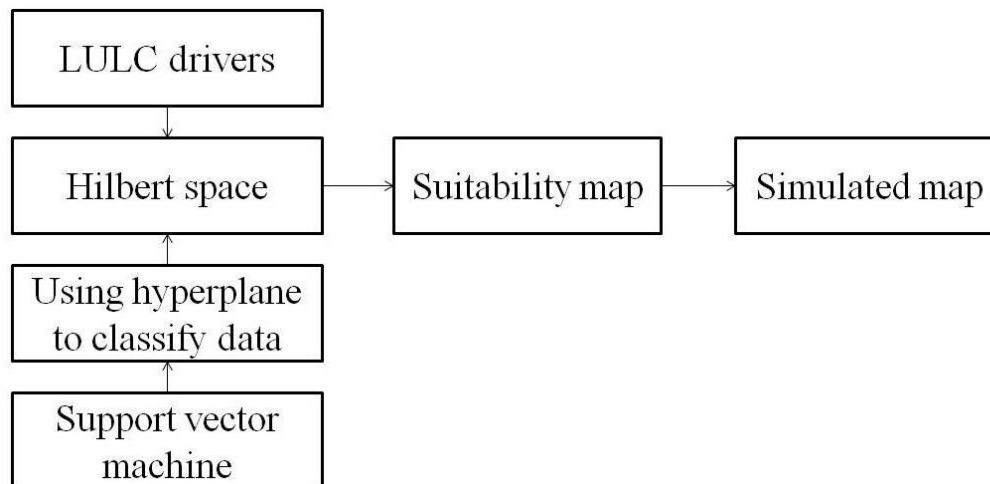


Figure 3-12: Structure of support vector machine model

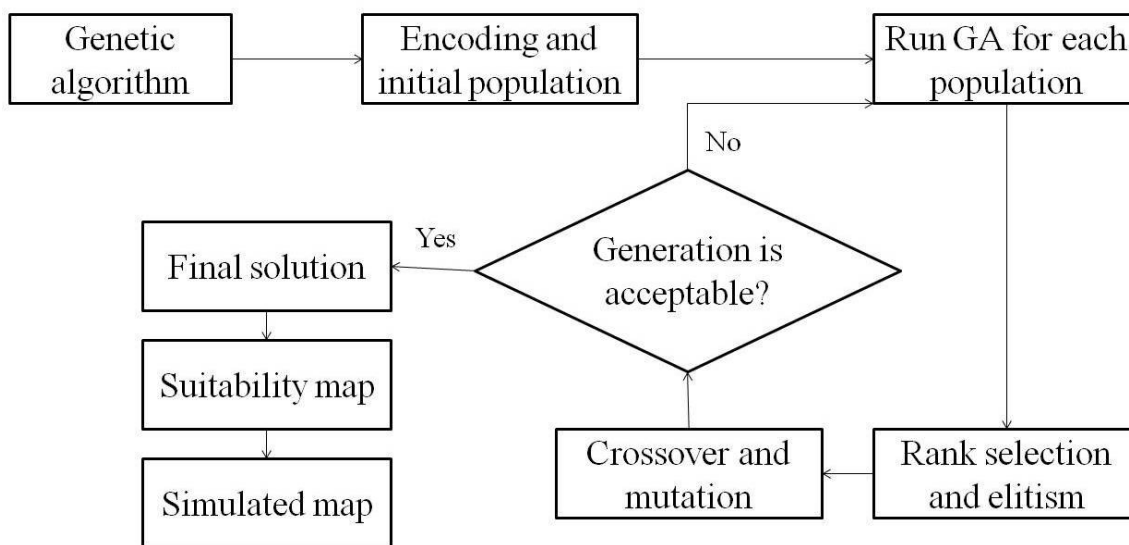


Figure 3-13: Structure of genetic algorithm model

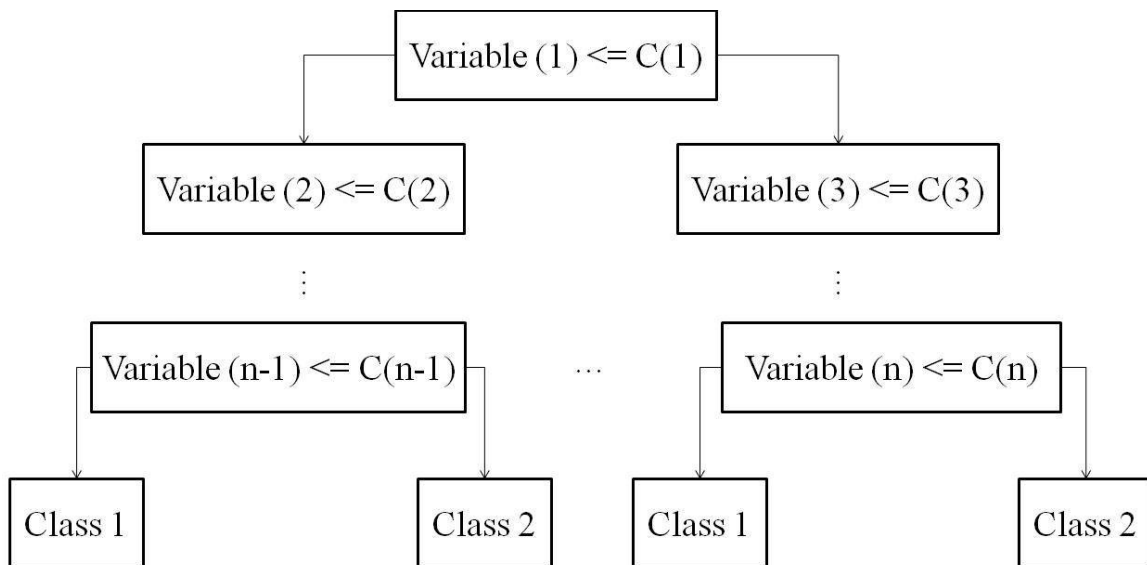


Figure 3-14: Structure of CART model

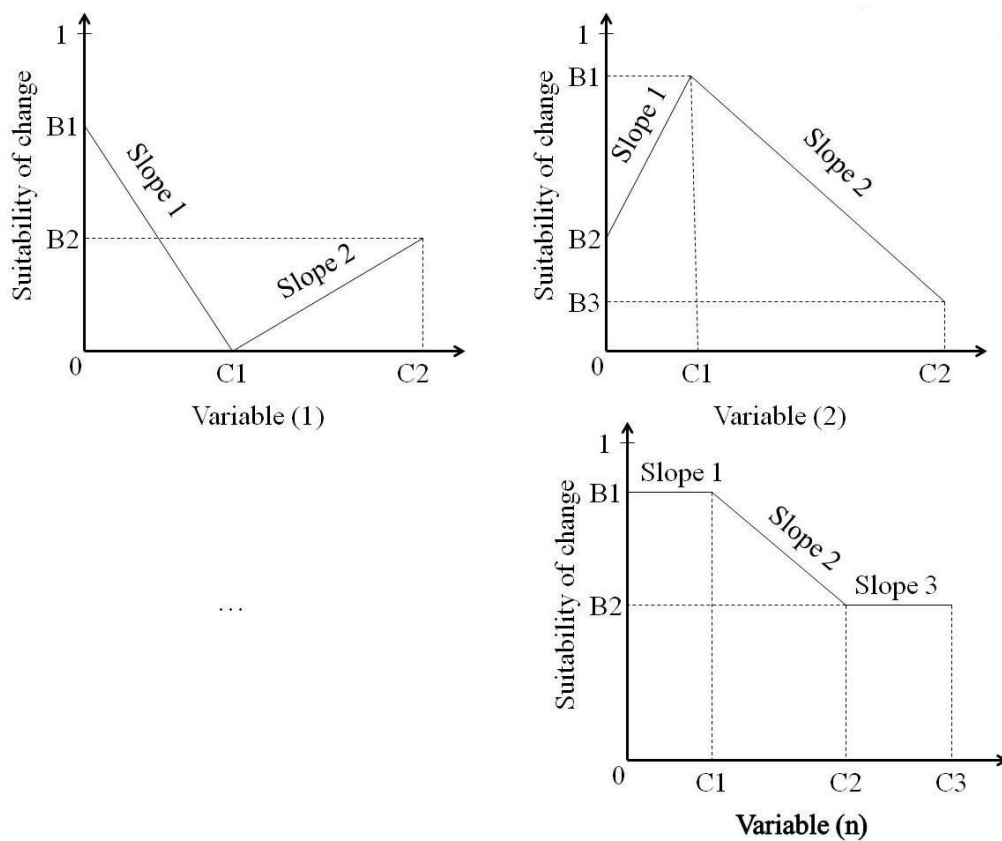


Figure 3-15: Structure of MARS model

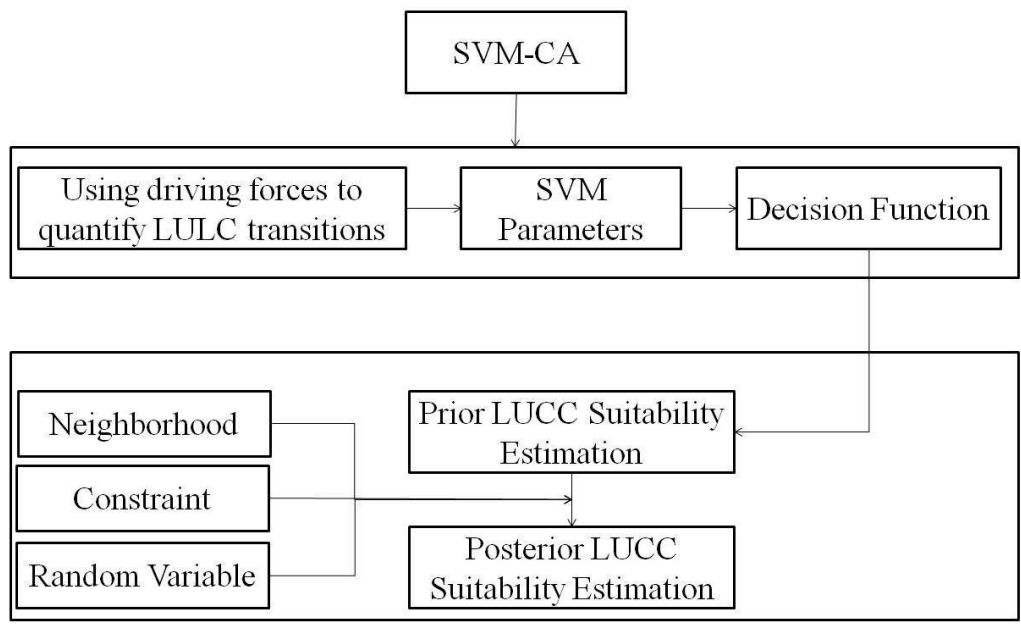


Figure 3-16: Structure of SVM-CA model adopted from Yang et al. (2008)

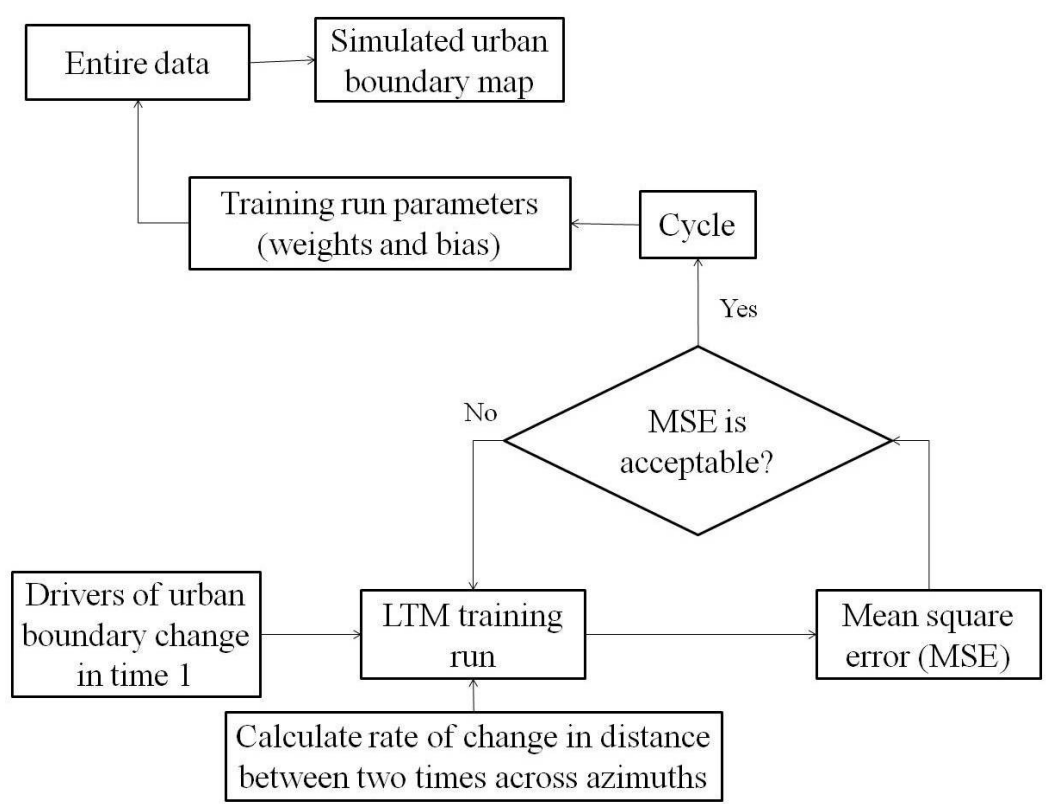


Figure 3-17: Structure of ANN-UGBM

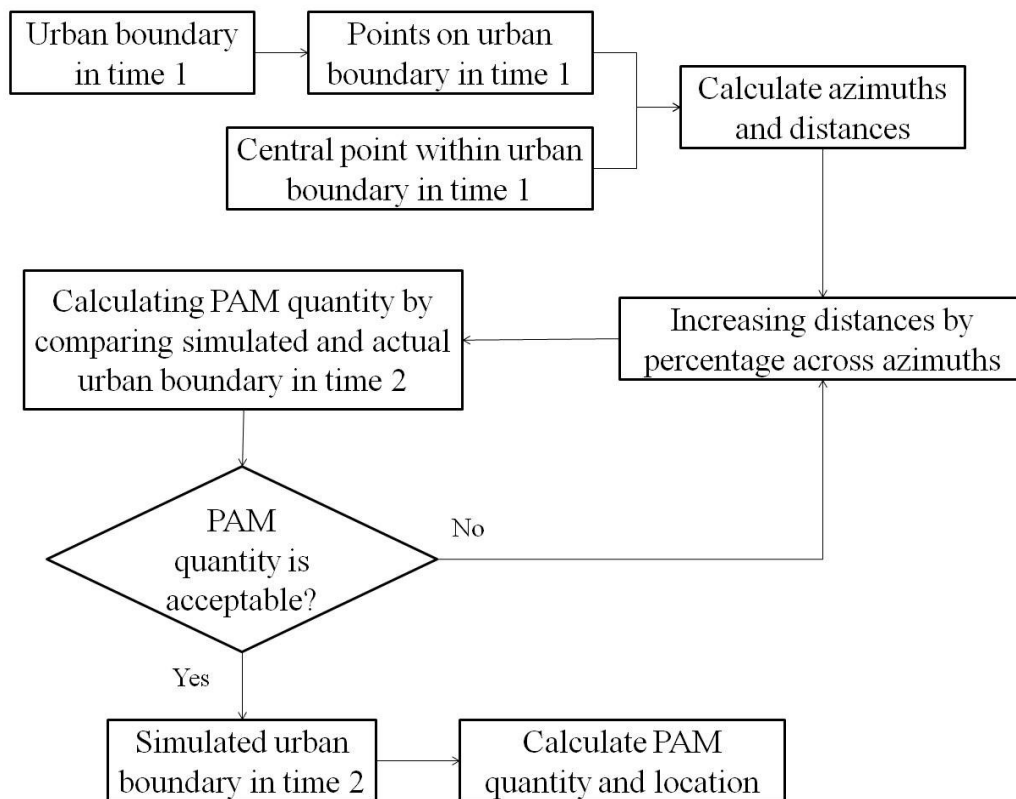


Figure 3-18: Structure of DDM

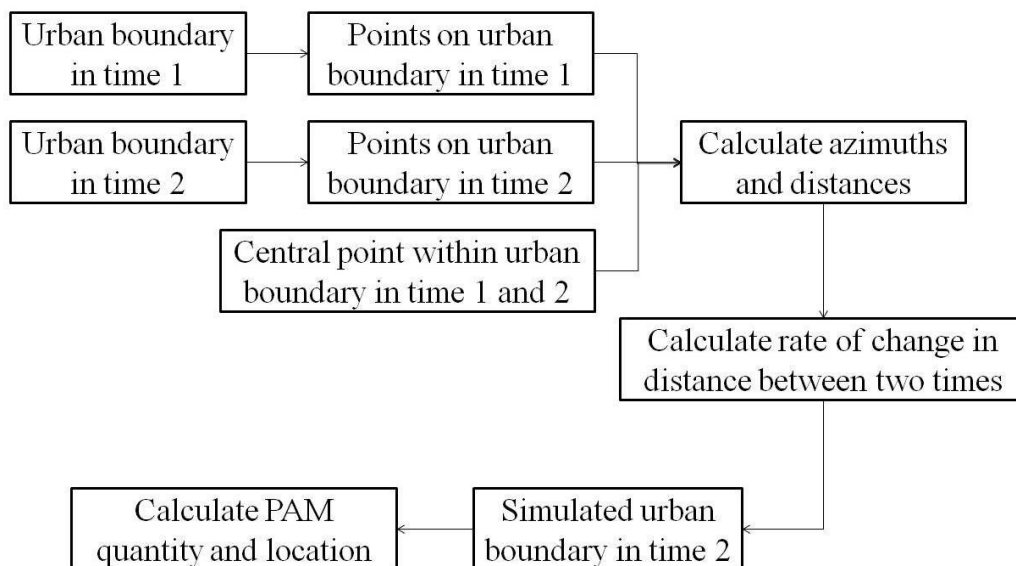


Figure 3-19: Structure of DIM

3.13 References

- Acosta-Michlik, L., Espaldon., V. (2008). Assessing vulnerability of selected farming communities in the Philippines based on a behavioural model of agent's adaptation to global environmental change. *Glob Environ Change* 18:554–563.
- Alkheder, S., and J. Shan, (2006). Change detection-Cellular automata method for urban growth modeling, Proceedings of International Society of Photogrammetry and Remote Sensing Mid-term Symposium, WG VII/5, The Netherlands.
- Almeida, C. M., Batty, M., Monteiro, A. M. V., Câmara, G., Soares-Filho, B. S., Cerqueira, G. C. (2003). Stochastic cellular automata modeling of urban land use dynamics: Empirical development and estimation. *Computers, Environment and Urban Systems*, 27, 481–509.
- Ana, M., Dragan, N., Leopold, C., (2004). Probabilistic SVM outputs for pattern recognition using analytical geometry. *Neurocomputing* 62, 293–303.
- Baesens, B., Gestel, T. V., Viaene, S., Stepanova, M., Suykens, J., Vanthienen, J., (2003). Benchmarking state-of-the-art classification algorithms for credit scoring. *Journal of the Operational Research Society* 54 (6), 627–635.
- Batty, M., and Xie, Y. (1994a). From cells to cities. *Environment and Planning B*, 21, 31-48.
- Batty, M., and Xie, Y. (1994b). Urban analysis in a GIS environment: population density modeling using ARC/INFO. In A. S. Fotheringham, & P. A. Rogerson, *Spatial analysis and GIS* (pp. 189-219). London: Taylor and Francis.
- Batty, M., Xie, Y., & Sun, Z. (1999). Modeling urban dynamics through GIS-based cellular automata. *Computers, Environment and Urban Systems*, 23, 205–233.
- Berry, M. J. A., & Linoff, G. S. (2004). *Data mining techniques: For marketing, sales, and customer relationship management* (2nd). Indiana: Wiley Publishing, Inc.
- Breiman, L., Friedman, J. H., Olshen, R. A., and Stone, C. J. (1984). *Classification and Regression Trees*. Belmont, CA: Wadsworth
- Candau, (2002). Temporal calibration sensitivity of the SLEUTH urban growth model. M.A. thesis. University of California, Santa Barbara.
- Caswell, H. (1988). Theory and models in ecology: A different perspective. *Ecological Modelling*, 43, 33-44.
- Clarke, K. C., and L. Gaydos. (1998). Loose-coupling a cellular automaton model and GIS: Long-term urban growth prediction for San Francisco and Washington/Baltimore. *International Journal of Geographic Information Science* 12: 699-714.
- Clarke, K.C., Hoppen, S., and Gaydos, L. (1997). A Self-Modifying Cellular Automaton Model of Historical Urbanization in the San Francisco Bay Area. *Environmental Planning B: Planning and Design*, 24, 247–261.
- Dietzel, C., & Clarke, K. C. (2006). The effect of disaggregating land use categories in cellular automata during model calibration and forecasting. *Computers, Environment and Urban Systems*, 30(1), 78–101.
- Drucker, H., Wu, D., Vapnik, V., (1999). Support vector machines for spam categorization. *IEEE Transactions on Neural Networks* 10 (5), 1048–1054.

- Eastman, J. R., and H. Jiang, (1996). Fuzzy measures in multi-criteria evaluation. In Proceedings of Second International Symposium on Spatial Accuracy Assessment in Natural Resources and Environmental Studies, Fort Collins, Colorado, May 21-23, pp. 527-534.
- Eastman, J. R., (1997). IDRISI for Windows: User's Guide, Version 2 (Worcester, Massachusetts, Clark University).
- Fielding, A. H., Bell, J. F., (1997). A review of methods for the assessment of prediction errors in conservation presence/absence models. *Environ. Conserv.* 24 (1), 38–49.
- Foley, J. A., DeFries, R., Asner, G. P., Barford, C., Bonan, G., Carpenter, S. R., Chapin, F. S., Coe, M. T., Daily, G. C., Gibbs, H. K., Helkowski, J. H., Holloway, T., Howard, E. A., Kucharik, C. J., Monfreda, C., Patz, J. A., Prentice, I. C., Ramankutty, N., and Snyder, P. K. (2005). Global Consequences of Land Use. *Science*, 309, 570-574.
- Fotheringham, A. S. and M. E. O'Kelly. (1989). *Spatial Interaction Models: Formulations and Applications*. Dordrecht, Kluwer Academic Publishers.
- Friedman, J. H. (1991). Multivariate Adaptive Regression Splines (with discussion). *Annals of Statistics* 19, 1.
- Gestel, T.V., Suykens, J., Baesens, B., Lambrechts, A., Lanckriet, G., Vandaele, B., Moor, B., Vandewalle, J., (2001). Financial time series prediction using least squares support vector machines with the evidence framework. *IEEE Transactions on Neural Networks* 12 (4), 809–821.
- Gibson, C., E. Ostrom, and T.-K. Ahn. (2000). The concept of scale and the human dimensions of global change: a survey. *Ecological Economics* 32:217-239.
- Goldberg, D. E., (1989). *Genetic Algorithms in Search, Optimization, and Machine Learning*, Addison-Wesley, Massachusetts.
- Goldstein, N. C., (2003). Brains vs. brawn-Comparative strategies for the calibration of a cellular automata-based urban growth model, Proceedings of the 7th International Conference on GeoComputation, 08–10 September, University of Southampton, Southampton, UK, unpagniated CD-ROM.
- Gotelli, N. J., and Graves, G. R. (1996). *Null models in ecology*. Smithsonian Institution Press.
- He, Z., Lo, C. (2007). Modelling urban growth in Atlanta using logistic regression. *Computer Environment Urban System*. 31(6):667–688.
- Holland, J. H., (1975). *Adaptation in Natural and Artificial Systems*, University of Michigan Press, Ann Arbor, Michigan.
- Holland, J. H. (1998). *Emergence: From Chaos to Order*. Reading, MA, Perseus Books.
- Jantz, C. A., S. J. Goetz, and M. K. Shelley. (2003). Using the SLEUTH urban growth model to simulate the impacts of future policy scenarios on urban land use in the Baltimore/Washington metropolitan area. *Environment and Planning B* 31: 251-271.
- Jantz, C. A., & Goetz, S. J. (2005). Analysis of scale dependencies in an urban land-use change model. *International Journal of Geographical Information Science*, 19(2), 217–241.
- Jenerette, G. D. and J. Wu. (2001). Analysis and simulation of land-use change in the central Arizona - Phoenix region, USA. *Landscape Ecology* 16:611-626.

- Kok, K., Farrow, A., Veldkamp, A., and Verburg, P. H. (2001). A Method and Application of Multi-Scale Validation in Spatial Land-Use Models. *Agriculture, Ecosystems and Environment*, 85, 223–238.
- Landis, J., and Zhang, M., (1998). The second generation of the California urban futures model. Part 1: model logic and theory. *Environment and Planning B: Planning and Design*, 30, 657–666.
- Lee, D.R., and G.T. Sallee, (1970). A method of measuring shape, *The Geographical Review*, 60:555–63
- Li, X., and Yeh, A. G. O., (2000). Modelling sustainable urban development by the integration of constrained cellular automata and GIS. *International Journal of Geographical Information Science*, 14, 131–152.
- Li, X., Yeh, A. G. O. (2002). Neural-network-based cellular automata for simulating multiple land use changes using GIS, *International Journal of Geographical Information Science*. 16(4): 323-343.
- Lu, C., Gestel, T.V., Suykens, J., Huffel, S., Vergote, I., Timmerman, D., (1999). Preoperative prediction of malignancy of ovarium tumor using least squares support vector machines. *Artificial Intelligence in Medicine* 28 (3), 281–306.
- Marceau, D. J. and N. Moreno. (2008). An object-based cellular automata to mitigate scale dependency. In: *Object-Based Image Analysis*, T. Blaschke, S. Lang, and G.J. Hay, eds, Springer-Verlag, pp. 43-73.
- Martens, D., Baesens, B., Van Gestel, T., Vanthienen, J., (2007). Comprehensible credit scoring models using rule extraction from support vector machines. *European Journal of Operational Research* 183 (3), 1466–1476.
- Matsinos, Y. G., & Troumbis, A. Y. (2002). Modeling competition, dispersal and effects of disturbance in the dynamics of a grassland community using a cellular automaton model. *Ecological Modelling*, 149, 71–83.
- Ménard, A., & Marceau, D. J. (2007). Simulating the impact of forest management scenarios in an agricultural landscape of southern Quebec, Canada, using a geographic cellular automata. *Landscape and Urban Planning*, 79(3–4), 253–265.
- Mitra, S., S. K. Pal and P. Mitra, (2002). Data mining in soft computing framework: A survey. *IEEE. Trans. Neural Networks*, 13: 3-14
- Moreno, N., & Marceau, D. J. (2006). A vector-based cellular automata model to allow changes of polygon shape. In *Proceedings of the 2006 SCS international conference on modeling and simulation – methodology, tools, software applications*, pp. 85-92. Canada: Calgary.
- Moreno, N. and D. J. Marceau, (2007). Modeling land-use changes using a novel vector-based cellular automata model. *The 18th IASTED International Conference on Modelling and Simulation*, May 30 – June 1, 2007, Montreal, Quebec.
- Moreno, N., Ménard, A., & Marceau, D. J. (2008). VecGCA: A vector-based geographic cellular automata model allowing geometrical transformations of objects. *Environment and Planning B: Planning and Design*, 35, 647–665.
- Moreno, N., F. Wang, and D. J. Marceau, (2009). Implementation of a dynamic neighborhood in a land-use vector-based geographic cellular automata model, *Computers, Environment and Urban Systems*, 33(1):44–54.

- Nagel, K., R. J. Beckman, and C. L. Barrett. (1999). TRANSIMS for urban planning. Los Alamos, NM, Los Alamos National Laboratory.
- Parker, D. C., Manson, S. M., Janssen, M. A., Hoffmann, M. J., Deadman, P. (2003). Multi-agent systems for the simulation of land use and land-cover change: a review. *Ann Assoc Am Geogr.* 93:314–337.
- Parker, D. C., Brown, D., Polhill, J., Deadman, P. J., Manson, S. M. (2008). Illustrating a new ‘conceptual design pattern’ for agent-based models of land use via five case studies—the Mr. Potatohead framework. In: Lo’pez Paredes A, Herna’ndez Iglesias C (eds) *Agent-based modelling in natural resource management*. Pearson Education, Upper Saddle River, pp 23–51
- Pijanowski, B. C., Daniel G. Brown, Bradley A. Shellito, Gaurav A. Manik. (2002). Using neural networks and GIS to forecast land use changes: a Land Transformation Model. *Computers, Environment and Urban Systems.* 26, 553-575.
- Pijanowski B. C., Pithadia S., Shellito B. A., Alexandridis, K. (2005). Calibrating a neural network based urban change model for two metropolitan areas of Upper Midwest of the United States. *International Journal of Geographical Information Science.* 19:197–215.
- Pijanowski, B. C., K. Alexandridis and D. Mueller. (2006). Modeling urbanization patterns in two diverse regions of the world. *Journal of land use science.* (1): 83-108.
- Pijanowski, B. C., Tayyebi, A., Delavar, M. R., and Yazdanpanah, M. J. (2009). Urban expansion simulation using geographic information systems and artificial neural networks. *International Journal of Environmental Research,* 3(4), 493-502.
- Pontius, Jr. R. G., J. Cornell., and C. Hall. (2001). Modeling the spatial pattern of land-use change with Geomod2: application and validation for Costa Rica. *Agriculture, Ecosystems & Environment* 85(1-3) p.191-203.
- Pontius, R. G., Jr., D. Huffaker, and K. Denman. (2004). Useful techniques of validation for spatially explicit land-change models. *Ecological Modelling* 179 (4): 445–61.
- Rykiel, Jr., E. J., (1996). Testing ecological models: the meaning of validation. *Ecol. Model.* 90, 229–244.
- Semboloni, F. (2000). The growth of an urban cluster into a dynamic self-modifying spatial pattern. *Environment and Planning B: Planning and Design,* 27(4), 549–564.
- Shan, J., S. Alkheder, J. Wang. (2008). Genetic Algorithms for the Calibration of Cellular Automata Urban Growth Modeling. *Photogrammetric Engineering & Remote Sensing* Vol. 74, No. 10, October 2008, pp. 1267–1277.
- Shi, W., and Pang, M. Y. C. (2000). Development of Voronoi-based cellular automata-an integrated dynamic model for geographical information systems. *International Journal of Geographical Information Science,* 14(5), 455–474.
- Silva, E. A., and K. C. Clarke. (2002). Calibration of the SLEUTH urban growth model for Lisbon and Porto, Portugal. *Computers, Environment and Urban Systems* 26: 525-552.
- Tayyebi, A., Pijanowski, B. C., Tayyebi, A. H. (2011a). An Urban Growth Boundary Model Using Neural Networks, GIS and Radial Parameterization: An Application to Tehran, Iran. *Landscape and Urban Planning,* 100, 35-44.

- Tayyebi, A., Pijanowski, B. C., Pekin, B. (2011b). Two rule-based urban growth boundary models applied to the Tehran metropolitan area, Iran. *Applied Geography*, 31(3), 908-918.
- Tayyebi, A., Pekin, B. K., Pijanowski, B. C., Plourde, J. D., Doucette, J., Braun, D. (2012). Hierarchical modeling of urban growth across the conterminous USA: Developing meso-scale quantity drivers for the Land Transformation Model. *Journal of Land Use Science*. DOI: 10.1080/1747423X.2012.675364.
- Valbuena, D., Verburg, P. H., Bregt, A. K. (2008). A method to define a typology for agent-based analysis in regional land-use research. *Agric Ecosyst Environ* 128:27–36.
- Vapnik, V., (1998). *Statistical Learning Theory*. Wiley, New York, 768pp.
- Veldkamp, A. and Fresco, L. O. (1996). CLUE-CR: an integrated multi-scale model to simulate land use change scenarios in Costa Rica. *Ecological modelling*, 91: 231-248.
- Verburg, P. H., Veldkamp, A., de Koning, G. H. J., Kok, K. and Bouma, J. (1999). A spatial explicit allocation procedure for modelling the pattern of land use change based upon actual land use. *Ecological modelling*, 116: 45-61.
- Verburg, P. H., Soepboer, W., Veldkamp, A., Limpiada, R. and Espaldon, V. (2002). Modeling the spatial dynamics of regional land use: the CLUE-S model. *Environmental Management*, 30(3): 391-405.
- Verburg, P. H. and Veldkamp, A. (2004). Projecting land use transitions at forest fringes in the Philippines at two spatial scales. In: *Landscape ecology*, 19, 1 pp. 77-98.
- Verburg, P. H., Nijs, T. C. M., Eck, J. R., Visser, H., & Jong, K. (2004). A method to analyze neighborhood characteristics of land use patterns. *Computers, Environment and Urban Systems*, 28(6), 667–690.
- Verburg, P. H. (2006). Simulating feedbacks in land use and land cover change models. *Landscape Ecol* 21:1171–1183.
- Von Neumann, J., and Burks, A. W. (1966). *Theory of self reproducing automata*. Urbana, Illinois: University of Illinois Press.
- White, R., and Engelen, G., (1993). Cellular automata and fractal urban form: a cellular modelling approach to the evolution of urban land use patterns. *Environment and Planning A*, 25, 1175-1199.
- White, R., Engelen, G., and Ujje, I., (1997). The use of constrained cellular automata for high-resolution modelling of urban land use dynamics. *Environment and Planning B: Planning and Design*, 24, 323-343.
- White, R., and Engelen, G. (2000). High resolution integrated modeling of the spatial dynamics of urban and regional systems. *Computers, Environment and Urban Systems*, 24, 383–400.
- White, R., Engelen, G., and Ujje, I. (2000). Modelling land-use change with linked cellular automata and socio-economic models: A tool for exploring the impact of climate change on the island of St. Lucia. In M. J. Hill & R. J. Aspinell (Eds.), *Spatial information for land-use management* (pp. 189-204). Amsterdam: Gordon and Breach.
- Wolfram, S. (1984). *Computer Software in Science and Mathematics*. Scientific American, September, pp. 188-203.
- Wu, F. (1998). SimLand: A prototype to simulate land conversion through the integrated GIS and CA with AHP-derived transition rules. *International Journal of Geographical Information Science*, 12, 63–82.

- Wu, F., and Webster, C. J., (1998). Simulation of land development through the integration of cellular automata and multi-criteria evaluation. *Environment and Planning B: Planning and Design*, 25, 103–126.
- Wu, F. (2002). Calibration of stochastic cellular automata: The application to rural-urban land conversions. *International Journal of Geographical Information Science*, 16(8), 795–818.
- Yang, X., and C. P. Lo. (2003). Modelling urban growth and landscape change in the Atlanta metropolitan area. *International Journal of Geographical Information Science* 17: 463-488.
- Yang, Q., Li, X., X. Shi, (2008). Cellular automata for simulating land use changes based on support vector machines. *Computers & Geosciences* 34, 592-602.
- Yassemi, S., Dragicevic, S., & Schmidt, M. (2008). Design and implementation of an integrated GIS-based cellular automata model to characterize forest fire behaviour. *Ecological Modelling*, 210, 71–84.

**CHAPTER 4: USING CART, MARS AND ANNS TO MODEL LAND USE LAND
COVER CHANGE: APPLICATION OF DATA MINING TOOLS TO THREE
DIVERSE AREAS IN THE USA AND AFRICA UNDERGOING LAND
TRANSFORMATION¹**

4.1 Introduction

Different disciplines (e.g. economics, medicine, engineering, psychology, and environmental science) have applied a variety of data mining approaches to extract underlying patterns in data (Imran et al. 2008). Data mining methods generally include two main groups of models—global parametric models (GPM) and local non-parametric models (LNPM)—that have been used to quantify the relationship between dependent and multiple independent variables. GPMs are the most common in the literature (Landis and Zhang 1998, Theobald and Hobbs 1998, Aspinall 2004); these approaches present all data to the model. In other words, one model is created that represents the entire dataset. GPMs can be statistical or belong to a class of tools referred to as machine learning. A variety of GPMs have been applied by modelers, particularly in land use science. Logistic regression is one of the most common statistical GPM applied to model land use cover

¹Current version has been submitted to Applied Soft Computing Journal.

change (e.g. He and Lo, 2007, Tayyebi et al. 2010, Mertens and Lambin 2000, Serneels and Lambin, 2001, Lambin et al. 1999, Lambin et al. 2001). Machine learning GPM tools for land use cover change modeling have focused on the use of artificial neural networks (ANNs), (Pijanowski et al. 2002a, Li and Yeh 2002, Shellito and Pijanowski 2003, Mas et al. 2004, Almeida et al. 2008), cellular automata (White and Engelen 1993, Batty and Xie 1994, Clarke et al. 1997, Dietzel and Clarke 2006, Stevens and Dragičević 2007) and genetic algorithms (Jenerette and Wu 2004, Seppelt and Voinov 2002), to name a few. LNPMs, on the other hand, subset all data and build separate (i.e. local) models of these subsets. Thus, multiple models are generated from partitioned data. To date, no studies in land use science have examined the potential of LNPM to model land use cover change.

It is quite conclusive to the land use science community (Veldkamp and Lambin 2001, Lambin et al. 2001, Irwin and Geoghegan 2001, Verburg et al. 2004, Lambin and Geist 2006; Pontius et al. 2008) that LUCC is a very complex process, with multiple drivers of LUCC operating at a variety of spatial and temporal scales from diverse sources: policy, behavior, economics, soils, and other natural features (e.g. streams, lakes). Thus, it is unlikely that statistical GPMs can appropriately characterize these systems as earlier studies have shown (cf. Lambin and Geist 2006). Statistical GPMs are likely to be insufficient when most of the statistical GPMs assume that the spatial predictors (especially in LUCC field) have to follow a normal distribution for proper modeling; however, data from the real world rarely have such distributions (Lumley, et al. 2002). Due to the complexity between social and economic factors and LUCC (Pijanowski et al. 2002b; Clarke et al. 1997), statistical GPMs may not detect the non-linear patterns in LUCC data. Furthermore, most of the functions that statistical GPMs

use require prior knowledge about the relationship between input and output (e.g. non-linear and linear functions). There are commonly auto-correlations between spatial predictors that affect the goodness of fit of LUCC models (Munroe et al. 2001; Read and Lam, 2002; Pontius et al. 2001; Gobim, et al. 2002); however, most of the statistical GPMs assume that input variables are independent from one other. Further problems arise with statistical GPMs when more spatial predictors are included in the modeling process of LUCC (Millington et al. 2007). More spatial predictors are usually added to help the model to find more complex patterns in data (Millington et al. 2007); however, more drivers increase the risk of multi-collinearity.

When using statistical GPMs, most of the assumptions are unwarranted in the cases of predictive LUCC modeling (Austin et al. 1994). In contrast, LNPMs are free from most of the limitations that exist in the statistical GPMs and may offer solutions to these challenges. To use LNPMs, one does not need to have prior knowledge about the distribution (i.e. normal distribution) of data, the form and parameters of the functions (i.e. linear or non-linear, means and standard deviations; Zhao, 2008). Moreover, the model structures of the LNPMs are not fixed and the model typically grows to fulfill the complexity in the data (Hardle et al. 2004). LNPMs are able to detect non-linear relationships in data, variable selection, data transformation and variable reduction (Stanton, 1997). Classification And Regression Tree (CART; Breiman et al. 1984) and Multivariate Adaptive Regression Splines (MARS; Friedman, 1991; De Andrés et al. 2011; Abdel-Aty and Haleem, 2011) are LNPMs that have been used widely in data mining, including predicting business failure (Li et al. 2009) and hypertension in people

(Ture et al. 2005). Most research suggests that CART and MARS generally provide very satisfactory results.

4.1.1 Literature review on LTM, CART and MARS

Comparative methodological data mining studies are becoming frequent in the literature. Many scientists have compared CART, ANN and MARS with one other and these comparative studies have shed light on important factors to consider in such studies. In an oral health study, CART, ANN and logistic regression were used for the study of factors contributing toward tooth decay; the performances of the three models were compared using the receiver operating characteristic curve or ROC (Gansky, 2003). ANN performed better than logistic regression and CART; Gansky concluded, however, that any comparative study of data mining tools such as ANN, MARS and CART need multiple model assessment tools and an iterative analysis approach (e.g. explore data, examine goodness of fit, re-evaluate predictors) to be useful.

In another application, CART and ANN were compared in a psychological study on short-term and long-term memory of people (Fong et al. 2010). In this study, researchers found that one tool performed better for data on long-term memory and but another tool did better for short-term memory suggesting that there is no one best technique even with very similar data. Yet in another study, canals in Bangkok were classified into 5 water quality class uses (Class 1 = extra clean, requires minimal processing for human use to Class 5 = use only for navigation) based on biophysical attributes such as pH value, dissolved oxygen, nitrate nitrogen, ammonia nitrogen and total coliform using CART and ANNs (Areerachakul and Sanguansintukul, 2010). Both

techniques yielded exceptional results generating greater than 98% fit suggesting that either approach can be used to automate the classification of canals in terms of water quality and potential use.

In a health care study, the prediction accuracy of ANN, CART and regression models were compared with each other using a set of data on smokers (Razi and Athappilly, 2005). ANN and CART models provide better compared to non-linear regression models when the inputs are categorical and the outputs are continuous; the authors concluded that either ANN or CART could be used. Finally, in a speech and learning study, separate and hybrid version of CART and MARS models were tested against each other to estimate speech and perception quality (Zha and Chan, 2005) of human voices. Classification of speech patterns were very reliable and fast using both methods, making these tools ideal for objectively classifying speech problems in a medical office. ANNs performed better than CART and MARS for predicting the risk of hypertension disease according to sensitivity, specificity and predictive rate (Ture et al. 2005) using 694 subjects (452 patients and 242 controls). ANNs and MARS were compared in terms of accuracy to recover different types of polynomial function (Psichogios and Ungar, 1992). MARS is often found to be more accurate and much faster than ANNs, and produced easy-to-interpret low order models; however, CART and MARS, in contrast to ANNs, were found to be more sensitive to the outliers in data (Psichogios and Ungar, 1992).

Comparison of different methods can be challenging. MARS was capable of outperforming other ANN models when judged based on speed and goodness of fit (Abraham et al. 2001), standard ways to compare these tools. However, predefined

thresholds (e.g. 0.5) used for assessment can vary for different applications of ANNs (Pijanowski et al. 2002a and 2005) making comparisons difficult as some methods have predefined rules for transforming data from continuous to binary. Additionally, there is very little research that shows that if mean squared error (MSE) values on test data are comparatively less, the models predictions are reliable.

Some researchers that have conducted comparative studies have found that characteristics of the study area such as sample size, quality of data, how models are built (i.e. training) and validated (i.e. testing), and patterns in data can influence which model performs best. For example, CART, MARS and ANN were explored for modeling different forest classes using satellite imagery and comparing this with *in situ* field data within five ecologically different regions in the Western US (Moisen and Frescino, 2002). MARS and ANNs showed tremendous advantages over CART for prediction; however, the differences between models were less distinct for the *in situ* data which had less noise. Thus, “noisy” data may be modeled best using ANN and MARS. ROC was used to compare CART and MARS for predicting the likelihood of emerging markets using financial data (Büyükbebec, 2009). The CART approach could give more accurate results in the training run; however, in testing runs, MARS gave more accurate results. Thus, some tools may over fit the data hindering its ability to generalize from one dataset to another.

4.1.2 Objectives and structure of chapter

It is surprising that, although the global parametric approach in modeling LUCC has received considerable attention during the last two decades (Clarke et al. 1997;

Pontius and Schneider, 2001; Pijanowski et al. 2002a and 2002b; Tang et al. 2005a and 2005b; He and Lo, 2007; Tayyebi et al. 2011a and 2010), we are aware of no studies that have compared global parametric models with local non-parametric models. Here, we apply the ANN-based LTM as a ML GPM model with two LNPMs—CART and MARS—to simulate agriculture, forest and urban growth patterns using land use maps from the Climate-Land Interaction Project (CLIP) study area in East Africa (Olson et al. 2008), the Muskegon River Watershed (MRW) study area in Michigan, USA (cf. Ray and Pijanowski 2010), and from a Southeast Wisconsin (SEWI) study area, respectively (cf. Pijanowski and Robinson 2011). This chapter has two main objectives. The first objective is to compare the power of the ANN-based LTM, CART and MARS to reveal the pattern of agriculture, forest and urban (spatial modeling). The second objective is to contrast the goodness of fit of three models in short (5 years intervals), intermediate (10 years intervals) and long (20 years intervals) periods (temporal modeling) to simulate single transition patterns in three study areas using the Percent Correct Match (PCM) and Relative Operating Characteristic (ROC) curve metrics. We selected three different regions because these three study areas—CLIP, MRW and SEWI—are agriculture-dominated, forest-dominated and urban-dominated, respectively.

The chapter is organized as follows. Section 4.2 provides comprehensive section about the ANN-based LTM, CART, MARS and accuracy assessment metrics (PCM and ROC) used to validate the models in three study areas. In Section 4.3, three study areas are briefly described. We showed how we used LTM and Salford Systems to build CART and MARS models. Section 4.4 describes the simulation results of agriculture, forest and urban growth in CLIP, MRW and SEWI and compares the PCM and ROC to evaluate the

results of experiments. Section 4.5 summarizes our conclusions about the use of each data mining method.

4.2 Methods

4.2.1 Global Parametric Model (Land Transformation Model)

Land Transformation Model (LTM) uses a Multi-Layer Perceptron (MLP) Artificial Neural Network (ANN) which has advantages to other types of ANNs (e.g. better approximation, simpler structures and faster algorithms). Models from ANNs class can be trained using supervised and unsupervised learning algorithms (Zurada, 1992). In supervised learning, ANNs fit a model to data based on the relationship between the input and the output. Conversely, in unsupervised learning, data are classified to different classes based on the similarity between input data (refer to cluster analysis; Zurada, 1992). The numbers of output classes (binary or multiple classes) are determined during the training run in a supervised classification by checking the unique values in output; however, in unsupervised classifications the user can decide before a training run or leave it to ANNs to select during training run based on correlation between input layers (Zurada, 1992).

MLP uses a supervised learning algorithm which can estimate a function between input-output pairs without knowledge of the form of the function (Pijanowski et al. 2009). LTM (Pijanowski et al. 2005 and 2006) uses data in at least two periods of time to train the networks. Mean Square Error (MSE) computes the difference between reference and calculated output of ANNs (See Eq. 4-1; Y is the calculated and O is the reference values of output node; n is number of observations) and LTM saves the MSE in a CSV

file for each 100 cycles (Pijanowski et al. 2002a and Tayyebi et al. 2012). The LTM couples ANNs and GIS using socio-economic and bio-physical factors in a raster environment (Pijanowski et al. 2002a) to simulate LUCC (Pijanowski et al. 2002b) and environmental impacts (Tang et al. 2005a and 2005b, Wiley et al. 2010, Ray et al. 2010, Yang et al. 2010, Pijanowski et al. 2011). LTM follows four sequential steps (Pijanowski et al. 2002a): (1) developing binary and continuous maps from spatial predictor variables; (2) applying predefined rules to relate spatial predictor variables to output; (3) using ANN to train the LTM and save training values of weight, bias and activation values; and (4) using ANN training values and GIS to create future prediction of LUCC. The weights and biases of LTM are saved in a network file for each 100 cycles automatically and analyzed. The best network is applied to testing data to estimate the output and construct a binary map.

$$MSE = \frac{\sum_{i=1}^n (O_i - Y_i)^2}{2} \quad (\text{Eq. 4-1})$$

4.2.2 Local Non-Parametric Models (CART and MARS)

Both CART and MARS fragment the data recursively and involve two sequential phases in model construction: (1) the forward step which increases the complexity of the model by adding nodes in CART or basis functions in MARS until it reaches the predefined level of complexity by the user and model prevented from over-fit of the data through a series of rules; (2) subsequently a backward phase called model selection which removes the less significant node in CART or basis functions in MARS from the model in terms of the goodness-of-fit in order to generalize the final model for new data.

4.2.2.1 Classification And Regression Tree (CART)

The CART is one of the popular data mining approaches that employs repetitive splitting techniques and decision trees to predict continuous (e.g. regression tree models) or categorical (e.g. classification tree models) variables using continuous or categorical predictors (Breiman, et al. 1984). The node of the tree associates the alternatives between predictors and a threshold while the leaves of the tree show the labeled output class (e.g. change or no-change in LUCC). Data can be divided on the same or different predictors across the hierarchical levels of CART sequentially if the prediction accuracy of CART improves significantly (Aertsen et al. 2011). The surrogate splitter is one of the unique characters in CART compared to other conventional models which is identified as a back-up for missing values or variables in data (Steinberg and Golovnya, 2006). The number of nodes required to classify the data in CART depends on the number of samples and type of patterns (e.g. linear or non-linear) in the data; however, large trees with a lot of terminal nodes have often over-fit the data and cannot be used for new data efficiently (Steinberg and Colla, 1997).

CART is characterized as a reliable approach and is known as an effective tree-growing model which uses new methods such as the Gini index to control the tree-growing and purity of each node (Steinberg and Golovnya, 2006). The node in the tree is called a terminal node if a node is a child of an upper node and parent of a lower node simultaneously (except the root node). It is called a non-terminal node if a node does not have a child (Breiman, et al. 1984). If-then else rules (Timofeev, 2004) or non-linear functions can be used to select the threshold on one predictor or linear combination of

predictors (Gelfand and Delp, 1991). CART follows a similar process to classify the data and calculate the accuracy for nodes in the tree ($N_C(t)$ and $N_{NC}(t)$ are numbers of change and non-Change in LUCC while $N_T(t)$, $N_L(t)$ and $N_R(t)$ are total samples of the parent node (node t), left and right child node t , respectively). Eq. 4-2 shows the proportion of samples in the node t of a tree with respect to the total sample (n total samples in data):

$$P(t) = \frac{N_T(t)}{n} \quad (\text{Eq. 4-2})$$

Eq. 4-3a and Eq. 4-3b calculate the conditional probability that CART classifies the change and non-change LUCC samples accurately in the node t of a tree:

$$P(C|t) = \frac{N_C(t)}{N_T(t)} \quad (\text{Eq. 4-3a}) \quad \text{and} \quad P(NC|t) = 1 - P(C|t) \quad (\text{Eq. 4-3b})$$

Similarly, Eq. 4-4a and Eq. 4-4b calculate the probability that CART classifies the change and non-change LUCC samples accurately in the subsequent (left and right child of node t):

$$P_L = \frac{N_L(t)}{N_T(t)} \quad (\text{Eq. 4-4a}) \quad \text{and} \quad P_R = 1 - P_L \quad (\text{Eq. 4-4b})$$

Thus, CART can calculate the accuracy of a binary classification in the parent and child node t of a tree using Eq. 4-3a, 4-3b, 4-4a and 4-4b. The Gini is usually implemented as a default approach which measures the splitting impurity for binary classifications for each node in a tree (Eq. 4-5; Breiman et al. 1984). The resultant tree from the Gini calculation usually performs better than other methods (e.g. Twoing,

Entropy and Least Squares). Gini commonly generates a smaller tree which is highly concentrated with the desired output class (Sut and Simsek, 2011):

$$Gini(t) = 1 - P(C|t)^2 - P(NC|t)^2 \quad (\text{Eq. 4-5})$$

A gain function (Eq. 4-6 below) is introduced to compare Gini before and after splitting to assess the change in the degree of impurity of the parent node with respect to the child node. A split that can maximize the gain function is selected to fragment data (t is parent node, t_L and t_R are left and right child of the parent node).

$$Gain = Gini(t) - (Gini(t_L)P_L + Gini(t_R)P_R) \quad (\text{Eq. 4-6})$$

4.2.2.2 Multivariate Adaptive Regression Splines (MARS)

MARS is a regression approach that divides data into different regions to establish the relationship between independent and dependent spatial variables using piecewise polynomial functions called basis functions where the basis function can change from each region to another (Friedman, 1991). In contrast to other non-linear models (e.g. ANNs or logistic regression) where the model fits only one set of coefficients to the data, MARS detects the non-linear pattern in data by fitting separate piecewise polynomial functions (a separate set of coefficients for each region) to each region (Kayri, 2010; Eq. 4-7):

$$Y = \sum_{m=1}^M \beta_m BF_m(X_1, \dots, X_p) + \varepsilon \quad (\text{Eq. 4-7})$$

In the above equation, M , p , ε , β , BF , X and Y are the number of sub regions, number of predictors, error terms, basis function coefficients, type of polynomial functions, independent and dependent variables, respectively. The difference between

calculated and observed values within each region indicates the lack of fit of the model. The objective of MARS is to minimize the sum of the square errors in order to determine the basis function coefficients for each region separately (Friedman, 1991). The interaction between basis function (e.g. linear or non-linear) can be allowed or prohibited by a user before model construction according to prior knowledge of the modeler about the application (Friedman, 1991).

MARS fits one basis function for the values on the right side of the threshold (Eq. 4-8a) and another basis function (called the mirror) for the values on the left side of threshold (Eq. 4-8b). The terms BF_{2m-1} and BF_{2m} (m refers to the number of splits or sub regions) refer to the basis functions for the right and left side of the knot where C is the threshold value for a predictor, X denotes a predictor variable (k can change from one to p) and Y is response variable. Because we consider two basis functions, one for the left and another for the right side of the threshold, the total number of basis function is equal to two times of number of sub regions. The basis functions across different regions are generally combined to generate the final model as such:

$$BF_{2m-1}(X_k) = \sum_{m=1}^M \max(X_{k,m} - C_{k,m}) \quad (\text{Eq. 4-8a})$$

$$BF_{2m}(X_k) = \sum_{m=1}^M \max(C_{k,m} - X_{k,m}) \quad (\text{Eq. 4-8b})$$

The total number of basis functions depends on the pattern in the data (linear or non-linear pattern), unique values across the data (related to the number of splits), and number and type (categorical or continues) of predictors. Adding basis functions sequentially makes MARS more flexible to model data with more variability and

complexity; however, MARS may over-fit data in the training run by adding unnecessary basis functions to the model or it may learn about useless patterns in data. Thus, a Generalized Cross Validation (GCV) procedure has been developed for use in MARS (Friedman and Silverman, 1989; Craven and Wahba, 1979) to calculate the lack of fit by MARS as the difference between reference and calculated response using basis functions in order to avoid over-fitting the data. GCV operates by removing the least important basis functions simultaneously (Eq. 4-9; where n is number of total observations in model) as such:

$$GCV = \frac{\frac{1}{n} \sum_{i=1}^n (Y_i - f_M(X_i))^2}{\left(1 - \frac{C(M)}{n}\right)^2} \quad (\text{Eq. 4-9})$$

In other words, the numerator in the GCV equation measures how good MARS is in simulating the output while at the same time the denominator penalizes the model for the added basis functions. This is an iterative process in MARS to ensure a balance between lack of fit and complexity in the model. The objective of MARS is to minimize the GCV across different sub regions and the best model is the one with the lowest GCV. LeBlanc (1993) developed a method to calculate $C(M)$ using Eq. 4-10 where d is the cost for each basis function and M is total number of basis functions in MARS.

$$C(M) = d \times M \quad (\text{Eq. 4-10})$$

4.2.3 Validation Metrics

Two approaches were employed here to assess the goodness of fit of the ANN-based LTM, CART and MARS models. Data saved randomly into two mutually

exclusive sets, training (approximately 5% of the data) and testing (the other 95% of data), were used to compare the three types of models with each other. The training data sets were used to generate the LTM, CART and MARS best fit models which were then evaluated with the testing data sets. The K-fold cross validation procedure is one of the procedures that can prevent an over-fitting problem in the training run and gives useful information regarding the sensitivity of outputs to small changes in the data (Lawrence et al. 1997). Training data set is fragmented into K mutually exclusive folds with equal size using a random selection of data points (Muñoz and Felicísimo, 2004). At each time, one fold is generally excluded and the other included K – 1 fold is used to develop the model (Refaeilzadeh, et al. 2008). The output of the excluded fold is calculated at each time using the generated model from the other K – 1 fold. Thus, we need to train the model (CART and MARS) K times for each fold separately and the total error of the model is calculated by taking the average of the estimated error from the K training runs. We used a 10-fold cross validation method, which is the most common one, to train MARS and CART (Muñoz and Felicísimo, 2004); however, we followed Pijanowski et al. (2002a and 2009) to train the LTM because LTM does not have this option (K-fold cross validation) for the training run. Models are usually built up to capture general underlying trends in the data to use for forecasting applications (Pijanowski et al. 2002a). Over-fitting (poor generalization abilities) is a major problem in the training run of the modeling process which occurs when the number of parameters (weight and bias) increase (Lawrence et al. 1997), the model converges to the local minimum instead of global minimum in ANNs (Jordanov and Rafik, 2004) or the model is generated from noisy data rather than the underlying patterns within the data (Last and Maimon, 2004;

Witten and Frank, 2000). Thus, evaluation via testing data is needed to avoid over-fitting in data and ensure that underlying patterns can apply to new data (Manel et al. 1999; Pontius and Millones, 2011).

The performance of the ANN-based LTM, CART and MARS models for simulating agriculture, forest and urban was compared using the Relative Operating Characteristic (ROC) curve and Percent Correct Match (PCM) in the CLIP, MRW and SEWI study areas, respectively. PCM (Eq. 4-11a shows PCM_P and Eq. 4-11b shows PCM_N; See Table 4-1) is one of the popular metrics that usually is used to compare the predicted and a reference map. PCM_P and PCM_N show the proportion of the reference change and non-change cells in the testing data that have been correctly predicted by the model, respectively (Pijanowski et al. 2002a and 2005).

$$PCM_{-P} = \frac{TP}{Ref_{-}Change} \quad (\text{Eq. 4-11a})$$

$$PCM_{-N} = \frac{TN}{Ref_{-}Non_{-}Change} \quad (\text{Eq. 4-11b})$$

The ROC is another popular metric that has been used in the LUCC field to compare a simulated and reference binary map (Pontius and Batchu, 2003; Pijanowski et al. 2006; Tayyebi et al. 2009a and 2009b; Pontius et al. 2004). In contrast to the PCM_P and PCM_N that only uses one threshold to assess the accuracy of the model, ROC is capable of calculating the accuracy across a range of threshold. TP rates (Eq. 4-12a; sensitivities) and FP rates (Eq. 4-12b; 1 - specificities) are calculated using contingency table (Table 4-1) for different thresholds (Pontius and Batchu, 2003). ROC curves plot the FP rate along the X axis and TP rate along the Y axis for different thresholds (He and

Lo, 2007). The area under the ROC curve shows the ability of the model to discriminate between change and no-change (Pontius and Batchu, 2003; 1 indicate perfect model and 0.5 indicate random model). The sensitivity is the probabilities that the model will correctly classify change cells while the specificity is the probability that the model will correctly classify non-change cells (Fielding and Bell, 1997).

$$Sen = \frac{TP}{TP + FN} \quad (\text{Eq. 12a})$$

$$1 - Spec = \frac{FP}{FP + TN} \quad (\text{Eq. 12b})$$

4.3 Study Areas and Model Building

The CLIP study area (Olson et al. 2008, Pijanowski et al. 2011) is located in East Africa encompassing 5 countries wholly (Kenya, Uganda, Rwanda, Burundi and Tanzania; Figure 4-1a). Approximately 15% of the study area is agricultural. Excessive population growth and the need to feed over 100 million people of this region are leading to rapid expansion of rainfed agriculture in this part of the world. The Southeastern Wisconsin (SEWI) region includes seven counties: Kenosha, Milwaukee, Ozaukee, Racine, Walworth, Washington and Waukesha Counties (Figure 4-1b; See Pijanowski et al. 2006). SEWI is currently dominated by urban in the east, agriculture in the north and south. The Muskegon River Watershed (MRW) located in the west-central Lower Peninsula of Michigan, USA (Figure 4-1c; See Pijanowski et al. 2007; Ray et al. 2012). This watershed is currently dominated by forest in the northeast, agriculture in the center, and urban in the southwest.

We downloaded Salford Systems Software which contained a trial version of CART and MARS (www.salford-systems.com); however, LTM is open source software which is available online (www.ltm.agriculture.purdue.edu). Three models were developed using 12, 16 and 17 spatial predictor variables to reveal agriculture, urban and forest growth pattern in CLIP, MRW and SEWI, respectively (Table 4-2). Cells of agriculture, forest and urban in 1995, 1978 and 1990 were aggregated into exclusionary zones and were not candidates as new agriculture, forest and urban growth in 2000, 1998 and 2000 in CLIP, MRW and SEWI, respectively. The output layers in CLIP, MRW and SEWI were reclassified into agriculture versus non-agriculture, forest versus non-forest and urban and non-urban cells, respectively. Because of the large sizes of the study areas in SEWI (near 7,733,720 samples; 30m) and in MRW (near 11,991,901 samples; 30m) that make model computation intensive for the entire region, we used random sampling to take 1,020,472 samples for SEWI and 1,867,150 samples for MRW. However, we could be able to use whole samples in CLIP because of coarser resolution of data (1 km resolution). The size of each simulation and the resolution of data are given in Table 4-3.

4.4 Results

4.4.1 CART

The CART for all three locations generated informative results. The tree in Figure 4-2 shows red and blue nodes indicating more changes and no-changes, respectively, while the intermediate colors show the nodes that contain more mixed cases. Figure 4-2 also shows (lower plot) a relative cost of the training run which measures the misclassification error against the tree size. This plot starts around 0.6, 0.7 and 0.5575 in

node 2 and then decreases significantly until node 10, 7 and 10 in CLIP, SEWI and MRW (0 means perfect fit and 1 represents the performance of random), respectively. SPM software halted the training run of CART at 17, 13 and 17 number of nodes (forward run of CART) where the relative cost reached their minimum value in CLIP, SEWI and MRW, respectively. The most accurate classifier (backward run of CART) is indicated by the green bar marking the low point on the error profile (Figure 4-2). The best tree displayed has 16, 10 and 13 terminal nodes which reached a relative cost of 0.475, 0.403 and 0.461 in CLIP, SEWI and MRW, respectively (Figure 4-2). The relative cost can be used to compare same-sized trees based on different variables. Comparing the relative cost and size of a tree in three study areas suggests that agriculture and forest expansion patterns in CLIP and MRW (with higher relative cost) are more complicated than urbanization in SEWI.

Figure 4-3 gives detailed node information, including the splitting criteria of each node, and surrogate variables to be used if the primary splitter is missing at each node (Table 4-4). The top competitors are displayed in decreasing order of importance for CLIP, SEWI and MRW in table 4-4. The improvement scores are a measure of the quality of the split (higher scores are better), this is where the variance reduction occurs due to the split. The improvement within a node has to be weighted by the fraction of cases reaching that node.

The best competitor, distance to big city, split at the value 46232.50 m and yielded an improvement of 0.09532, quite similar to the main splitter (distance to town) where we observed an improvement of 0.09539 in CLIP study area. CART starts with the cells that are located within red nodes (e.g. node 4, 7 and 15) that have the highest

suitability for agriculture change and CART identifies those cells as agriculture first (Figure 4-2 and 4-3). Then, CART converts the cells with lower suitability for agriculture change that is located within light red nodes (e.g. node 5 and 11). This procedure continues until CART satisfies the total number of reference agriculture transitions in CLIP (Table 4-3). Similarly, distance to road as the best competitor, split at the value 157.20 m and yielded an improvement of 0.04514, about half of the main splitter (distance to urban) improvement of 0.08669 in SEWI. Similarly, the cells within node 3, 8 and 9 are more probable for urbanization in SEWI. Following these nodes, cells within node 6 have the highest suitability for urbanization. It is not surprising that the distance to urban variable contains unique information not reflected in the other variables (Figure 4-3). Finally, distance to forest as the best competitor, split at the value of 377.68 m and yielded an improvement of 0.08790, similar to the main splitter (distance to shrub) improvement of 0.09776 in MRW. Finally, the cells within node 3, 5, 6, 7 and 9 are first candidates for transition to forest in MRW. Following these nodes, cells within node 4, 11 and 12 have the highest suitability for forest transition. Similarly, CART continues this procedure until it satisfies the total number of reference urban and forest transitions in SEWI and MRW, respectively (Table 4-3).

4.4.2 MARS

Figure 4-4 shows the point where GCV most minimizes the error. The best MARS model is expressed using 38 basis functions for 12 variables in CLIP, 34 basis functions for 17 variables in SEWI and 40 basis functions for 16 variables in MRW (Table 4-5). Backward step runs to select the best model with the lowest GCV. Figure 4-4

also shows that the lowest GCV (i.e. optimal MARS model) is 0.1495, 0.1363 and 0.1567 for the MARS model in CLIP, SEWI and MRW (0 means perfect fit and 1 represents the performance close to random), respectively. R-squared values improved as a result from using additional basis functions and a different functional form for the regression equations (Figure 4-5). The largest R-squared value was 0.3850 in CLIP, 0.45386 in SEWI and 0.3697 in MRW. GCV, R-squared values and the number of basis functions in three study areas also indicate that (like relative cost in CART) agriculture and forest regrowth patterns in CLIP and MRW (higher GCV; lower R-square; more basis function) are more complicated than the urbanization pattern in SEWI.

The ANOVA summarizes the MARS model and the output by aggregating the basis functions involving one variable which are grouped together (Figure 4-6). The variable with the larger standard deviation has the greater contribution to the overall explanatory power of the MARS model (Figure 4-6). Distance to big city, with a standard deviation of 0.11483 and 2 basis functions (Table 4-5), distance to urban with a standard deviation of 0.28264 and 1 basis function, and distance to forest with a standard deviation of 0.180589 and 2 basis functions, show greater contributions to the simulation of agriculture, urban and forest growth in CLIP, SEWI and MRW, respectively (Table 4-5; Figure 4-6). Following the most significant variables, distance to town, distance to road and distance to shrub with a standard deviation of 0.09445, 0.12943 and 0.125071, and 3, 2 and 2 basis functions, indicate greater contributions to the simulation of agriculture, urban and forest growth in CLIP, SEWI and MRW, respectively (Table 4-5; Figure 4-6). Precipitation in CLIP with 8 basis functions, density of urban in SEWI with 5 basis functions and elevation in MRW with 10 basis functions include the highest number of

basis functions in MARS because these three variables show the most changes across their ranges of values (Table 4-5).

Table 4-5 shows the optimal model of MARS models for agriculture, urban and forest growth in CLIP, SEWI and MRW. MARS found two knots (around 10.816 km and 52.086 km) or three sub-regions (Figure 4-7) for distance to big city driver in CLIP (Table 4-5). The slope is zero for the distance less than 10.816 km and negative for the other two following intervals (Figure 4-7). The cells are located less than 11 km to the town (i.e. buffer 11 km around the town) have the similar and constant suitability, 0.48, for agriculture change. Thereafter, the suitability of agriculture change drop sharply for the distance between 10.816 km and 52.086 km. Lastly, the probability of agriculture drops slowly (smaller coefficient) for the distance between 52.086 km and 200 km.

For the urban growth simulation in SEWI, MARS found only one knot (around 67 m) or two sub-regions for distance to urban driver (Table 4-5). The slope is negative for the distance less than 67 m and zero for distance over 67 m (Figure 4-7). The suitability of urban change drop from 0.9 to 0.7 for sites nearer to existing urban areas (less than 67 m); however, the probability is constant for the distance between 67 m to 1500 m (Figure 4-7). For forest growth simulation in MRW, MARS also found one knot (around 67.082 m) or two sub-regions for distance to forest driver (Figure 4-7). The slopes are negative for the both sub-regions. The suitability of forest growth drops from 0.6 to 0.5 for the sites nearer to existing forest areas (less than 67 m); however, it changes from 0.5 to 0.3 for the distance between 67 m and 1800 m (Figure 4-7).

We also compared the calculated split in CART with the obtained knot in MARS, which create sub-regions, for significant drivers in three study areas (Table 4-4 and 4-5).

For CLIP, the calculated splits in CART, and the obtained knots in MARS, are 11.112 km and 18.384 km for distance to town and 46.232 km and 52.086 km for distance to big city (Table 4-4 and 4-5). Similarly in SEWI, for CART and MARS distance to urban split in 142 m and 67 m and distance to road split in 157 m and 218 m (Table 4-4 and 4-5). Finally in MRW, for CART and MARS, distance to shrubland split in 150 m and 140 m while distance to forest split in 377 m and 67 m (Table 4-4 and 4-6). Figure 4-7 also shows that the distance to road indicates an opposite behavior for urban and forest growth in SEWI and MRW, respectively. The coefficients are negative for the both sub-regions in SEWI; however, the coefficients are positive for both sub-regions in MRW (Figure 4-7). Thus, the suitability of urban growth is more likely when we are closer to the roads; however, the probability of forest growth is more likely when we are further from the roads (Figure 4-7).

4.4.3 LTM

Figure 4-8 plots the MSE across training cycles of the LTM for each of the three study areas. MSE starts around 0.123, 0.17 and 0.145 (0 means perfect fit and 1 represents the performance of random), drops through 5000 cycles in CLIP, MRW and SEWI, respectively. We halted the training after 50,000 cycles in three study areas where the MSE reached a stable minimum; at 0.114, 0.14 and 0.125 in CLIP, MRW and SEWI, respectively. The network files from the training results were saved and used to create the probability and prediction map in three study areas (Tayyebi et al. 2012). In contrast to the CART that all cells within a node have similar and exact suitability value, each cell in LTM and MARS usually has a unique suitability value for change.

4.4.4 Ranking variables in CART and MARS

The model variables were ranked from most to least important and displayed for MARS and CART in Table 4-6. To calculate variable importance scores, MARS refits the model after dropping all terms involving the variable and calculating the reduction in goodness-of-fit. Similarly, the variable importance is given a rank in the CART model as a variable's contribution to the overall tree when all nodes are examined. The column "relative priority" lists the relative importance (in percentage) of each variable. CART and MARS agree with most of the significant drivers to simulate agriculture in CLIP and urban in SEWI. But these models determined different significant drivers for forest growth simulation in MRW. Distance to town, distance to big city and precipitation were found to have a maximum influence on agriculture growth simulation in CLIP. Distance to urban, distance to road and distance to wetland are significant variables to simulate urban growth in SEWI. Distance to shrub, distance to road and distance to forest are significant factors according to the CART model while distance to forest, distance to shrub land and wetland are the most significant variables to simulate forest growth in MRW according to the MARS.

4.4.5 Terminal node in CART

Figure 4-9 provides a representation of the ability of the tree to capture the agriculture, urban and forest expansion across the terminal nodes. We sorted the nodes according to the growth so that the nodes with the highest concentrations of agriculture, urban and forest growth in CLIP, SEWI and MRW are located to the right in the tree (Figure 4-9). Nodes 12, 1 and 8 (follow figure 4-3 to find the node numbers) have the

lowest concentration of agriculture, urban and forest growth while nodes 2, 9 and 2 have the highest concentration of agriculture, urban and forest growth in CLIP, SEWI and MRW, respectively (Figure 4-9).

4.4.6 Calibration of three models using cross tabulation matrices and ROC values

Figure 4-10 shows the reference agriculture change and error maps that are derived from three models by comparing the simulated agriculture growth with reference change for CLIP. We could not show the error maps for SEWI and MRW because we took random samples from the entire study area as stated before. For the CART models, most of the FP occurs around the TP because CART simulates the new growth in buffers and is not dependent upon the probability of cell for growth such as MARS and LTM. However, the error map of MARS and LTM are more similar to each other.

The cross tabulation matrix (Figure 4-11) shows how many samples were correctly classified in LTM, CART and MARS for the testing run. Results show that CART, MARS and LTM simulate agriculture growth 61.72%, 65.13% and 68.63% correctly and non-agriculture 86.01%, 87.26% and 88.54% correctly in CLIP for testing data, respectively. Similarly, CART, MARS and LTM simulate urban growth 76.45%, 80.15% and 80.70% correctly and non-urban 78.15%, 81.59% and 82.10% correctly in SEWI for testing data, respectively. Finally, CART, MARS and LTM simulate forest growth 64.42%, 68.89% and 70.16% correctly and non-forest 81.38%, 83.73% and 84.39% correctly in MRW for testing data, respectively (Figure 4-11).

Table 4-7 summarizes the comparison of ROC for the three study areas. Although the three model's results were similar to each other, improvement of LTM and MARS

over CART was evident for three data sets across testing data. Furthermore, ROC for LTM and MARS for three study areas were similar to each other. However, the LTM performed slightly better than MARS. In the three data sets, the best results were obtained with LTM to simulate urban growth in SEWI across the testing data (ROC = 0.8958). A good model needs to deliver substantially larger values than an ROC of 0.50. Thus, CART, MARS and LTM models show excellent performance as all produced values of ROC over 0.80 across cross validation and testing data (Table 4-7).

4.4.7 Comparison of LTM, CART and MARS simulations using cross tabulation matrix

We employed a cross tabulation matrix used to compare the projections of LTM, CART and MARS, for the three study areas with each other. The rows show the predicted class from the first model and the columns of the table represent the predicted class from the second model. Diagonal entries indicate agreement and off-diagonal entries indicate disagreement of predicted maps between two models. We compared two models at each time in three study areas (CART vs LTM; CART vs MARS and LTM vs MARS). CART and MARS were more similar to each other having 92.61% and 79.77% agreement in non-agriculture and agriculture projection in CLIP (Figure 4-12). Similarly, LTM and MARS were more similar to each other having 92.57% and 91.98% agreement in non-urban and urban projection in SEWI (Figure 4-12). Lastly, LTM and MARS again were more similar to each other having 94.35% and 89.20% agreement in non-forest and forest projection in MRW (Figure 4-12).

4.5 Discussion

Each of models shows some characteristics which may be interesting in the context of LUCC. CART and MARS models are easier to interpret, especially for identifying the relative importance of predictor variables (Table 4-6) as well as their critical values (Table 4-4 and 4-5). Calibrations of CARTs (terminal and non-terminal nodes) and MARS (basis function) are much easier to understand than ANNs (weights and biases). When predictive accuracy is a key concern, the LUCC modelers need to choose ANNs rather than MARS and CART (Table 4-7 and Figure 4-11). Information about importance of predictor variables and their ranges will be helpful both for better calibrating of LUCC models, urban planners, policy makers and natural resource management. Therefore CART and MARS may be preferred to ANNs when ease of explanation rather than predictive accuracy is required. The effectiveness of any model is largely dependent upon the characteristics of the data structure used to fit the model (Goss and Vozikis, 2002). ANN and non-linear regression models provided comparably satisfactory predictions in reverse engineering applications (Pijanowski et al. 2007; Ray and Pijanowski, 2010) using all non-categorical variables (Feng and Wang, 2002); however, the regression model produced a slightly better performance in model verification. ANNs do better than CART models on multimodal classification problems for large data sets with few attributes (Brown et al. 1993); however, the CART model did better than the ANNs with smaller data sets and with large numbers of irrelevant attributes.

We explored different scenarios across space and time to dissect the performance of CART, MARS and ANNs models in LUCC. MARS is as good as ANN for analyzing complex structures which are commonly found in LUCC data (e.g. non-linearity and interactions; Table 4-7). CART models are scalable to large problems and can handle smaller data sets than ANN models (Marcham et al. 2000). The small decision trees (CART) or small number of basis functions without interaction (MARS) are easier (simple models) to explain to urban planners, decision makers and natural resource managers for LUCC modelers (Domingos, 1999). CART with more than 7-10 branches are not needed for capturing most human multi-attribute decision-making problems (Ben-David and Sterling, 2009). We found that CART, with 15-20 nodes, is enough to simulate LUCC. ANNs and MARS have been compared in a time series forecasting task using the noisy and clean data (Calvo et al. 1998). ANN outperformed MARS on the clean data set. In an application of identifying important factors in fraud, the ANN outperformed MARS, though the results were not statistically significant. However, the results were obtained on a relatively small database and may not generalize to other databases. In addressing nominal level variables, MARS is able to cluster together the categories of the variables that have similar effects on the dependent variable (Francis, 2001) ANN is not able to do that. CART and MARS can create surrogates for the missing variables and can be used on applications using data with missing values on many variables. In the future, each of the three models (MARS, ANNs and CART) can be combined into a hybrid model to improve predictive accuracy of LUCC models.

CART and MARS models are normally quite fast but were slower in our case (SPM software) because of the forward and backward procedures used to calculate the

best tree size in CART and best number of basis functions calculated for the MARS models. Of the three methods, ANNs were the slowest for simulating LUCC. Outliers in data (Ray et al. 2012) can significantly change the position of splits, number of levels (i.e. nodes) and basic function values in CART and MARS; in other words, outliers can change the local nature of the model. To train ANNs (in our case approximately 30,000 samples), it typically takes approximately 15 minutes on a Quad-core Windows 7 based workstation class computer while CART and MARS requires approximately 5 minutes (e.g. maximum 60 nodes or basis function). The Salford version of MARS and CART is able to automatically prune the model. This is a very attractive feature, together with the significant speed up that MARS and CART provide a clear advantage over standard ANNs, which can be redundant and are in general slow to train. The concept of pruning can be applied to ANNs as well but is much more computationally demanding. However, when using ANNs, one must be much more careful to avoid over-fitting the data (Bishop, 1995), a problem which is particularly apparent on smaller data sets as the number of adjustable parameters may exceed the number of available data points. From our perspective, the predictive ability of ANN models was in general better than MARS and CART models in LUCC (Table 4-7). However, as the number of available data points increases, ANNs, MARS and CART reach approximately the same level of accuracy (Table 4-7).

It was not surprising that CART performed worse than ANN and MARS in the three study areas for LUCC modeling. When we explored all three LUCC simulation areas, more advantages were seen in the use of MARS and ANN for agriculture and urban prediction in CLIP and SEWI, but smaller differences were observed for forest

simulation in MRW because of the lack of non-linear relationships between the response and predictor variables. While little appreciable difference was detected between the models, better fit may be obtained using more flexible statistical techniques. CART produced the greatest accuracy when interactions were present in the data. It was also among the most accurate methods in the case of strictly linear population models (Holden et al. 2011).

4.6 Conclusion

This chapter attempts to compare one global parametric model (e.g. LTM) with two local non-parametric models (e.g. MARS and CART) to simulate LUCC patterns. This study aimed to investigate the performance of LTM, CART and MARS methods in predictions of the agriculture, forest and urban growth in three different regions. A comparison is carried out that indicates the LTM can simulate slightly better than MARS and CART. Unlike other well-known conventional global parametric models, MARS and CART do not obtain a regression equation for the population in the data. Instead, they split the whole model into linear regions and produce separate functions for each generated linear area. CART is much simpler to interpret than the MARS and LTM, making it more likely to be practical in a LUCC model.

4.7 References

- Abraham, A., N. Philip and B. Joseph, (2001). Will We Have a Wet Summer? Soft Computing Models for Long Term Rainfall Forecasting. In: 15th European Simulation Multiconference (ESM, August/September 2001), Modeling and Simulation 2000, Kerckhoffs, E.J.H. and M. Snorek (Eds.). Czech Republic, Prague: 1044-1048.
- Abdel-Aty, M., Haleem. K., (2011). Analyzing angle crashes at unsignalized intersections using machine learning techniques. *Accid Anal Prev.* 43(1):461-70.
- Aertsen W, Kint V, Van Orshoven J, Muys B. (2011). Evaluation of modeling techniques for forest site productivity prediction in contrasting ecoregions using stochastic multicriteria acceptability analysis (SMAA). *Environ Modell Softw* 26:929–937.
- Almeida, A. P .G., Galão, R. P., Sousa, C. A., Novo, M. T., Parreira, R., Pinto, J., Piedade, J. and Esteves, A. (2008). Potential mosquito vectors of arboviruses in Portugal: species, distribution, abundance and West Nile infection. *Transactions of the Royal Society of Tropical Medicine and Hygiene* 102, 823-832.
- Areerachakul, S., and Sanguansintukul, S. (2010). Classification and Regression Trees and MLP Neural Network to Classify Water Quality of Canals in Bangkok, Thailand. *International Journal of Intelligent Computing Research (IJICR)*, Volume 1, Issue 1/2, March/June 2010.
- Armesto, J. J., Smith-Ramírez, C., Carmona, M. R., Celis-Diez, J. L., Díaz, I. A., Gaxiola, A., Gutiérrez, A. G., Nuñez-Avila, M. C., Pérez, C. A., Rozzi, R.. (2009). Old-growth temperate rainforests of South America: Conservation, plant–animal interactions, and baseline biogeochemical processes. Pages 367–390 in Wirth C, Gleixner G, Heiman M, eds. *Old-Growth Forests*. Springer.
- Areerachakul, S. and Sanguansintukul, S., (2010). Classification and Regression Trees and MLP Neural Network to Classify Water Quality of Canals in Bangkok, Thailand. *International Journal of Intelligent Computing Research (IJICR)*, Volume 1, Issue 1/2, March/June 2010.
- Aspinall, R. J. (2004) Modelling land use change with generalized linear and generalized additive models – a multi-model analysis of change between 1860 and 2000 in Gallatin Valley, Montana. *Journal of Environmental Management*, 72, 91-103.
- Austin, M. P. and Gaywood, M. J. (1994). Current problems of environmental gradients and species response curves in relation to continuum theory. *J. Veg. Sci.* 5: 473-482.
- Batty, M. and Y. Xie, (1994). From cells to cities, *Environment and Planning B*, 21, s31-s48.
- Ben-David, A., Sterling, L., Tran, T. (2009). Adding monotonicity to learning algorithms may impair their accuracy. *Expert Systems with Applications* 36 (2009) 6627–6634.
- Bishop, C.M. (1995), *Neural Networks for Pattern Recognition*, Oxford: Oxford University Press.
- Breiman, L., Friedman, J. H., Olshen, R.A., and Stone, C.J. (1984). *Classification and Regression Trees*. Belmont, CA: Wadsworth.
- Brown, D. E., Corruble, V., & Pittard, C. L. (1993). A comparison of decision tree classifiers with backpropagation neural networks for multimodal classification problems. *Pattern Recognition*, 26(6), 953–961.

- Cai, Z., S. Sawamoto, C. Li, G. Kang, J. Boonjawat, A. Mosier, and R. Wassmann. (2003). Field validation of the DNDC model for greenhouse gas emissions in East Asian cropping systems. *Global Biogeochem. Cycles* 17(4), doi:10.1029/2003GB002046.
- Calvo, R. A., Partridge, M. G., & Jabri, M. A. (1998). A comparative study of principal component analysis techniques. In *Proceedings of the ninth Australian conference on neural networks*, Brisbane, QLD.
- Carmona, A., Nahuelhual, L., Echeverría, C., Báez, A., (2010). Linking farming systems to landscape change: an empirical and spatially explicit study in southern Chile. *Agr. Ecosyst. Environ.* 139, 40–50.
- Clarke, K.C., Hoppen, S., Gaydos, L., (1997). A self-modifying cellular automaton model of historical urbanization in the San Francisco Bay area. *Environmental Planning B: Planning and Design* 24, 247–261.
- Cravne, P. and Wahba, G. (1979). Smoothing noisy data with Spline functions: estimating the correct degree of smoothing by the method of generalized cross-validation. *Numer. Math.*, 31, 377-403.
- De Andrés Suárez, J.; Lorca Fernández, P.; Cos Juez, F.J. de; Sánchez-Lasheras, F. (2011). Bankruptcy forecasting: A hybrid approach using Fuzzy cmeans clustering and Multivariate Adaptive Regression Splines (MARS)., *Expert Systems with Applications*, 38(3), pp. 1866-1875.
- Diaz, G. I., Nahuelhual, L., Echeverría, C., Marín, S. (2011). Drivers of land abandonment in Southern Chile and implications for landscape planning. *Landscape and Urban Planning* 99 (2011) 207–217.
- Dietzel, C., and Clarke, K. C. (2006). Decreasing computational time of urban cellular automata through model portability. *Geoinformatica*. vol. 10, no. 2. pp. 197-211.
- Domingos, P., (1999). MetaCost: A general method for making classifiers cost-sensitive. In: *Proc. Fifth ACM SIGKDD Internat. Conf. on Knowledge Discovery and Data Mining*, pp. 155–164.
- FAO. (2009). Seed security for food security in the light of climate change and soaring food prices: challenges and opportunities. Rome, FAO. (available at <ftp://ftp.fao.org/docrep/fao/meeting/016/k4275e.pdf>).
- Feng, C.-X., and Wang, X. (2002). Digitizing uncertainty modeling for reverse engineering applications: Regression versus neural networks. *Journal of Intelligent Manufacturing*, 13(3), 189–199.
- Fielding, A. H. and Bell, J. F. (1997). A review of methods for the assessment of prediction errors in conservation presence/absence models. *Environmental Conservation*, 24, 38–49.
- Francis, L. (2001). *Neural Networks Demystified*. Casualty Actuarial Society Forum, pp 253-320.
- Friedman, J. H. and Silverman, B. W. (1989). Flexible parsimonious smoothing and additive modeling (with discussion). *Technometrics*, 31, 3-39.
- Friedman, J. H. (1991). Multivariate Adaptive Regression Splines (with discussion). *Annals of Statistics* 19, 1.
- Gansky, S. A. (2003). Dental data mining: potential pitfalls and practical issues. *Adv Dent Res* 17:109–114.

- Gelfand, S. B. and Delp, E. J. (1991). On Tree Structured Classifiers, in Sethi and Jain (eds.), pp. 51-70.
- Gobim, A, Campling, P, Feyen, J. (2002). Logistic modeling to derive agricultural land determinants: a case study from southeastern Nigeria. *Agriculture, Ecosystem and Environment*, 89, pp. 213-228.
- Goss, E. and Vozikis, G. S. (2002). Improving Health Care Organizational Management Through Neural Network Learning. *Health Care Management Science*; 5(3), 221-227.
- Hardle, W., M. Müller, S. Sperlich, and A. Werwatz. (2004). *Nonparametric and Semiparametric Models*. Berlin: Springer Series in Statistics.
- He, Z. and Lo, C. (2007). Modeling urban growth in Atlanta using logistic regression. *Computers, Environment and Urban Systems*, 31(6), 667-688.
- Holden, Z. A., Crimmins, M., Cushman, S. A., Littell, J. (2011). Empirical modeling of spatial and temporal variability in warm season nocturnal air temperatures across two North Idaho mountain ranges, USA. *Agr. For. Meteorol.* 151, 261–269.
- Irwin, E., Geoghegan, J. (2001). Theory, data, methods: developing spatially-explicit economic models of land use change. *Agric. Ecosyst. Environ.* 85, 7-24.
- Imran, K., Ture, M., A. Kurum. T. (2008). Comparing performances of logistic regression, classification and regression tree, and neural networks for predicting coronary artery disease. *Expert Systems with Applications*, 34, 366–374.
- Jenerette, G. D. and Wu, J. (2004). Interactions of ecosystem processes with spatial heterogeneity in the puzzle of nitrogen limitation. *Oikos* 107: 273-282.
- Jordanov, I., and T. Rafik. (2004). Local Minima Free Neural Network Learning, Proc. of IEEE IS'04 International Conference on Intelligent Systems, Bulgaria, pp. 34-39.
- Kalnay, E., Cai, M., (2003). Impacts of urbanization and land-use change on climate, *Nature*, 423, 528-531.
- Kayri, M. (2010). The Analysis of Internet Addiction Scale Using Multivariate Adaptive Regression Splines. *Iranian J Publ Health*, Vol. 39, No.4, 2010, pp.51-63.
- Kirschbaum, M. U. F. (2000). Forest growth and species distribution in a changing climate. *Tree Physiology* 20, 309–322.
- Lambin, E., Baulies, X., Bockstael, N., Fischer, G., Krug, T., Leemans, R., Moran, E., Rindfuss, R., Sato, Y., Skole, D., Turner II, B. and Vogel, C. (1999). *Land-Use and Land-Cover Change (LUCC) Implementation Strategy*, IGBP Report 48.
- Lambin, E. F., Turner, B. L., Geist, H. J., Agbola, S. B., Angelsen, A., Bruce, J. W., Coomes, O. T., Dirzo, R., Fischer, G., Folke, C., George, P. S., Homewood, K., Imbernon, J., Leemans, R., Li, X., Moran, E. F., Mortimore, M., Ramakrishnan, P. S., Richards, J. F., Skanes, H., Steffen, W., Stone, G. D., Svedin, U., Veldkamp, T. A., Vogel, C., Xu, J. (2001). The causes of land-use and land-cover change: moving beyond the myths. *Global Environmental Change* 11 261–269.
- Lambin, E. F., and H. J. Geist, eds. (2006). *Land-use and Land-Cover Change: Local Processes and Global Impacts*. Berlin: Springer.
- Landis, J., Zhang, M., (1998). The second generation of the California urban futures model: part 2. Specification and calibration results of the land-use change sub-model. *Environment and Planning A* 25, 795–824.
- Last, M., and O. Maimon, (2004). A Compact and Accurate Model for Classification, *IEEE Transactions on Knowledge and Data Engineering*, Vol. 16, No. 2, pp. 203-215.

- Lawrence, S., C. L. Giles, and A. C. Tsoi. (1997). Lessons in neural network training: Overfitting may be harder than expected. In *Proceedings of the Fourteenth National Conference on Artificial Intelligence (AAAI-97)*, pages 540–545.
- LeBlanc, M. (1993). An adaptive expansion method for regression. Technical Report, Department of Statistics, University of Toronto.
- Li, X., and Yeh, A. G. O., (2002). Neural-network-based cellular automata for simulating multiple land use changes using GIS. *International Journal of Geographical Information Science* 16(4): 323-343.
- Li, X., G. C. Nsofor., L. Song. (2009). A comparative analysis of predictive data mining techniques, *International Journal of Rapid Manufacturing* 1 (2) 150–172.
- Lumley T, Sutherland P, Rossini A, Lewin-Koh N, Cook D, Cox Z. (2002). Visualising high-dimensional data in time and space: ideas from the Orca project. *Chemometrics and Intelligent Laboratory Systems* 60: 189-95.
- Manel, S., Dias, J. M., Ormerod, S. J. (1999). Comparing discriminant analysis, neural networks and logistic regression for predicting species distributions: a case study with a Himalayan river bird. *Ecological Modelling* 120 (1999) 337–347.
- Marcham, I. S., Mathieu, R. G. and Wray, B. A. (2000). Kanban setting through artificial intelligence: A comparative study of artificial neural networks and decision trees. *Integrated Manufacturing*, 11(4), 239.
- Mas, J. F., Vela'zquez, A., Di'az-Gallegos, J. R., Mayorga-Saucedo, R., Alcantara, C., Bocco, G., Castro, R., Fern'andez, T., Pe'rez-Vega, A., (2004). Assessing land/use cover changes: a nationwide multirate spatial database for Mexico. *International Journal of Applied Earth Observation Geoinformatics* 5, 249–261.
- Mertens, B. Lambin, E. F. (2000) Land-Cover-Change Trajectories in Southern Cameroon. *Annals of the Association of American Geographers*, 90(3), pp467-494.
- Millington, J.D.A., Perry, G.L.W., Romero-Calcerrada, R. (2007). Regression techniques for examining land use/cover change: a case study of a Mediterranean landscape. *Ecosystems* 10, 562–578.
- Moisen, G. G. and Frescino, T. S. (2002). Comparing five modeling techniques for predicting forest characteristics. *Ecological Modelling* 157: 209-225.
- Muñoz, J. and Felicísimo, Á. M. (2004). Comparison of statistical methods commonly used in predictive modeling. *Journal of Vegetation Science*, 15: 285-292.
- Munroe, D., Southworth, J. and Tucker, C. M. (2001). The dynamics of land-cover change in western Honduras: Spatial autocorrelation and temporal variation. *Conference Proceedings. American Agricultural Economics Association. AAEA-CAES 2001 Annual Meeting* Accessed July 10, 2004: http://agecon.lib.umn.edu/cgi-bin/pdf_view.pl?paperid=2611.
- Nair, P. K. R. (1993). *An introduction to agroforestry*. Dordrecht, Netherlands, Kluwer Academic Publishers.
- NRC, (2005). *Radiative Forcing of Climate Change: Expanding the Concept and Addressing Uncertainties*. National Research Council, 208 pp.
- NCR, (2007). *Earth Science and Applications from Space: National Imperatives for the Next Decade and Beyond*. National Research Council, 456 pp.

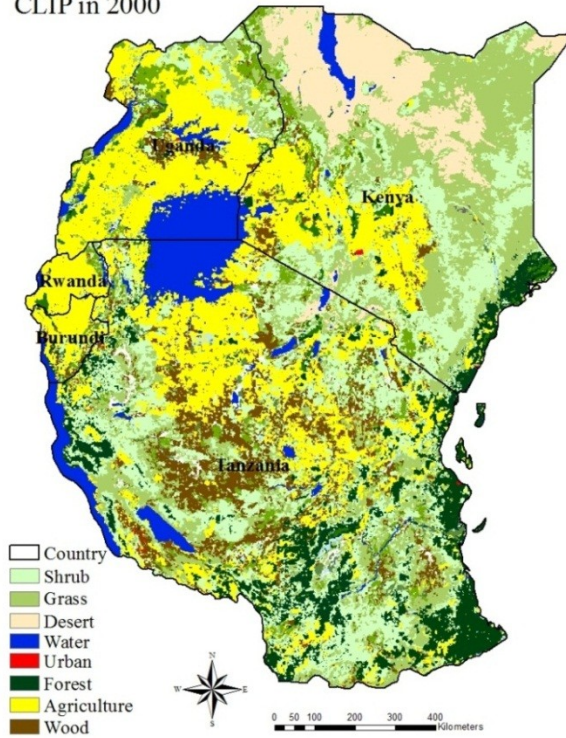
- Olson, J., G. Alagarwamy, J. Andresen, D. Campbell, A. Davis, J. Ge, M. Huebner, B. Lofgren, D. Lusch, N. Moore, B. Pijanowski, J. Qi, P. Thornton, N. Torbick, J. Wang. (2008). Integrating Diverse Methods to Understand Climate-Land Interactions in East Africa. *GeoForum* 39(2):898-911.
- Peng, Y., U. Lohmann, R. Leitch, C. Banic, and M. Couture, (2002). The cloud albedocloud droplet effective radius relationship for clean and polluted clouds from RACE and FIRE.ACE. *J. Geophys. Res.*, 107 (D11), doi:10.1029/2000JD000 281.
- Pielke, R. A. Sr. (2005). Land Use and Climate Change. *Science* 310, 1625 (2005). DOI: 10.1126/science.1120529.
- Pijanowski, B. C., Daniel G. Brown, Bradley A. Shellito, Gaurav A. Manik. (2002a). Using neural networks and GIS to forecast land use changes: a Land Transformation Model. *Computers, Environment and Urban Systems*. 26, 553–575.
- Pijanowski, B. C., Shellito, B., Pithadia, S., Alexandridis, K. (2002b). Forecasting and assessing the impact of urban sprawl in coastal watersheds along eastern Lake Michigan. *Lakes & Reservoirs: Research and Management* 2002 7: 271–285.
- Pijanowski B. C., Pithadia S., Shellito B. A., Alexandridis, K. (2005). Calibrating a neural network based urban change model for two metropolitan areas of Upper Midwest of the United States. *International Journal of Geographical Information Science*. 19:197–215.
- Pijanowski, B. C., K. Alexandridis and D. Mueller. (2006). Modeling urbanization patterns in two diverse regions of the world. *Journal of land use science*. (1): 83-108.
- Pijanowski, B., D. K. Ray, A. D. Kendall, J. M. Duckles, and D. W. Hyndman. (2007). Using back-cast land-use change and groundwater travel time models to generate land-use legacy maps for watershed management. *Ecology and Society* 12 (2):25.[online] URL: <http://www.ecologyandsociety.org/vol12/iss2/art25/>.
- Pijanowski, B. C., Tayyebi, A., Delavar, M. R., and Yazdanpanah, M. J. (2009). Urban expansion simulation using geographic information systems and artificial neural networks. *International Journal of Environmental Research*, 3(4), 493-502.
- Pijanowski, B., L. Iverson, C. Drew, H. Bulley, J. Rhemtulla, M. Wimberly, A. Bartsch and J. Peng. (2010). Addressing the Interplay of Poverty and the Ecology of Landscapes: A Grand Challenge Topic for Landscape Ecologists? *Landscape Ecology*. doi:10.1007/s10980-009-9415-z.
- Pijanowski, B. C., Moore, N., Mauree, D., Niyogi, D. (2011). Evaluating Error Propagation in Coupled Land–Atmosphere Models. *Earth Interact.*, 15, 1–25.
- Pijanowski, B.C., and K. D. Robinson. (2011). Rates and patterns of land use change in the Upper Great Lakes States, USA: A framework for spatial-temporal analysis. *Landscape and Urban Planning*. DOI:10.1016/j.landurbplan.2011.03.014.
- Pontius, R. G. Jr., J. Cornell and C. Hall. (2001). Modeling the spatial pattern of land-use change with GEOMOD2: application and validation for Costa Rica. *Agriculture, Ecosystems & Environment* 85(1-3): 191-203.
- Pontius, R. G. Jr., and L. Schneider. (2001). Land-use change model validation by a ROC method for the Ipswich watershed, Massachusetts, USA. *Agriculture, Ecosystems & Environment* 85(1-3) p.239-248.

- Pontius Jr., R. G. and Batchu, K. (2003). Using the Relative Operating Characteristic to Quantify Certainty in Prediction of Location of Land Cover Change in India. *Transactions in GIS*, 7(4): 467–484.
- Pontius, R. G. Jr., Huffaker, D., Denman, K. (2004). Useful techniques of validation for spatially explicit land-change models. *Ecological Modeling*, 179(4), 445-461.
- Pontius, R. G. Jr., Boersma, W., Castella, J. C., Clarke, K., T de Nijs, C Dietzel, Z Duan, E Fotsing, N Goldstein, K Kok, E Koomen, C D Lippitt, W McConnell, A Mohd Sood, B Pijanowski, S Pithadia, S Sweeney, T N Trung, A T Veldkamp, and P H Verburg. (2008). Comparing input, output, and validation maps for several models of land change. *Annals of Regional Science*, 42(1): 11-47.
- Pontius, R. G. Jr and M. Millones. (2011). Death to Kappa: birth of quantity disagreement and allocation disagreement for accuracy assessment. *International Journal of Remote Sensing* 32(15): 4407-4429.
- Psichogios, D. C., Ungar, L. H. (1992). A Hybrid Neural Network-First Principles Approach to Process Modeling. *AIChE J.* 1992, 38, 1499-1511.
- Razi, M. A. and Athappilly, K. (2005). A comparative predictive analysis of neural networks (NNs), nonlinear regression and classification and regression tree (CART) models. *Expert Systems with Applications* 29 (2005) 65–74.
- Ray, D. K., and B. C. Pijanowski, (2010). A backcast land use change model to generate past land use maps: application and validation at the Muskegon river watershed of Michigan, USA, *journal of land use science*, 5: 1, 1-29.
- Ray, D. K., Pijanowski, B. C., Kendall, A. D., Hyndman, D. W. (2012). Coupling land use and groundwater models to map land use legacies: Assessment of model uncertainties relevant to land use planning. *Applied Geography* 34 (2012) 356-370.
- Read, J. and N. Lam (2002). Spatial methods for characterizing land cover and detecting land-cover changes for the tropics. *International Journal of Remote Sensing* 23(12): 2457-2474.
- Refaeilzadeh, P., Tang, L. & Liu, H. (2008). Cross-validation, <http://www.public.asu.edu/~ltang9/papers/ency-cross-validation.pdf>
- Seppelt, R., Voinov, A., (2002). Optimization methodology for land use patterns using spatially explicit landscape models. *Ecological Modeling*. 151 (2/3), 125–142.
- Serneels, S., and E.F. Lambin. (2001). Proximate causes of land-use change in Narok District, Kenya: a spatial statistical model. *Agriculture, Ecosystems and Environment* 85 (2001) 65–81.
- Shellito, B. and B. C. Pijanowski. (2003). Using neural nets to model the spatial distribution of seasonal homes. *Cartography and Geographic Information Systems* 30 (3):281-290.
- Stanton, R. (1997). A Nonparametric Model of Term Structure Dynamics and the Market Price of Interest Rate Risk. *Journal of Finance*. 52, 1973-2002.
- Steinberg, D. and Colla, P. (1997). *CART—Classification and Regression Trees: A Supplementary Manual for Windows*, Salford Systems Inc., San Diego.
- Steinberg, D., Golovnya, M. (2006). *CART 6.0 User's Manual*. Salford Systems, San Diego, CA.

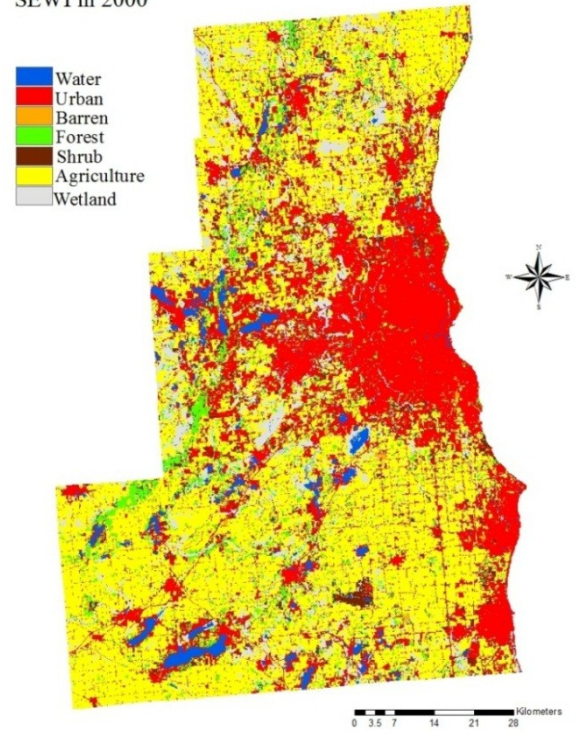
- Stevens, D. and Dragičević, S. (2007). A GIS-based irregular cellular automata model of land-use change. *Environment and Planning B: Planning and Design* 2007, volume 34, pages 708-724.
- Sut, N., and Simsek, O. (2011). Comparison of regression tree data mining methods for prediction of mortality in head injury. *Expert Systems with Applications* 38, 15534-15539.
- Tang, Z., B. Engel, K. Lim, B. Pijanowski and J. Harbor. (2005a). Minimizing the impact of urbanization on long-term runoff. *Journal of the Water Resources Association*. 41(6): 1347-1359.
- Tang, Z., B. A. Engel, B.C. Pijanowski, and K. J. Lim. (2005b). Forecasting Land Use Change and Its Environmental Impact at a Watershed Scale. *Journal of Environmental Management*. 76: 35-45.
- Tayyebi, A., Delavar M. R., Pijanowski, B. C., Yazdanpanah, M. J. (2009a). Accuracy assessment in urban expansion model. In: Devillers R, Goodchild H (eds) *Spatial data quality, from process to decisions*. Taylor and Francis, CRC Press, Canada, pp 107–115.
- Tayyebi, A., Delavar, M. R., Pijanowski, B. C., Yazdanpanah, M. J. (2009b). Spatial variability of errors in Urban Expansion Model: Implications for error propagation, *Spatial Data Quality, From Process to Decisions*, Edited by R. Devillers and H. Goodchild, Taylor and Francis, CRC Press, Canada, pp. 134–135.
- Tayyebi, A., Delavar, M. R., Pijanowski, B. C., Yazdanpanah, M. J., Saeedi, S., and Tayyebi, A. H. (2010). A spatial logistic regression model for simulating land use patterns, a case study of the Shiraz metropolitan area of Iran. In E. Chuvieco, J. Li, & X. Yang (Eds.), *Advances in earth observation of global change*. Springer Press.
- Tayyebi, A., Pijanowski, B. C., A. H. Tayyebi, (2011a). An urban growth boundary model using neural networks, GIS and radial parameterization: An application to Tehran, Iran. *Landscape and Urban Planning* 100, 35-44.
- Tayyebi, A., Pijanowski, B. C., B. Pekin, (2011b). Two rule-based urban growth boundary models applied to the Tehran metropolitan area, Iran. *Applied Geography* 31, 908-918.
- Tayyebi, A., Pekin, B. K., Pijanowski, B. C., Plourde, J. D., Doucette, J., Braun, D. (2012) Hierarchical modeling of urban growth across the conterminous USA: Developing meso-scale quantity drivers for the Land Transformation Model. *Journal of Land Use Science*. DOI: 10.1080/1747423X.2012.675364.
- Tayyebi, A. H., S. Homayouni, J. Shan, M. J. Yazdanpanah, B. C. Pijanowski and A. Tayyebi. (2011a). Model Parameter Uncertainty Assessment in Land Transformation Model. 7th International Symposium on Spatial Data Quality. Coimbra, Portugal, October 12-14, Edited by: Cidalia C. Fonte, Luisa Goncalves, Gil Goncalves, Page 77-82.
- Tayyebi, A. H., S. Homayouni, J. Shan, M. J. Yazdanpanah , B. C. Pijanowski and A. Tayyebi. (2011b). Multi-Scale Analysis Approach of Simulating Urban Growth Pattern using a Land Use Change Model, 7th International Symposium on Spatial Data Quality. Coimbra, Portugal, October 12-14, Edited by: Cidalia C. Fonte, Luisa Goncalves, Gil Goncalves, Page 207-210.

- Theobald, D. M., and N. T. Hobbs. (1998). Forecasting rural land use change: a comparison of regression- and spatial transition-based models. *Geographical and Environmental Modeling* 2(1):57–74.
- Timofeev, R. (2004). Classification and regression trees (CART) theory and applications. Master's thesis, Humboldt University Berlin.
- Ture, M., I. Kurt, A. T. Kurum, and K. Ozdamar. (2005). Comparing Classification Techniques for Predicting Essential Hypertension. *Expert Systems with App.*, 29, 583-588. (Available at: <http://www.elsevier.com/locate/eswa>).
- Turner, B. L., D. Skole, S. Sanderson, G. Fischer, L. Fresco, and R. Leemans. (1995). Land-use and land-cover change science/research plan. IGBP report no. 35 and HDP report no. 7.
- Veldkamp, A., Lambin, E. F., (2001). Editorial: predicting land-use change. *Agriculture, Ecosystems and Environment* 85, 1–6.
- Verburg, P. H., Schot, P. P., Dijst, M. J., Veldkamp, A. (2004). Land use change modeling: current practice and research priorities. *GeoJournal*, 61(4): 309-324.
- Warner, B. and Misra, M. (1996). Understanding neural networks as statistical tools. *The American Statistician*, 50(4), 284–293.
- Washington, C., B. Pijanowski, D. Campbell, J. Olson, J. Kinyamario, E. Irandu, J. Nganga, and P. Gicheru. (2010). Using a role-playing game to inform the development of land-use models for the study of a complex socio-ecological system. *Agricultural Systems*. doi: 10.1016/j.agsy.2009.10.002.
- Wernick, I. K. (2007). Global Warming and the Industrial System, International Relations and Security Network (ISN), Zurich, Switzerland. See <http://www.isn.ethz.ch/pubs/ph/details.cfm?lng=en&id=30366>.
- White, R. and Engelen, G. (1993). Cellular automata and fractal urban form. *Environment and Planning A*. 25, 1175–1199.
- Wiley, M., D. Hyndman, B. Pijanowski, A. Kendall, C. Riseng, E. Rutherford, S. Cheng, M. Carlson, R. Richards, R. Seelbach and J. Koches. (2010). A multi-modeling approach to evaluate the impacts of global change on river ecosystems. *Hydrobiologia* 657:243-262.
- Willert, M. V., Windhorst, K., Techel, G. (2010). Modeling of forest growth and yield in Uganda, Final report, Kampala, Study Commissioned by SPGS, 2010.
- Witten, I. H. and E. Frank. (2000). *Data Mining: Practical Machine Learning Tools and Techniques with Java Implementations*. Morgan Kaufmann, San Francisco.
- Yang, G., L. Bowling, K. Cherkauer, B. Pijanowski and D. Niyogi. (2010). Hydrologic response of watersheds to urbanization in the White River basin, Indiana. *Journal of Hydrometeorology*. doi: 10.1175/2009JHM1143.1.
- Zha, W. and Chan, W-Y. (2005). Objective Speech Quality Measurement Using Statistical Data Mining. *EURASIP Journal on Applied Signal Processing* 2005:9, 1410–1424.
- Zhao, Z. (2008). Parametric and nonparametric models and methods in financial econometrics, *Statistics Surveys*. Vol. 2 (2008) 1-42. ISSN: 1935-7516.
- Zurada, J. M. (1992), *Introduction to Artificial Neural Systems*, Boston: PWS Publishing Company.

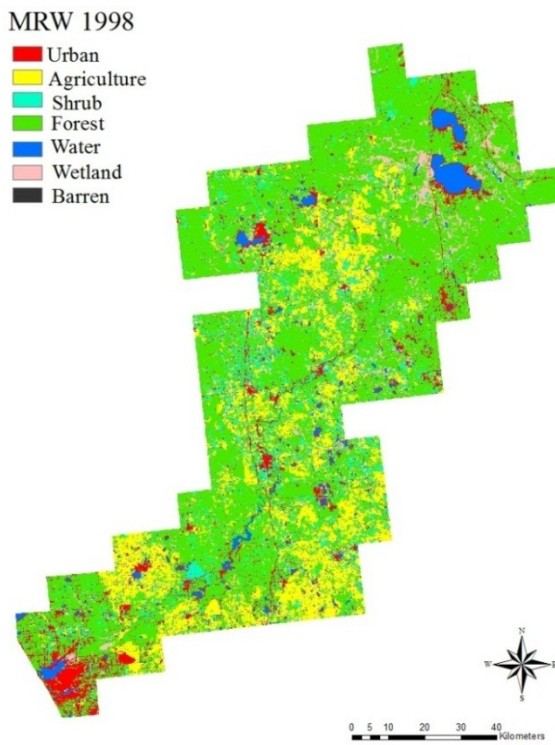
CLIP in 2000



SEWI in 2000



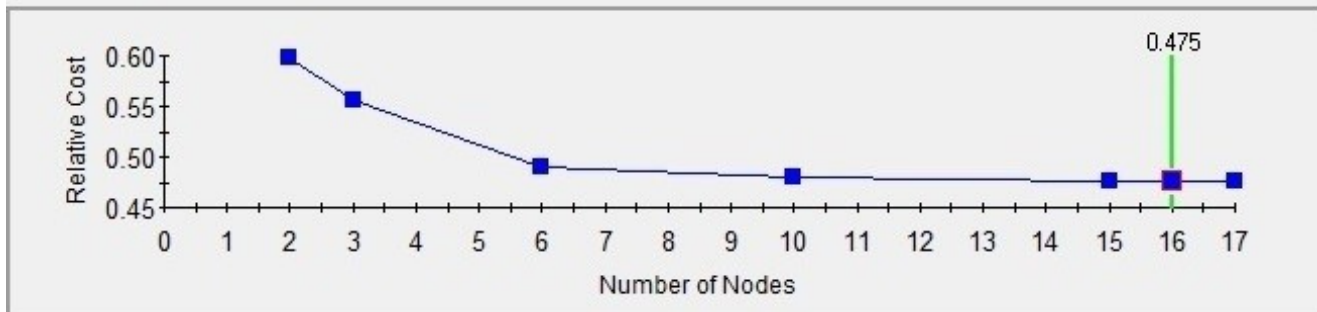
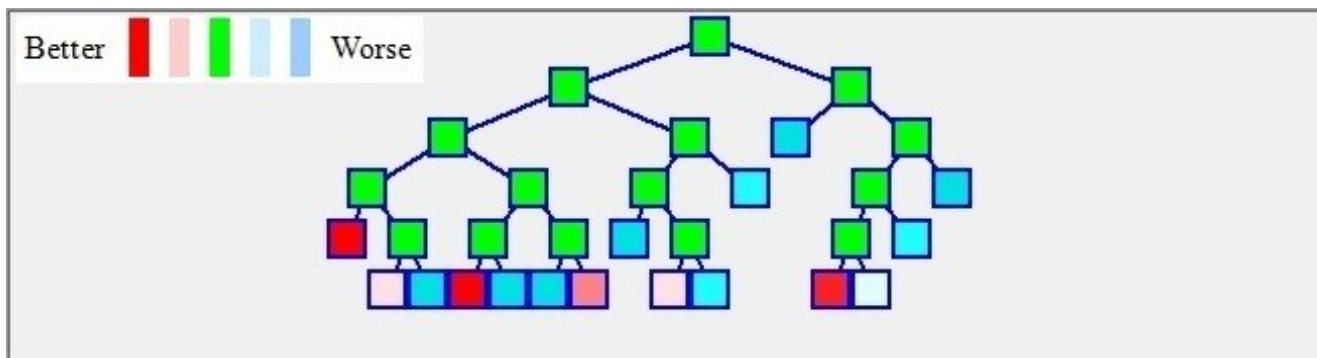
CLIP in 2000



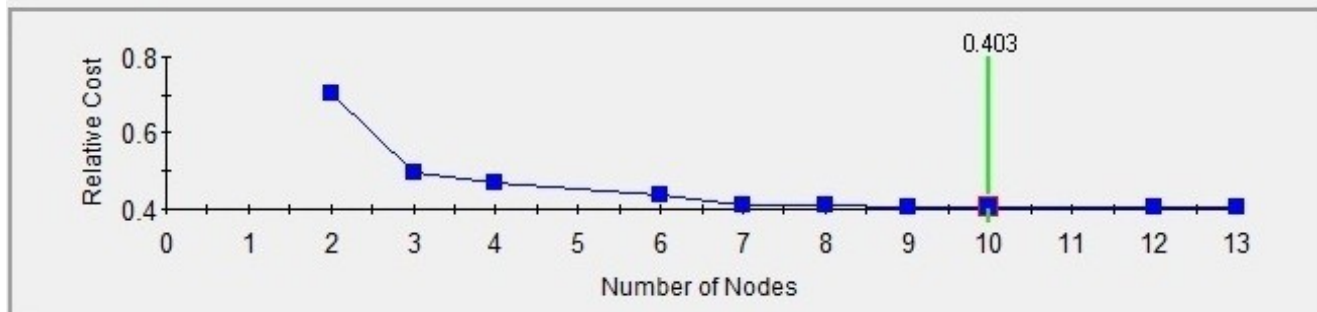
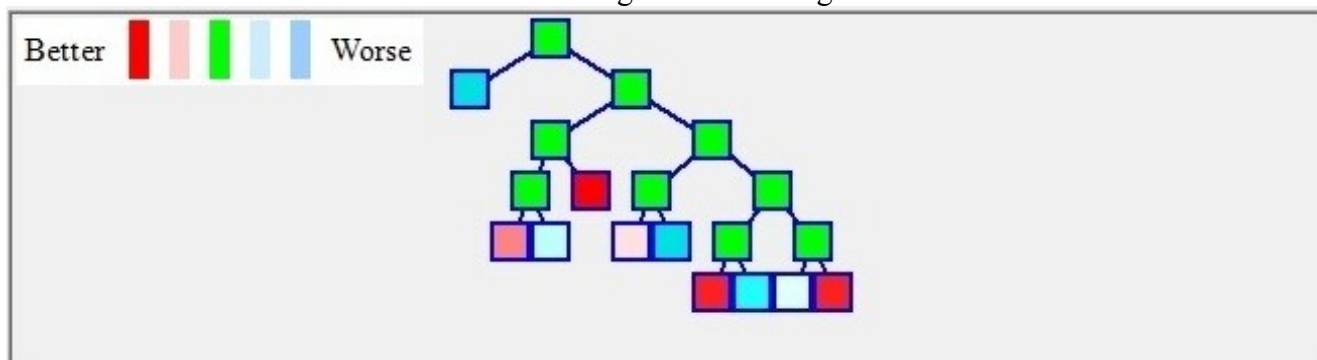
SEWI in 2000

MRW in 1998

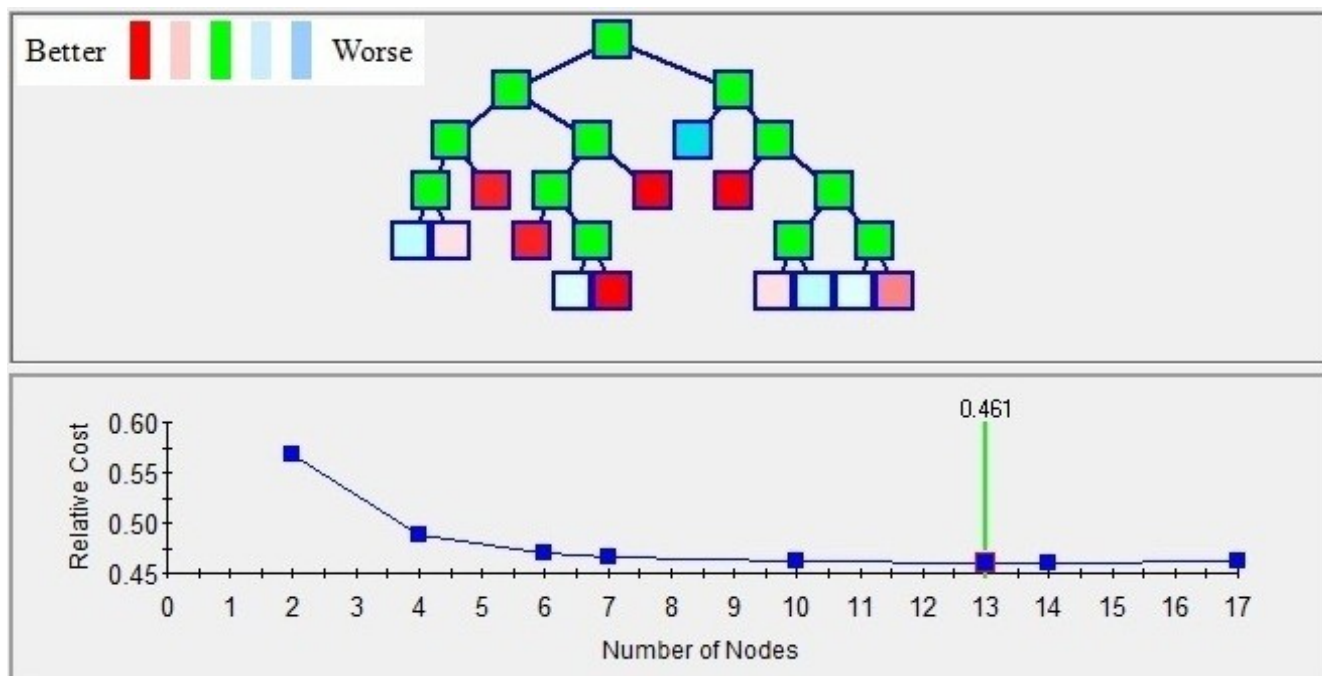
Figure 4-1: Three study areas



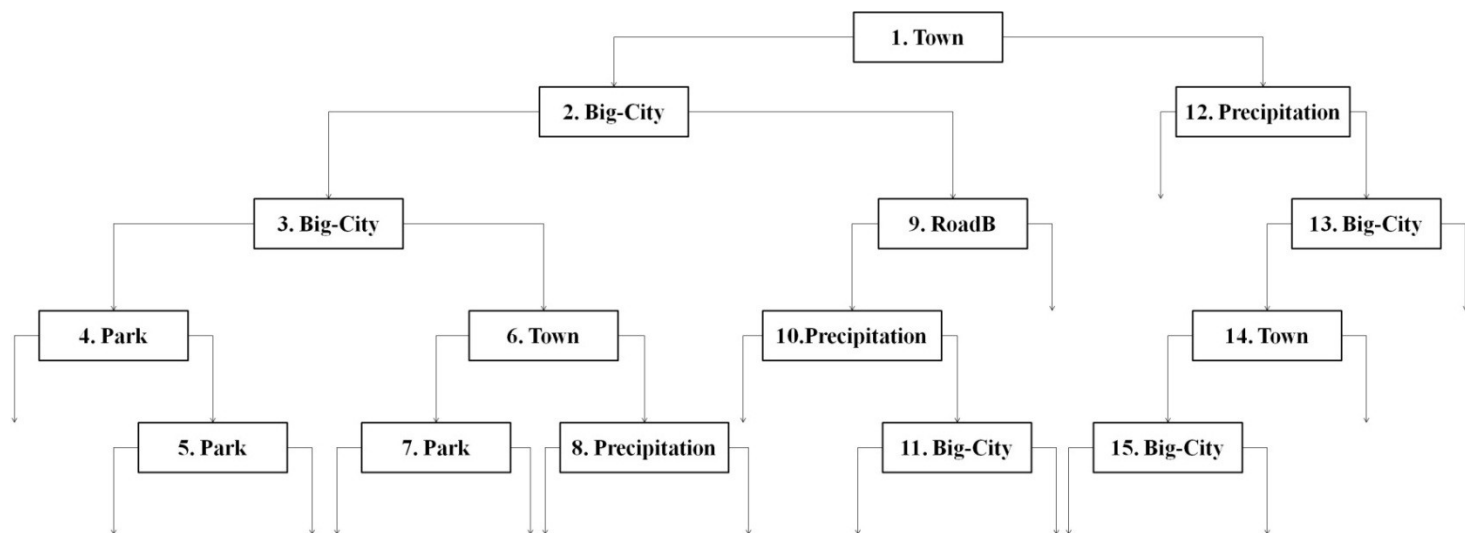
CLIP – Agriculture Change



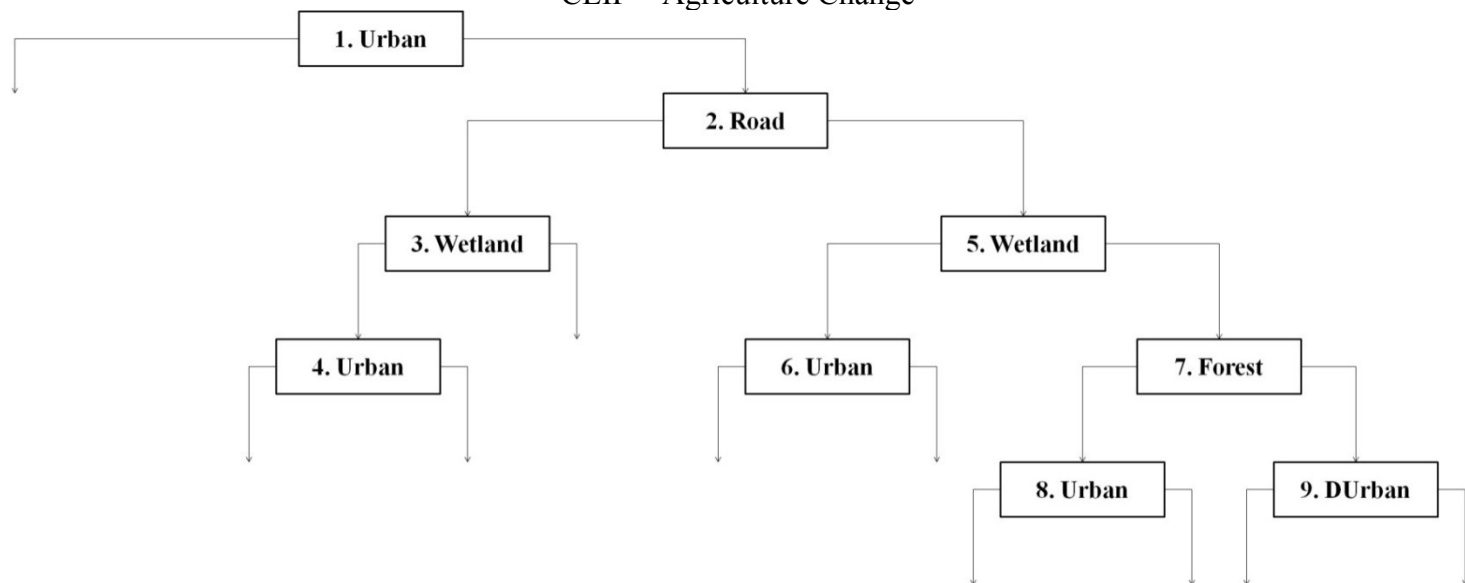
SEWI – Urban Change



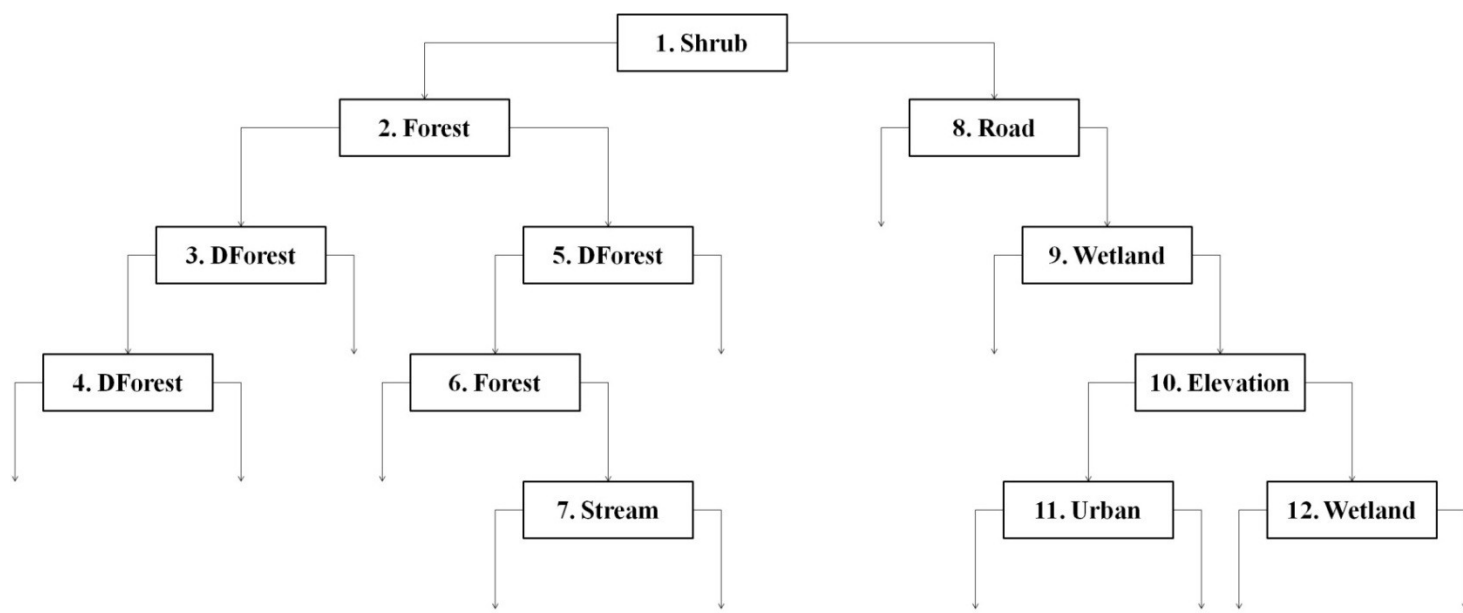
MRW – Forest Change
Figure 4-2: Tree Navigator in CART



CLIP – Agriculture Change



SEWI – Urban Change



MRW – Forest Change

Figure 4-3: CART models for each study area

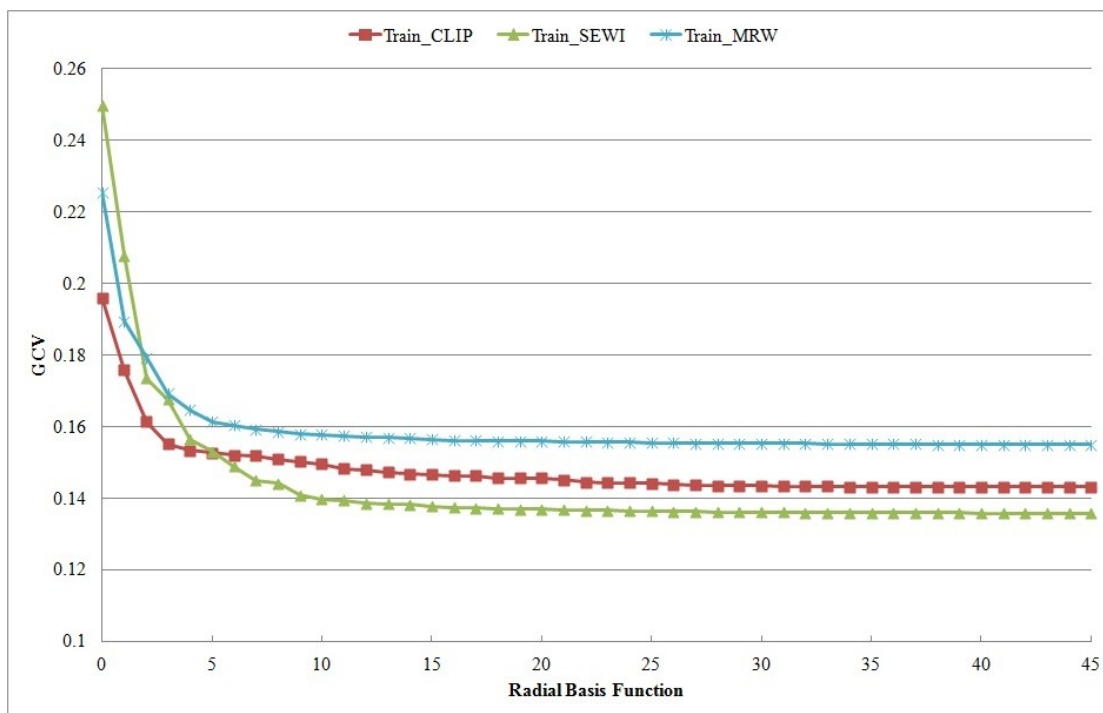


Figure 4-4: GCV across adding radial basis functions to MARS

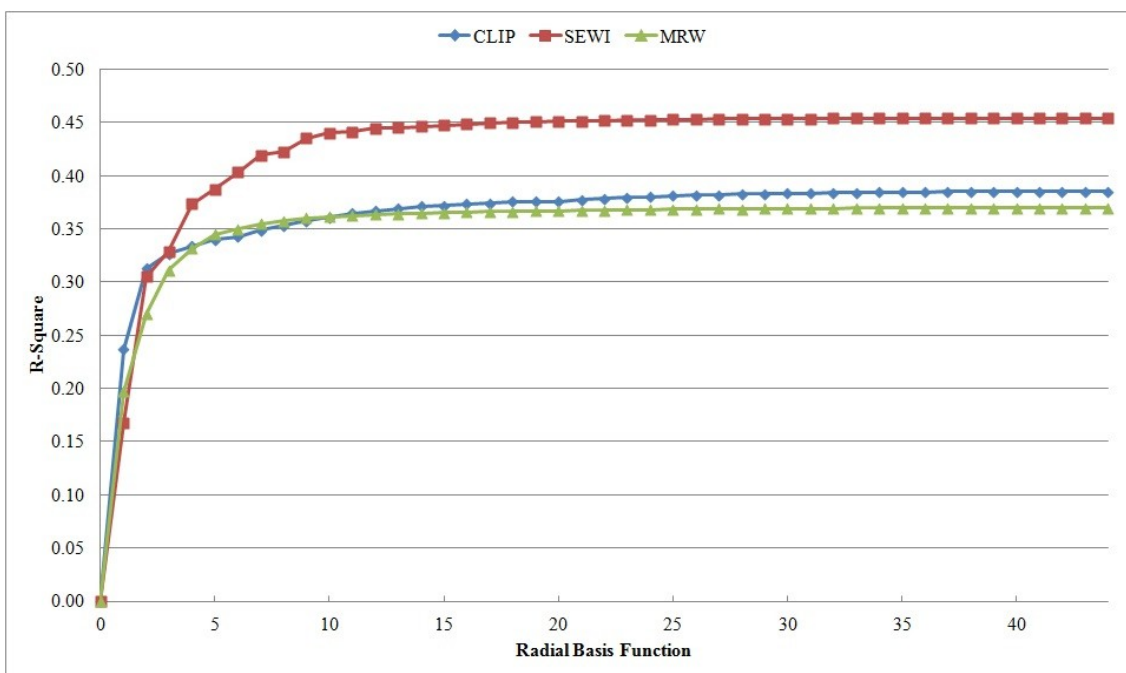
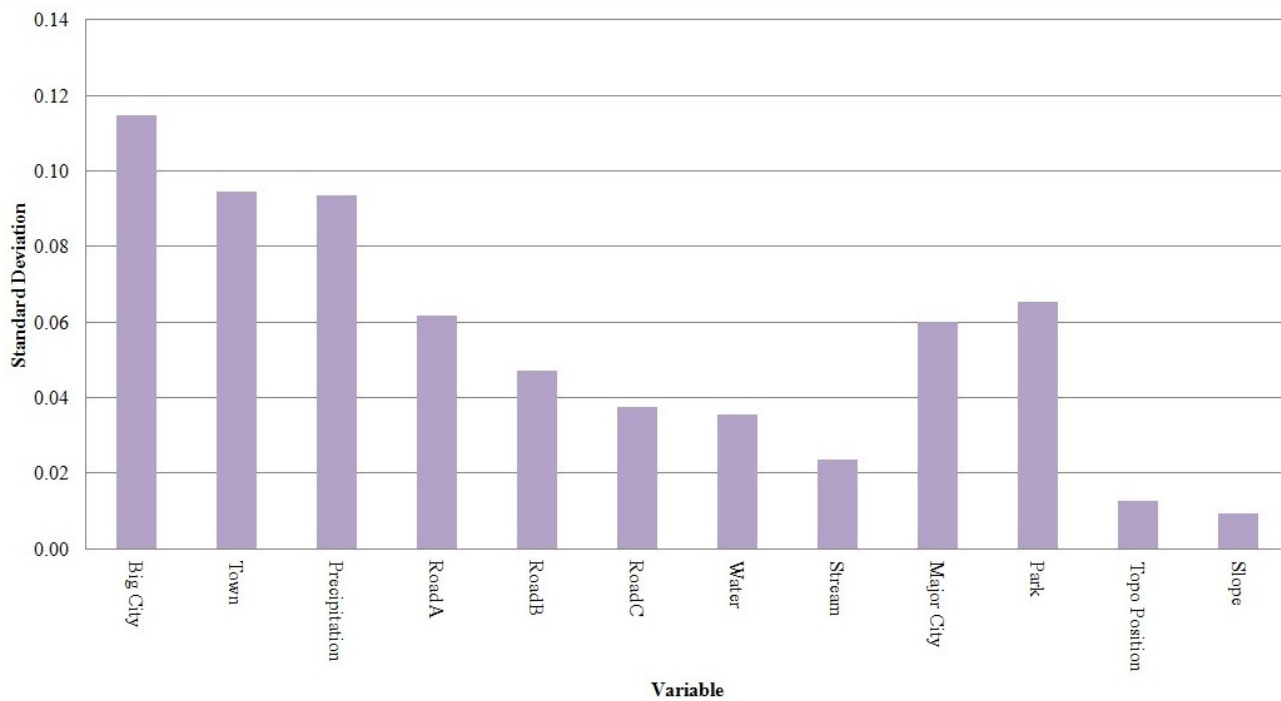
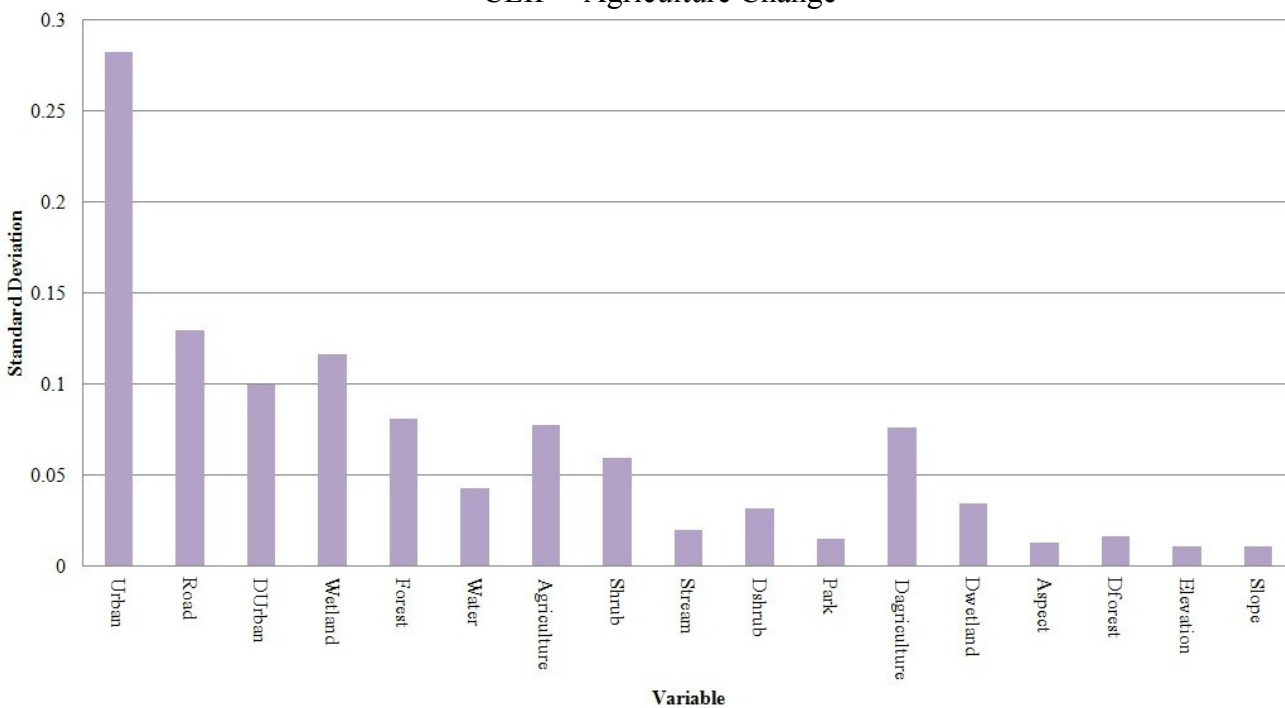


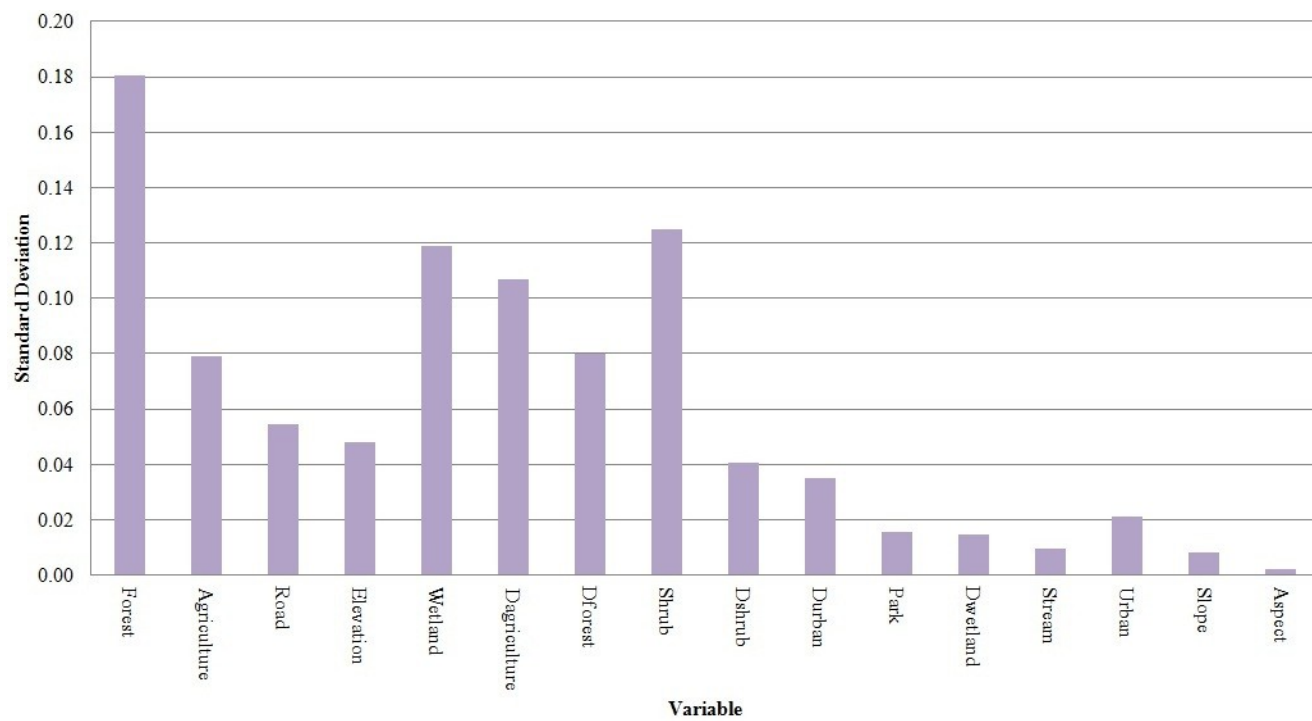
Figure 4-5: R-square across adding radial Basis functions in MARS



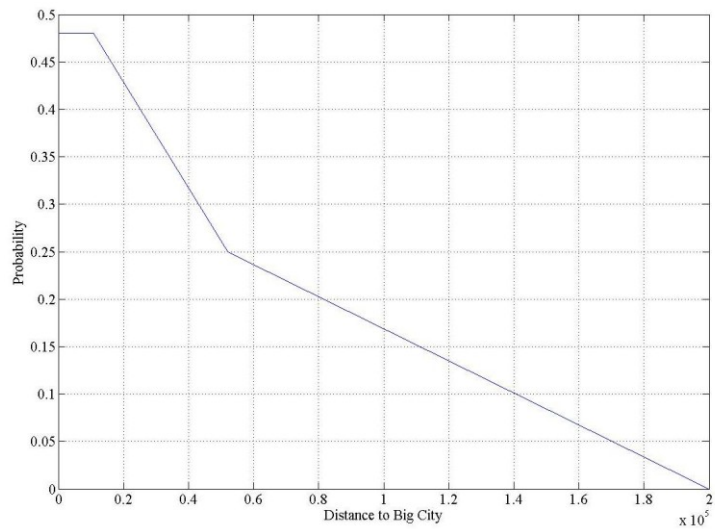
CLIP – Agriculture Change



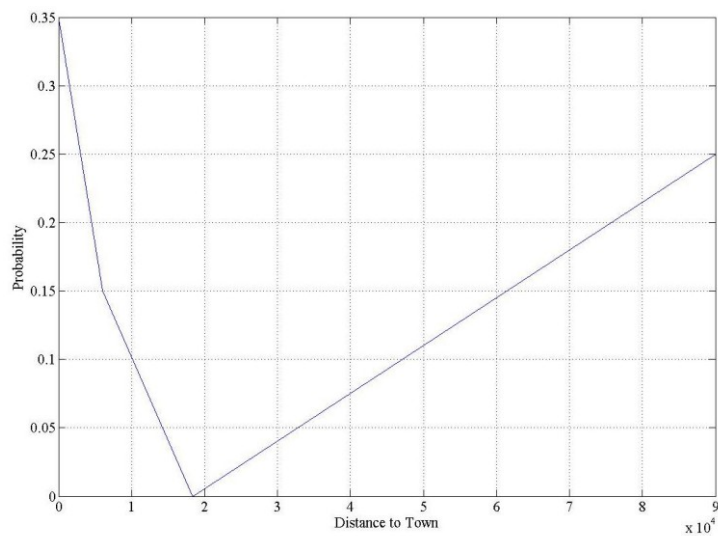
SEWI – Urban Change



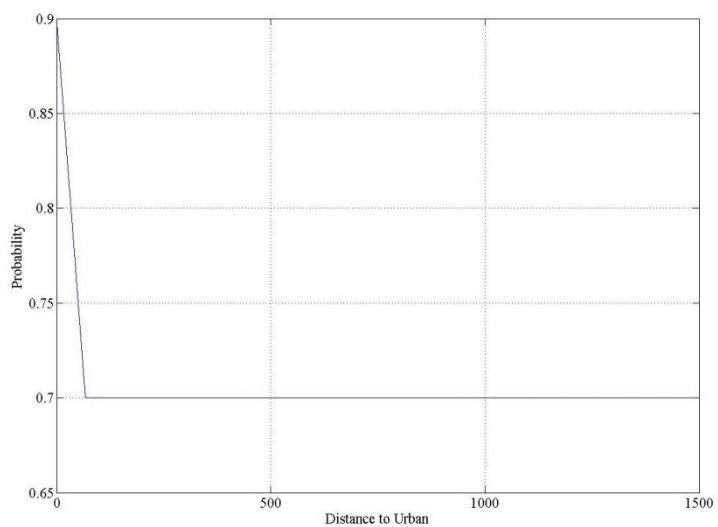
MRW – Forest Change
Figure 4-6: ANOVA in MARS



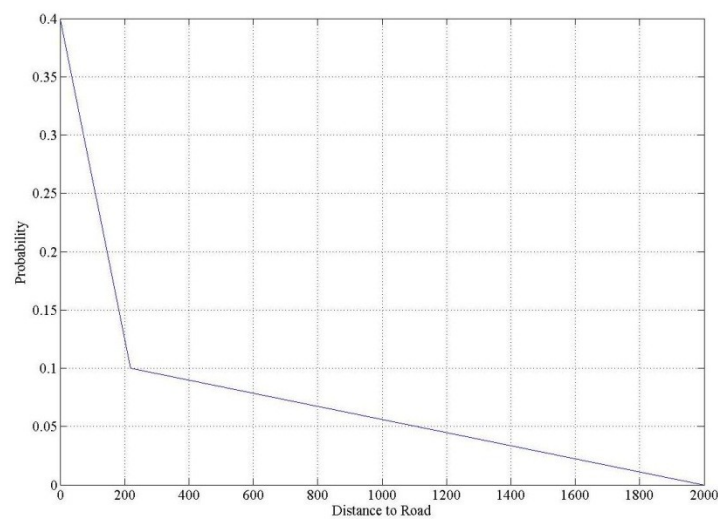
CLIP- Distance to Big City



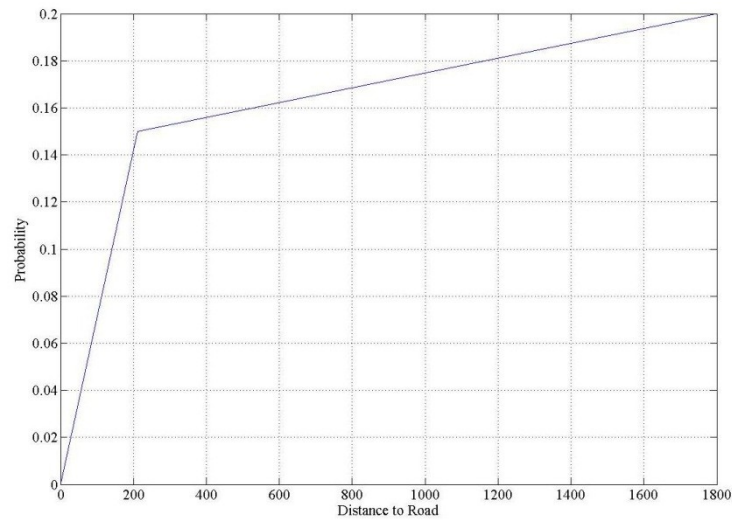
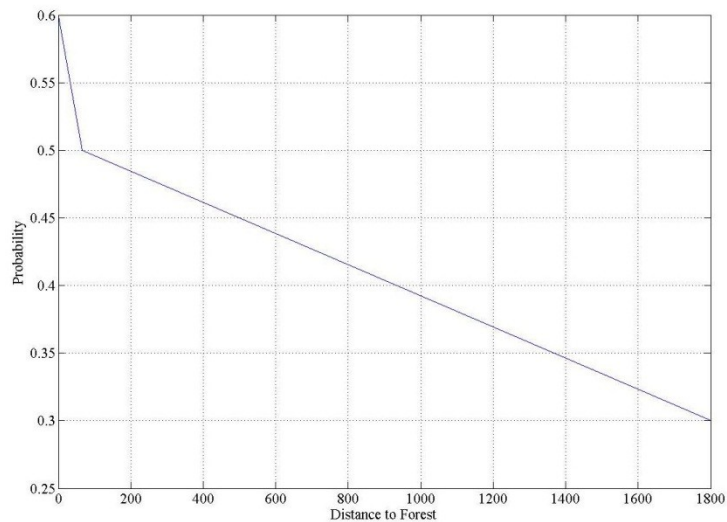
CLIP - Distance to Town



SEWI - Distance to Urban



SEWI - Distance to Road



MRW - Distance to Forest

MRW - Distance to Road

Figure 4-7: BF's for significant drivers in CLIP, SEWI and MRW

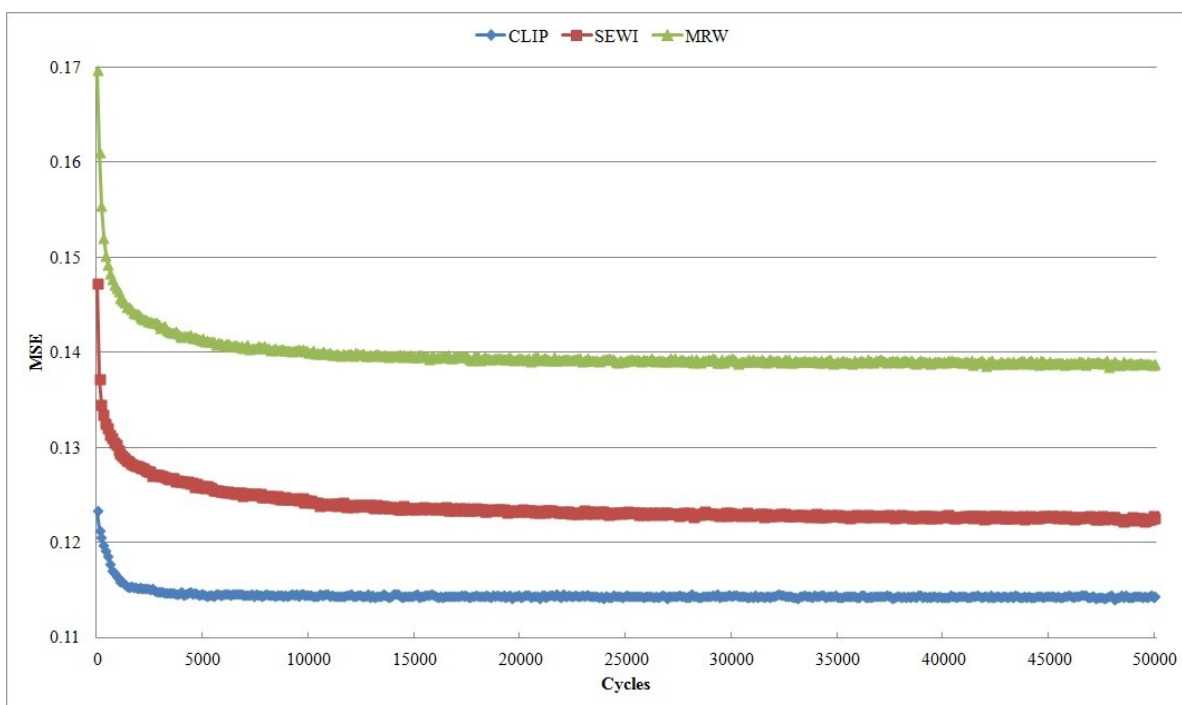
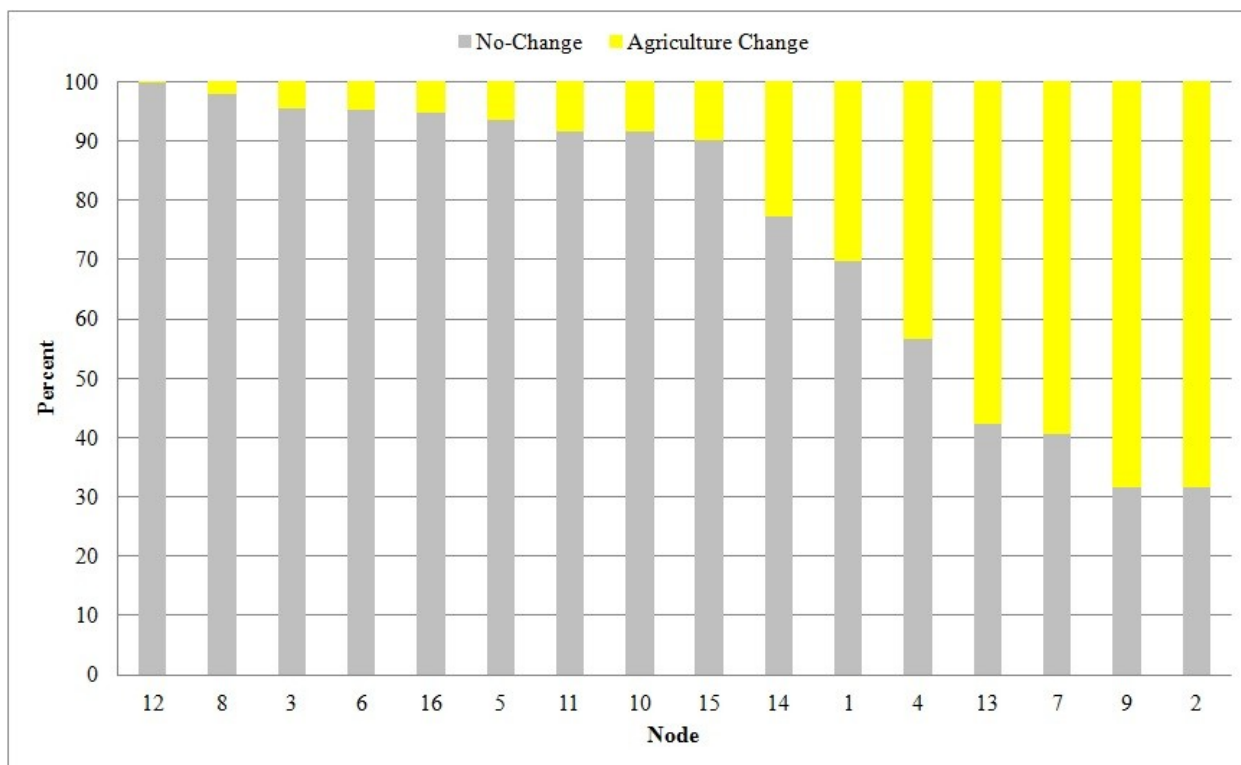
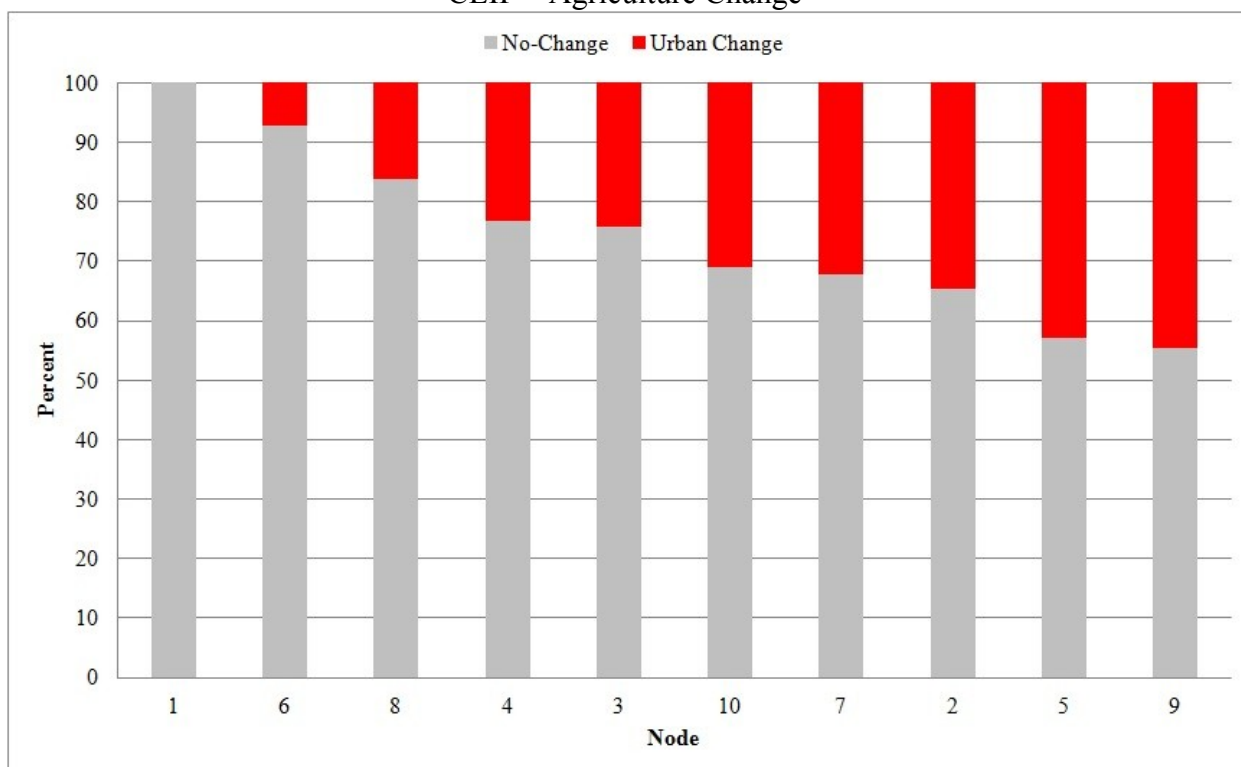


Figure 4-8: Training run of LTM



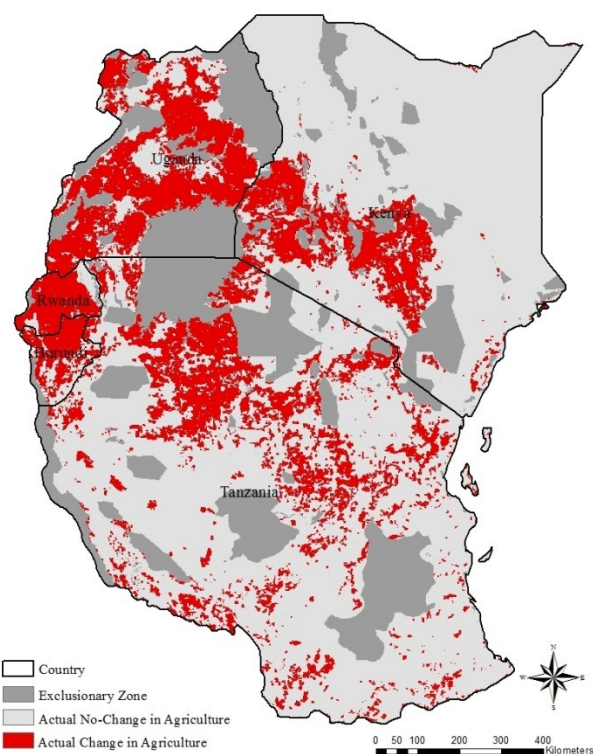
CLIP - Agriculture Change



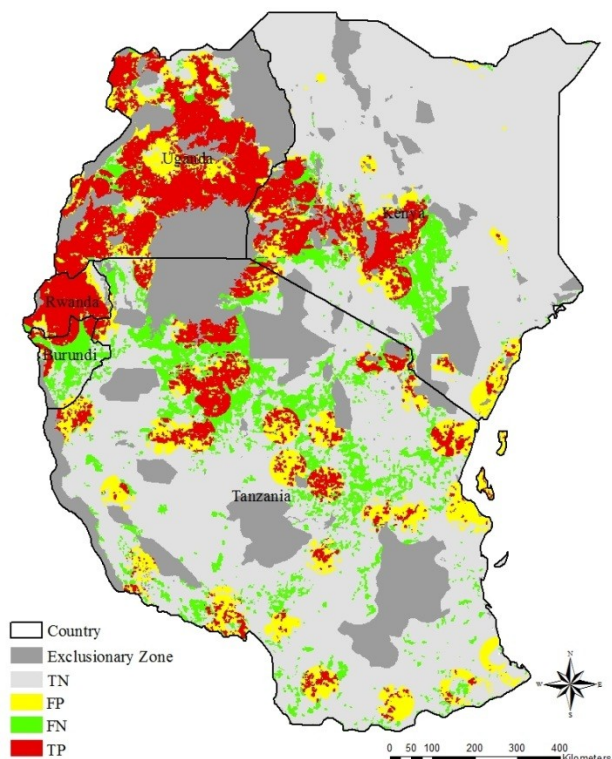
SEWI - Urban Change



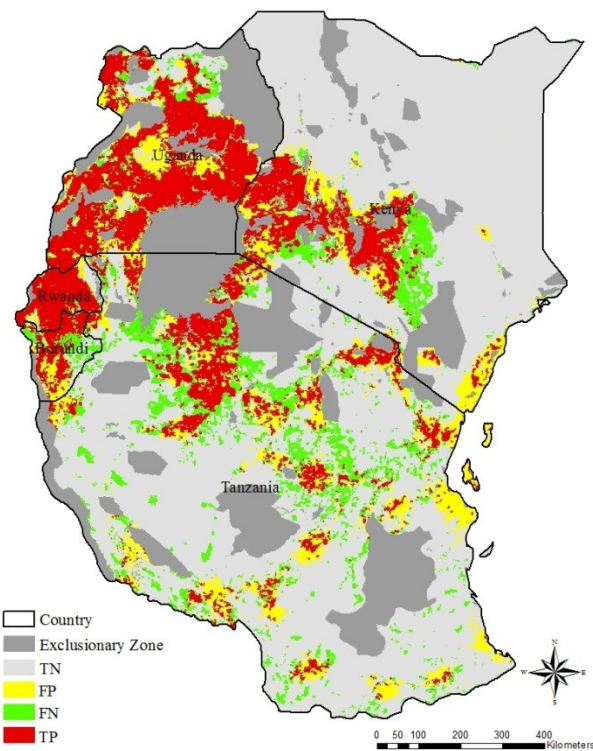
MRW – Forest Change
Figure 4-9: Terminal node in CART



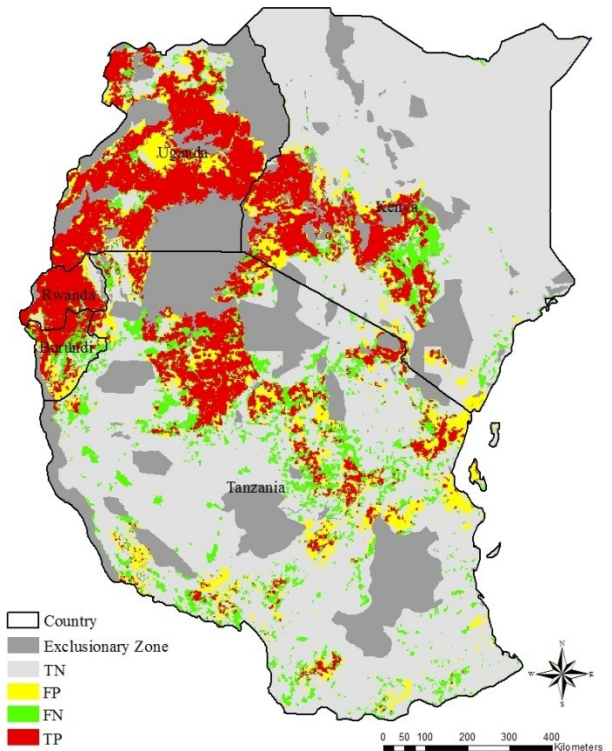
Reference Change



Error Map from CART



Error Map from MARS



Error Map from LTM

Figure 4-10: Reference agriculture change and error maps of three models in CLIP

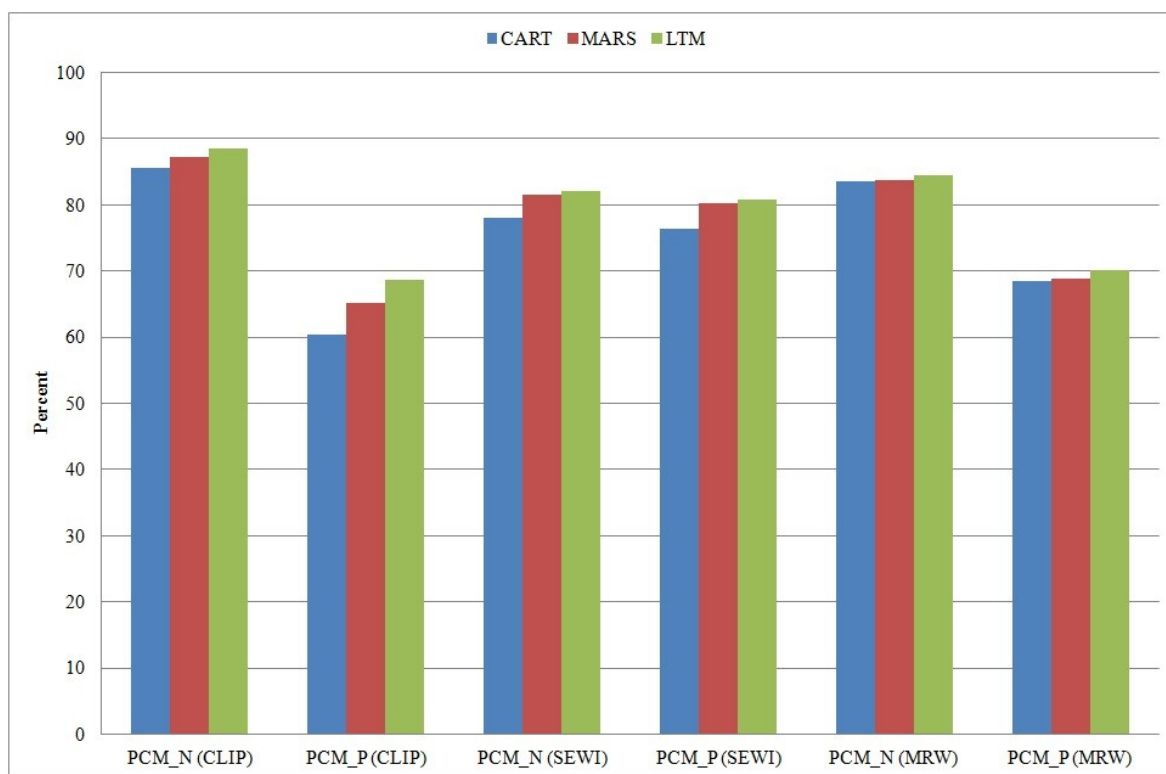


Figure 4-11: PCM_N and PCM_P values for CART, MARS and LTM

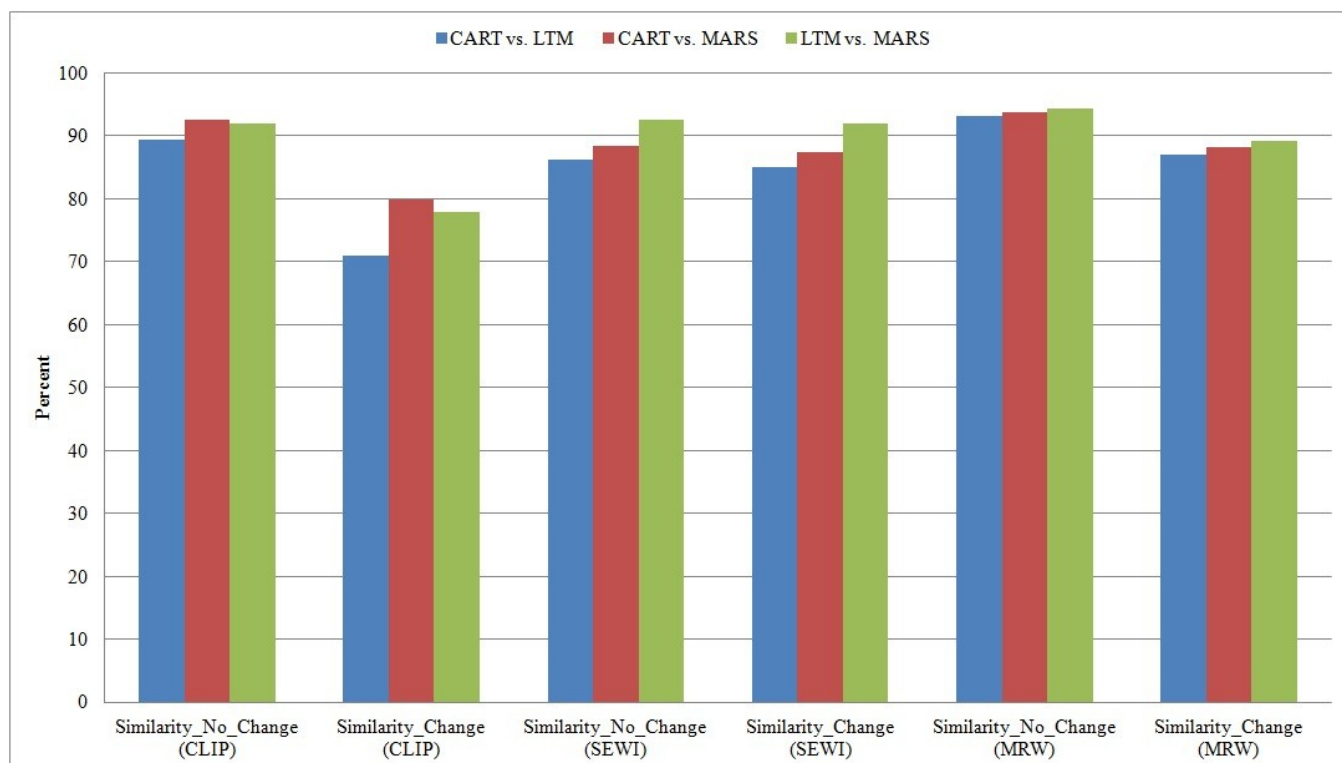


Figure 4-12: Similarity values for LTM, CART and MARS simulations

Table 4-1. Coding system employed here for the contingency table calculations used to compare simulated and reference LUCC map

		Reference map	
		Non-Change	Change
Simulated map	Non-Change	True Negative (TN)	False Negative (FN)
	Change	False Positive (FP)	True Positive (TP)

Table 4-2: Spatial predictor variables in CLIP, SEWI and MRW

Predictor	CLIP (Agriculture Change)	SEWI (Urban Change)	MRW (Forest Change)
1	Distance to major city	Elevation	Elevation
2	Distance to town	Aspect	Aspect
3	Distance to big city	Distance to Urban	Distance to Urban
4	Distance to park	Density of Urban	Density of Urban
5	Distance to water	Distance to Forest	Distance to Forest
6	Distance to stream	Density of Forest	Density of Forest
7	Precipitation	Distance to Agriculture	Distance to Agriculture
8	Slope	Density of Agriculture	Density of Agriculture
9	Topo-Position	Distance to Shrub	Distance to Shrub
10	Distance to road-A	Density of Shrub	Density of Shrub
11	Distance to road-B	Distance to Wetland	Distance to Wetland
12	Distance to road-C	Density of Wetland	Density of Wetland
13	----	Distance to Park	Distance to Park
14	----	Distance to Stream	Distance to Water
15	----	Distance to Road	Distance to Stream
16	----	Slope	Distance to Road
17	----	----	Slope

Table 4-3: Size of samples and resolution of data in CLIP, SEWI and MRW

Study Area	Change	Non-Change	Total	Resolution
CLIP	339,845	930,244	1,270,089	1km×1km
SEWI	491,031	529,441	1,020,472	30m×30m
MRW	641,237	1,225,913	1,867,150	30m×30m

Table 4-4: Competitor, split and improvement in CART

	Competitor	Split	Improvement
Main	Town	11112.50	0.09539
1	Big-City	46232.50	0.09532
2	Precipitation	534.50	0.08024
3	RoadA	33263.50	0.05939
4	Major-City	350957	0.03956
5	Water	49223.50	0.03464
6	RoadB	42005.90	0.03319
7	RoadC	13527.50	0.01944
8	Park	171412.50	0.01342
9	Slope	9.50	0.00199
10	Stream	15082.50	0.00155
11	Topo-Position	2.50	0.00097

CLIP – Agriculture Change

	Competitor	Split	Improvement
Main	Urban	142.50	0.08669
1	Road	157.20	0.04514
2	Wetland	2475.47	0.04450
3	Agriculture	1156.20	0.04196
4	DUrban	0.15	0.02024
5	DWetlan	0.10	0.01330
6	Forest	1736.20	0.01315
7	Shrub	2488.65	0.01276
8	Stream	2248.04	0.00993
9	Water	1140.08	0.00806
10	Park	2057.02	0.00564
11	DShrub	0.07	0.00402
12	DForest	0.15	0.00390
13	DAgriculture	0.01	0.00130
14	Elevation	274.50	0.00109
15	Aspect	0.50	0.00096
16	Slope	0.17	0.00096

SEWI – Urban Change

	Competitor	Split	Improvement
Main	Shrub	150.13	0.09776
1	Forest	377.68	0.08790
2	Road	196.66	0.02411
3	Agriculture	296.22	0.01363
4	Wetland	5794.66	0.01351
5	DShrub	0.12	0.01142
6	DAgriculture	0.40	0.00658

7	DForest	0.25	0.00596
8	Elevation	356.50	0.00562
9	Urban	211.06	0.00372
10	Durban	0.04	0.00301
11	Stream	938.43	0.00202
12	Park	1898.07	0.00143
13	Slope	1.28	0.00053
14	DWetlan	0.58	0.00046
15	Aspect	164.37	0.00026

MRW – Forest Change

Table 4-5: Coefficients, variables and knots in MARS

BFs	Coefficient	Variable	Sign	Knot
0	2.42441368			
1	0.00000347	Big-City	+	52,086
2	-0.00001659	Town	-	18,384
3	0.00003251	Town	+	18,384
4	0.00475980	Precipitation	-	700
5	-0.00319349	Precipitation	+	700
6	-0.00000039	RoadA	-	34,132
7	0.00000371	RoadA	+	34,132
8	0.00000245	RoadB	-	64,536
9	-0.00000267	RoadC	+	15,264
10	0.00000575	RoadC	-	15,264
11	0.00001954	Water	+	94,111
12	-0.00001774	Water	-	94,111
13	-0.00001823	RoadA	+	166,928
14	-0.00000952	Stream	-	7,615
15	0.00002031	Town	+	5,999
16	-0.00000249	Major-City	-	267,134
17	0.00000100	Major-City	+	267,134
18	0.00140561	Precipitation	-	988
19	-0.00277690	Precipitation	+	769
20	-0.00078533	Precipitation	-	1,228
21	0.00000180	Major-City	+	387,865
22	-0.00000646	Park	-	99,126
23	0.00000333	Park	+	99,126
24	0.00000165	Major-City	-	102,078
25	0.00000176	Major-City	+	509,574
26	0.00000312	RoadA	-	120,739
27	0.00244000	Topo-Position	+	5
28	0.00690933	Topo-Position	-	5
29	0.00001333	RoadA	+	173,954
30	0.00000378	Park	-	14,559
31	0.00235258	Precipitation	+	459
32	-0.00358714	Precipitation	-	268
33	-0.00162222	Precipitation	+	557
34	-0.03954992	Slope	-	8
35	-0.00000621	Park	+	278,352
36	0.00000375	Park	-	212,397
37	-0.00000520	Big-City	+	10,816
38	-0.00001910	Water	-	4,471

CLIP – Agriculture Change

BFs	Coefficient	Variable	Sign	Knot
0	1.45167184			
1	-0.02966011	Urban	-	67
2	0.00397150	Wetland	+	94
3	-0.00401613	Wetland	-	94
4	-0.00006609	Road	+	218
5	0.00121700	Road	-	218
6	1.25214827	DUrban	-	0.53
7	-1.69810307	DUrban	+	0.53
8	0.00119909	Forest	-	108
9	-0.00125138	Forest	+	108
10	-0.00452334	Water	-	60
11	0.00186062	Agriculture	+	150
12	-0.00211285	Agriculture	-	150
13	0.00106522	Shrub	+	123
14	-0.00176804	Shrub	-	123
15	0.48514801	DShrub	+	0.02
16	1.44921708	DShrub	-	0.02
17	0.00000770	Park	+	6,363
18	0.30609438	DAgriculture	-	0.07
19	-0.54288918	DAgriculture	+	0.07
20	0.51860422	DWetlan	-	0.21
21	-0.11628491	DWetlan	+	0.21
22	0.00020825	Aspect	+	127
23	0.00024565	Aspect	-	127
24	0.54309684	DForest	-	0.36
25	-0.11845764	DForest	+	0.36
26	-0.90340024	DUrban	-	0.06
27	0.00030453	Elevation	+	198
28	0.00304598	Elevation	-	198
29	-0.00327487	Slope	+	0.33
30	-0.09363096	Slope	-	0.33
31	-1.95366967	DUrban	+	0.91
32	-0.23361279	DUrban	-	0.25
33	-0.00021901	Stream	+	216
34	0.00005888	Stream	-	1,276

SEWI – Urban Change

BFs	Coefficient	Variable	Sign	Knot
0	1.50715065			
1	-0.00091195	Forest	+	67
2	-0.01736367	Forest	-	67
3	0.00001416	Road	+	212
4	-0.00074109	Road	-	212
5	0.01144137	Elevation	+	302
6	-0.01030203	Elevation	-	302
7	0.23848380	DForest	+	0.44
8	-0.81003433	DForest	-	0.44
9	0.53589106	DAgriculture	+	0.29
10	-0.22906694	DAgriculture	-	0.29
11	0.00177329	Wetland	+	90
12	0.01014404	Wetland	-	90
13	0.97863191	DShrub	+	0.48
14	-0.24052025	DShrub	-	0.48
15	1.30380857	DUrban	+	0.47
16	-0.43899977	DUrban	-	0.47
17	0.00000175	Park	-	3,604
18	0.00000936	Park	+	3,604
19	-0.00023166	Agriculture	-	256
20	0.88562632	DWetlan	+	0.46
21	-0.08965859	DWetlan	-	0.46
22	-0.00516677	Elevation	+	390
23	-0.00001095	Stream	+	752
24	-0.00003991	Stream	-	752
25	-0.35395181	DForest	+	0.74
26	-0.00128250	Urban	-	408
27	0.00104839	Urban	+	408
28	0.00369674	Slope	+	0
29	-0.42668161	DUrban	-	0.21
30	0.02683787	Elevation	+	228
31	-0.01943569	Elevation	-	193
32	-0.00818860	Elevation	+	241
33	-0.02244085	Elevation	-	220
34	0.01282837	Elevation	+	204
35	0.00002618	Park	+	18,434
36	0.00447845	Elevation	-	417
37	0.00171197	Elevation	+	356
38	0.00001693	Aspect	-	0
39	-0.00000279	Shrub	+	140
40	0.00855425	Shrub	-	140

MRW – Forest Change

Table 4-6: Ranking variables in CART and MARS

CART		MARS	
Variable	Relative Priority	Variable	Relative Priority
Town	0.24976	Big-City	0.1647
Big-City	0.23843	Town	0.1495
Precipitation	0.20375	Precipitation	0.1425
Major-City	0.08524	RoadA	0.1016
Water	0.07465	RoadB	0.0846
RoadA	0.05332	Park	0.0744
RoadB	0.04858	RoadC	0.0669
RoadC	0.03584	Major-City	0.0662
Park	0.00992	Water	0.0640
Stream	0.00046	Stream	0.0443
Slope	0.00006	Topo-Position	0.0235
Topo-Position	0.00000	Slope	0.0179

CLIP – Agriculture Change Simulation

CART		MARS	
Variable	Relative Priority	Variable	Relative Priority
Urban	0.34791	Urban	0.2847
Road	0.25453	Road	0.1321
Wetland	0.16571	Wetland	0.1197
DUrban	0.08083	Forest	0.0871
DWetlan	0.03940	DUrban	0.0552
Stream	0.03867	Agriculture	0.0526
Forest	0.02398	Water	0.0509
Agriculture	0.02228	Shrub	0.0486
DForest	0.00647	DShrub	0.0304
DAgriculture	0.00600	DWetlan	0.0262
Water	0.00535	DAgriculture	0.0249
Shrub	0.00347	Stream	0.0240
Slope	0.00246	Park	0.0172
Elevation	0.00163	Aspect	0.0149
Park	0.00124	DForest	0.0126
DShrub	0.00000	Elevation	0.0095
Aspect	0.00000	Slope	0.0085

SEWI – Urban Change Simulation

CART		MARS	
Variable	Relative Priority	Variable	Relative Priority
Shrub	0.33051	Forest	0.1532
Forest	0.17097	Shrub	0.1321
Road	0.15222	Wetland	0.1063
Wetland	0.08137	DForest	0.1046
DAgriculture	0.06735	Elevation	0.1032
DForest	0.04819	Road	0.0761
DShrub	0.04475	DAgriculture	0.0688
Agriculture	0.02748	Agriculture	0.0493
Elevation	0.02446	DShrub	0.0453
DWetlan	0.01564	DUrban	0.0362
Urban	0.01556	Urban	0.0356
Stream	0.01048	Park	0.0306
DUrban	0.00548	DWetlan	0.0229
Park	0.00501	Stream	0.0170
Slope	0.00048	Slope	0.0166

MRW – Forest Change Simulation

Table 4-7: ROC of CART, MARS and LTM obtained from the cross validation with the testing data

		CLIP - Agriculture	SEWI – Urban	MRW - Forest
CART	Cross validation	0.8415	0.8698	0.8468
	Testing run	0.8398	0.8429	0.8421
MARS	Cross validation	0.8688	0.8927	0.8640
	Testing run	0.8680	0.8904	0.8631
LTM	Testing run	0.8927	0.8958	0.8623

**CHAPTER 5: SIMULATING MULTIPLE LAND USE CLASSES USING THE
ARTIFICIAL NEURAL NETWORK-BASED LAND TRANSFORMATION
MODEL AND TWO NONLINEAR DATA MINING TOOLS²**

5.1 Introduction

Land use change (LUC) drivers operate across a variety of spatial-temporal scales in a very nonlinear way (Veldkamp and Lambin, 2001) and thus nonlinear tools are needed to simulate these dynamics. Many LUC models use nonlinear techniques (e.g. Clarke et al. 1997; Pijanowski et al. 2002a) but a comparison of several tools in different locations has been lacking, which limits our understanding of how nonlinear approaches can aptly simulate the scale of drivers and the complexity of LUC patterns. Furthermore, within a given region, multiple land use changes occur. For example, it is quite common for some areas to be converted from agriculture to urban while nearby forests are converted to agriculture (Alexandridis et al. 2007; Washington-Ottombre et al. 2010; Pijanowski and Robinson, 2011). However, few researchers have considered multiple land use transitions in the same model and thus oversimplifying the land use change process. In modeling, simulating more than one outcome often creates what is known as the multiple classification (MC) problem (Ho, 2000).

² Current version has been submitted to International Journal of GIS.

Many rules have been proposed to handle MC problems but determining which rule is best requires careful parameterization of the model and the quantification of model goodness of fit.

5.1.1 Nonlinear Modeling Tools

Statistically-based machine learning tools are data intensive and are of two types: global parametric models (GPMs) and local non-parametric models (LNPM). A variety of GPM-based approaches, such as artificial neural networks (ANNs) (e.g. Pijanowski et al. 2002b), cellular automata (e.g. Batty and Xie, 1994; Dietzel and Clarke, 2006), genetic algorithms (e.g. Shan et al. 2008; Jenerette and Wu, 2001) and logistic regression (e.g. Tayyebi et al. 2010; Pontius and Schneider, 2001; He and Lo, 2007), have been used extensively by LUC modelers over the last two decades. Statistical GPMs find the relationship between input and output (e.g. numerical, categorical or mixed variables) and often fit better to data than traditional linear models like multiple regression. However, GPMs suffer from several assumptions, such as the need for data to be normally distributed (Lumley, et al. 2002) and forcing variables to act globally over the entire dataset (Siegel and Castellan, 1988).

Local non-parametric models (LNPM), on the other hand, split the data into subsets and have fewer model assumptions than GPMs. The variables are added sequentially to the LNPMs as necessary to fit the data (Hardle et al. 2004) and functions (e.g. linear or non-linear) can be different for each subset. Users can also limit the LNPMs to quantify interaction between subsets (Steinberg and Colla, 1997). LNPMs are able to detect non-linear patterns that may not be easily found using statistical GPMs.

Thus, LUC modelers may be able to adapt LNPMs to simulate LUC. Recently developed LNPMs include multivariate adaptive regression splines (MARS) and classification and regression trees (CART) (Breiman et al. 1984; Friedman, 1991). CART calculates the likelihood of the outcomes using multiple spatial predictors to develop monotone outcomes. MARS, on the other hand, overcomes the restriction of the piecewise constant functions in CART by generating piecewise linear models using basis functions between the subsets (Friedman, 1991).

5.1.2 Multiple Classification (MC) Problem

Data mining tools have been applied to the problem of multiple classifications (MC) frequently. The central objective of MC is to integrate data from all classes simultaneously. However, learning each class separately in a binary mode usually yields better results than integrating information as an independent task. A central question of MC is “how can one combine a variety of classes together (referred to model structure and coding scheme) to model more than one outcome?” There are two ways available for employing MC using data mining tools. One method is for an MC to be converted into numerous binary classifications that are solved using binary classifiers. Alternatively, binary classifications can be extended to the MC which need special formulations to perform the separation; this is accomplished using tools such as fuzzy sets (Zadeh, 1965), voting (Lam and Suen, 1995), k-nearest neighbor rules (Bay, 1998) or support vector machines (Cortes and Vapnik, 1995). To our knowledge, few studies have applied and addressed MC problems in LUC modeling (e.g. Li and Yeh, 2002). In this chapter, we limited our study on the MC modeling using one model to simulate multiple land use

classes. This has the advantage that it minimizes the total number of models that need to be executed and takes into account the correlation between different output classes simultaneously.

5.1.2.1 Decomposing MC into binary classification

Several methods have been suggested to decompose the multiple classifications (MC) into numerous binary classifications. The following, which are also illustrated in Figure 5-1:

One-Verses-All (OVA): OVA is a popular approach has been proposed by several researchers in recent years (Rifkin and Klautau, 2004; Dubchak et al. 1999; Figure 5-1A). The OVA is the simplest approach of those employed, where each modeling run discriminates a one class from the other $n - 1$ classes (Rifkin and Klautau, 2004). This procedure is repeated for each of the n classes, leading to n binary classifiers. OVA has several shortcomings in the training run of machine learning because one class usually have few cells compared to the large number of other classes at each time. Thus, machine learning may classify land use cells as other classes due to the overabundance of cells (coded as 0), or may over fit the one class (code 1) due to the presence of very few cells. Rifkin and Klautau, (2004) defended the OVA approach for MC and Tsoumakas et al. (2010) summarized several ways to improve the OVA method;

All-Verses-All (AVA): AVA is another popular approach for treating MC, which considers all possible mutual binary classifiers between n classes while ignoring the rest of the classes (Hastie and Tibshirani, 1998; Figure 5-1B).

This method requires building $\binom{n}{2} = n(n-1)/2$ binary classifiers ($(n-1)/2$ more models than OVA). For the testing run, each cell receives a vote from all possible binary classifiers and the land use class with the dominate votes is assigned to the cell. AVA is very difficult to analyze due to the large number of binary classifiers. Moreover, both methods, OVA and AVA, also ignore the correlations between the outputs (Tsoumakas et al. 2010);

5.1.2.2 Extensible data mining coding scheme for multiple classifications (MC)

The data mining coding scheme for binary applications can be extended for MC as well. ANN provides a natural extension to the MC problem. The idea is to use numerous binary classifiers to solve multiple binary classification problems simultaneously. The model structure and output code scheme corresponding to each class can be chosen as follows (after Dietterich and Bakiri, 1995):

(1) **One-per-class coding:** Instead of just having one neuron in the output layer, with binary output, we could have n binary neurons. Each output neuron is designated the task of identifying a given class. The output code for that class should be 1 at this neuron and 0 for the others. Therefore, we will need n neurons in the output layer, where n is the number of classes or

(2) **Distributed output coding:** Each class receives a unique binary code that can change from 0 to $2^n - 1$, where n is the number of output neurons. During the testing run, the calculated code is compared to the code for the reference n classes. The closer the value is to the observed class, according to

distance measure (e.g. Hamming or Euclidean distance), that class becomes the winning class.

5.1.3 Land Use Land Cover Change Models and Multiple Classifications (MC)

The main objective of LUC models is to assign the cells in a maps into future classes (Pontius and Connors, 2006) so that land use forecasts can be assessed for environmental impacts (cf. Pijanowski et al. 2002b and 2007; Ray et al. 2010). Several approaches have been developed during the last three decades to simulate land use using numerous environmental variables. However, most of them limited their application to only a single land use transition (e.g. see models of Clarke et al. 1997; Verburg et al. 1999; Pontius et al. 2001; Pijanowski et al. 2002a).

Land Transformation Model (LTM) uses ANN to learn about the patterns between input (i.e. drivers) and output (e.g. historical LUC) data but it has been used in a variety of places around the world to simulate only a single land use transition (Pijanowski et al. 2005, 2006, 2009 and 2011). The LTM has also been successfully applied in many areas of research such as LUC impacts on hydrology (Pijanowski et al. 2007, Ray et al. 2012), developing historical LUC maps (Ray and Pijanowski, 2010), urban boundary simulation (Tayyebi et al. 2011a and 2011b), LUC simulation at national or continental scale (Tayyebi et al. 2012), the nature of different errors within LTM (Tayyebi et al. 2011a, b and c), land-climate-people multi-model simulations (Moore et al. 2010, Pijanowski et al. 2011), LUC impacts on fish community structure (Wiley, 2010), and land-climate feedback simulation (Pijanowski et al. 2011). Although the statistical GPMs have received a lot of attention during the last three decades in LUC

fields, there are no studies that compare GPMs with LNPMs for a multiple classification (MC) problem.

This chapter attempts to extend the current LTM (Pijanowski et al. 2005 and 2006) and reconfigure the model as a MC problem; we refer to this version of the LTM as LTM-MC. Moving from binary to MC in LUC modeling presents several challenges. First, we need to determine how well an MC version of a model performs. To accomplish this, we modified the LTM's model structure for MC using a one-per-class coding strategy (see 5.1.2.1 for more details) where the number of nodes in an output layer is equal to the number of desired outputs (Figure 5-2). In order to determine how well the LTM-MC performs, we compared this version of the LTM to two other data mining tools that are easy to configure for MC; Classification and Regression Trees or CART (Loh, 2010) and Multiple Adaptive Regression Splines or MARS (Gooijer and Ray, 2003). A second challenge is to determine how to structurally treat the land use classes. Should they be treated individually for MC (Figure 5-3) or should they be treated as a group in a single record? Here, we treated the LTM-MC as multiple land use classes individually (Figure 5-3); however, we decided that MARS and CART had to treat multiple land use classes as a group in a single record (scale from 0 to n). In such a case, 0 represents the persistence of land use classes and other numbers (1, 2, ..., n) were used to code land use transitions between two times. The third challenge is to determine the coding scheme for the nodes for output layer had to be changed from the original LTM model (see 5.1.2.2 for more details). Code 1 and 0 still represents change and no-change of land use classes as with the original model (see Pijanowski 2002a) and the nodes in the output layer are labeled as discriminate output classes (Figure 5-2 and 5-3). Finally, a comparison of

models is challenging as the LTM-MC and CART develops unique probability maps for each output; however, MARS develops one suitability map that scale from 0 to n (number of output class; Figure 5-4a). There are some cells that may change to more than one class in CART and LTM-MC (Figure 5-4b; we call these ambiguous predictions); however, each cell can belong only to one land use class in the future. Here, we create simple rules to eliminate ambiguous predictions between mutual land use simulations.

The specific aims of this chapter are to (1) reconfigure three data mining tools for multiple land use transition that have already been developed for single LUC (LTM, CART and MARS); (2) develop effective rules to overcome the ambiguous predictions in MC; (3) compare the multiple land use transitions of three data mining techniques with one other in terms of their potential for agriculture, forest and urban change simulation in MRW and SEWI using relative operating characteristic (ROC) and percent correct match (PCM) and (4) to explore the advantages and disadvantages of the model structure and coding scheme (treating dependent variables as individual or in a group) for MC. We argue that the results of this work provide an effective and appropriate methodology for assessing how well multiple land use transition models perform.

The chapter is organized as follows. Section 5-2 gives an overview of MC using three data mining approaches (LTM-MC, CART and MARS) and summarizes the accuracy assessment metrics used to validate the three models. In section 5-3, two study areas are briefly described and we explain how we implemented the SNNS software to run LTM-MC, and SPM software to run CART and MARS. Section 5-4 describes the simulation results of agriculture, forest and urban transitions of three models in MRW

and SEWI and compares the results of MC simulations with one another. Section 5-5, we conclude with a summary of our findings.

5.2 Methods

5.2.1 LTM-MC as a GPM

LTM is a feed-forward ANN, which uses the supervised learning algorithm (back-propagation algorithm) to forecast LUC (Pijanowski et al. 2002a). The number of layers, nodes per layer and connections between nodes in consecutive layers usually define the model structure of the LTM. The original version of the LTM followed two main changes including: first, we modified the original structure of the LTM for binary classification, where the number of nodes in output layer is equal to the number of the desired output (Figure 5-2) and second, we used one-per-class coding strategy for the output layer, which use a combination of k -binary numbers to represent k -category attributes, each associated with one of the transition. A k -class pattern classification problem can be implemented into a single ANN architecture with k outputs (Figure 5-2). In order to show the state of transition for each land use class, only one of the k numbers in the output layer need to be coded as one while the others stay zero (Figure 5-2 and 5-3). All the nodes in output layer are coded zero if land use persists between two times. Our LTM-MC enables a user to define I inputs, H hidden units and O output units (Figure 5-2). The output of the j^{th} hidden unit is obtained by first forming a weighted linear (w_{ij}) combination of the I input values, and adding a bias (Eq. 5-1a):

$$a_j = \sum_{i=1}^I w_{ji} X_i + b_{j0} \quad (\text{Eq. 5-1a})$$

Here, w_{ji} denotes a weight in the first layer, going from input i to hidden unit j , X_i shows the spatial predictor (unit i) as inputs of LTM-MC and b_{j0} denotes the bias for hidden unit j . The activation of hidden unit j is then obtained using the activation function of LTM-MC (logistic function) for hidden layers (Eq. 5-1b):

$$Z_j = f(a_j) \quad (\text{Eq. 5-1b})$$

The output of unit k is obtained by transforming the activations of the hidden units using a second layer of processing elements. Thus, for each unit k , we construct a linear combination of the outputs of the hidden units of the form (Eq. 5-2a):

$$p_k = \sum_{j=1}^H w_{kj} Z_j + b_{k0} \quad (\text{Eq. 5-2a})$$

Similarly, w_{kj} denotes a weight in the hidden layer, going from hidden j to output unit k , Z_j shows the output of the unit j hidden unit and b_{k0} denotes the bias for output unit k . The activation of output unit k is then obtained using the activation function (identity function) of LTM-MC for output layers (Eq. 5-2b):

$$Y_k = g(p_k) \quad (\text{Eq. 5-2b})$$

By combining the Eqs 5-1a, 5-1b, 5-2a and 5-2b, we obtain an explicit expression for the complete function represented by the LTM-MC in the form of Eq. (5-3):

$$Y_k = g\left(\sum_{j=1}^H w_{kj} f\left(\sum_{i=1}^I w_{ji} X_i + b_{j0}\right) + b_{k0}\right) \quad (\text{Eq. 5-3})$$

Where I is the number of input nodes, H is the number of hidden nodes, O is the number of output nodes. Thus, i , j and k can change from 1 to I , H and O , respectively. The objective of the training run is to adjust the weights and biases

iteratively in order to minimize the error function (Bishop, 1995). Training run can be stopped when the change in weights between two consecutive epochs become smaller than the specific threshold, the percentage of misclassified values become smaller than some threshold, or a predefined the number of epochs has expired. In this article, we use the maximum number of epochs (50,000 cycles) to stop the training run (Pijanowski et al. 2005 and Tayyebi et al. 2012).

5.2.2 CART and MARS as multiple classification LNPMs

CART and MARS within the SPM software over-grow first to make sure that stopping rules do not avoid the model to extract the underlying patterns in data (this prevents under-fitting in training run) and consequently pruning back by penalizing the complexity of the model and removing the unnecessary growth of the model that does not improve the accuracy significantly (i.e. prevents over-fitting in training run) to obtain the best and optimum model (Steinberg and Colla, 1997).

5.2.2.1 Classification And Regression Tree (CART)

CART is a recursive partitioning procedure that classifies the categorical (classification tree) or continuous (regression tree) data at each node (e.g. parent) using a set of if-then-else rules (Sut and Simsek, 2011). The process begins with the root node at the top of the tree, which contains the entire data for the training run (Yap et al. 2011). A node in the CART model is either a terminal node (a node without children), or non-terminal node (a node with children; Chen, 2011). The tree structure represents spatial drivers of LUC organized hierarchically (levels in the tree are representative of the level of significance of variables) and series of splits for each predictor (Ture et al. 2005).

CART seeks the split using search algorithms to classify the data into binary or multiple classes by checking all unique values across the range of data values of different predictors. Binary decision trees fragment the data into the clusters slower than MC and find patterns that are more complex across data values (Ayoubloo et al. 2011).

CART calculates the probability (p_j) of the land use classes in the root node of the tree using relative frequencies in the entire learning data ($p_j = \frac{N_j}{N}; j = 1, 2, \dots, J$; where N_j is the number of cells belong to land use class j from the entire data N ; Loh, 2010). Afterward, $p(j, t)$ denotes the probability of land use class j (Eq. 5-4a) which is estimated from the data within node t (where $N_j(t)$ is the number of cells in node t belonging to class j). $p(j|t)$ denotes the conditional probability that CART classifies the land use classes accurately (Eq. 5-4b; where $p(t) = \sum_j p(j, t)$):

$$p(j, t) = p_j \times \frac{N_j(t)}{N_j} \quad (\text{Eq. 5-4a})$$

$$p(j|t) = \frac{p(j, t)}{p(t)} \quad (\text{Eq. 5-4b})$$

Gini is usually used as a node impurity function to define a splitting rule (Camdeviren et al. 2007) for each unique value in model predictors to find the best split to fragment data (uniform cost; Eq. 5-5a and non-uniform cost; Eq. 5-5b). $C(i|j)$ represents the cost of misclassifying a cell that belongs to land use class j into land use class i as follows:

$$d(t) = \sum_{j=1}^J \sum_{i=1}^{J-1} p(i|t)p(j|t) = \frac{1}{2} \left(1 - \sum_{j=1}^J p^2(i|t) \right) \quad (\text{Eq. 5-5a})$$

$$d(t) = \sum_{j=1}^J \sum_{i=1}^{J-1} p(i|t)p(j|t)(C(i|j) + C(j|i)) \quad (\text{Eq. 5-5b})$$

The best split in node t is the one that maximizes the node impurity function ($d(t)$) in the children of node t (Loh, 2010). The gain function (Eq. 5-6) can be used to determine the goodness of a split (Kurt et al. 2008; split s for node t). The gain function uses a distribution of data before and after splitting to make a more homogenous subset than the previous node (Chang and Chen, 2009). A splitting value is adopted at node t that maximizes the reduction in diversity obtained by the split. Where p_L and p_R are the proportions of cells going to nodes t_L (left) and t_R (right) respectively:

$$\Delta d(s, t) = d(t) - p_L d(t_L) - p_R d(t_R) \quad (\text{Eq. 5-6})$$

5.2.2.2 Multivariate Adaptive Regression Splines (MARS)

MARS is capable of finding optimal variable transformations and interactions between inputs (Friedman, 1991; Friedman, 1996). Knots are responsible in MARS to break the independent variables into subsets (Chang et al. 2011). Any arbitrary function with an irregular shape can be approximated using a large number of knots (Andrés et al. 2011). The coefficients of MARS can change for different intervals as well as different predictors (Lee and Chen, 2005). MARS have been generalized for incorporation into the MC. We assume that $y = (y_1, y_2, \dots, y_k)^T \in R^k$ contains a k-dimensional output which depends on p-dimensional variables $x = (x_1, x_2, \dots, x_p)^T \in R^p$ (Gooijer and Ray, 2003; N observations; 0 represent no-change while the other integer numbers show LUC; Eq. 5-

7). Specifically, each regression function is modeled as a linear combination of $S > 0$ basis function $b_s(x_j)$, so that for a function f (where i and j can change from 0 to k and p , respectively), using an ordinary least squares estimation:

$$y_i = \hat{f}(x_j) = \sum_{j=1}^p \sum_{s=1}^{S_j} \beta_j b_s(x_j) \quad (\text{Eq. 5-7})$$

Here, S_j denotes the number of the knots for the corresponding predictors (x_j) and β_j are regression parameters. In order to have a fast and easy interpretable MARS model, we limit the basis functions to linear terms (only $(x_j - t_{js})_+$ and $(t_{js} - x_j)_+$ where t_{js} is the knot for driver j). The best MARS model is chosen using generalized cross-validation (GCV). For GVC, those pairs of basis functions that contribute less to the goodness-of-fit are eliminated in a backward phase. GCV takes into account not only the estimation errors, but also the complexity of the model (Eq. 5-8; Li et al. 2010). GVC is calculated as such, where λ is the effective number of degrees of freedom whereby the GCV adds a penalty for adding more input variables to the model (Gooijer and Ray, 2003):

$$GCV = \frac{1}{N} \frac{\sum_{i=1}^N (y_i - f(x_i))^2}{\left(1 - \lambda/N\right)^2} \quad (\text{Eq. 5-8})$$

The ability of MARS to simulate LUC can be also evaluated using an R^2 value (Samui and Kothari, 2011; Eq. 5-9), where y_i and $f(x_i)$ are the reference and predicted response values, respectively, \bar{y} and $\overline{f(x_i)}$, are mean of reference and predicted response values:

$$R^2 = \frac{\sum_{i=1}^N (y_i - \bar{y})(f(x_i) - \overline{f(x_i)})}{\sqrt{\sum_{i=1}^N (y_i - \bar{y})^2} \sqrt{\sum_{i=1}^N (f(x_i) - \overline{f(x_i)})^2}} \quad (\text{Eq. 5-9})$$

5.2.3 Adapted Rules to Remove Conflicts in MC

Multiple classifications (MC) should assign each cell to a unique land use class; however, there are often cells that may be assigned to more than one land use class. These ambiguous predictions occur due to the complexity of the LUC patterns, where data mining approaches cannot draw distinct boundaries between land use classes. A simple method is suggested here to solve the conflicts problems. We added a new step after the land use predictions by applying a two-way comparison between all the classes with ambiguous prediction results. CART and LTM-MC develops unique suitability maps for each output; however MARS creates one suitability maps scale from 0 to n (n is integer and equal to the number of outputs). MARS uses one suitability map to simulate MC without any conflicts (Figure 5-4a); however, CART and LTM-MC experience ambiguous predictions, there are often cells that may change to more than one land use class (Figure 5-4b). The number of cells in this condition depends on the ability of data mining procedures to discriminate between land use classes, strength of drivers, quantity of reference changes for land use classes and number of output land use classes.

A new sub-component was written in C# to eliminate cells that undergoes ambiguous predictions. First, this sub-component, hereafter we call conflict removal, employs a contingency table to count the number of reference land use transitions between the initial and subsequent land use maps. The land use classes receive a rank

value from high to low based on the number of reference transitions; a higher rank is assigned for the output with more reference land use transitions. Thereafter, suitability maps of each land use classes derive from MC are produced; employed to predict LUC (Step 1 in Figure 5-4b). Second, this sub-component counts and saves the number and location of conflicted cells between the simulated land use maps with the highest rank and the other lower rank land use maps mutually ($k-1$ comparison; Step 2 in Figure 5-4b). At each run ($k-1$ times), those ambiguous cells are removed from the lower rank cells in the suitability map (those cells assign to zero in the final map; Step 3 in Figure 5-4b) and the lower rank suitability map uses to predict land use class again. The highest rank prediction map in a first run is a prediction map that does not change because the changes occur in the land use prediction map with the lower rank. Finally, the whole process is repeated for the other $k-1$ classes again. We follow this procedure sequentially to remove the conflicted cells. For MC problems with k outputs, $(k-1)!$ comparison is necessary (Step 4 in Figure 5-4b).

5.2.4 Calibration and validation runs

Modelers usually split data into two mutually exclusive sets: (1) calibration data (e.g. 05% of data) used to build and test the goodness of fit of the models and (2) validation data, used to (e.g. other 95% of data) assess the accuracy of the models (Tayyebi et al. 2012). For the calibration run, SPM software use a k -fold cross validation procedure to examine the model performance (Figure 5-5; Refaeilzadeh et al. 2008). Calibration data (5% of data) are randomly segmented into the k equal sized fold data partitions. One of the k folds is used for the testing run and the remaining $k-1$ fold

data are used to build the model for the learning run at each time. At each iteration (k possible iterations), the $k - 1$ fold is used to find the pattern in data and following that the learned pattern is applied to the testing fold. The SPM software (Steinberg and Golovnya, 2006) takes the average of k iterations to give the accuracy of the model. We used the most common cross validation procedure ($10 - fold$). Because this option is not available in SNNS software, all calibration data (5% of data) were used for training run. Following the training run, the best LTM-MC, CART and MARS models derived from the calibration run is applied to the validation data (other 95% of data) that were not used in calibration run (Tayyebi et al. 2012).

A cross tabulation matrix used to compute the proportion of cells that contained the similar (on-diagonals) and different (off-diagonals) land use classes compared to the reference land use map (Table 5-1). The percent correct match (PCM) indicates the percentage of the cells for the land use class that were classified correctly by the spatial explicit models (Pijanowski et al. 2009). PCM can be used to calculate the proportion of cases that undergo change and no-change. The relative operating characteristic (ROC) curve can be used to evaluate the performance of binary (Pontius and Batchu, 2003; Pijanowski et al. 2006; Tayyebi et al. 2010) and MC (Hand and Till, 2001) problems. For the binary classification problem, a series of cutoffs is applied to predict the land use class. Sensitivity and specificity are computed for each cutoff and the ROC is computed; however, for MC, we followed Hand and Till (2001) that extended the ROC for MC by averaging pair-wise comparisons. The MC problem is decomposed into all possible binary problems and the area under the curve is calculated for each class pair. For a specific class, the maximum area under the curve is used as the ROC measure. Because

CART and LTM-MC develop unique suitability maps for each of land use classes, the application of CART and LTM-MC for MC can be treated as a binary classification using the conventional ROC (Pontius and Batchu, 2003; Pijanowski et al. 2006). In contrast, due to one suitability map for all land use classes ranging from 0 to n (the maximum number of land use classes) resulting from the MARS model, we followed the adapted ROC for MC given by Hand and Till (2001).

5.3. Study Areas, Data Preparation and Model Building

5.3.1 Study Areas

We built three models for two areas (Figure 5-6). The Southeastern Wisconsin (SEWI) region includes seven counties: Kenosha, Milwaukee, Ozaukee, Racine, Walworth, Washington and Waukesha Counties (Pijanowski and Robinson, 2011). SEWI is currently dominated by urban in the east, agriculture in the north and south. Most of the growth has historically occurred close to the city of Milwaukee. Development, especially along highway and road corridors, accounts for most of the suburban growth. Between 1990 and 2000, the amount of urban increased from 24.1% to 28.4%; however, the amount of agriculture and forest decreased from 51.8% to 46.8% and from 6.9% to 6.7%, respectively. The Muskegon River Watershed (MRW) is located in the Lower Peninsula of Michigan, USA (Pijanowski et al. 2007). MRW watershed is currently dominated by forests in the north, agriculture in the central portion, and urban in the south. The southern portion of the watershed was used to grow very high-value crops (Alexander et al. 2007). Between 1978 and 1998, the amount of urban and forest in the watershed

increased from 4.2% to 7.3% and from 55.3% to 57.6%, respectively; however, the amount of agriculture decreased from 22.2% to 17%.

5.3.2 Data Preparation

The land use maps were developed and digitized from aerial photographs at Anderson Level 1 (7 land use classes) and were converted to raster maps in ArcGIS10. Elevation and slope for both regions were obtained from the USGS's Shuttle Radar Topography Mission (SRTM). All spatial layers were resampled to a spatial resolution of 30m×30m. Euclidean distances were calculated to urban, forest, wetland, shrub and agriculture in 1978 for MRW and in 1990 for SEWI. For density calculation, neighborhood function (focal function) used to compute the value at each location based on the input cells in a neighborhood of the central cell. We used circle to define the neighborhoods of the central cell and mean as neighborhood statistic to compute the mean of the values in the neighborhood (Figure 5-6). Three models were developed using 16 and 17 spatial predictors to simulate agriculture, urban and forest change pattern (Table 5-2) using identical data in MRW and SEWI, respectively. Due to the large size of data in both study areas, random sampling was implemented (Table 5-3).

5.3.3 Model Building

CART and MARS models were developed in a commercial product (SPM software, <http://www.salford-systems.com>); however, LTM-MC (based on Stuttgart Neural Network Simulator (SNNS) software), which is open source software (<http://itm.agriculture.purdue.edu>), was implemented in this study. For LTM-MC, inputs drivers were scaled to a range of [0, 1] by dividing by the maximum value and LTM-MC

was trained for 50,000 epochs and saved for in step 100 increments. As a rule of thumb, the maximum number of nodes in CART and basis functions in MARS should be at least two to four times the number of inputs (Steinberg and Golovnya, 2006). We allowed a maximum of 45 nodes in CART and 45 basis functions in MARS (average three times of inputs; 17 and 16 spatial drivers in SEWI and MRW). An effective way to make MARS less locally adaptive is to specify a minimum number of observations between knots. The minimum node sample size specifies the minimum number of cases required in a node for splits to be considered. We set the minimum to 200 in large samples for the smallest node (Steinberg and Golovnya, 2006). The parent node limit must be at least twice the terminal node limit to allow CART to consider a reasonable number of alternative splitters.

5.4 Results and Discussion

5.4.1 CART

The color-coding in CART helps to locate interesting terminal nodes. Red and blue nodes (Figure 5-7) contain more cells that encounter land use changes and no-changes, respectively. The lower plots indicate a relative cost of the training run that traces the relationship between classification errors and tree size. The SPM software halted the training run at 21 nodes (forward run of CART in SEWI) and 25 nodes (forward run of CART in MRW) where the relative cost reached their minimum value. The best tree size or the most accurate classifier (pruned back in CART) is indicated by the green bar (Figure 5-7). The best tree size has 21 and 20 terminal nodes where a relative cost reached 0.33 and 0.55 in SEWI and MRW, respectively (Figure 5-7). Comparing the relative cost and size of a tree in two study areas suggests that LUC

patterns in MRW (higher relative cost and more terminal nodes) are more complicated than LUC pattern in SEWI. The structure of best trees were saved and used for validation data.

Figure 5-8 gives a simple overview of the main drivers we used for the models. Distance to forest and agriculture, distance to agriculture, road and forest are the most significant drivers to simulate urban, forest and agriculture change simultaneously in SEWI and MRW, respectively (Figure 5-8). The top competitor splits in decreasing order of importance are displayed for SEWI and MRW in Table 5-4. The improvement scores are a measure of the quality of the split (larger scores are better); this is where the variance reduction occurs due to the split. Distance to agriculture split at the value 75m yield an improvement of 0.06582 much lower than the main splitter (distance to forest with 0.09451 improvement) in SEWI. Similarly, distance to shrub is the best competitor, split at the value 51m, which yield an improvement of 0.06486, quite similar to the main splitter, distance to shrub with 0.06570 improvements and distance to agriculture with 0.06587 improvements in MRW (Table 5-4).

The cells located within the red nodes with larger suitability values have the greatest chance for LUC (Figure 5-7 and 5-8). In SEWI, the cells within the node 8 (distance to forest less than 65m), the node 20 (distance to wetland over 55m) and the node 18 (distance to agriculture less than 65m) has the greatest suitability for forest, urban and agriculture change, respectively (Figure 5-7 and 5-8). Similarly in MRW, the cells within node 17 (distance to shrub over 45m), node 14 (density of urban greater than 0.03544) and node 18 (distance to wetland over 45m) has the greatest suitability for forest, urban and agriculture change, respectively (Figure 5-7 and 5-8). This procedure

continues from red node with greater suitability values to blue nodes with lower suitability value until CART satisfies the total number of reference LUC (the quantity of LUC between two times were fixed; Table 5-3).

5.4.2 MARS Training

The best MARS model is the one with the smallest GCV, which is selected in the backward run. GCV displays the contribution of the basis functions were added to the model. Figure 5-9 shows the point where GCV most minimizes error where the MARS is expressed using 39 and 40 basis functions in SEWI and MRW, respectively (Table 5-5 and 5-6). Figure 5-9 also shows that the lowest GCV values are 0.35 and 0.54 in SEWI and MRW, respectively (Figure 5-9). GCV for SEWI is lower than MRW (Figure 5-9). R^2 improved because of additional basis functions (Figure 5-9) and reaches to its maximum at 0.43 and 0.25 in SEWI and MRW, respectively. GCV, R^2 values and the number of basis functions also indicate that LUC patterns in MRW (higher GCV; lower R^2 more basis function) are more complicated than LUC pattern in SEWI. The basis function of the best MARS models were saved and used for validation data in two study areas.

The variable with the larger standard deviation (in an ANOVA table) has the more explanatory power to describe the relationship between the inputs and outputs. Distance to agriculture with standard deviation 0.74321 and 0.29275 in SEWI and MRW show greater contributions to simulate land use transitions, respectively (Figure 5-10). Following those variables, distance to urban with standard deviation of 0.31399 in SEWI, distance to shrub with standard deviation 0.25686 in MRW indicate greater contribution

to simulate land use transitions, respectively (Figure 5-10). Distance to shrub with 4 basis functions in SEWI and elevation with 8 basis functions in MRW include the highest number of basis functions in the MARS (Table 5-5). Table 5-5 shows the pruned model of MARS models developed in SEWI and MRW.

5.4.3 LTM-MC Training

Figure 5-11 plots the mean squared error (MSE) across training cycles in SEWI and MRW using LTM-MC. MSE starts around 0.32 in SEWI and 0.37 in MRW. The MSE of two scenarios drop through 10,000 cycles in SEWI and MRW. We halted the training at 50,000 cycles where the MSE reached a stable minimum of 0.23 in SEWI and 0.33 in MRW. The best network files from the training run were saved and used to create the suitability map in two study areas.

5.4.4 Variable rankings in CART and MARS

The model variables were ranked from most to least important for MARS and CART (Table 5-6). The least important variable is the one with the smallest impact on the model's goodness-of-fit and the most important variable is the one that, when omitted, degrades the model fit the most. It is essential to pay attention to the level of significance of the predictors because they show the character of LUC in the study area. In SEWI, CART identified distance to agriculture, forest and urban as the main variables; however, MARS selected distance to agriculture, wetland and urban as the best drivers to model forest, urban and agriculture (Table 5-6). In MRW, CART and MARS agree about the most significant spatial drivers (distance to agriculture, road, forest and shrub); however, these drivers do not have same order (Table 5-6).

5.4.5 Terminal node in CART

Figure 5-12 provides a representation of the ability of the nodes in CART to capture the LUC pattern. We sorted the nodes according to the highest concentrations of change (see Figure 5-8 to find the node number). Nodes 3, 5, 7 and 14 have the highest concentration of agriculture, urban, forest change and no-change in SEWI, respectively (Figure 5-12 and 5-8). Similarly, nodes 11, 10, 19 and 13 have the highest concentration of agriculture, urban, forest change and no-change in MRW, respectively (Figure 5-12 and 5-8).

5.4.6 Validation of three models using PCM and ROC

Figure 5-13 summarizes the comparison of the three models for MC using PCM and ROC. According to the PCM, LTM-MC and CART had similar accuracy and were more accurate than MARS to simulate urban, agriculture and forest change in both regions. There is an exceptional case for forest change modeling in SEWI where the difference between LTM-MC and CART with MARS is huge because there are few cells that experienced forest change during 10 years (around 7.7%). According to ROC, LTM-MC and CART outperformed MARS using validation data significantly and LTM-MC performed slightly better than CART (Figure 5-13). ROC for three models was similar to each other in SEWI; however, ROC for LTM-MC and CART were greater than the ROC for MARS in MRW. CART and LTM-MC models showed adequate performance as they produced ROC values over 0.80 (Figure 5-13).

5.5 Discussion

Most of the LUCC models have been designed for single classification predictions (Clarke et al. 1997; Pijanowski et al. 2002; Pontius et al. 2001; Veldkamp and Fresco, 1996), it is called hard classification (Pontius and Connors, 2006). Data analysis with hard classification is straightforward where scientists usually use contingency table to compare maps with series of categories (Pijanowski et al. 2006). For binary classification, a model classifies the data into binary classes. However, very few studies have focused on building a LUCC model for MC (Li and Yeh, 2002) which has received attention recently, there are two types of models that can use to classify the cells into distinct and mutual LULC classes: (1) using series of binary models to simulate multiple LULC classes (e.g. using OVA or AVA): This process is time consuming and depend on the number of LULC classes and (2) developing a model which can classify the cells in LULC maps to distinct LULC classes simultaneously which is the focus of this paper. This process only needs one model to assign cells in the map to mutual LULC classes. This paper has explored issues related to the MC problem in LUCC modeling. To accomplish this, we extended the original version of the single class transition LTM, to include MC transitions.

LULC classes may be poorly defined or understood, classification of LULC cells within those categories may be correspondingly uncertain. Thus, each cell can belong to multiple LULC classes (e.g. partial membership), it is called soft classification or partial membership (Pontius and Connors, 2006). The idea here is to develop a model which can classify the cells in LULC maps into more than one LULC class (or multiple

memberships). Pontius and Connors (2006) developed new approaches which compare two maps with cells that belong simultaneously to several LULC classes or have partial membership to multiple LULC classes. Results show that proper interpretation of these methods can reveal patterns in the maps. Fuzzy set theory is another way (Woodcock and Gopal, 2000) to compare maps which a given cell can have multiple membership.

Models with MC are unstable when there are small changes in training data or in model structure; these often lead to large changes in the output values (Breiman, 1998). These MC challenges are apparent in many pattern recognition applications. For instance, in word speech recognition, a major cause of errors is the inaccurate detection of the beginning and ending patterns of speech (Shin et al. 2000). A robust speech/non-speech classification method, which uses CART to combine the multiple features (e.g. linear prediction error energy, pitch, and band energy), was proposed in noisy environments for speech recognition of voice dialing cellular phone (Shin et al. 2000). The results showed that the proposed method using multiple features performed better than using a single feature by 4 to 10%.

Scientists usually use exact data for training run to compare models, and choose the best models (Wen et al. 2009). LUCC models for MC generate both false positive (i.e. assigning a cell to an incorrect LULC class) and false negative (i.e. not assigning a cell to a correct LULC class) errors. Models with different algorithms have not only different classification performance, but also their misclassification rates (false positive and false negative) are variable in spatial and temporal scale (Wen et al. 2009). Using only the best model is critical since we may ignore information from other models. Models may complement each other; misclassified by one model may detect by another

model. Using hybrid models as an alternative, which are at least combination of more than one model (e.g. CA-GA, CA-ANN, CA-SVM), have received more attention during last 10 years to fill this gap. A manager, natural resource, decision maker and planner require the ranking of various models, based on both types of errors. However, additional complexity is no guarantee for improvement in practical usefulness. There are possibly other ways to simulate MC simultaneously compared to that we employed in this paper. There is also substantial need for improvement in overall performance of the models such as using hybrid models.

5.6 Conclusion

Classification algorithms help to understand the existing pattern in data and can be used to predict the land use class of the new cell while comparisons of suitable techniques remain a meticulous task. This chapter presented a comprehensive study on multiple land use classifications with focuses on issues, (1) architecture and encoding schemes for multiple LUC models and (2) suggesting a solution for confliction problems in multiple land use classification, including three data mining procedure (LTM-MC, CART and MARS). Our study compares three data mining approaches for MC pattern recognition using ROC and PCM. A systematic comparison is important to understand the performance of the different algorithms. Result support that LTM-MC, CART and MARS are potential in dealing with high dimensional LULC data, mixed data (e.g. categorical, continuous or ordinal) and complex relationships between dependent and independent drivers (e.g. linear or non-linear). CART and MARS gives the lowest and highest rate of false positive and false negatives predictions for MC, respectively while

LTM-MC gives better accuracy than CART and MARS overall. POLYMARS, which is an extension of MARS that allows for multiple responses (Kooberberg et al. 1997), can be used for MC in future effort.

5.7 References

- Alexandridis, K., B. C. Pijanowski and Z. Lei. (2007). Assessing Multi-Agent Parcelization Performance in the MABEL Simulation Model using Monte Carlo Replication Experiments. *Environment and Planning B*. 34:223-244.
- Andrés, J. D., P. Lorca, F. J. C. Juez., F. Sánchez-Lasheras. (2011). Bankruptcy forecasting: A hybrid approach using Fuzzy c-means clustering and Multivariate Adaptive Regression Splines. *Expert Systems with Applications* 38, 1866–1875.
- Ayoubloo, M. K., H. M. Azamathulla, E. Jabbari, M. Zanganeh. (2011). Predictive model-based for the critical submergence of horizontal intakes in open channel flows with different clearance bottoms using CART, ANN and linear regression approaches. *Expert Systems with Applications*, 38 (2011) 10114-10123.
- Bay. D. S. (1998). Combining nearest neighbor classifiers through multiple feature subsets. In *Proceedings of the 17th International Conference on Machine Learning*, pages 37–45, Madison, WI.
- Batty, M. and Y. Xie, (1994). From cells to cities, *Environment and Planning B*, 21, s31-s48.
- Bishop, C. M. (1995), *Neural Networks for Pattern Recognition*, Oxford: Oxford University Press.
- Breiman, L., Friedman, J. H., Olshen, R. A., and C. J. Stone. (1984). *Classification and Regression Trees*. Belmont, CA: Wadsworth.
- Camdeviren, H. A., Yazici, A. C., Akkus, Z., Bugdayci, R., & Sungur, M. A. (2007). Comparison of logistic regression model and classification tree: An application to postpartum depression data. *Expert Systems with Applications*, 32, 987–994.
- Chang, C., C. Wang., B. C. Jiang. (2011). Using data mining techniques for multi-diseases prediction modeling of hypertension and hyperlipidemia by common risk factors. *Expert Systems with Applications* 38, 5507–5513.
- Chang, C. L., & Chen, C. H. (2009). Applying decision tree and neural network to increase quality of dermatologic diagnosis. *Expert Systems with Applications*, 36, 4035–4041.
- Chen, M. Y. (2011). Predicting corporate financial distress based on integration of decision tree classification and logistic regression. *Expert Systems with Applications*, 38 (2011) 11261–11272.
- Clarke, K.C., Hoppen, S., Gaydos, L., (1997). A self-modifying cellular automaton model of historical urbanization in the San Francisco Bay area. *Environmental Planning B: Planning and Design* 24, 247–261.
- Cortes, C. and V. Vapnik. (1995). Support-vector networks. *Machine Learning*, pages 273-297.
- Gooijer, D. J. G., B. K. Ray. (2003). Modeling vector nonlinear time series using POLYMARS. *Computational Statistics and Data Analysis*, 42 (2003) 73-90.
- Hastie, T., and R. Tibshirani. (1998). Classification by pairwise coupling. In Michael I. Jordan, Michael J. Kearns, and Sara A. Solla, editors, *Advances in Neural Information Processing Systems*, volume 10. The MIT Press.

- Dietterich, T. G. and G. Bakiri. (1995). Solving multiclass learning problems via error correcting output codes. *Journal of Artificial Intelligence Research*, 39:1-38.
- Dietzel, C., and Clarke, K. C. (2006). Decreasing computational time of urban cellular automata through model portability. *Geoinformatica*. vol. 10, no. 2. pp. 197-211.
- Dubchak, I., Muchnik, I., Mayor, C., Dralyuk, I. and Kim, S. H. (1999). Recognition of a protein fold in the context of the Structural Classification of Proteins (SCOP) classification. *Proteins*, 35, 401-407.
- Friedman, J. H. (1991). Multivariate Adaptive Regression Splines (with discussion). *Annals of Statistics* 19, 1.
- Friedman, J. H. (1996). Another approach to polychotomous classification. Technical report, Stanford University.
- Hand, D. J. and R. J. Till. (2001). A simple generalization of the area under the ROC curve for multiple class classification problems. *Machine Learning*, 45, 171-186.
- Hardle, W., M. Müller, S. Sperlich, and A. Werwatz. (2004). *Nonparametric and Semiparametric Models*. Berlin: Springer Series in Statistics.
- He, Z., Lo, C., (2007). Modeling urban growth in Atlanta using logistic regression. *Computers, Environment and Urban Systems*, 31(6), 667-688.
- Ho, T. K. (2000). Complexity of classification problems and comparative advantages of combined classifiers. *Lect. Notes Comput. Sci.* 2000; 1857: 97–106.
- Jenerette, G. D. and J. Wu. (2001). Analysis and simulation of land-use change in the central Arizona – Phoenix region, USA. *Landscape Ecology* 16: 611-626.
- Kurt, I., Ture, M., & Kurum, A. (2008). Comparing performances of logistic regression, classification and regression tree, and neural networks for predicting coronary artery disease. *Expert System with Applications*, 34, 366–374.
- Lam, L., C. Y. Suen. (1995). Optimal combinations of pattern classifiers. *Pattern Recognition Letters* 16 (1995) 945-954.
- Lee, T. S., & Chen, I. F. (2005). A two stage hybrid credit scoring model using artificial neural networks and multivariate adaptive regression splines. *Expert Systems with Applications*, 28, 743–752.
- Li, X. and Yeh, A. G. O., (2002). Neural-network-based cellular automata for simulating multiple land use changes using GIS. *International Journal of Geographical Information Science*, 16(4), pp. 323-343.
- Li, H., Sun, J., & Wu, J. (2010). Predicting business failure using classification and regression tree: An empirical comparison with popular classical statistical methods and top classification mining methods. *Expert Systems with Application*. doi:10.1016/j.eswa.2010.02.016.
- Loh, W-Y. (2010). Tree-structured classifiers. *WIREs Comp Stat* 2010, 2:364–369.
- Lumley T, Sutherland P, Rossini A, Lewin-Koh N, Cook D, Cox Z. (2002). Visualising high-dimensional data in time and space: ideas from the Orca project. *Chemometrics and Intelligent Laboratory Systems* 60: 189-95.
- Moore, N., N. Torbick, B. Pijanowski, B. Lofgren, J. Wang, J. Andresen, D. Kim, and J. Olson. (2010). Adapting MODIS-derived LAI and fractional cover into the Regional Atmospheric Modeling System (RAMS) in East Africa. *International Journal of Climatology*. doi: 10.1002/joc.2011.

- Pijanowski, B. C., Daniel G. Brown, Bradley A. Shellito, Gaurav A. Manik. (2002a). Using neural networks and GIS to forecast land use changes: a Land Transformation Model. *Computers, Environment and Urban Systems*. 26, 553–575.
- Pijanowski, B. C., Shellito, B., Pithadia, S., Alexandridis, K. (2002b). Forecasting and assessing the impact of urban sprawl in coastal watersheds along eastern Lake Michigan. *Lakes & Reservoirs: Research and Management* 2002 7: 271–285.
- Pijanowski B. C., Pithadia S., Shellito B. A., Alexandridis, K. (2005). Calibrating a neural network based urban change model for two metropolitan areas of Upper Midwest of the United States. *International Journal of Geographical Information Science*. 19:197–215.
- Pijanowski, B. C., K. Alexandridis and D. Mueller. (2006). Modeling urbanization patterns in two diverse regions of the world. *Journal of land use science*. (1): 83-108.
- Pijanowski, B., D. K. Ray, A. D. Kendall, J. M. Duckles, and D. W. Hyndman. (2007). Using back-cast land-use change and groundwater travel time models to generate land-use legacy maps for watershed management. *Ecology and Society* 12 (2):25.[online] URL: <http://www.ecologyandsociety.org/vol12/iss2/art25/>.
- Pijanowski, B. C., Tayyebi, A., Delavar, M. R., and Yazdanpanah, M. J. (2009). Urban expansion simulation using geographic information systems and artificial neural networks. *International Journal of Environmental Research*, 3(4), 493-502.
- Pijanowski, B.C., and K. D. Robinson. (2011). Rates and patterns of land use change in the Upper Great Lakes States, USA: A framework for spatial-temporal analysis. *Landscape and Urban Planning*. DOI:10.1016/j.landurbplan.2011.03.014.
- Pijanowski, B. C., Moore, N., Mauree, D., Niyogi, D. (2011). Evaluating Error Propagation in Coupled Land–Atmosphere Models. *Earth Interact.*, 15, 1–25.
- Pontius, R. G. Jr., J. Cornell and C. Hall. (2001). Modeling the spatial pattern of land-use change with GEOMOD2: application and validation for Costa Rica. *Agriculture, Ecosystems & Environment* 85(1-3): 191-203.
- Pontius Jr., R. G. and Batchu, K. (2003). Using the Relative Operating Characteristic to Quantify Certainty in Prediction of Location of Land Cover Change in India. *Transactions in GIS*, 7(4): 467–484.
- Pontius, R. G. Jr and J. Connors. (2006). Expanding the conceptual, mathematical, and practical methods for map comparison. *Conference proceedings of the meeting of Spatial Accuracy*. Lisbon, Portugal. 16p.
- Refaeilzadeh, P., Tang, L. & Liu, H. (2008). Cross-validation, <http://www.public.asu.edu/~ltang9/papers/ency-cross-validation.pdf>
- Ray, D. K., and B. C. Pijanowski, (2010). A back-cast land use change model to generate past land use maps: application and validation at the Muskegon river watershed of Michigan, USA, *journal of land use science*, 5: 1, 1-29.
- Ray, D. K., Duckles, J. M., & Pijanowski, B. C. (2010). The impact of future land use scenarios on runoff volumes in the Muskegon river watershed. *Environmental Management*, 46(3), 351-366.
- Ray, D. K., Pijanowski, B. C., Kendall, A. D., Hyndman, D. W. (2012). Coupling land use and groundwater models to map land use legacies: Assessment of model uncertainties relevant to land use planning. *Applied Geography* 34, 356-370.

- Rifkin, R. and A. Klautau. (2004). Parallel networks that learn to pronounce English text. *Journal of Machine Learning Research*, pages 101-141.
- Samui, P. and D. P. Kothari. (2011). Application of Multivariate Adaptive Regression Splines to Evaporation Losses in Reservoirs. *Earth Science India*, ISSN: 0974-8350. Vol. 4(I), January, 2011, pp.15-20.
- Shan, J., S. Alkheder, J. Wang. (2008). Genetic Algorithms for the Calibration of Cellular Automata Urban Growth Modeling, *Photogrammetric Engineering and Remote Sensing*, Journal of the American Society for Photogrammetry and Remote Sensing, Vol. 74, No. 10, pp. 1267-1277.
- Siegel, S., and Castellan, N. J. (1988). *Nonparametric statistics for the behavioral science*. New York: McGraw-Hill.
- Steinberg, D. and Colla, P. (1997). *CART-Classification and Regression Trees: A Supplementary Manual for Windows*, Salford Systems Inc., San Diego.
- Steinberg, D., Golovnya, M. (2006). *CART 6.0 User's Manual*. Salford Systems, San Diego, CA.
- Sut, N., and Simsek, O. (2011). Comparison of regression tree data mining methods for prediction of mortality in head injury. *Expert Systems with Applications*, doi:10.1016/j.eswa.2011.06.006.
- Tayyebi, A., Delavar, M. R., Pijanowski, B. C., Yazdanpanah, M. J., Saeedi, S., and Tayyebi, A. H. (2010). A spatial logistic regression model for simulating land use patterns, a case study of the Shiraz metropolitan area of Iran. In E. Chuvieco, J. Li, & X. Yang (Eds.), *Advances in earth observation of global change*. Springer Press.
- Tayyebi, A., Pijanowski, B. C., A. H. Tayyebi, (2011a). An urban growth boundary model using neural networks, GIS and radial parameterization: An application to Tehran, Iran. *Landscape and Urban Planning* 100, 35-44.
- Tayyebi, A., Pijanowski, B. C., B. Pekin, (2011b). Two rule-based urban growth boundary models applied to the Tehran metropolitan area, Iran. *Applied Geography* 31, 908-918.
- Tayyebi, A., Pekin, B. K., Pijanowski, B. C., Plourde, J. D., Doucette, J., Braun, D. (2012) Hierarchical modeling of urban growth across the conterminous USA: Developing meso-scale quantity drivers for the Land Transformation Model. *Journal of Land Use Science*. DOI: 10.1080/1747423X.2012.675364.
- Tayyebi, A. H., S. Homayouni, J. Shan, M. J. Yazdanpanah, B. C. Pijanowski and A. Tayyebi. (2011a). Model Parameter Uncertainty Assessment in Land Transformation Model. 7th International Symposium on Spatial Data Quality. Coimbra, Portugal, October 12-14, Edited by: Cidalia C. Fonte, Luisa Goncalves, Gil Goncalves, Page 77-82.
- Tayyebi, A. H., S. Homayouni, J. Shan, M. J. Yazdanpanah, B. C. Pijanowski and A. Tayyebi. (2011b). Multi-Scale Analysis Approach of Simulating Urban Growth Pattern using a Land Use Change Model, 7th International Symposium on Spatial Data Quality. Coimbra, Portugal, October 12-14, Edited by: Cidalia C. Fonte, Luisa Goncalves, Gil Goncalves, Page 207-210.

- Tayyebi, A. H., S. Homayouni, J. Shan, M. J. Yazdanpanah, B. C. Pijanowski and A. Tayyebi. (2001c). Uncertainty Framework in Land Use Change Models: An Application of Data, Model Parameter and Model Outcome Uncertainty in Land Transformation Model, 7th International Symposium on Spatial Data Quality. Coimbra, Portugal, October 12-14, Edited by: Cidalia C. Fonte, Luisa Goncalves, Gil Goncalves, Page 211-213.
- Tsoumakas, G., I. Katakis, and I. Vlahavas. (2010). Mining multi-label data. In Oded Maimon and Lior Rokach, editors, *Data Mining and Knowledge Discovery Handbook*, chapter 34, pages 667–685. Springer, 2nd edition, 2010.
- Ture, M., Kurt, I., Kurum, T. A., & Ozdamar, K. (2005). Comparing classification techniques for predicting essential hypertension. *Expert Systems with Application*, 29(3), 583–588.
- Veldkamp, A., Lambin, E. F., (2001). Editorial: predicting land-use change. *Agriculture, Ecosystems and Environment* 85, 1-6.
- Verburg, P. H., de Koning, G. H. J., Kok, K., Veldkamp, A., Bouma, J. (1999). A spatial explicit allocation procedure for modelling the pattern of land use change based upon actual land use. *Ecological Modeling*, 116, 45-61.
- Washington, C., B. Pijanowski, D. Campbell, J. Olson, J. Kinyamario, E. Irandu, J. Nganga, and P. Gicheru. (2010). Using a role-playing game to inform the development of land-use models for the study of a complex socio-ecological system. *Agricultural Systems*. doi: 10.1016/j.agsy.2009.10.002.
- Wiley, M., D. Hyndman, B. Pijanowski, A. Kendall, C. Riseng, E. Rutherford, S. Cheng, M. Carlson, R. Richards, R. Seelbach and J. Koches. (2010). A multi-modeling approach to evaluate the impacts of global change on river ecosystems. *Hydrobiologia* 657:243-262.
- Yap, B. W., S. H. Ong, N. H. M. Husain. (2011). Using data mining to improve assessment of credit worthiness via credit scoring models. *Expert Systems with Applications*, 38 (2011) 13274-13283.
- Zadeh, L. (1965). Fuzzy sets, *Information and Control*, 8: 338–353.

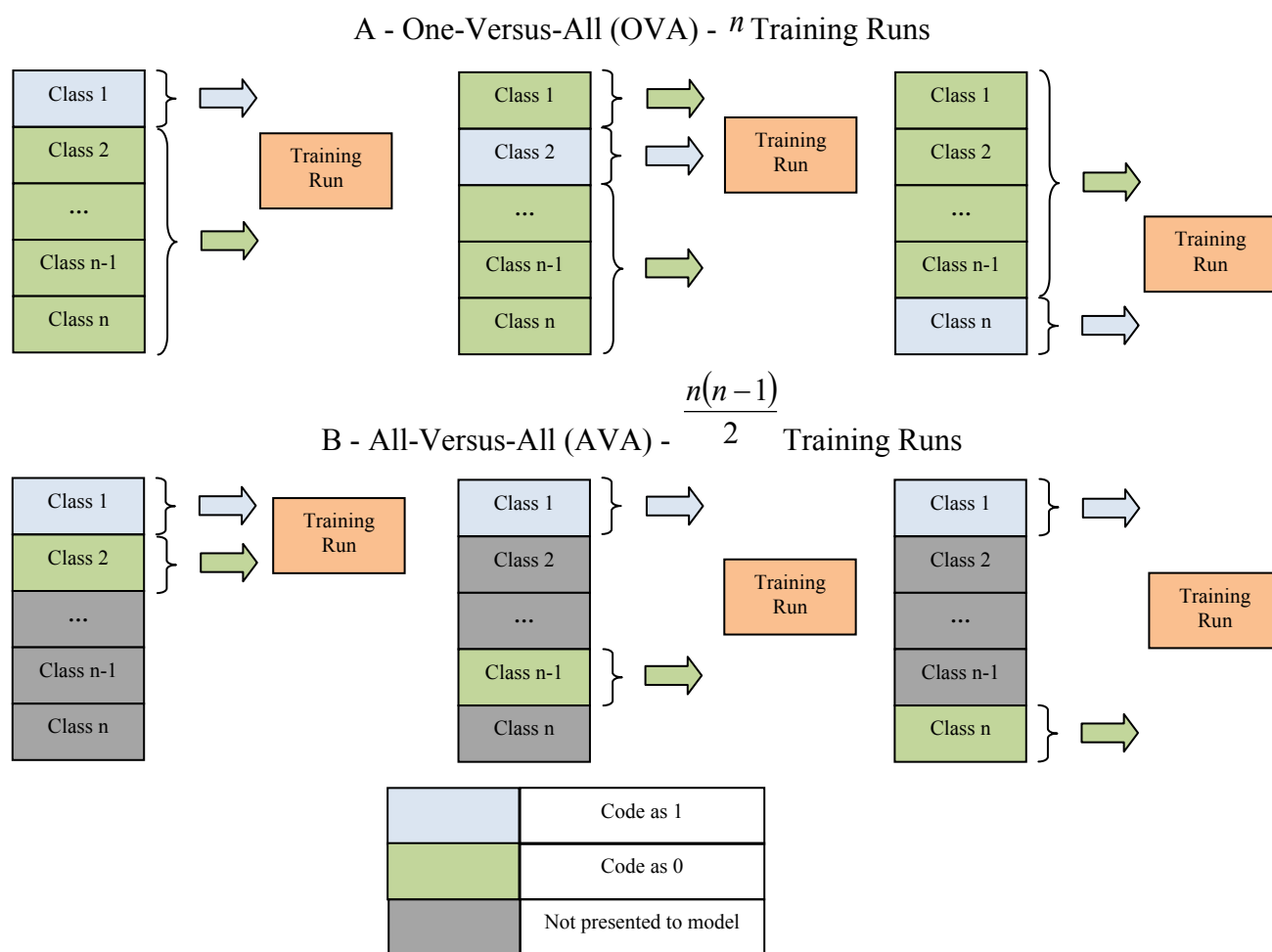


Figure 5-1: The idea of One-Versus-All (OVA) and All-Versus-All (AVA) procedures for MC

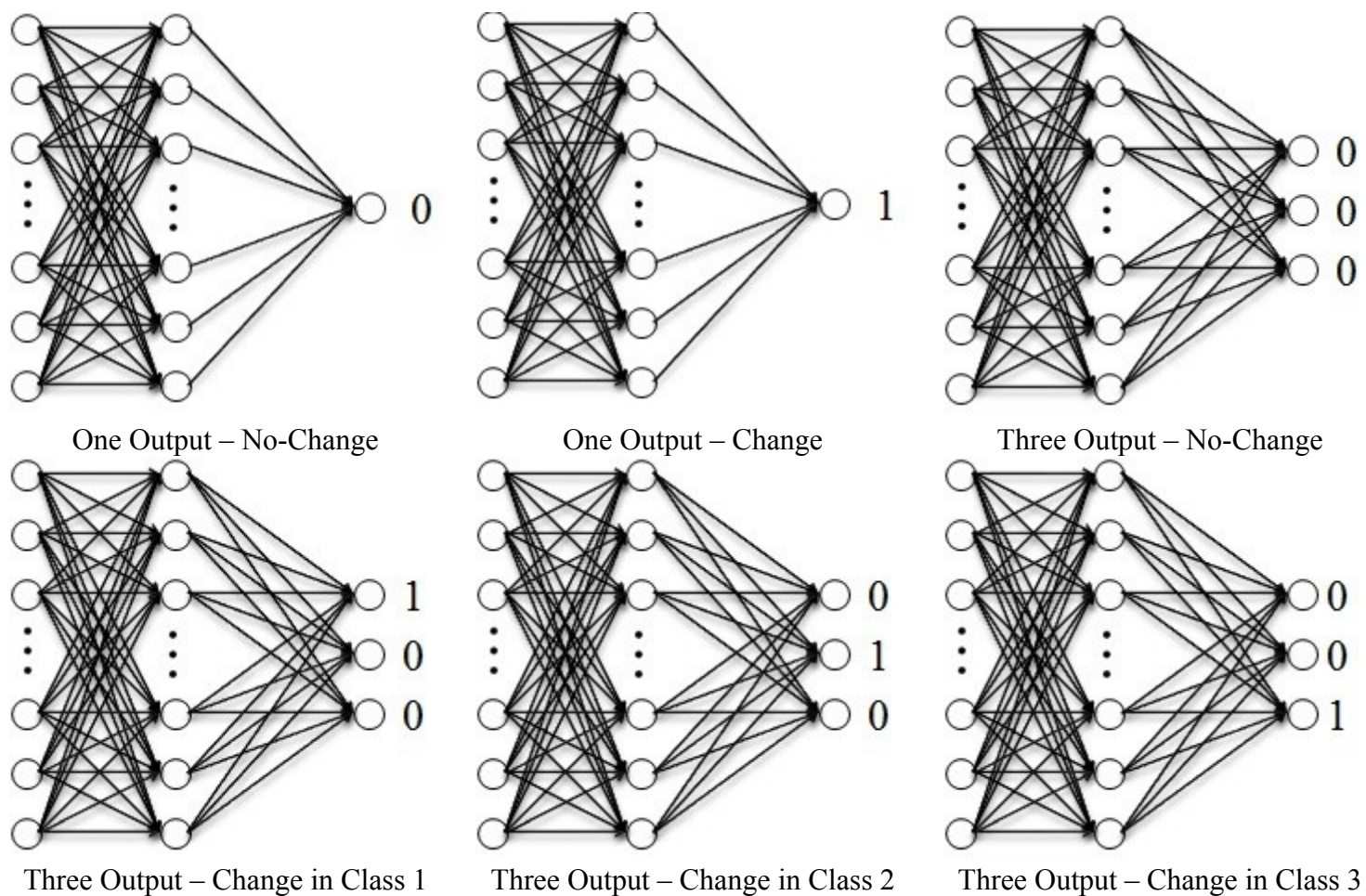


Figure 5-2: Model structure and coding scheme of LTM-MC

```

LTM-MRW-03.pat - Notepad
File Edit Format View Help
SNNs pattern definition file v3.2
generated at Tuesday June 21 13:30:09 2011
No. of patterns : 36579
No. of input units : 16
No. of output units : 3

0.49128 0.25208 0.01958 0.01638 0 0.89499 0.93884 0 0.23422 0.01638 0.31451 0 0 0.00862 0.01987 0.02387
0 1 0 Change in Class 2
0.48837 0.17849 0.07442 0.01096 0 0.91167 0.90938 0 0.17894 0.01547 0.30656 0 0 0.00431 0.01405 0.10657
0 1 0
0.48837 0.62604 0.09504 0.00932 0 0.91725 0.89834 0 0.17495 0.01399 0.30504 0 0 0.01363 0.01987 0.02532
0 0 1 Change in Class 3
0.47965 0.37673 0.09604 0.00444 0 0.88519 0.89382 0 0.07899 0.05324 0.26795 0 0 0.00431 0.04215 0.01688
0 1 0
0.49709 0.30089 0 0 0.97587 0.80109 0 0.16948 0.01797 0.34985 0 0 0.0431 0.07759 0
0 0 0 No-Change
0.49419 0.62604 0.25397 0 0 0.99949 0.76637 0 0.26797 0.00051 0.28185 0 0 0.06964 0.11239 0.00844
0 0 0
0.49419 0.75069 0.24579 0 0 0.94085 0.81199 0 0.04852 0.01785 0.29328 0 0 0.03554 0.02221 0.02387
0 1 0
0.49419 0 0.28993 0 0 0.96634 0.77242 0 0.17495 0.02805 0.30703 0 0 0.02891 0.08487 0
0 0 0
0.49419 0 0.27884 0 0 0.9694 0.76489 0 0.1854 0.02805 0.2955 0 0 0.03475 0.09983 0
0 0 0
0.48256 0.55245 0.2254 0 0 0.93677 0.81876 0 0.10904 0.01785 0.26114 0 0 0.00862 0.03974 0.03774
0 1 0
0.50872 0.66145 0 0.01562 0.74637 0.66891 0 0.23371 0.00323 0 0.20517 0 0.19473 0.11627 0
1 0 0 Change in Class 1
0.47965 0.62604 0.25589 0 0 0.94085 0.80276 0 0.03255 0.01836 0.27526 0 0 0.01363 0.02221 0.04219
0 1 0
0.49419 0.32566 0.30978 0 0 0.93932 0.77731 0 0.03069 0.02805 0.31143 0 0 0.02513 0.03582 0.02669
0 1 0
0.50291 0.37673 0.70644 0 0.0221 0.74494 0.66348 0 0.31069 0 0 0.20972 0 0.22567 0.18664 0.01688
1 0 0
0.49128 0 0.23826 0 0 0.98878 0.74171 0 0.19195 0.01122 0.25564 0 0 0.06004 0.16049 0
0 0 0
    
```

LTM-MC (Three Outputs; e.g. MRW)

```

SPM-MRW-03.txt - Notepad
File Edit Format View Help
Elevation Aspect Urban Durban Forest DForest Agriculture DAgiculture Shrub DShrub wetland Dwetlan Park Stream Road Slope Output
344 216.5377 283.0194 0.0133438 0 0.877551 10182.78 0 488.3646 0.0400314 2095.71 0 0 67.08204 0 2.052775 2 Change in Class 2
341 271.442 9447 0.01121372 0 0.8641161 10029.2 0 331.3608 0.06134565 1965.63 0 0 60 30 0.9548413 2
345 0 1899.737 0 0.9714431 8554.788 0 510 0.02600714 2207.193 0 0 234.3075 283.0194 0 0
344 0 1546.383 0 0.9989801 8340.054 0 745.1846 0.001019888 1890.238 0 0 551.5433 323.1099 0 0
343 0 1698.117 0 0 0.9490056 8868.896 0 120 0.01886792 2163.747 0 0 300 30 0 2
344 136 1674.097 0 0 0.9449261 8850 0 42.42641 0.01886792 2036.468 0 0 174.9286 30 1.350224 3 Change in Class 3
345 0 1865.074 0 0 0.9597144 8428.933 0 445.9821 0.02804692 2133.589 0 0 174.9286 240 0 0
345 0 2063.904 0 0 0.9408465 8523.38 0 134.1641 0.02804692 2256.391 0 0 120 67.08204 0 2
368 249.1986 742.7651 0.0005099439 30 0.972463 7145.103 0 0 0.02702703 1230.366 0 0 1537.335 189.7367 2.569503 1 Change in Class 1
344 0 1574.071 0 0 0.9867415 8156.746 0 488.3646 0.0127486 1824.829 0 0 379.4733 445.9821 0 0
345 0 2110.474 0 0 0.9388067 8457.074 0 150 0.02804692 2246.597 0 0 108.1665 60 0 2
373 323.125 579.3962 0.03416624 67.08204 0.9388067 7133.253 0 0 0.02702703 1061.508 0 0 1712.367 379.4733 2.719923 1
344 226 1716.566 0 0 0.9551249 8187.527 0 339.4113 0.02447731 1934.244 0 0 218.4033 284.605 0.3376147 0
342 27.56505 1578.924 0 0 0.9398266 8884.509 0 417.8517 0.01784804 1612.762 0 0 60 0 1.06752 2
350 342.5651 4576.647 0 42.42641 0.7751773 7162.716 0 931.9335 0 0 0.1851064 0 1622.498 582.4946 1.509527 1
344 0 1140.395 0 0 1 7707.256 0 759.5393 0 1328.495 0 0 685.4196 442.9447 0 0
345 0 2193.285 0 0 0.9311576 8220.219 0 189.7367 0.02804692 1985.674 0 0 108.1665 30 0 2
339 121.9638 2259.779 0 0 0.9306476 8185.603 0 240 0.02804692 1892.142 0 0 30 84.85281 4.16874 2
346 199.435 2460.732 0 0 0.7965324 6273.516 0 1299.731 0 90 0.2034676 0 335.4102 0.7548945 0
347 226 2346.913 0 0 0.8143804 6150.659 0 1382.932 0 174.9286 0.1856196 0 67.08204 450 1.01275 0
344 226 2482.035 0 0 0.8485467 6003.674 0 1557.691 0 210 0.1514533 0 351.141 0.3376147 0
343 0 2103.426 0 0 0.9551136 8855.083 0 361.2478 0.009659091 384.1875 0.03522727 732.3933 403.6087 256.3201 0 2
343 0 2101.928 0 0 0.9469388 9011.293 0 570.7889 0.01156463 268.3282 0.0414966 849.0583 283.0194 254.5584 0 2
343 0 2191.849 0 0 0.9427994 8951.922 0 582.4946 0.01144011 192.0937 0.04576043 924.1753 212.132 192.0937 0 2
343 0 2225.062 0 0 0.9414285 8977.672 0 647.611 0.01 134.1641 0.04857143 982.7004 150 127.2792 0 2
353 316 4085.841 0 0 0.9005609 6063.341 0 1524.106 0 60 0.09943906 0 1441.25 540.8327 1.01275 0
342 0 2289.651 0 0 0.9463337 8667.561 0 342.0526 0.009032943 335.4102 0.04463337 840.5355 366.1967 300 0 2
353 0 4060.209 0 0 0.9077002 6025.819 0 1548.709 0 30 0.09229985 0 1405.205 502.8916 0 0
342 91 2382.121 0 0 0.9447052 8585.243 0 381.8377 0.008868023 335.4102 0.04642671 900 349.8571 318.9044 0.9548413 2
342 0 2401.687 0 0 0.9330269 8815.407 0 658.6349 0.01050558 30 0.0564675 1098.59 60 42.42641 0 2
342 0 2468.947 0 0 0.9395055 8348.368 0 466.6905 0.008942662 276.5863 0.05155182 990.4545 284.605 234.3075 0 2
343 0 782.3043 0 0 0.9882713 6023.13 0 1299.731 0 457.9301 0.01172871 0 1087.06 241.8677 0 0
343 0 2547.882 0 0 0.9607343 8175.042 0 391.1521 0.008669047 551.5433 0.03059663 768.3749 67.08204 60 0 2
343 0 840.5355 0 0 0.9892912 5921.866 0 1324.424 0 576.2812 0.01070882 0 1124.5 212.132 0 0
342 109.435 2452.305 0 0 0.9439062 8291.514 0 484.6648 0.008669047 366.1967 0.04742478 973.4988 284.605 212.132 0.7548945 2
343 0 2441.823 0 0 0.9490056 8181.644 0 483.7355 0.008669047 424.2641 0.04232534 894.986 192.0937 123.6932 0 2
343 117.565 2424.252 0 0 0.9847017 7832.528 0 658.6349 0.003569607 700.3571 0.01172871 642.028 30 174.9286 1.06752 2
342 0 2317.002 0 0 0.9341164 8327.526 0 657.9514 0.008171604 189.7367 0.05771195 1164.989 189.7367 150 0 2
342 0 2323.984 0 0 0.945436 8102.5 0 602.9926 0.007649159 349.8571 0.04691484 966.0745 283.0194 30 0 2
    
```

CART or MARS (Three Outputs; e.g. MRW)

Figure 5-3: Coding scheme of LTM-MC, CART and MARS to model MC

Suitability map

1.05	2.25	2.64
0.15	2.88	0.52
1.82	0.83	1.35

$$N(0) = 2$$

$$N(1) = 3$$

$$N(2) = 3$$

$$N(3) = 1$$

Simulated map

1	2	2
0	3	0
2	1	1

Three Outputs

Figure 5-4a: Simulated land use maps for three outputs (suitability map scale from 0 to 3) using MARS. Where in $N(i) = j$, i and j show the code and number of transition for each land use class, respectively

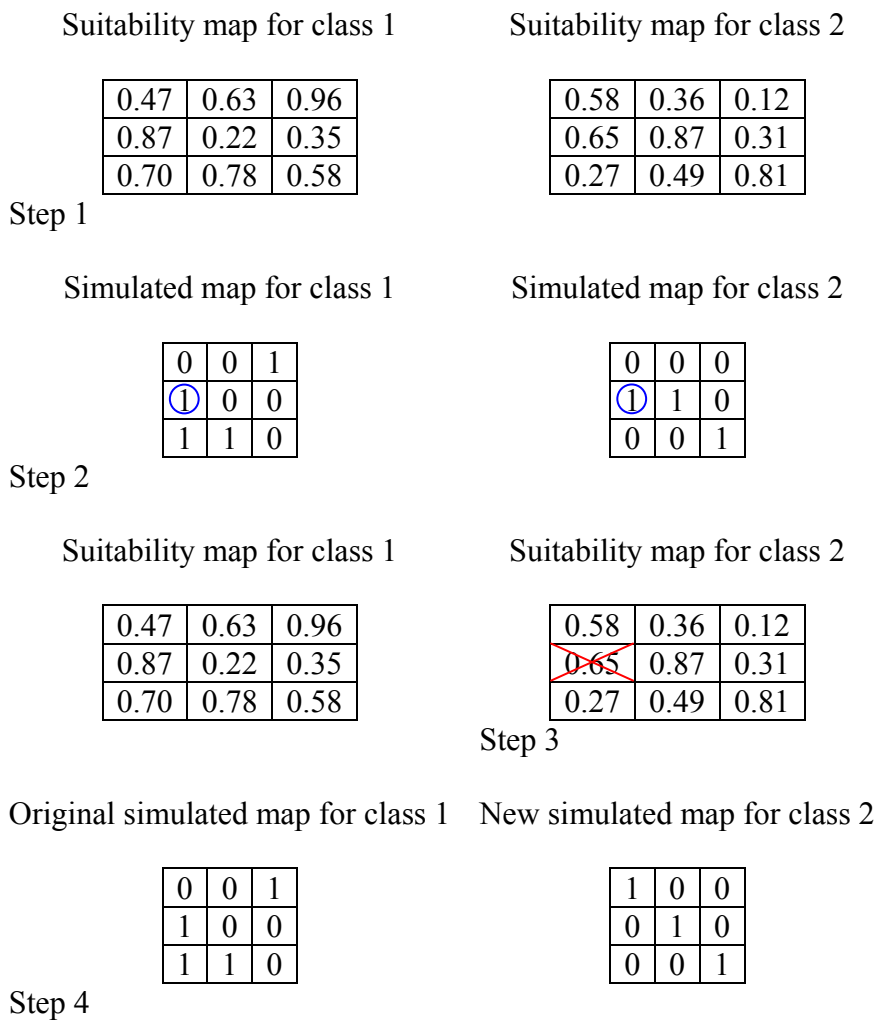


Figure 5-4b: Blue circle show the conflict cell between two land use simulated maps (0 and 1 represent no-change and change, respectively). Class 1 and 2 with 4 and 3 reference land use transition receive rank 1 and 2, respectively. Red Cross shows the conflict cell that removed from the suitability map with the lower rank (rank 2)

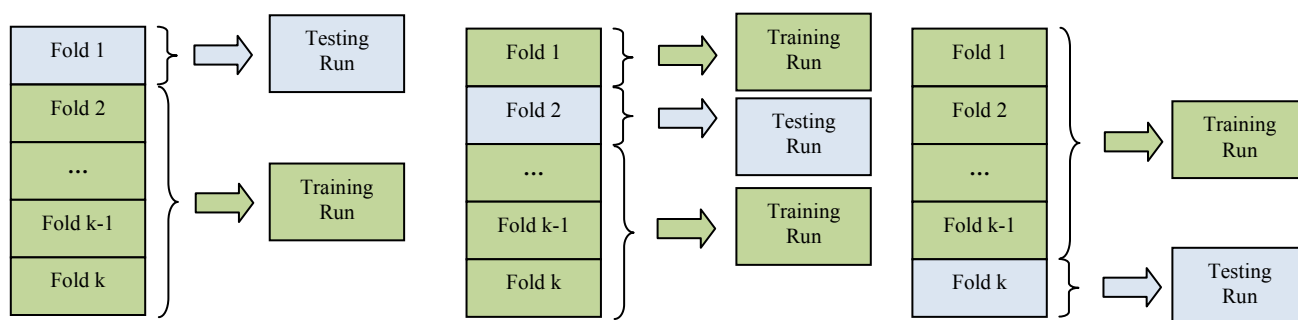
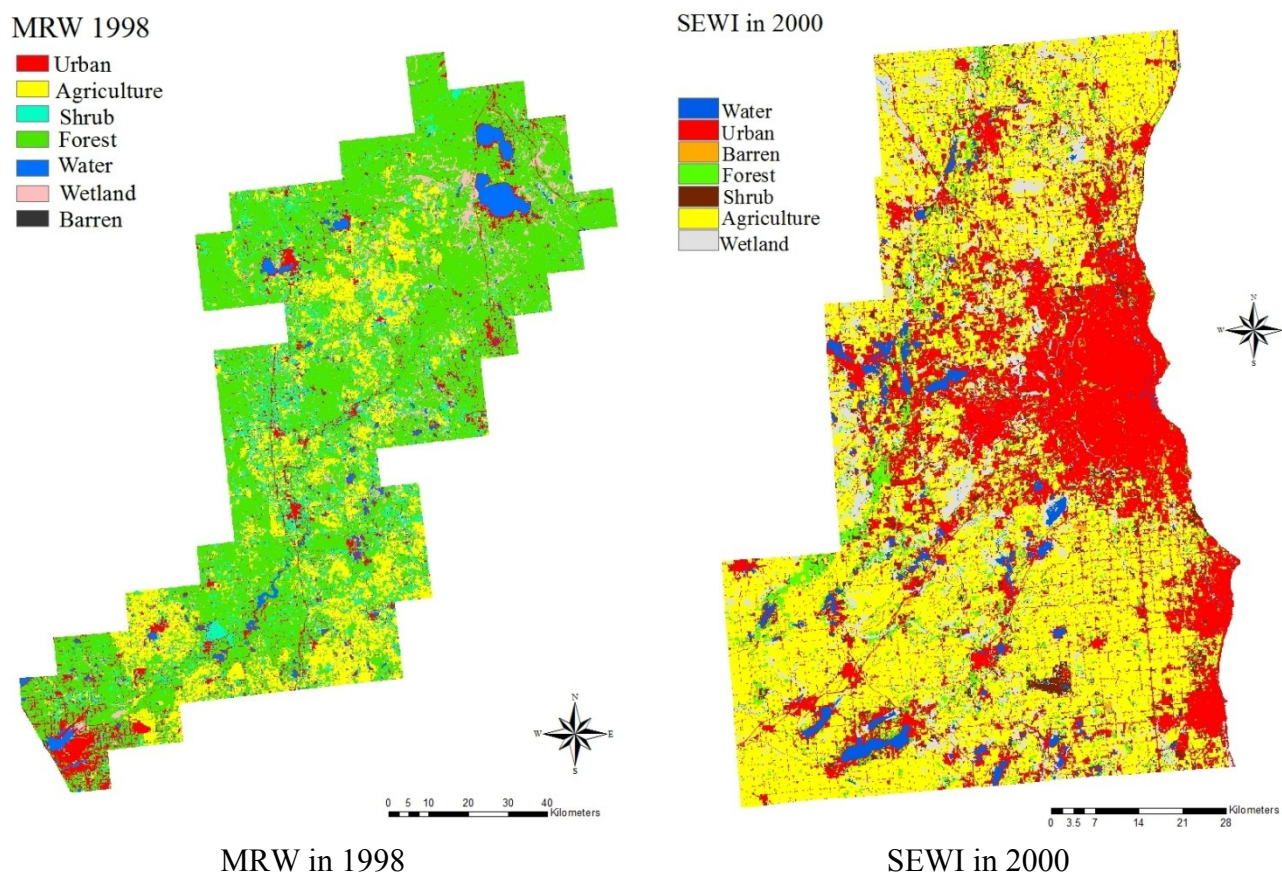


Figure 5-5: k – fold cross validation procedure in SPM software



MRW in 1998

SEWI in 2000

Figure 5-6: Study area in MRW and SEWI

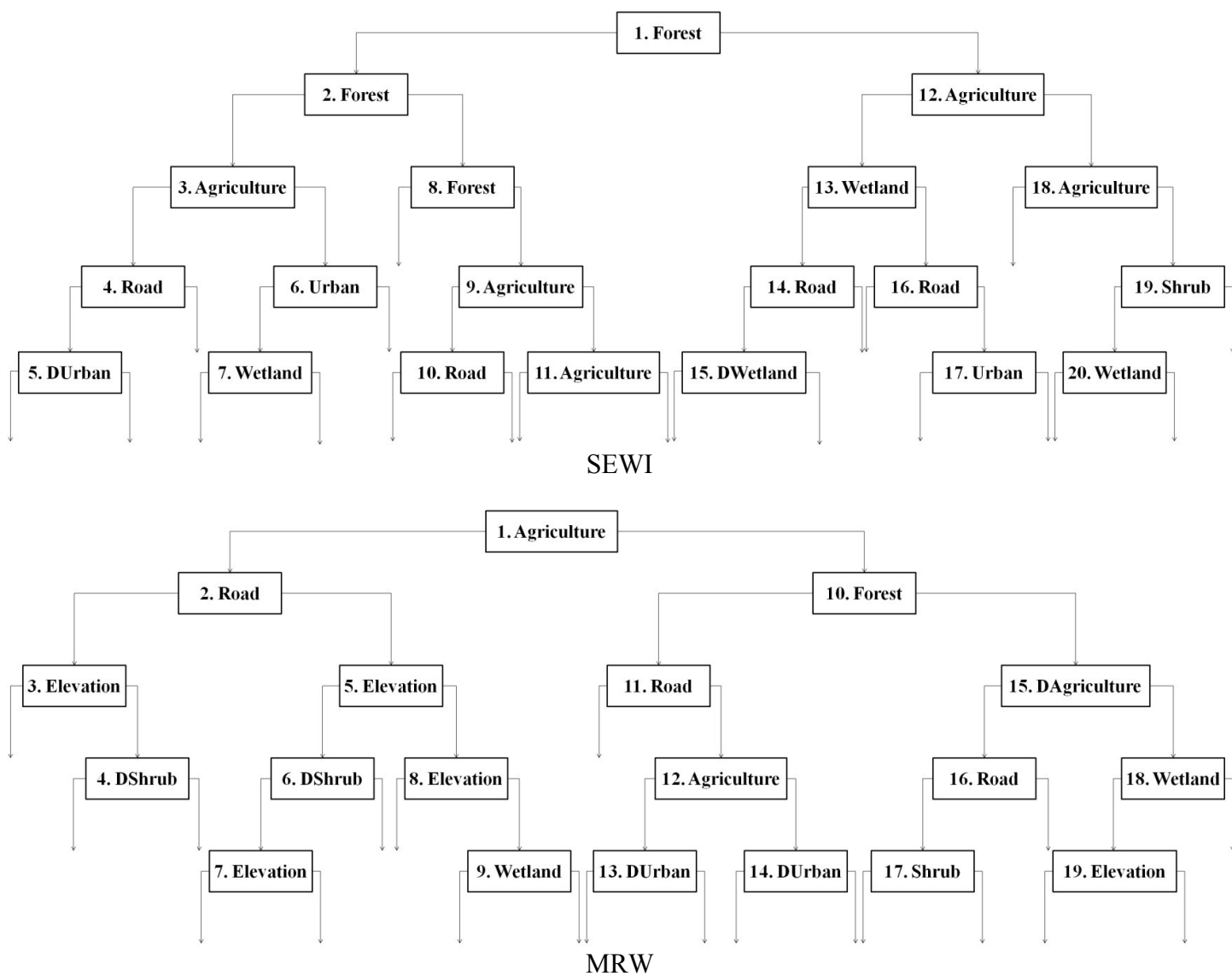


Figure 5-8: Viewing the main splitter in CART

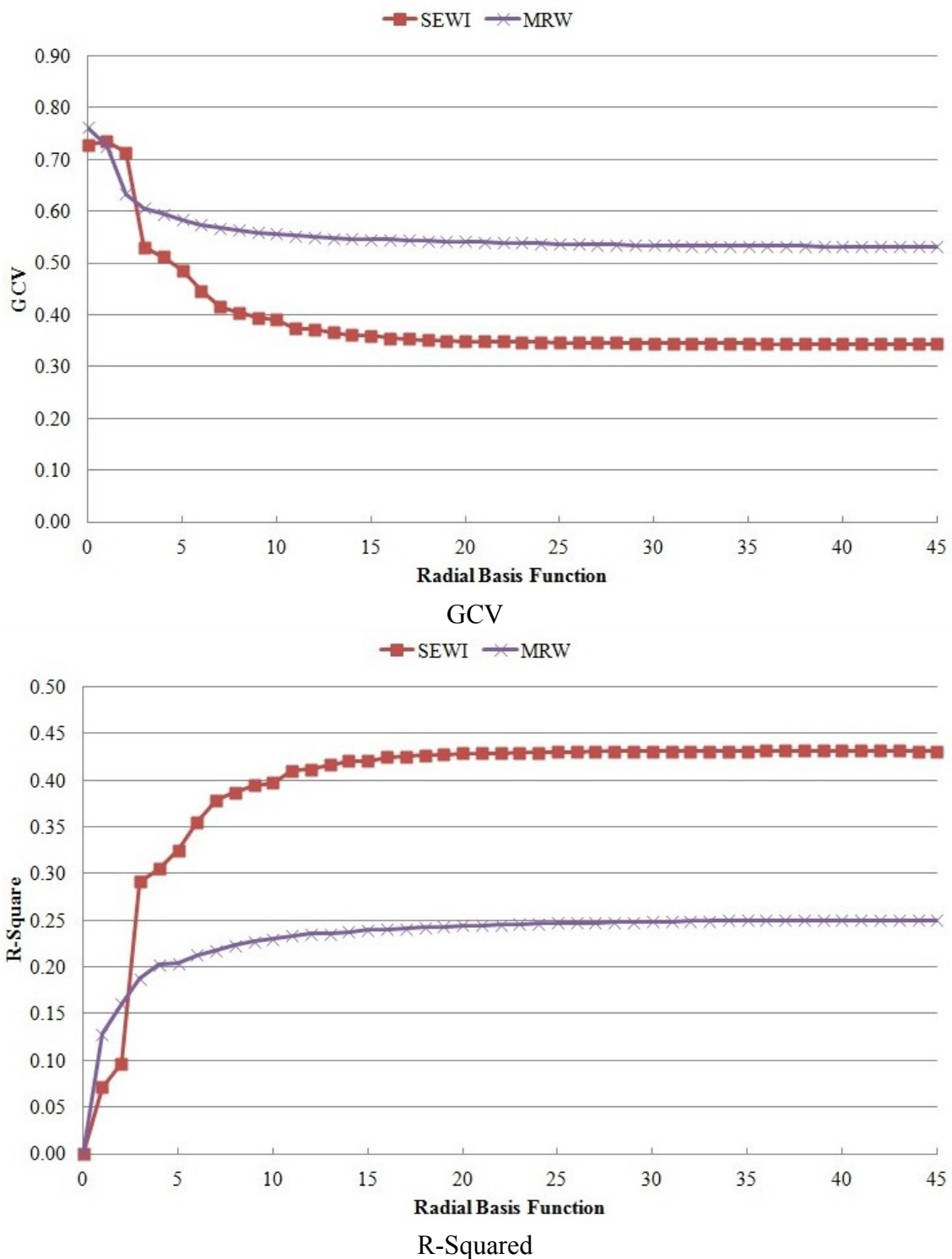


Figure 5-9: GCV and R-squared across number of radial basis functions in MARS

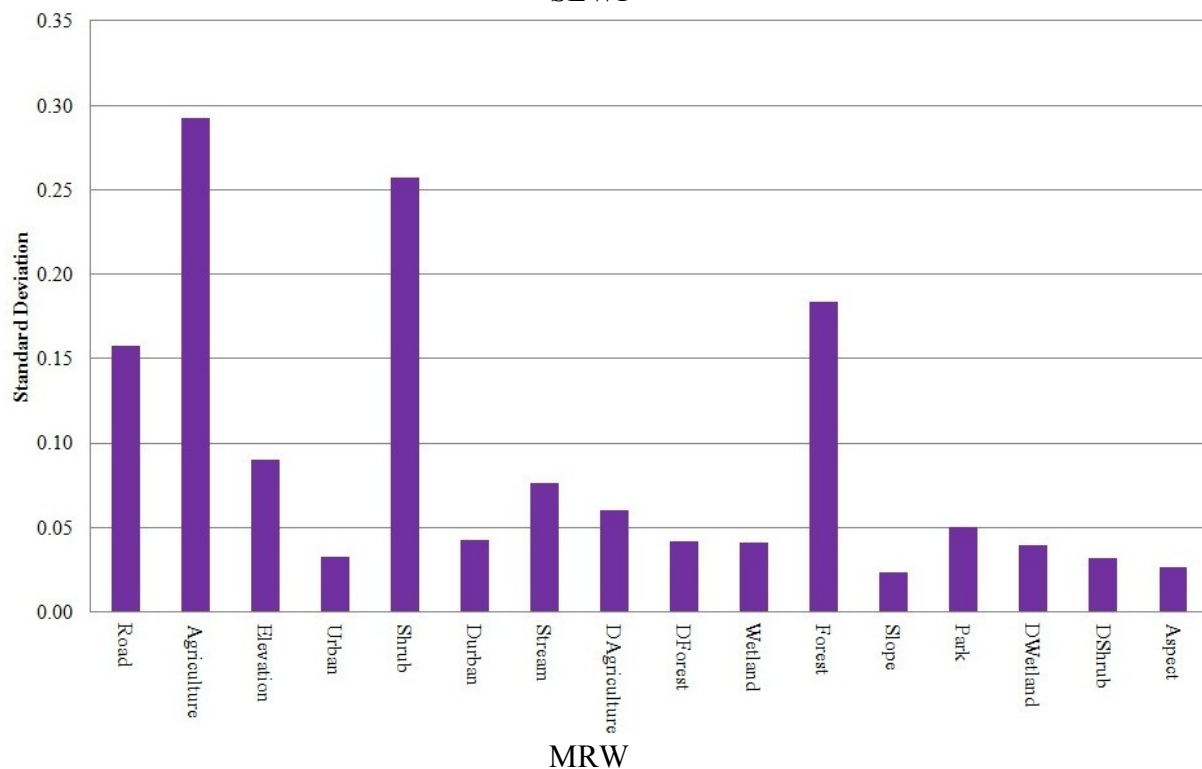
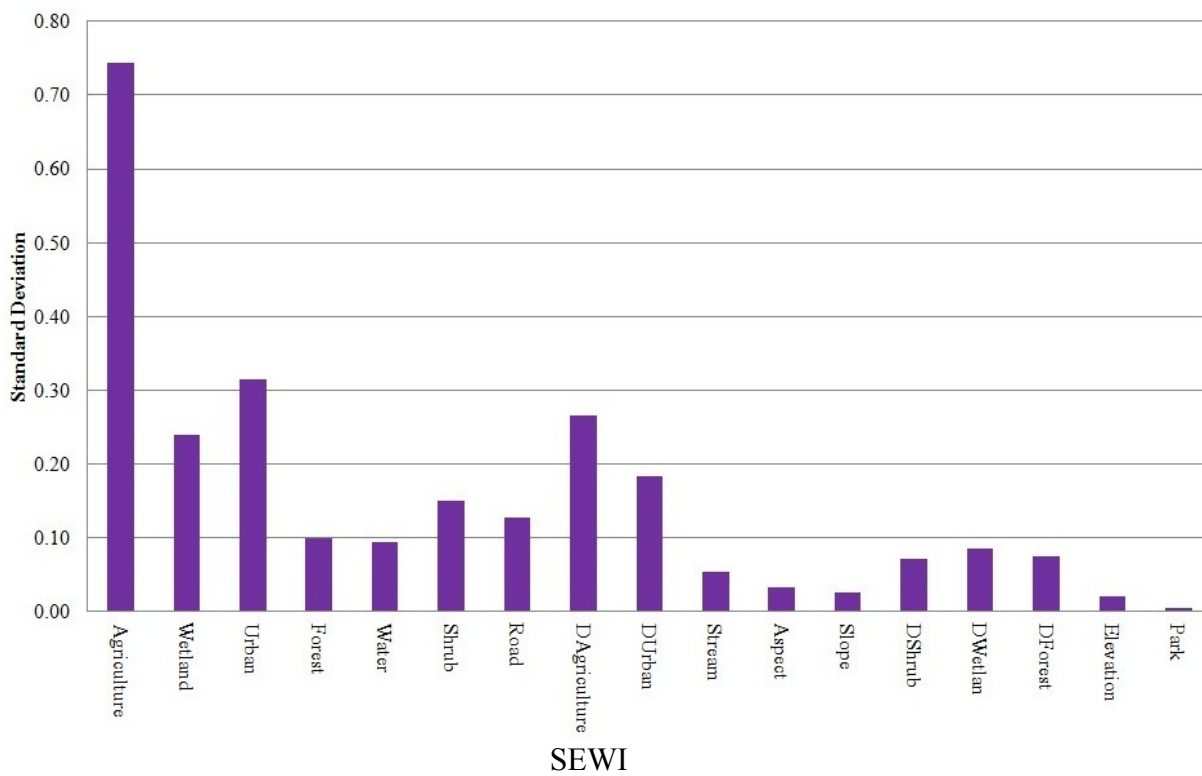


Figure 5-10: ANOVA in MARS

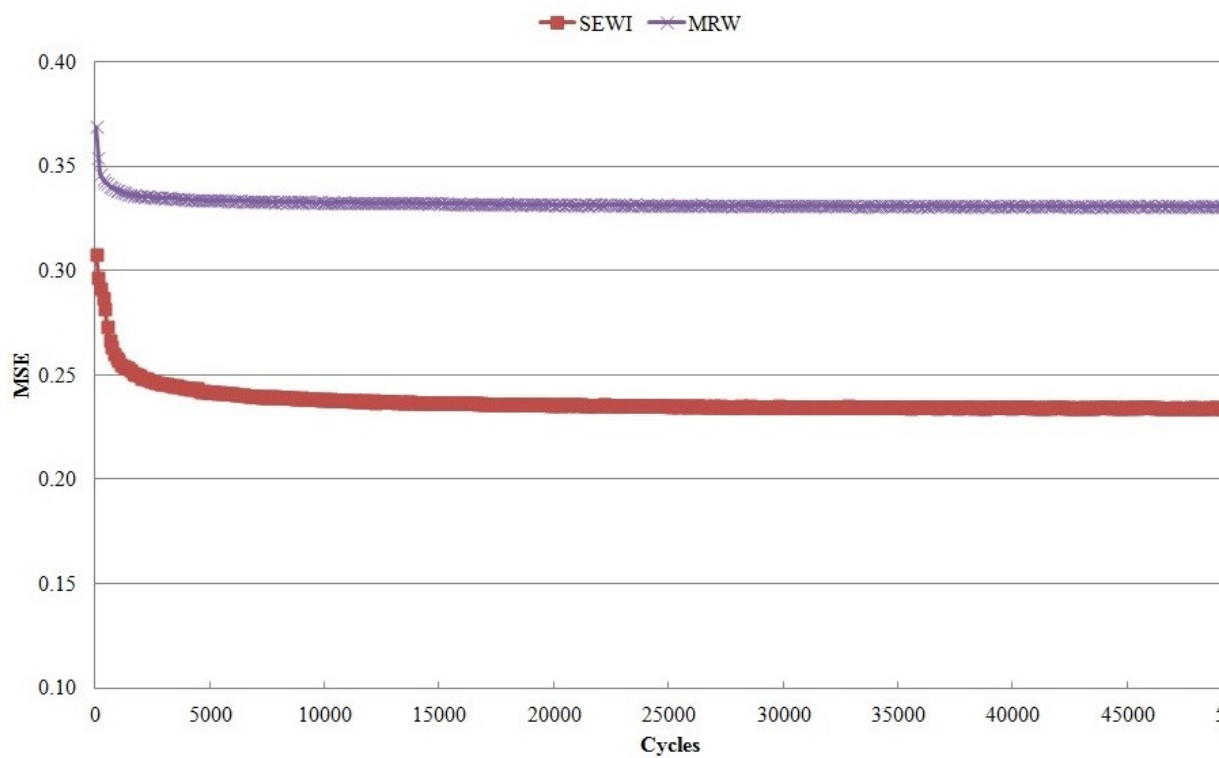


Figure 5-11: Training run of LTM-MC

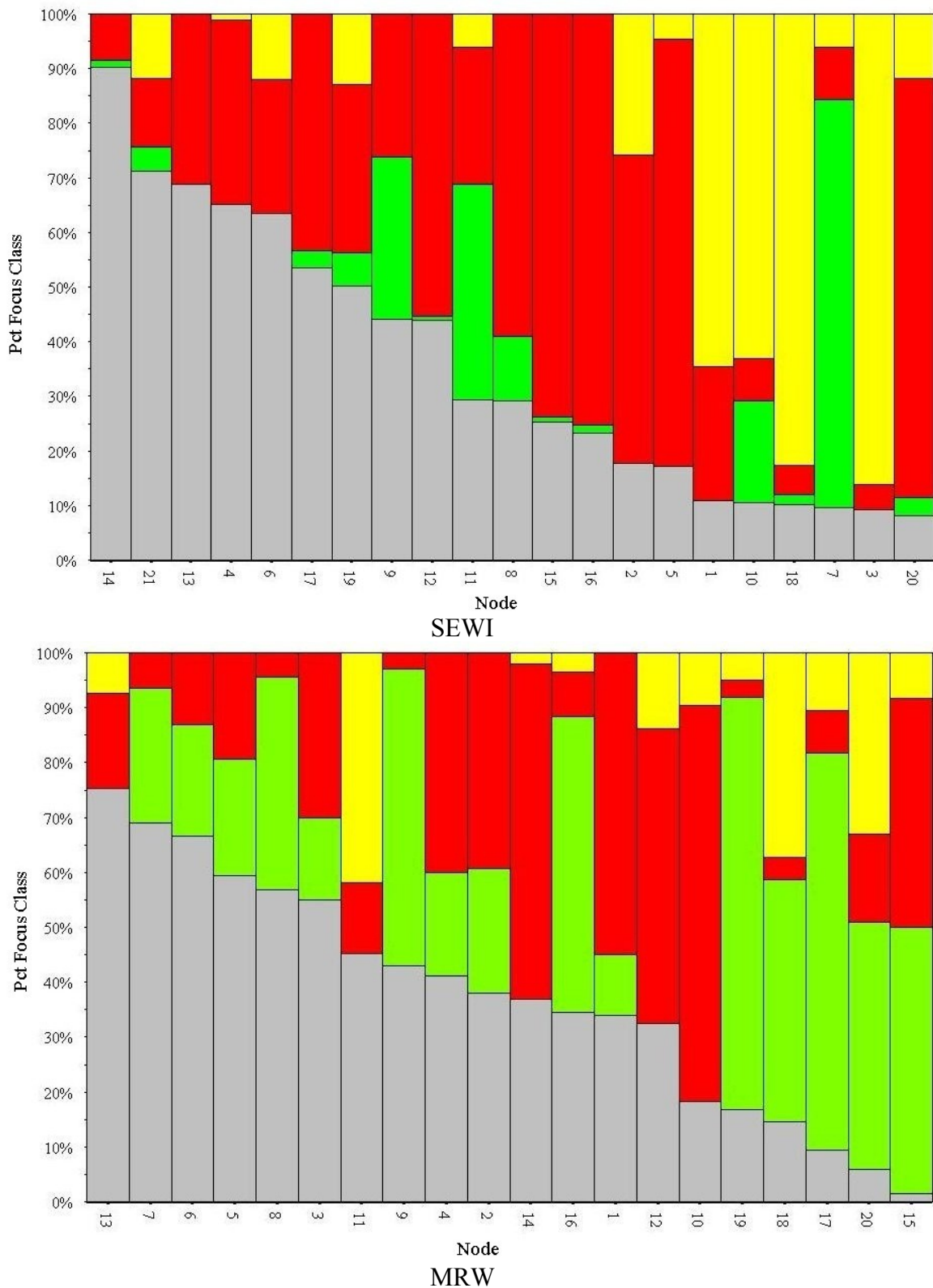


Figure 5-12: Terminal node in CART (gray, red, yellow and green represent no-change, urban change, agriculture change and forest change, respectively)

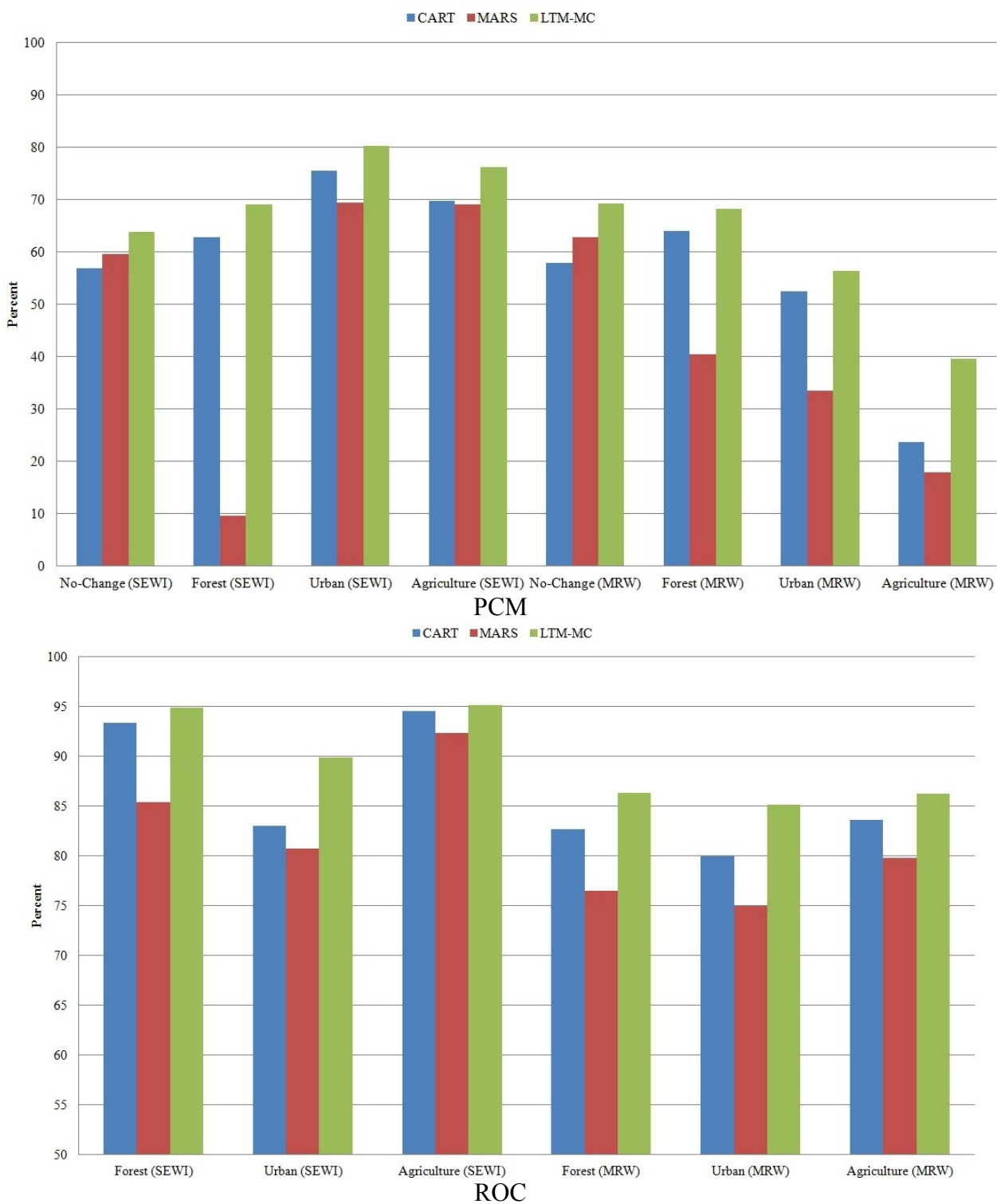


Figure 5-13: PCM and ROC for CART, MARS and LTM-MC

Table 5-1. A contingency table to compare simulated and reference land use maps

		Reference Map					Sum of row
		1	2	3	...	J	
Simulated Map	1	n_{11}	n_{12}	n_{13}		n_{1J}	$S_1 = \sum n_{1j}$
	2	n_{21}	n_{22}	n_{23}		n_{2J}	$S_2 = \sum n_{2j}$
	3	n_{31}	n_{32}	n_{33}		n_{3J}	$S_3 = \sum n_{3j}$
	⋮						⋮
	J	n_{J1}	n_{J2}	n_{J3}		n_{JJ}	$S_J = \sum n_{Jj}$
	Sum of column	$A_1 = \sum n_{j1}$	$A_2 = \sum n_{j2}$	$A_3 = \sum n_{j3}$...	$A_J = \sum n_{jJ}$	Total = $\sum_{j=1}^J A_j = \sum_{j=1}^J S_j$

Table 5-2: Spatial predictor variables for SEWI and MRW

	SEWI	MRW
1	Elevation	Elevation
2	Aspect	Aspect
3	Distance to Urban	Distance to Urban
4	Density of Urban	Density of Urban
5	Distance to Forest	Distance to Forest
6	Density of Forest	Density of Forest
7	Distance to Agriculture	Distance to Agriculture
8	Density of Agriculture	Density of Agriculture
9	Distance to Shrub	Distance to Shrub
10	Density of Shrub	Density of Shrub
11	Distance to Wetland	Distance to Wetland
12	Density of Wetland	Density of Wetland
13	Distance to Park	Distance to Park
14	Distance to Stream	Distance to Water
15	Distance to Road	Distance to Stream
16	Slope	Distance to Road
17	----	Slope

Table 5-3: Size of samples and resolution of data for SEWI and MRW

Study Area	Agriculture Change	Forest Change	Urban Change	Non-Change	Total	Resolution
SEWI	135,709	79,467	491,031	314,265	1,020,472	30m×30m
MRW	120,013	641,237	412,302	693,598	1,867,150	30m×30m

Table 5-4: Competitor, split and improvement for CART

A - SEWI	Competitor	Split	Improvement
Main	Forest	63	0.09451
1	Agriculture	75	0.06582
2	Urban	51	0.03752
3	DForest	0.11346	0.02820
4	Road	121	0.01776
5	Durban	0.16735	0.01632
6	Wetland	51	0.01451
7	DAgriculture	0.43037	0.01371
8	Slope	3.14572	0.01317
9	Shrub	142	0.00712
10	Park	1499	0.00648
11	DShrub	0.05948	0.00610
12	DWetland	0.09972	0.00473
13	Elevation	265	0.00458
14	Water	101	0.00456
15	Stream	121	0.00418
16	Aspect	0.50	0.00349

B - MRW	Competitor	Split	Improvement
Main	Agriculture	345	0.06587
1	Shrub	51	0.06486
2	Road	114	0.03823
3	Forest	190	0.03040
4	Durban	0.03543	0.01517
5	Urban	270	0.01333
6	DAgriculture	0.14085	0.00980
7	Elevation	266	0.00939
8	Wetland	875	0.00910
9	DShrub	0.13359	0.00829
10	DWetland	0.04490	0.00374
11	DForest	0.37794	0.00346
12	Stream	915	0.00227
13	Park	2772	0.00110
14	Slope	1.14232	0.00089
15	Aspect	5.58117	0.00056

Table 5-5: Coefficients, variables and knots in MARS

BFs in SEWI	Coefficient	Variable	Sign	Knot
0	-0.984680			
1	-0.061248	Agriculture	-	67
2	0.035816	Agriculture	+	67
3	-0.031057	Urban	+	42
4	-0.015252	Wetland	-	161
5	0.014962	Wetland	+	161
6	-0.001308	Road	-	161
7	0.003081	Road	+	161
8	-0.022361	Wetland	+	60
9	-0.000101	Water	-	90
10	-0.006427	Water	+	90
11	-0.004736	Shrub	-	366
12	0.004286	Shrub	+	366
13	0.000015	Forest	-	67
14	-0.004473	Forest	+	67
15	0.012819	Urban	-	42
16	-3.674577	DUrban	+	0.7726
17	-1.079093	DUrban	-	0.7726
18	-3.326859	DAgriculture	+	0.0790
19	-2.891896	DAgriculture	-	0.0790
20	-0.007839	Shrub	+	134
21	0.000535	Aspect	+	145
22	0.000145	Aspect	-	145
23	-0.722788	DShrub	+	0.3728
24	-1.050544	DShrub	-	0.3728
25	0.999261	DWetland	+	0.1020
26	0.056512	DWetland	-	0.1020
27	0.792730	DForest	+	-0.0000
28	-0.006119	Slope	-	2.8624
29	-0.027395	Slope	+	2.8624
30	0.003083	Shrub	-	174
31	-0.000693	Elevation	+	267
32	-0.001118	Elevation	-	267
33	-1.464719	DWetland	+	0.5492
34	0.002106	Urban	+	84
35	-0.000475	Stream	+	240
36	0.000135	Stream	-	1,218
37	0.000110	Water	+	684
38	4.434641	DAgriculture	-	0.1045
39	0.000002	Park	+	0.0001

BFs in MRW	Coefficient	Variable	Sign	Knot
0	1.916899			
1	-0.023503	Agriculture	-	1,214
2	-0.000051	Road	+	189
3	0.002369	Road	-	189
4	0.000130	Wetland	+	84
5	-1.712863	DAgriculture	-	0.0122
6	4.617346	DAgriculture	+	0.0122
7	0.000037	Stream	-	108
8	-0.002620	Stream	+	108
9	-0.005666	Elevation	-	339
10	-0.004297	Elevation	+	339
11	0.019570	Shrub	+	984
12	0.016237	Forest	+	445
13	-0.498543	DWetland	-	0.0602
14	0.611026	DWetland	+	0.0602
15	0.000564	Agriculture	-	1,214
16	-0.000770	Shrub	+	984
17	8.710874	DForest	-	0.9444
18	-1.011644	DUrban	+	0.5038
19	-0.500216	DUrban	-	0.5038
20	-0.000134	Park	+	12,554
21	-0.000334	Aspect	-	64
22	-0.001198	Aspect	+	64
23	-0.000096	Urban	-	2,323
24	0.000019	Urban	+	2,323
25	0.222987	DShrub	-	0.2228
26	0.452830	DShrub	+	0.2228
27	0.000119	Park	-	17,017
28	0.000030	Park	+	5,964
29	-0.000777	Forest	-	445
30	1.990626	DAgriculture	+	0.0755
31	-0.014505	Slope	-	2.6350
32	-0.023725	Slope	+	2.6350
33	0.011041	Elevation	-	216
34	0.083747	Elevation	+	239
35	-0.037933	Elevation	-	254
36	-0.066528	Elevation	+	228
37	0.007891	Elevation	-	298
38	0.005506	Elevation	+	356
39	-0.000250	Wetland	-	1,130
40	0.000162	Wetland	+	2,165

Table 5-6: Ranking variables in CART and MARS

CART - SEWI	
Variable	Relative Priority
Agriculture	0.2581
Forest	0.2306
Urban	0.1238
DAgriculture	0.0680
Wetland	0.0641
Shrub	0.0616
Durban	0.0469
DForest	0.0407
DShrub	0.0314
Park	0.0213
Road	0.0192
Slope	0.0185
DWetland	0.0063
Elevation	0.0056
Stream	0.0022
Water	0.0011
Aspect	0.0001

MARS - SEWI	
Variable	Variable Priority
Agriculture	0.3123
Wetland	0.1273
Urban	0.1117
Shrub	0.0734
Road	0.0678
Water	0.0494
DUrban	0.0491
DAgriculture	0.0376
Forest	0.0362
Stream	0.0291
DWetland	0.0253
DShrub	0.0246
DForest	0.0212
Aspect	0.0176
Slope	0.0101
Elevation	0.0073

CART - MRW	
Variable	Relative Priority
Agriculture	0.2282
Shrub	0.1994
Forest	0.1215
Road	0.0924
DAgriculture	0.0875
DUrban	0.0658
Urban	0.0549
DForest	0.0534
Elevation	0.0288
DShrub	0.0200
Wetland	0.0183
Park	0.0154
DWetland	0.0077
Stream	0.0062
Slope	0.0003
Aspect	0.0001

MARS - MRW	
Variable	Relative Priority
Road	0.1568
Agriculture	0.1560
Shrub	0.1280
Forest	0.1090
Elevation	0.0833
Stream	0.0737
Park	0.0483
DAgriculture	0.0409
DForest	0.0387
DUrban	0.0318
Urban	0.0288
DWetland	0.0253
Wetland	0.0226
Aspect	0.0217
DShrub	0.0197
Slope	0.0155

**CHAPTER 6: AN URBAN GROWTH BOUNDARY MODEL USING
NEURAL NETWORKS, GIS AND RADIAL PARAMETERIZATION: AN
APPLICATION TO TEHRAN, IRAN³**

6.1 Introduction

Urban growth boundaries, or UGBs, are planning tools used by local governments to constrain urban development to a fixed area (Calthorpe and Fulton, 2001). The overall objectives are to promote higher urban densities, protect non-urban lands such as agriculture that are outside the boundary, and to reduce urban infrastructure costs, such as transportation, sewer, etc. (APA, 2002). Thus, this planning approach creates urban areas that are clearly separated from rural uses.

UGBs are implemented using various approaches, but most involve the development of a boundary within which development over the next 10 to 25 years is allowed to occur (Calthorpe and Fulton, 2001). Local governments that implement UGBs need to estimate the amount of urban land required in the future given anticipated growth of housing, business, recreation and other urban uses required within the boundary. The boundary most frequently occurs across several local government units, and as such, is considered to be a regional planning tool (APA, 2002).

³ Current version has been published in *Landscape and Urban Planning*.

UGBs have been promoted most often in high growth areas, such as metropolitan areas along the west coast of the United States, and are argued by some as an effective means to preserve open space surrounding large cities and as tool that ensures efficient use of land (APA, 2002). UGBs have been implemented in various countries around the world, including the United States (Phillips and Goodstein, 2000; Wassmer, 2002), Great Britain (Gunn, 2007), China (Han et al. 2009), Saudi Arabia (Mubarak, 2004), Canada (Gordon and Vipond, 2005), Albania (Turner et al. 1992), Australia (Coiacetto, 2007), and Korea (Bengston and Youn, 2006), to name a few. In the United States, several states, including Washington, Oregon, Maine and Tennessee, have required all local governments to develop comprehensive plans that include urban growth boundaries. Given the considerable attention to the problems occurring as a result of urban sprawl (Batty, 2005; Van and Mahler, 2005; Verburg, 2006; Acevedo et al. 2007; He and Lo, 2007; Alkheder, 2008a and b), and the increasing attention given to UGBs as a regional planning tool, it is thus surprising that very little research has focused on developing models that assist planners in delineating the urban boundary (cf. Knaap and Hopkins, 2001). Models are needed as the many factors that drive urban change operate across different spatial and temporal scales in a very complex way (Brown et al. 2007; Entwisle et al. 2007; Evans and Kelley, 2007) and thus a simple delineation of boundaries is not feasible. To assist planners and others in identifying future urban growth boundaries, we develop and apply a model to project the future extent of rapidly growing urban areas.

6.1.1 Literature Review on UGBs

UGBs are used throughout the world although they are known by other names. Establishing urban boundaries can be traced back to the 1930s where they were used as an urban planning tool in Great Britain (Elson, 1993). Referred to there as “green belts”, it was enacted as a planning tool to protect rural areas outside London from development by containing urban growth within a carefully defined area. Large urban areas in Japan in the 1950s (Eaton and Eckstein, 1994) and 1960s also experiencing rapid development have employed urban growth boundaries. In Albania, the yellow line system (Turner et al. 1992) has been used for decades as a means to define “inhabitation centers” that demarcate urban and rural areas. In South Africa, an Integrated Development Plan requires a the development of a Spatial Development Framework which includes the demarcation of a city’s urban edge, sometimes called an “urban fence” (Metropolitan Durban, 1974). UGBs have been proposed as one of the first urban growth management tools in countries such as Saudi Arabia (Al-Hathloul and Mughal, 2004) where explosive urban growth, as much as 6% per annum, is straining urban infrastructure in its major cities (Mubarak, 2004).

In the United States, UGBs are used in various ways, generally guided by state policy. In some places, they are referred to as Urban Growth Areas or UGAs. In California, state law requires each county to have a Local Agency Formation Commission, which sets UGBs for each city and town in a county. In Tennessee, urban boundaries are used solely to define long-term city boundaries rather than control urban sprawl. In Texas the UGB delineations, called Extra Territorial Jurisdictional boundaries,

are used to map out future city growth with the goal of minimizing competitive annexations.

UGBs are also common regional planning tools in Canada (Smith and Haid, 2004). For example, the metropolitan areas of Vancouver, Toronto, Ottawa and Waterloo, Ontario, have established urban growth boundaries to restrict urban growth to certain areas and to preserve green space. In British Columbia, UGBs are part of a larger regional planning initiative called the Agricultural Land Reserve Program that was established in the 1970s to protect valuable farmland from being converted to urban.

Not surprisingly, UGBs have come under considerable scrutiny in the past 10 years especially on the West Coast of the United States (Jaeger and Plantinga, 2007). For example, it has been argued that UGBs inflate housing prices (Staley and Mildner, 1999; although see Wassmer and Baass, 2006) and that UGBs have been ineffective in reducing urban growth rates (Pendall, 1999). Others have argued that it suffocates economic development (Jaeger and Plantinga, 2007) because it sets stringent growth limits especially during times of heightened economic growth. However, many UGBs require frequent updating thus in general, planning can respond to short-term growth spurts in areas. In Portland, Oregon, for example, the housing boom of the late 1990s drove the planning authority to substantially increase the UGB in 2004, which was required by Oregon State law (Jaeger and Plantinga, 2007; Walsh et al. 2008).

Within the context of Iran's planning system, UGB has tremendous potential as a regional planning tool. The country is divided into two planning domains, one simply referred to as urban planned districts and the other as non-urban planned districts and thus UGBs compliment the broader planning structure in this country. UGB planning could be

beneficial to those urban regions which are experiencing rapid growth and are interested in preserving natural areas outside the city boundaries. One such illustrious place is the Tehran Metropolitan Area (TMA), located in the Islamic Republic of Iran, where city planners are interested in introducing a range of policy directions to provide for a more compact city, minimize speculation on the city's fringe, and retain open spaces in the surrounding rural areas. Tehran is the fastest growing city in Iran. Currently, there is no consistent approach for deciding where urban growth can occur and where non-urban land should persist. To date, the boundary separating urban and non-urban areas in TMA has been determined by referencing regional or local policy documents, zoning decisions and legislation, all prepared at different times by different authorities and for different purposes. This has led to uncertainty in the decision-making process. This uncertainty has had undue effects by negatively impacting investment choices of landowners and developers, while raising concerns in the wider community about the long-term direction of urban growth and the erosion of TMA's green spaces. An urban growth boundary was proposed recently as a planning tool to accomplish two major objectives: (1) to promote efficiency in urban management with an emphasis on focusing residential development in established and planned suburbs, and in areas where there is already significant investment in infrastructure, and (2) to protect high value land adjacent to the urban boundary in recognition that this land makes significant contributions to the nation's economy.

The current shape of the city of Tehran is obviously driven by a variety of factors, including configuration of transportation networks, topography, and natural resources such as rivers and lakes which help support industry and recreation. These factors

interact in complex ways to form the current urban boundary. Thus, the first requirement of an urban growth boundary model is to quantify how these factors interact to create its current geometry. The second requirement is to allow these factors to persist through time so that a future urban growth boundary can be created that takes into account those urban growth variables that contribute to the evolution of the boundary's form and that accommodate the need for new urban area.

6.1.2 Research questions and chapter structure

We have selected the Tehran Metropolitan Area (TMA) for our study because (1) considerable remote sensing and geospatial data exist to help delineate urban boundaries and (2) an urban growth boundary model (UGBM) could be a useful tool for regional planning by combining a variety of spatial attributes within a GIS. Our research questions are (1) How can remote sensing maps of urban and various spatial predictor variables be used to parameterize an UGBM? and (2) How can an urban growth boundary map derived from an UGBM can be used by regional planners to develop future UGBs? We describe here the structure of an UGBM that uses Artificial Neural Networks, vector and raster GIS routines and inputs from remote sensing imagery. The model is calibrated and then used to develop future UGBs around TMA.

We organize the remainder of this chapter as follows. Section 6.2 summarizes the basic principles of ANNs as it has been applied to land change modeling, provides a broad conceptual overview of UGBM and describes the study area and data sources used. Section 6.3 illustrates how we parameterize UGBM using a set of spatial interaction rules derived from GIS routines. The results of the spatial-temporal patterns of UGB for our

TMA application, developing a forecast UGB map for TMA and the implications of forecasting map for spatial planning are discussed in section 6.4. The chapter concludes with section 6.5 that discusses the UGB and its potential for managing growth in Tehran, Iran.

6.2 Materials and Methods

6.2.1 Background on Artificial Neural Networks

Our UGBM uses many of the same parameterization methods of the ANN-based Land Transformation Model (LTM) of Pijanowski et al. (2000, 2002, 2005, 2006, and 2009). The use of ANN has increased substantially over the last several years in many fields because of the advances in computing performance (Aisa et al. 2008) and the increased availability of powerful and flexible ANN software. ANNs are machine learning tools that recognize complex patterns in data (Skapura, 1996). These tools are fashioned after the way that a network of neurons in the mammalian brain processes multiple input signals (Fisher, 2001). ANNs have traditionally been composed of several layers of nodes; an input layer, one or more hidden layers and an output layer (Figure 6-1), forming what is called a multilayer perceptron. The training of such a network involves three phases including the feed forward of the input training pattern with weights associated with each node, the back propagation of the associated error and the adjustment of the weights using a standard delta rule. Each input unit receives a signal and broadcasts this signal to each of the hidden units while hidden unit sums the signal with different weights, then applies what is called an activation function to compute its output signal and sends this signal to the unit in the output layer. The output unit receives

a signal from each hidden layer and sums the signals with corresponding weights and computes the output value which is typically between 0 and 1.

Weights in an ANN are determined by using a training algorithm, the most popular is the Back Propagation (BP) algorithm. The BP algorithm randomly selects the initial weights, and compares the calculated output for a given observation with the expected output for the observations. The mean square error (MSE) -- the difference between the expected and calculated output values across all observation -- is computed with each pass, called a cycle. Once the training is stopped, biases and weights are obtained and saved; and these biases and weights are then used with other data to estimate output values; this is called testing. The output values are then used to assess model goodness of fit (i.e. calibration) against known values.

6.2.2 Urban Growth Boundary Model

Our Urban Growth Boundary Model (UGBM) differs from the LTM in several ways. First, the UGBM uses only the values of pixels located on the urban boundary as input from the first satellite image and as output from the first and second one to simulate UGB pattern. Second, raster data are used as a source of inputs of ANN while outputs of ANN vector data. Our UGBM requires six sequential steps (Figure 6-2) including: (1) base map development; (2) boundary delineation along azimuths; (3) coding of data and applying spatial functions; (4) ANN training and testing; (5) estimation of goodness of fit for UGBM and (6) applying training weights to create a forecast of the UGB. A collection of routines written in Java was used to process and analyze the data.

6.2.2.1 Base Map Development. All GIS data need to be converted to the same projection and raster maps standardized to the same cell size and grid dimensions (number of rows and columns). Creation of predictor maps can be accomplished using most GIS software packages, here, we use ArcGIS Spatial Analyst to calculate predictor variables such as distance to roads, slope, etc. Two land use maps, separated in time with enough urban growth occurring (viz. 10 or more years) are also needed as inputs to the ANN training.

6.2.2.2 Urban Boundary Delineation. The urban boundary for each of the two years was developed using the following procedure in ArcGIS. First, all urban cells in each map were set to a value of 1 and all other cells to 0. The region group procedure in ArcGIS was used to group all contiguous urban cells in the raster map to create urban patches. The largest contiguous urban patch was then selected and saved and the edge pixels were used to define the urban boundary.

A central point inside the urban boundary was selected and used as a reference point. Euclidean distances between this reference point and the urban boundary was calculated. Azimuths and distance of these lines based on coordinates of point coordinates were computed following Eqs. (6-1) and (6-2). This process is repeated for the first and the second satellite image.

$$S_{it} = \sqrt{(X_i - X_t)^2 + (Y_i - Y_t)^2} \quad (\text{Eq. 6-1})$$

$$\text{Azimuth}_{it} = \tan^{-1}\left(\frac{X_i - X_t}{Y_i - Y_t}\right) \quad (\text{Eq. 6-2})$$

where X_t is the easting coordinate of a central point in the urban area, Y_t is the northing coordinate of a central point in the urban area, X_i is the easting coordinate of point i on urban boundary, Y_i is the northing coordinate of point i on urban boundary, S_{it} represents the distance between a central point t in the region and point i on urban boundary; and $Azimuth_{it}$ is the azimuth between a central point t in the region and point i on the urban boundary.

Distances from the reference point depend on azimuth interval. A scale factor (SF) for each azimuth was used to normalize distances from 0.0 to 1.0 by dividing the distances between the two consecutive times along the same azimuth by the distance at the first time using Eq. (6-3):

$$SF_i = \frac{S_{it}(t_2) - S_{it}(t_1)}{S_{it}(t_1)} \quad (\text{Eq. 6-3})$$

where SF_i is the scale factor of distance between a central point in the region and point i on the urban boundary. The scale factor across different azimuths was used as output targets to train the ANNs.

6.2.2.3 Coding of Data. To investigate the input data required for the UGBM, urban boundary derived from the second satellite image in vector format is overlaid on the first satellite image. Coding of the predictive variables and spatial functions are performed and applied on the first satellite image. Following Pijanowski et al. (2002), each value in an entire predictor variable map (e.g. distance to roads) was normalized from 0.0 to 1.0 by dividing each value by the maximum value contained in predictor variable map. Eventually, pixels in the first satellite image located under the urban

boundary directly are selected and values at these predictor variable grids are used as inputs to the ANN routine in the UGBM. In fact, each point in the vector file (the former time) that made the urban boundary is matched with a pixel at a later time).

6.2.2.4 Simulation. We follow Pijanowski et al. (2002) in our use of ANNs. A back-propagation, feed-forward neural network with one hidden layer is created using predictor variables as inputs. Training is followed over a set of cycles (e.g. every 100 cycles) and the MSE is plotted and trends inspected in order to identify a minimum MSE to halt training. Once the training is stopped, activation function weights, bias and node weights are saved to a network file. All values from the network file are then presented to the neural network as a testing run where all inputs are kept but the outputs (SF values) are removed so that they can be estimated.

6.2.2.5 Model Calibration. There are several features of the UGBM that require an assessment of how well the model performs. These include: (1) the fit of the simulated distance versus real distance during each training cycle; (2) the sensitivity of each predictor variable on model output; (3) the goodness of fit for each simulated distance along each azimuth to the true distance and (4) the goodness of fit of the total area created by the model versus the size of the observed area in the second urban map.

6.2.2.6 Forecasting UGB geometry. In the forecasting process, after the ANN is trained and tested successfully, biases and weights are obtained, the feed-forward algorithm is used to estimate a new distance from the reference point along each azimuth. The forecasting process uses normalized predictor variable values as input from cells on the urban boundary in the study area; however, the output values are removed. After getting scale factor as output of ANN, scale factor is multiplied to real distances in each

azimuth in subsequent time to get distances across different azimuths in future (Eq. (6-4)). With the azimuths and distances, the forecasted urban boundary is determined. In fact, the azimuths are constant in different time periods and they are employed only for normalization of the rate of distances using:

$$S_{it}(t_3) = SF_i \times S_{it}(t_2) + S_{it}(t_2) \quad (\text{Eq. 6-4})$$

6.2.3 Study Area and Data Sources

Iran's rapid economic growth from 1985 to 2005 transformed the country to an industrialized nation. Tehran Metropolitan Area (TMA) is located (Latitude 35° 45' N and Longitude 51° 30' E) in the northern portion of Iran. TMA has exhibited an accelerated rate of urban growth especially over the last three decades. TMA has supported a great deal of economic and social development in terms of urban change and the rapid growth of infrastructure. TMA with a daytime population of over 10 million and with a metropolitan area of over 2000 km² is the center of commercial, financial, cultural and educational activities in Iran. Rapid urban growth has resulted from a high population growth rate and increased rural-urban migration combined with a strong tradition of centralization of government activities focussed in the capital.

National topographic data base (NTDB) of the National Cartographic Centre (NCC), at a scale of 1:25000, was used as the main source of UGBM data for TMA. Two Landsat TM images of TMA with a 28.5m resolution for 1988 and 2000 were acquired. NTDB and its extracted digital elevation model (DEM) at 30m resolution were used. NCC topographic data were integrated with our database to provide the appropriate inputs to the GIS-based model. Locations of service centres were obtained from country

road maps at a scale of 1:25000 and stored as point coverage. Data on land use, transportation, natural features, public lands, digital elevation model and political boundaries were incorporated into the GIS database for subsequent modeling.

6.3 Parameterization of our UGBM for TMA

This section presents a complete description for our UGBM implemented for TMA. From previous work (Tayyebi et al. 2008a, b; Pijanowski et al. 2009), we found that seven independent variables affect urban growth boundary in TMA: elevation, slope, aspect, and distance from built area, service centre locations, green spaces and roads.

6.3.1 Base map development

Satellite images have been used extensively to document spatio-temporal changes associated with increased urbanization in TMA (Syphard et al. 2005; Tan et al. 2005; Salami and Akinyede, 2006). Two Landsat images were geometrically registered to the Universal Transverse Mercator (UTM) WGS 1984 Zone 39N. Registration errors were about 0.50 pixels. Supervised classification was utilized to classify the images to different LUCC categories. All land use/land cover classes for TMA were also reclassified from their original classification to Anderson Level I classification scheme (Anderson et al. 1976). Three classes of different LUCC categories were selected in the images; namely road, build-up area and green space. Locations of service centres were produced and stored as point coverage. The Kappa quantity for the Landsat TM image of 1988 was 81.72% and 84.61% for that of 2000 (Pontius and Marco, 2008). Figure 6-3 illustrates the image registration and classification results for TMA.

The boundary of TMA was identified on the first and second satellite images. Boundary extraction process was performed with digitization of urban boundary in the two satellite images and both of them were exported as vector format. The two maps were overlaid and a composite map was produced which represents urban boundary of TMA in 1988 and 2000 (Figure 6-4). Therefore, after considering a central point in each boundary and measuring azimuths and distances (Eq. (6-1, 6-2)) in both of the times, scale factors were computed following Eqs. (6-3). In fact, each azimuth has different value of scale factors between two consecutive time of urban boundary and the same azimuth have different scale factors at a different two consecutive time.

6.3.2 Urban Boundary Delineation

When the boundary of TMA from the first and second satellite images was identified, the circle centred at a central point was plotted over the boundary image to prepare datasets for centre configuration following Alkheder and Shan (2005). Therefore, at every azimuth starting from zero to 360 degrees at an interval of 1 degree, two measurements were recorded representing the azimuths and distances from urban boundary at 1988 and 2000. Distances were normalized from 0.0 to 1.0 (Scale Factor) by dividing rate of distances between two consecutive times (1988-2000) in the same azimuth by distance in the first image (Eq. (6-3)). Numbers of points that make the urban boundary map depend on the spatial interval. Vectors of 360 by 1 measurements were assigned as output for training and testing run of ANN. Figure 6-5 shows the distance variables as output compiled in Arc/Info Grid format at the year 2000. A program in Java was written with user interface which gets central point in the region, azimuth interval

and urban boundary map at the two time interval as input to calculate scale factor at the specified azimuths.

6.3.2.1 Absorbing Excursion Spaces: Each cell contains distance from service centre, green space and build-up areas. The distance of each cell from its nearest absorbing cell was calculated and stored as a separate variable grids. These variable grids represented the potential effect of a location for growth of the urban boundary.

6.3.2.2 Transportation: Another influencing factor is the distance of each cell from the nearest road cell calculated and stored. The hypothesis is that humans need roads to access areas where resources are used resulting in urban boundary change. Therefore, areas closest to roads have a greater likelihood of being developed.

6.3.2.3 Landscape Features: Landscape topography is an effective factor contributing towards build-up areas utilization. Elevation is important in the flood landscape prone areas. Slope and aspect are important to minimize landscape costs.

6.3.2.4 Constraints: A constraint is a physical or legal characteristic of a cell that prevents the cell from being extended. There are two constraints that we considered for simulation of urban boundary. First, are cells that have limitations for urban boundary change because exterior situations such as physical condition. For example, in this paper, elevation and location of mountains are two factors that prevent growth of urban boundary. Second, cells that are protected legally from urban growth by the government. These lands are considered inappropriate for urban boundary changes around TMA which are forests, wetlands and barren lands.

Coding of the predictive variables and spatial functions are performed and applied on the first and second satellite images. Pixels from the first satellite image which were

located directly within the urban boundary map of TMA derived from the second satellite image were selected. In fact, each point in urban boundary map from the second satellite image was matched only with a pixel from the first satellite image. Therefore, there are different values for each pixel based on the predictor variables that we have considered as input that can influence on the UGB. The map layers have been stored in grid format then each location contained its spatial configuration value from each driving variable grid. For each cell in the study area, there are seven measurements as input of ANN. Vectors of 360 by 7 measurements located on urban boundary were assigned as input for training and testing of ANN. Figure 6-6 shows seven variables compiled in Arc/Info Grid format as inputs at 1988.

6.3.3 Simulation

The ANN toolbox of Matlab software was used for the design, training and prediction of the ANN. All input grids were stored an Arc/Info Grid (ESRI, 2009) format, were then normalized to a range from 0.0 to 1.0 and converted into ASCII representations (called a pattern file). The pattern file contained information from the 7 final input grids and an output file so that each line in the pattern file corresponded to one location. The output of the ANN represents the growth of urban boundary. Tan-sigmoid transfer activation function was used for the activation of hidden and output neurons (Tsoukalas and Uhrig, 1997).

To avoid over-training of the network (cf. Skapura, 1996; Bishop 1999), the ANN was trained with a partial set of input data. To further reduce over-fitting, data were presented to the ANN in random order for each cycle. The ANN was trained with the

training data and the MSE generated by Matlab and each cycle was stored in a file for the analysis. The ANN was tested as follows. First, the network files generated from the training run were applied to a pattern file that contained all of the cells on the urban boundary. Matlab used the pattern and the ANN files to generate an output file of the activation values. The resultant file contained values ranged from 0.0 to 1.0. Testing run was completed by comparing the simulated urban boundary with the observed urban boundary, based on the radial distances at the specified azimuths. The MSE was used to assess the performance of the UGBM. Therefore, MSE values generated for each iteration with Matlab software and each cycle was stored in a file for the analysis. Then, the MSE values are plotted against the number of training cycles to identify the best fitting model.

6.3.4 Calibration Metrics

We calculated the average and standard deviation of the difference between predicted distance and observed distance across all azimuths, MSE of the training run for each drop one out simulation and the seven predictor variable model, and the difference in size of the predicted year 2000 urban area and the observed urban area in 2000. We also used a Percent Area Match (PAM) metric to evaluate our UGBM. PAM compares (Eq. 6-5) areas that are predicted correctly to change according to our UGBM with areas that are converted to new areas in our observed map as follows:

$$\text{Percent Area Match} = \frac{\text{Area predicted to change}}{\text{Area actually to change}} \quad (\text{Eq. 6-5})$$

PAM is expressed as a percentage. Values less than 100 indicate that the model underestimates the size of the urban area; values greater than 100 reflect that the model overestimates urban area.

6.4 Results

6.4.1 Training of UGBM

The simulation points in our study area included 360 cells of which 54 cells (15%) were removed due to limitations of undergoing expansion. Figure 6-7 illustrates training run of UGBM in which MSE was plotted across training cycles. The MSE of the UGBM starts around 0.4 and drops linearly through 4,000 cycles, and then decreases its decline between 4,000 and 8,000 cycles; it then levels off below 0.02 after 8,000 cycles. We halted the training at 10,000 cycles where the MSE was 0.0138.

6.4.2 Testing Run and Model Validation

We used several goodness of fit statistics to compare the UGBM predicted and observed maps of the UGBs. We calculated the differences between predicted and reference distances across all azimuths; mean and standard deviation of these differences were 4 km and 1 km, respectively. The average distances were 20 km, so the model underestimated distances by 20%. We also followed MSEs across training cycles for a “drop one out” experiment (Figure 6-8) following Pijanowski (2002) and Washington et al. (2010). The MSE plots show that all six predictor variable models follow a similar trend during training; MSEs are larger (> 0.4) than the seven variable model at the start but fall to less than 0.1 after 5,000 cycles. All reach a minimum MSE around 7,000 cycles. Table 6-1 lists the MSEs after training was stopped at 10,000 cycles. Most MSEs

are close to the seven variable MSEs. Removing the predictor variable aspect produced the best (i.e. least MSE) six variable model; removing distance to road yielded a model with the greatest MSE (least fit to the data) suggesting this was the most important predictor variable in the UGBM.

PAM for the best fit simulation was 80%. We also measured PAM in each of the cardinal directions (North, South, East and West as north = 315 through 45, east = 45 through 135; south= 135 through 225 and west= 225 through 315) to determine if the model performed better in any one direction. Results show (Table 6-2) that values of PAM are 80% or greater in all cardinal directions, indicating that there are no significant biases in any of the cardinal directions although it is clear that the model more frequently underestimates, rather than overestimates, the distances.

6.4.3 Prediction

After the ANN was successfully trained and calibrated, biases and weights were saved and used to forecast the boundary into the future. Predictor maps were developed for areas outside the urban growth boundary of 2000 and these values along with biases and weights from the training runs were then applied to another testing run to estimate distances from the reference point. Boundary location points for the future (2012) were derived using Eq. (6-6):

$$S_{it}(t_3=2012) = SF_i \times S_{it}(t_2=2000) + S_{it}(t_2=2000) \quad (\text{Eq. 6-6})$$

Values for each point around all azimuths were then assembled into a vector polygon to create the future UGB.

Figure 6-9 shows the spatial configuration of the UGBs for 2012; this boundary is overlaid on TMA in 1988 and 2000 for comparison. Note that a great deal of boundary growth is anticipated in the south, southeast, east and northeast portions of TMA. However, less boundary growth may also occur into the west and north, but no boundary growth is predicted into the southwest and northwest of the TMA. This is because in the northwest, urban growth is constrained by a mountain and there are legal restrictions on growth by government in the southwest.

6.5 Conclusion and Discussion

The purpose of delineating urban planned districts is to guide and regulate the location and intensity of land development controlled under Iran's UGB plan. The purpose of designating non-urban planned districts is the conservation of environmentally sensitive areas and to protect rural landscapes. In Iran, citizens, policy makers, and natural resource managers have begun to propose the use of UGBs, both locally and nationally. In Iran, policies related to land use intends to support efficient use of natural resources and to improve socio-economic development. Social cohesion should be considered and economic growth should not favor environmental degradation. Thus, a tool like our UGBM is necessary to support the planning process in a complex urbanizing region like Tehran.

UGBM provides information which can be used as input in urban planning: (1) UGBM can be used to determine which predictor variable has the most important role on UGB simulation. Therefore, urban planners can focus on this factor more and consider essential requirements to prepare the city for better urban expansion. In addition,

environmentalist can also provide better conditions to prevent pollution in these areas. (2) UGBM determines to which direction urban boundary will extend.

This model differs in form and function from other urban growth models. First, the UGBM integrates raster and vector GIS routines in ways that attempt to delineate boundaries of large cities. Many land change models, such as the SLEUTH cellular-automaton model of Clark et al. (1997 and 1998), use a raster based environment to growth and transition cells on the basis of complex rules and learning algorithms. Input and output are all raster maps. Our UGBM uses raster as input and creates a vector map as output. The CLUE model of Verburg et al. (2002) uses a series of hierarchical rules coupled to logit models to transition cells, also entirely in a raster environment. Pijanowski's Land Transformation Model (LTM) is very similar to our UGBM, as it uses ANNs to assign rank order probabilities of transition and a simple rule to adjust the quantity of transitions into the future. Model calibration is generally performed on the probability distribution of cells (Verburg et al. 2004) or on the spatial shape of groups of cells (e.g. Pijanowski et al. 2006). The SLEUTH, CLUE and LTM has, to our knowledge, not been configured for urban growth boundary and used to predict the size and shape of a large urban area. This reconfiguration of Pijanowski's LTM represents one of several (Yin and Xu, 1991; Li and Yeh, 2002; Shellito and Pijanowski, 2003; Müller and Mburu, 2009; Pijanowski et al. 2007; Ray and Pijanowski, 2010) configurations for modeling land use patterns using ANNs. Our UGBM reconfiguration has also produced new ways to measure model goodness of fit. Comparing SFs along various axes emanating from a central reference point can potentially assist modelers with assessing how well their

models grow in different directions. Comparing the size of the predicted and observed urban area is simple but rarely done in modeling studies.

There are a variety of ways that urban growth boundaries are developed. In Tennessee, USA for example, state policy mandates that a County Growth Plan, developed by a County Coordinating Committee, establish UGBs. These are often included as part of the comprehensive plan as a map developed using GIS layers of zoning, natural resources, transportation, etc. Our method of delineating the UGB used Landsat TM imagery. These images were used to classify urban cells and then urban edges of the largest urban patch assigned to the urban boundary. This method was employed because no official UGB map for Tehran exists. This method could be employed in some areas of the world however where land use maps are not readily available.

In this chapter, our UGBM has been developed which takes advantage of GIS, ANN and RS based on the utilization of a variety of social and environmental factors. UGBM examines the relationship between seven predictor variables as inputs and radial extent of the boundary at specified azimuths as outputs to simulate UGB. GIS and RS have the potential to support such models by providing data and analytical tools for the study of urban planning while ANNs learn about complex spatial relationships of factors that correlate with UGB. Applying the proposed UGBM to the TMA resulted from variables has been successfully examined. The delineation of the UGB for TMA provides a new and easily understood way of defining where urban growth will be encouraged or not permitted. It clearly distinguishes land that is designated urban, to be used for housing, industry and commerce, from that which is non-urban. Non-urban land is to be

used for activities such as conservation, agriculture, resource development and suitable community infrastructure like airports, water supply and sewage treatment facilities that require large areas of open land.

6.6 References

- Acevedo, M. F., Callicott, J. B., Monticino, M., Lyons, D., Palomino, J., Rosales, J., Delgado, L., Ablan, M., Davila, J., Tonella, G., Ramirez, H., & Vilanova, E., (2007). Models of natural and human dynamics in forest landscapes: Cross-site and cross-cultural synthesis. *Geoforum*, 39, 846-866.
- Aisa, B., Mingus, B., O'Reilly, R.C., (2008). The emergent neural modelling system. *Neural Networks*, 21, 1045-1212.
- Al-Hathloul, S., Mughal, M.A., (2004). Urban growth management-the Saudi experience. *Habitat Int.*, 28(4), 609-623.
- Alkheder, S, and Shan, J., (2005). Urban growth simulation using remote sensing imagery and neural networks. Third International Symposium Remote Sensing and Data Fusion Over Urban Areas (URBAN 2005) and the 5th International Symposium on Remote Sensing of Urban Areas (URS 2005), March 14- 16, 2005, Tempe, Arizona.
- Alkheder, S., Wang, J., Shan, J., (2008a). Fuzzy inference guided cellular automata urban growth modeling using multi-temporal satellite images, *Int. J. Geogr. Inf. Syst.*, 22 (11-12), 1271-1293.
- Alkheder, S., Shan, J., (2008b). Calibration and assessment of multitemporal image-based cellular automata urban growth modeling, *Photogramm. Eng. Rem. S.*, 74 (12), 1539-1550.
- American Planning Association, (2002). *Growing Smart Guidebook*. Chapter 6 – Regional Planning, Retrieved February 16, 2010 from <http://www.planning.org/growingsmart/guidebook/six02.htm>.
- Anderson, J. R., Hardy, E. E., Roach, J. T., Witmer, R. E., (1976). A land use and land cover classification system for use with remote sensor data. US Geological Survey, Professional Paper 964: 28, Reston, VA.
- Batty, M., (2005). *Cities and Complexity Understanding Cities with Cellular Automata, Agent-based Models, and Fractals*. Cambridge, Mass., MIT Press.
- Bengston, D. N., Youn, Y., (2006). Urban containment policies and the protection of natural area: the case of Seoul's greenbelt. *Ecol. Soc.*, 11(1), No. 3.
- Bishop C.M., (1995). *Neural Networks for Pattern Recognition*, Oxford University Press. pp. 116-137.
- Brown, D. G., Robinson, D. T., Nassauer, L., Zellner, J., Rand, I., Riolo, W., Low, B., Wang, Z., (2007). Exurbia from the bottom-up: Modeling multiple actors and their landscape interactions. *Geoforum*, 39, 805–818.
- Calthorpe, P., Fulton, W., (2001). *The regional city: Planning for the end of sprawl*. Island Press, Washington D.C., pp. 304.
- Clarke, K. C., Hoppen, S., and Gaydos, L., (1997). A self-modifying cellular automaton model of historical urbanization in the San Francisco Bay area. *Environ. Plann. B*, 24, 247-261.
- Clarke, K. C., Gaydos L., (1998). Loose coupling a cellular automaton model and GIS: Long-term growth prediction for San Francisco and Washington/Baltimore. *Int. J. Geogr. Inf. Syst.*, 12 (7), 699-714.

- Coiacetto, E., (2007). Residential sub-market targeting by developers in Brisbane. *Urban Pol. and Res.* 25 (2), 257-274.
- Eaton, J., Eckstein Z., (1994). Cities and growth: Theory and evidence from France and Japan. NBER Working Paper Series. No. 4612. pp 235-267. National Bureau of Economic Research. Cambridge MA.
- Elson, M.J., (1993). Effectiveness of green belts. HMSO Books, London. 267 pp.
- Entwisle, B., Rindfuss, R. R., Walsh, S. J., Page, P. H., (2007). Population growth and its spatial distribution as factors in the deforestation of Nang Rong, Thailand. *Geoforum*, 39, 879-897.
- ESRI, (2009). ArcGIS 9.2 Software.
- Evans, T., Kelley, H., (2007). The influence of landowner and topographic heterogeneity on the pattern of land cover change in South-central Indiana. *Geoforum*, 39, 819–832.
- Fischer, M. M., (2001). Computational neural networks - Tools for spatial data analysis. In Fischer, M. M. and Leung, Y. (eds.): *Geo-Computational Modeling: Techniques and Applications*. Springer, New York. 15-34.
- Gordon, D. L.A., Vipond, S., (2005). Gross density and new urbanism. *J. Amer. Plann. Assoc.*, 71 (2), 41-54.
- Gunn, S.C., (2007). Green belts: A review of the region's responses to a changing housing agenda. *Environ. Plann. B.* 50 (5), 595-616.
- Han, H., Lai, S., Dang, A., Tan, Z., Wu, C., (2009). Effectiveness of urban construction boundaries in Beijing: An assessment. *Journal of Zhejiang University Science A*, 10 (9), 1285-1295.
- He, Z., Lo, C., (2007). Modeling urban growth in Atlanta using logistic regression. *Comput. Environ. Urban*, 31 (6), 667-688.
- Jaeger W. G., Plantinga A. J., (2007). How have land-use regulations affected property values in Oregon? OSU Extension.
- Knaap, G. J., Hopkins, L. D., (2001). The inventory approach to urban growth boundaries. *J. Am. Plann. Assoc.* 67 (3), 314-326.
- Li, X.,A. Yeh., (2002). Neural-network-based cellular automata for simulating multiple land use changes using GIS. *Int. J. Geogr. Inf. Syst.*, 16 (4), 323-343.
- Mubarak, F., (2004). Urban growth boundary policy and residential suburbanization: Riyadh, Saudi Arabia. *Habitat Int.*, 28 (4), 567-591.
- Müller, D., J. Mburu., (2009). Forecasting hotspots of forest clearing in Kakamega Forest, Western Kenya. *Forest Ecol. Manag.* 257 (2), 968-977.
- Pendall, R., (1999). Do land use controls cause sprawl? *Environ. Plann. B.*, 26, 555-571.
- Phillips, J., Goodstein, E., (2000). Growth Management and Housing Prices: The Case of Portland, Oregon. *Contemporary Economic Policy*. 18 (3), July 2000. Available at SSRN: <http://ssrn.com/abstract=234341>.
- Pijanowski, B.C., Gage, S., D.T. Long, D., Cooper W., (2000). A land transformation model: Integrating policy, socioeconomics and environmental drivers using a Geographic Information System; Pages 123-157 in *Landscape Ecology: A Top Down Approach*, Larry Harris and James Sanderson, eds. CRC Press, Boca Raton, Florida
- Pijanowski, B. C., Brown, D. G., Shellito, B. A., Manik, G. A., (2002). Using neural networks and GIS to forecast land use changes: a land transformation model. *Comput. Environ. Urban* 26 (6), 553-575.

- Pijanowski, B. C., Pithadia, S., Shellito, B. A., Alexandridis, K., (2005). Calibrating a neural network-based urban change model for two metropolitan areas of Upper Midwest of the United States. *Int. J. Geogr. Inf. Syst.*, 19 (2), 197-215.
- Pijanowski, B. C., Alexandridis, K. T., Muller, D., (2006). Modeling urbanization patterns in two diverse regions of the world. *Journal of Land Use Science*, 1 (2-4), 83-109.
- Pijanowski, B.C., Tayyebi, A., Delavar, M. R., Yazdanpanah, M. J., (2009). Urban expansion simulation using geographic information systems and artificial neural networks, *Int. J. Environ. Res.* 3 (4), 493-502.
- Pontius Jr. R. G., Marco M., (2008). Problems and solutions for kappa-based indices of agreement. *Conference Proceedings of Studying, Modeling and Sense Making of Planet Earth*. Mytilene, Greece.
- Ray, D., Pijanowski, B. C., (2010). A backcast land use change model to generate past land use maps: applications and validation at the Muskegon River Watershed of Michigan, USA. *Journal of Land Use Science*, 5, 1-29.
- Ref. Metropolitan Durban - Draft Guide Plan, Natal Town and Regional Planning Reports, (1974), Volume 28.
- Salami, A. T., Akinyede, J., (2006). Space technology for monitoring and managing forest in Nigeria, *Proc., International Symposium on Space and Forests, United Nations Committee on Peaceful Uses of Outer Space (UNOOSA), Vienna, Austria.*
- Shellito, B., Pijanowski, B., (2003). Using neural nets to model the spatial distribution of seasonal homes. *Cartogr. Geogr. Inform.*, 30 (3), 281-290.
- Skapura, D., (1996). *Building Neural Networks*. ACM Press, New York.
- Smith, B. E., Hald, S., (2004). The rural-urban connection: growing together in Great Vancouver. In *Planning – the State of the Art*. Canadian Institute of Planners.
- Staley, S., Mildner, G., (1999). *Urban growth boundaries and housing affordability*. Reason Public Policy Institute. Los Angeles.
- Syphard A. D., Clarke, K. C., Franklin, J., (2005). Using a cellular automaton model to forecast the effects of urban growth on habitat pattern in southern California. *Ecol. Complex.*, 2, 185-203.
- Tan, M. H., Li, X. B., Lu, C. H., (2005). Urban land expansion and arable land loss of the major cities in China in the 1990s. *Land Use Policy*, 22 (3), 187-196.
- Tayyebi, A., Delavar, M. R., Saeedi, S., Amini, J., (2008a). Monitoring the Urban Expansion by Multi-Temporal GIS Maps, Application of Remote Sensing and Imagery (TS 5B), Integrating Generations, FIG Working Week 2008 and FIG/UN-HABITAT Seminar, Stockholm Sweden, June 14–19, 2008.
- Tayyebi, A., Delavar, M. R., Saeedi, S., Amini, J., Alinia, H., (2008b). Monitoring Land Use Change by Multi-Temporal Landsat Remote Sensing Imagery. *The International Archives of the Photogrammetry, Remote Sensing and Spatial Information Sciences*. Vol. XXXVII. Part B7. Beijing 2008, China, pp. 1037-1043.
- Tsoukalas, L. H., Uhrig, R. E., (1997). *Fuzzy and neural approaches in engineering*. John Wiley and Sons, Inc., New York.
- Turner, B., Hegedus J., Tosics, I., (1992). *The reform of housing in Eastern Europe and the Soviet Union*. Routledge Press, London.

- Van, P. C., Mahler, B. J., (2005). Trends in hydrophobic organic contaminants in urban and Reference Lake sediments across the United States, 1970–2001. *Environ. Sci. Technol.* 39 (15), 5567-5574.
- Verburg, P.H., Soepbaer, W., Veldkamp, A., Limpiada, R., Espaldon, V., Mastura, S., 2002. Modeling the spatial dynamics of regional land use: the CLUE S Model. *Environ. Manage.* 30 (2), 391-405.
- Verburg, P.H., Overmars K. P., Witte, N., (2004). Accessibility and land-use patterns at the forest fringe in the northeastern part of the Philippines. *Geogr. J.*, 170 (3), 238-255.
- Verburg, P. H., (2006). Simulating feedbacks in land use and land cover change models. *Landscape Ecol.* 21 (8), 1171-1183
- Walsh, S. J., Messina, J. P., Mena, C. F. Malanson, G. P., (2008). Complexity Theory, Spatial Simulation Models, and Land Use Dynamics in the Northern Ecuadorian Amazon. *Geoforum*, 39 (2), 867-878.
- Washington, C., Pijanowski, B., Campbell, D., Olson, J., Kinyamario, J., Irandu E., Nganga, J., Gicheru, P., (2010.) Using a role-playing game to inform the development of land-use models for the study of a complex socio-ecological system. *Agr. Syst.*, 103 (3), 117-126.
- Wassmer, R. W., (2002). Focalization of land use, urban growth boundaries and non-central retail sprawl in the Western United States. *Urban Stud.* 39 (8), 1307-1327.
- Wassmer, R. W., Baass, M. C., 2006. Does a more centralized urban form raise housing prices? *J. Policy Anal. Manag.* 25 (2), 439-462.
- Yin, Y., X. Xu., (1991). Applying neural net technology for multi-objective land use planning. *J. Environ. Manage.* 32 (4), 349-356.

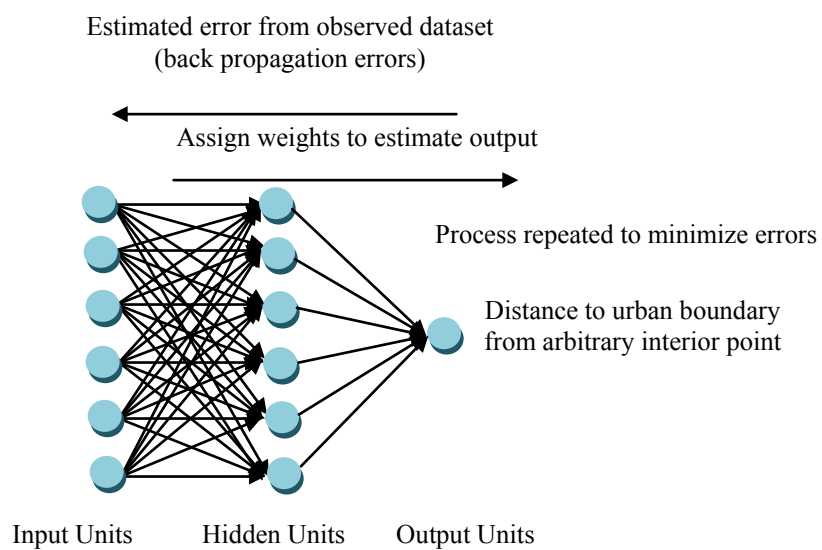


Figure 6-1: A typical architecture of feed-forward back propagation ANN

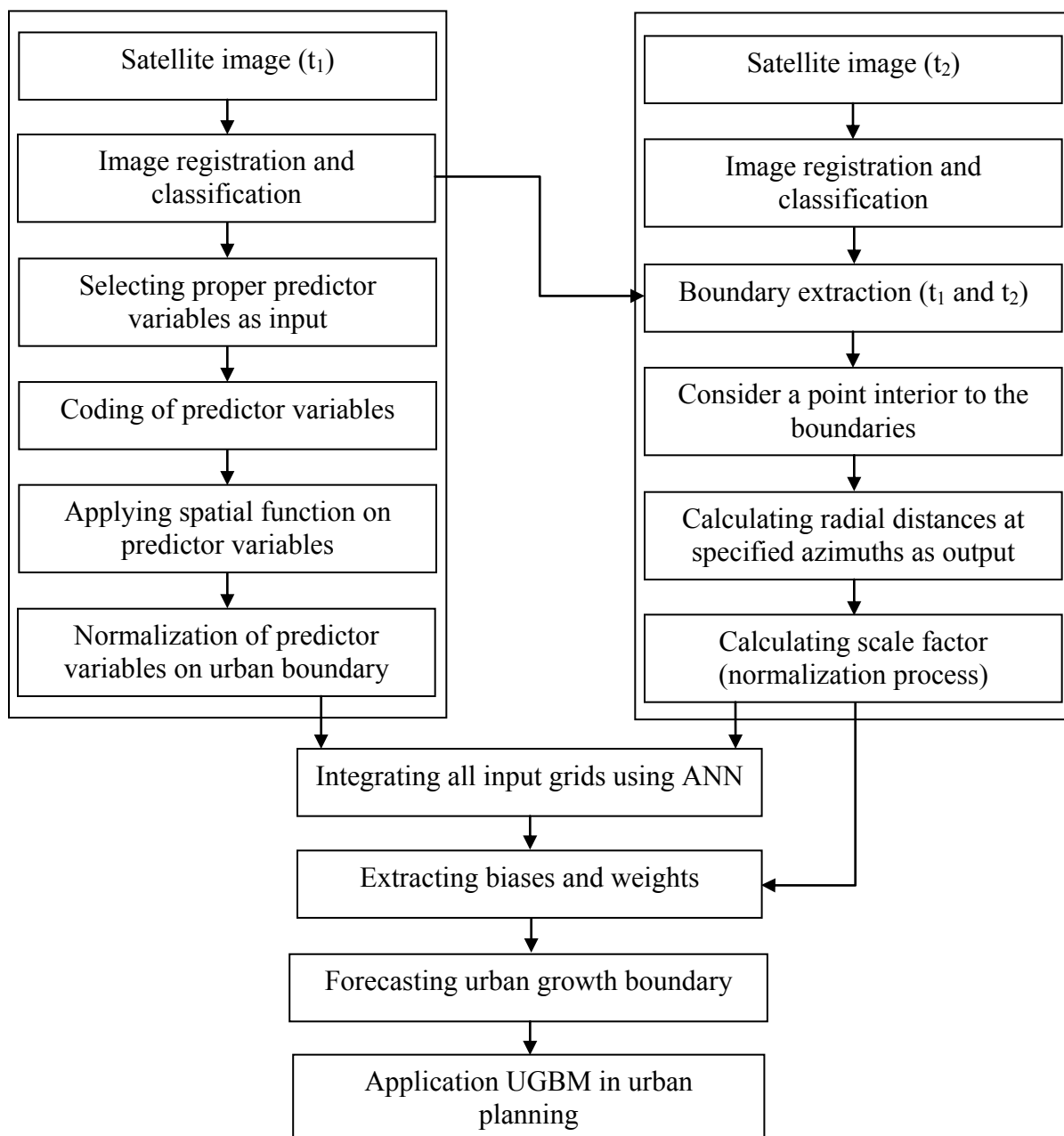
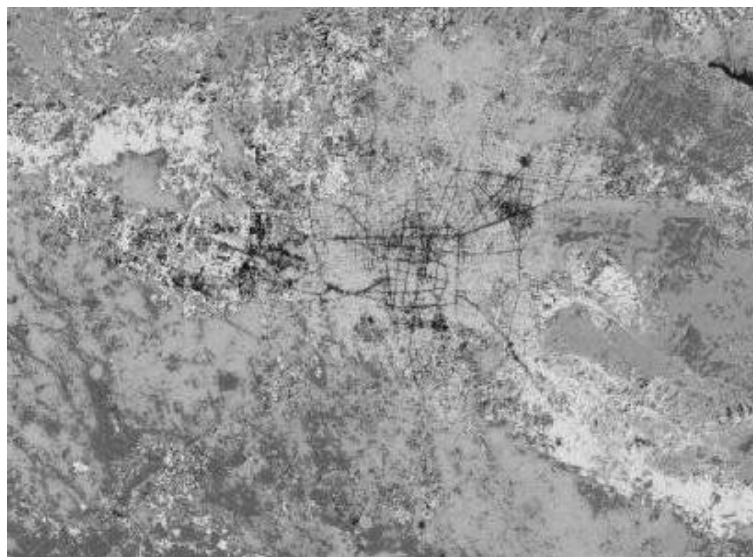
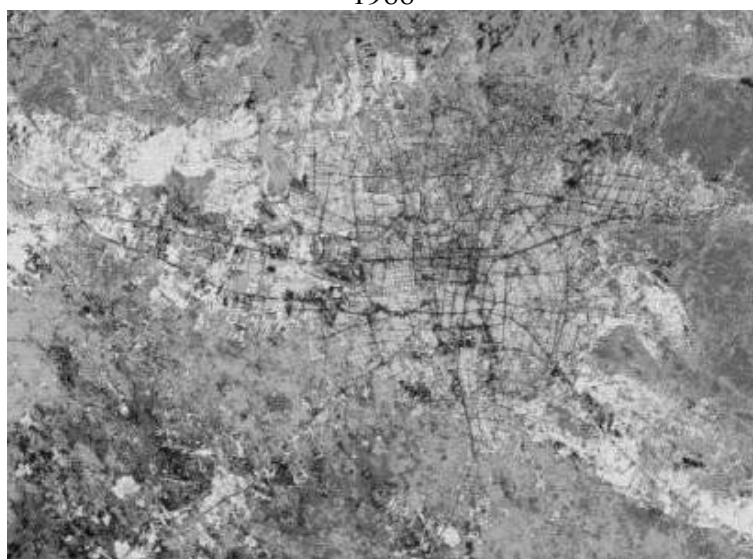


Figure 6-2: Conceptual model of UGBM



1988



2000

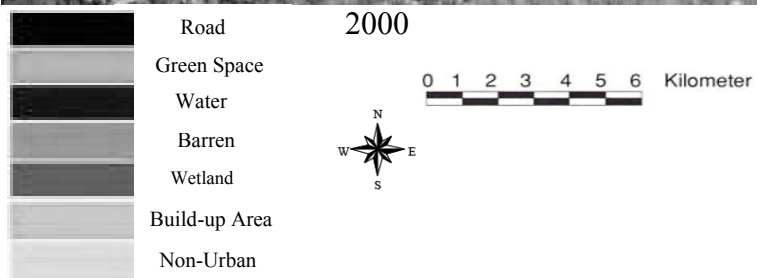


Figure 6-3: Image classification results for TMA in 1988 and 2000

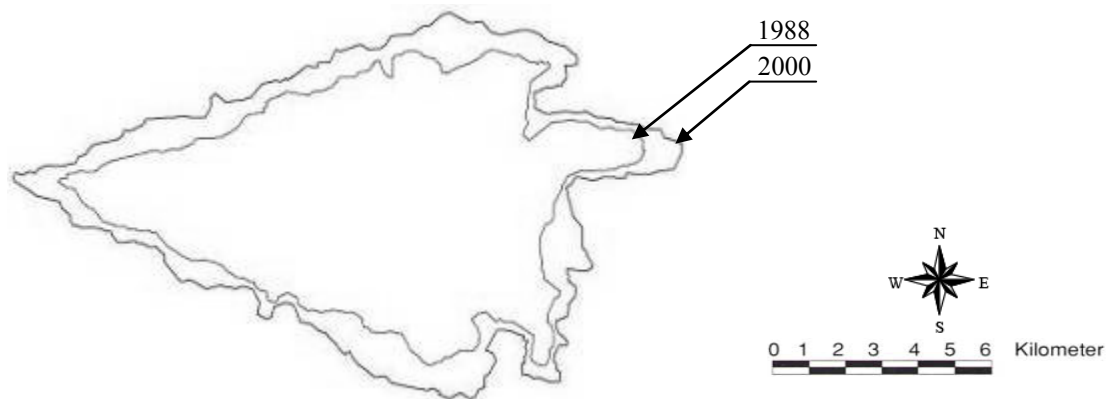


Figure 6-4: Urban boundary of TMA for the years 1988 and 2000

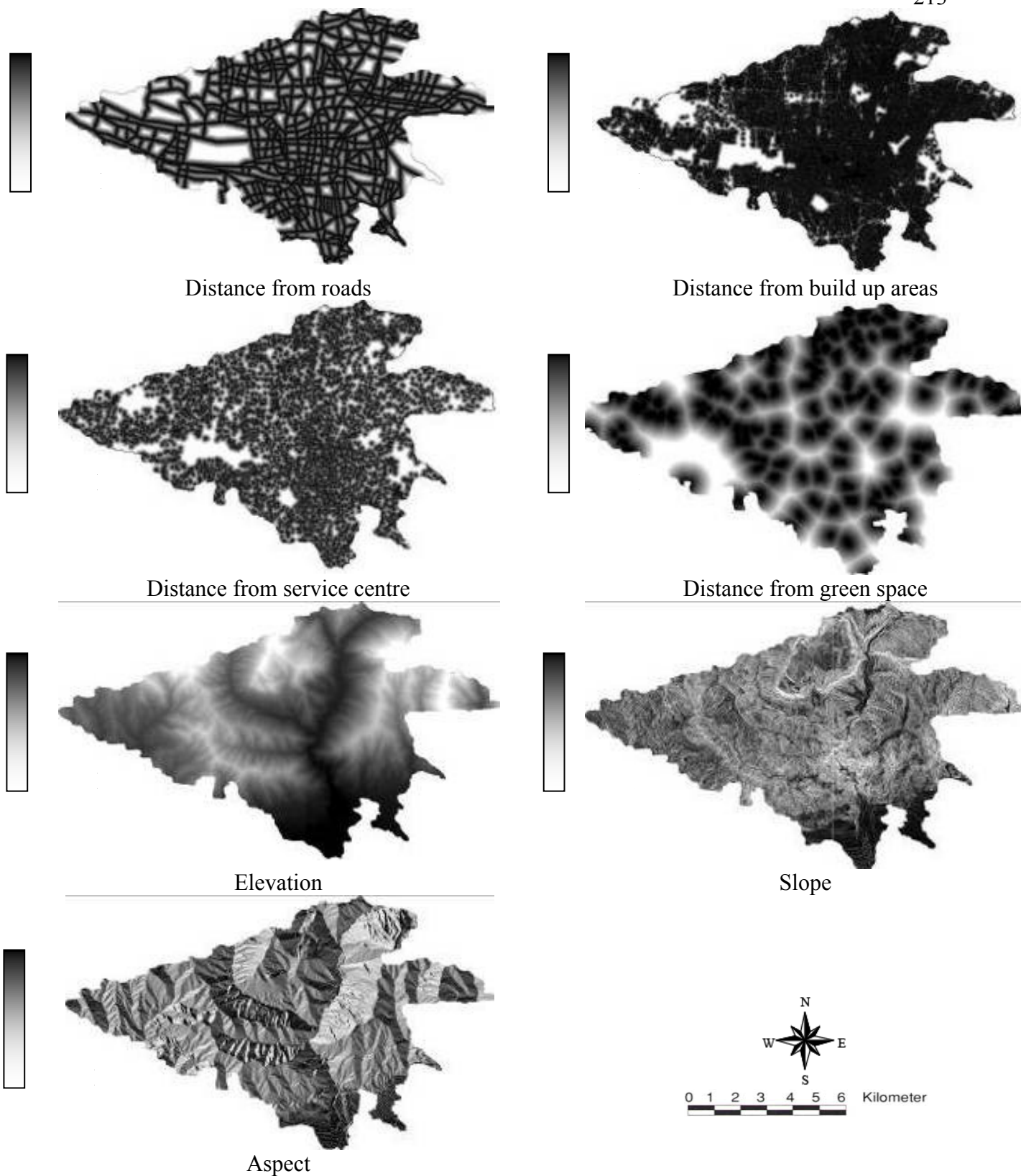


Figure 6-5: Maps of the seven variables in 1988 used as input for ANN

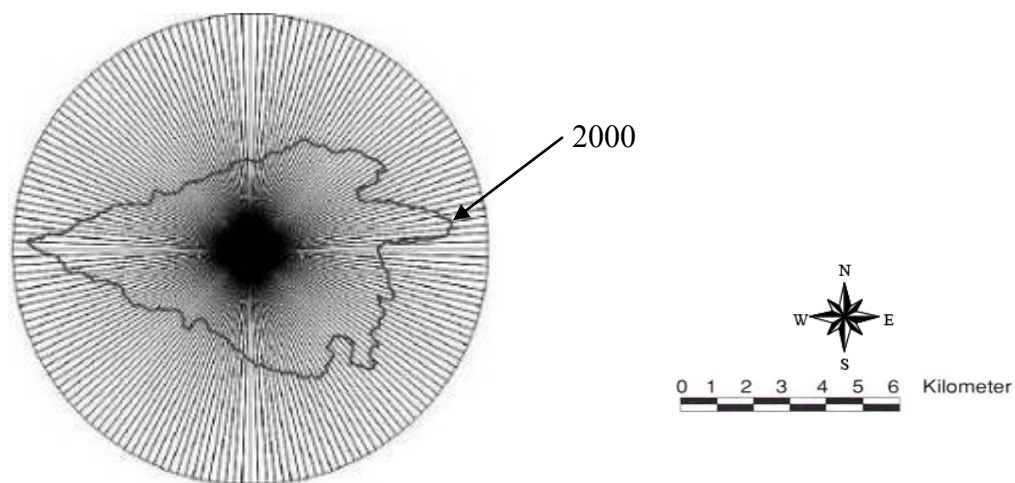


Figure 6-6: Centre configuration used as output for training data collection in 2000, TMA
 centre location: $(x, y) = (534694.929, 3953534.460)$ meters

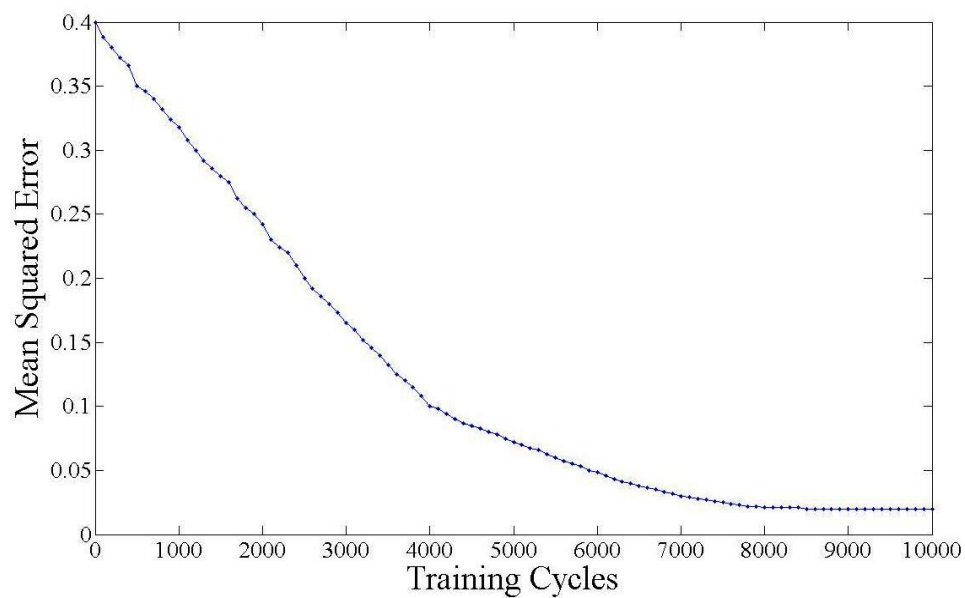


Figure 6-7: MSE value across training cycles

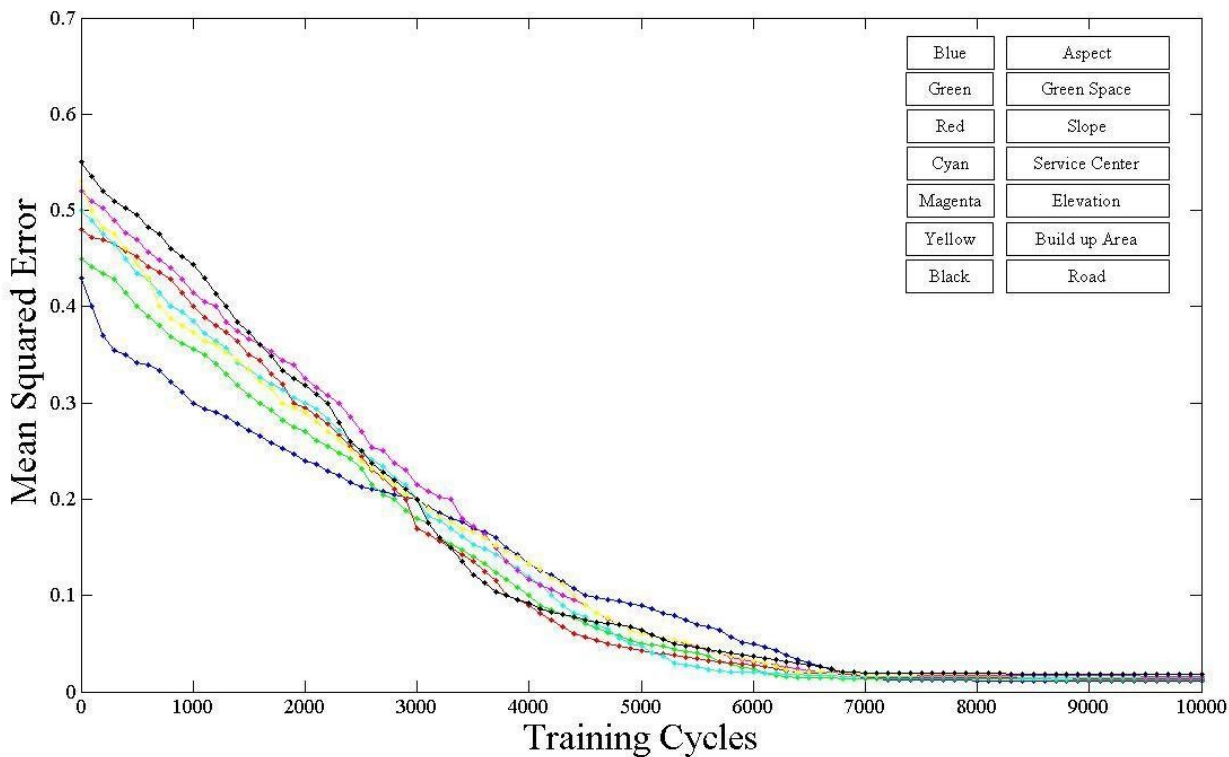


Figure 6-8: MSEs across training cycles for the drop one out predictor variable sensitivity analysis. Each curve is labelled with the predictor variable that is left out of the training

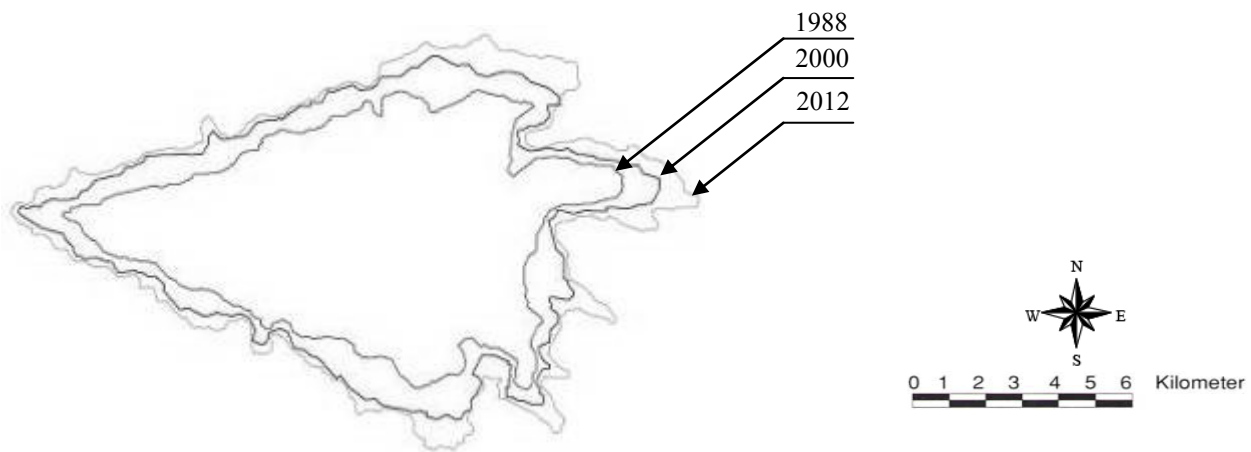


Figure 6-9: Illustration of the result of UGB predictions of TMA in 2012

Table 6-1: MSE of UGBMs with reduced-variable for the statistical analysis

Reduced-variable	MSE value
Distance to road	0.0182
Distance to build up area	0.0178
Elevation	0.0162
Distance to service centre	0.0145
Slope	0.0136
Distance to green space	0.0124
Aspect	0.0107

Table 6-2: PAM values for different cardinal directions

Direction	Domain (Degree)	Area actually transitioning (km ²)	Area predicted to change (km ²)	PAM
North	315° to 45°	25	21	84
East	45° to 135°	22	17.60	80
South	135° to 225°	34	27.54	81
West	225° to 315°	19	15.58	82
Total	0° to 360°	100	81.72	82

CHAPTER 7: TWO RULE-BASED URBAN GROWTH BOUNDARY MODELS APPLIED TO THE TEHRAN METROPOLITAN AREA, IRAN⁴

7.1 Introduction

7.1.1 Urban Growth Boundaries (UGBs)

Urban growth modeling has attracted considerable attention over the last two decades (Veldkamp et al. 1997; Verburg et al. 2002; Clarke and Gaydos 1998; Pijanowski et al. 2002; Batisani and Yarnal, 2009; Dewan and Yamaguchi, 2009; He et al. 2006; Tayyebi et al. 2008a, 2010; Serra et al. 2009; Shalaby and Tateishi, 2007). The focus of much of this research has been exclusively on modeling change in individual urban pixels. Surprisingly, urban growth modeling has failed to directly address the delineation of Urban Growth Boundaries (UGBs) which are common planning tools used to demarcate limits for urban growth over a particular period of time, generally 20 years (Calthorpe and Fulton, 2001). UGBs have been used by state, regional, or local planning agencies in various countries around the world (Phillips and Goodstein, 2000; Wassmer and Baass, 2006; Gordon and Vipond, 2005; Coiacetto, 2007; Bengston and Youn, 2006; Tayyebi et al. 2008b).

⁴ Current version has been published in Applied Geography.

Most land change simulations treat urban areas as groups of similarly classified pixels and are not specifically designed to simulate the edges of the urban area. Furthermore, the few UGB models that exist do not specifically address the location of the urban boundary per se, but rather supply users with a means to calculate the total area needed within the urban area. UGBs have been extensively adopted in the United States, particularly in Oregon, Washington, Minnesota, Maryland, Montana, Florida, and California (Anderson, 1999; Jaeger and Plantinga, 2007; Staley and Mildner, 1999). For example, Baltimore County in the state of Maryland has had an urban/rural demarcation line in place since the 1970s which defines the areas where sewer and water can be provided (Anderson, 1999). The primary objectives of restricting urban development within a defined boundary are to: (1) control urban sprawl by encouraging in-fill development where services and utilities were generally available, (2) reduce the cost of infrastructure provision for new development by having better coordination between its provisions and economic development plans, and (3) preserve resources in the surrounding landscape (APA 2002; Gunn, 2007; Han et al. 2009; Acevedo et al. 2007; Bengston and Youn, 2006). Hence, land inside the UGB is available for urban development while the land outside the UGB is set aside for farming, forestry, and low-density residential development where conditions for farming are particularly poor (Nelson and Moore, 1993). UGBs have also been proposed as one of the first urban growth management tools in countries such as Saudi Arabia (Al-Hathloul and Mughal, 2004) where explosive urban growth is straining urban infrastructure in its major cities (Mubarak, 2004). Despite the preponderance of UGBs around the world, it is surprising that very little research has focused on developing models that can be used to determine

how UGBs should be implemented (Knaap and Hopkins, 2001, Alkheder and Shan 2005).

A vital component of the research on land use/cover change is the development of land use/cover change models for decision making (GLP, 2005; Houet et al. 2009; Lambin and Geist, 2006; Rindfuss et al. 2004; Turner et al. 2007). The impact of urban planning policies in large cities is often a major concern for those involved in modeling, forecasting, and policy making related to planning sustainable urban development (Barredo et al. 2004; Evans and Kelley, 2007). Therefore, the spatial and temporal boundaries of UGBs deserve serious study by urban planners, urban geographers and policy makers. In Iran, the growing necessity for infrastructure provision due to the accelerating rate of urban growth encouraged the government to introduce UGBs, and decision makers have recently started to use spatial analytical and planning tools to simulate and evaluate the consequences of urban planning prior to implementing them. However, urban development inevitably reaches the UGB, creating the need to define UGBs that can realistically accommodate future urban expansion (Nelson and Moore, 1993).

Urban dynamics are often simulated with rule-based Urban Growth Models (UGMs), e.g. Cellular Automata (CA) and Agent Based Models (ABMs). CA has been employed to study different types of urban forms and development densities (Yeh and Li, 2002), evolution of urban spatial structure over time (White and Engelen, 2000), patterns of pedestrian movement (Batty 2003), and to explore urban growth and sprawl (Clarke et al. 1997). In Rule-Based UGMs, universal transition rules specify how a cell will evolve under certain conditions through time. They have also incorporated real data through GIS

and relax many of the assumptions, such as homogeneity of space, uniformity of neighborhood interactions, and universal transition functions (White and Engelen 2000). ABM also allows for the modeling of interactions between human and natural systems by defining different agents (Matthews et al. 2007; Parker et al. 2008; Robinson et al. 2007; Berger and Schreinemachers, 2006; Le et al. 2008). Agents can have different internal characteristics which allow them to interact with other agents and their environment (Bonabeau, 2002; Sawyer, 2003). However, ruled-based models have not been used to specifically model urban boundary change. In the following sections, we present two Urban Growth Boundary Models (UGBMs) and describe how they represent the spatial location and quantity of area within urban boundary more accurately than traditional Urban Growth Models; hence provide more useful information for developing and implementing UGBs.

7.1.2 Urban Growth Boundary Models (UGBMs) versus Urban Growth Models (UGMs)

UGMBs differ from other UGMs in that they predict the change in the spatial location and quantity of area within urban boundary whereas UGMs simulate the change in individual pixels in a study area from non-urban to urban. UGBMs utilize solely vector GIS routines in ways that attempt to delineate urban boundaries. Many land change models, like the current SLEUTH model, grow by pixels and complex spatial rules to govern the growth patterns of these pixels (Jantz and Goetz, 2005; Clarke and Gaydos, 1998). Similarly, the CLUE model of Verburg et al. (2002) uses a series of hierarchical rules coupled to logit models to transition cells in a raster environment. The Land Transformation Model (LTM) also uses pixels to simulate the relationship between inputs

and output (Pijanowski et al. 2002; Pijanowski et al. 2005; Pijanowski et al. 2006; Pijanowski et al. 2010). Calibration for the CLUE model is performed on the probability distribution of cells (Verburg, 2006) and on the spatial shape of groups of cells for the LTM (Pijanowski et al. 2006; Tayyebi et al. 2009). None of the UGMs have attempted to predict the size and shape of urban boundaries directly. Further, UGMs use accuracy assessment parameters like Percent Correct Match (PCM), Kappa Statistic (KS), and Relative Operating Characteristic (ROC) that are only applicable to comparing pixels classified either as binary maps (PCM and KS) or probabilities of change (ROC). In contrast, to assess a boundary, one needs to use shape and size to measure model goodness of fit and determine the distance of urban growth from a central reference point across different azimuths, which can potentially inform planners on how the urban boundary grows in particular directions. Furthermore, comparing the size of the predicted and observed urban area is rarely done in modeling studies. Thus, modeling urban boundary and urban growth are different and we have not been able to find (in the geography, urban planning, land change or economic literature) any model that focuses specifically on simulating an UGB.

7.1.3 Research question and chapter structure

In this chapter, we demonstrate two approaches for simulating urban boundary growth using rule-based simulation UGBMs, one which we call the Distance Dependent Method (DDM) and the other referred to as the Distance Independent Method (DIM). We compare these UGBMs with a null UGBM to assess their accuracy in predicting the location and quantity of urban boundary change. Both DDM and DIM use azimuths and

distances from a central point in the region to simulate urban boundary change. Distances across different azimuths from points on the urban boundary to a central point are measured in the interior of the urban area and then used to simulate urban boundary. The relative accuracy of the urban boundary predictions are assessed by comparing the Percent Area Match (PAM) in *quantity* and *location* goodness of fit metric of the projection from each UGBMs with the reference urban boundary for the same year. The current chapter is unique in that it is the first to develop rule-based simulation UGBMs to predict urban boundary change. The research questions are: (1) How can spatial predictor variables (azimuth and distances) be used to parameterize UGBs with rule-based modelling approaches (i.e. DDM and DIM)? (2) Do these rule-based UGBMs more accurately predict urban boundaries than a null UGBM? and (3) How can UGB maps derived from rule-based simulation UGBMs be used by regional planners to develop future UGBs?

We organize the remainder of this chapter as follows. Section 7.2 summarizes the basic principles of rule-based simulation UGBMs and the concept of a Null model relevant to urban boundary change modelling. Section 7.3 describes the study area, Tehran Metropolitan Area (TMA), and the data source used in the models and illustrates how we parameterize rule-based simulation UGBMs and Null UGBM using a set of spatial interaction rules derived from GIS routines. The projections for the TMA and comparison between the rule-based simulation UGBMs and Null UGBM are discussed in section 7.4. The chapter concludes with a discussion on simulation of UGB in TMA and its application in urban planning.

7.2 Urban Growth Boundary Models (UGBMs)

7.2.1 Application of Null model to UGBMs

Null models are pattern generating models that allow for randomization of data or random sampling from a known or imagined distribution (Gotelli and Graves, 1996). Null models are widely used in ecology and biogeography, particularly when conventional statistical analyses fall short (Nitecki and Hoffman, 1987; Manly, 1991; Gotelli and Graves, 1996; Colwell and Lees, 2000). In contrast to other modelling approaches, the null model deliberately excludes a mechanism being tested (Caswell, 1988). We compare output from our ruled-based UGBMs with output from null UGBMs to assess how well our model predicts the patterns in the real data compared to a simple model that does not incorporate any predictor variables.

We can generate a null UGBM using an algorithm or set of rules based on procedures that are created using random values. A polygon of the urban boundary of the study area in initial time can be expanded using GIS software to produce new urban boundaries, each corresponding to a separate expansion increment. Therefore, each run of the null UGBM generates a different simulated map that has a different spatial location and quantity of area within urban boundary, depending on the particular run's parameters and the random selection. This can be done until an under-estimated and over-estimated of the reference urban boundary in subsequent time is achieved.

7.2.2 Rule-based simulation UGBMs

7.2.2.1 Distance Dependent Method (DDM)

The DDM approach uses the points on the urban boundary in initial time and takes advantage of a suitable prediction method to anticipate the urban boundary in any subsequent time. The suitable prediction method projects a new urban boundary by increasing distances by percentage increments across different azimuths. Central points in the city are defined visually based on different constraints (discussed in section 7.2.2.4) and the distance from the central point to points on the urban boundary are computed for the different azimuths (Figure 7-1) using Eq. 7-1 and 7-2.

$$S_{it} = \sqrt{(X_i - X_t)^2 + (Y_i - Y_t)^2} \quad (\text{Eq. 7-1})$$

$$\text{Azimuth}_{it} = \tan^{-1}\left(\frac{X_i - X_t}{Y_i - Y_t}\right) \quad (\text{Eq. 7-2})$$

In Eq. 7-1 and 7-2: X_t is the Easting coordinate of a central point in the city; Y_t is the Northing coordinate of a central point in the city; X_i is the Easting coordinate of point i on urban boundary; Y_i is the Northing coordinate of point i on urban boundary; S_{it} is the distance between an central point in the city and point i on the urban boundary; and Azimuth_{it} is the azimuth between a central point in the city and point i on the urban boundary.

Eq. 7-3 is used to ensure that the reference change in distance across different azimuths and for different increments is consistent in percentage. In Eq. 7-3, $S_{it'}$ and S_{it}

are the new predicted distance and initial distance from central point to urban boundary for the different azimuths respectively, and *Growth-Factor*(*GF*) is the percent of increment change in distances where $GF = 1.0; i = 1 \dots n$.

$$S_{it'} = GF * S_{it} \quad (\text{Eq. 7-3})$$

$S_{it'}$ is then used to calculate coordinates of new urban boundaries for different percent distance increments.

7.2.2.2 Distance Independent Method (DIM)

In contrast to DDM, DIM simulates the urban boundaries using data from two time periods and measure distances from central points to urban boundaries. DIM uses central points to indicate an azimuth for measuring the rate of change in distance between the two urban boundaries using a Rate of Change in Distances over Time (RCDT). The central points used to compute the distances and azimuths are the same across the two time periods. The RCDT is measured across different azimuths using Eq. 7-4, which is repeated for all points along the urban boundary so that each point on urban boundary has its own RCDT.

$$RCDT_i = \frac{S_{it}(t_2) - S_{it}(t_1)}{S_{it}(t_1)} \quad (\text{Eq. 7-4})$$

In Eq. 7-4, $RCDT_i$ is the Rate of Change in Distances over Time between a central point in the city and point i on the urban boundary across different azimuths; $S_{it}(t_1)$ is the distance between a central point and point i on urban boundary in initial

time; and $S_{it}(t_2)$ is the distance between a central point and point i on urban boundary in subsequent time.

Each central point is assigned to a region on the urban boundary based on which central point is used to measure the RCDT for points on that region (see section 7.2.4 for details). The RCDTs for all points within the region on the urban boundary map coinciding with each central point are averaged using Eq. 7-5, giving an Average RCDT (ARCDT) for each central point. Final Average RCDT (FARCDT) is computed as the average of all ARCDTs (Eq. 7-6). The ARCDT of different central points and the FARCDT can be applied to predict new urban boundaries for the different regions on the urban boundary map.

$$ARCDT_j = \frac{\sum_{i=1}^n RCDT_{ij}}{n} \quad (\text{Eq. 7-5})$$

$$FARCDT = \frac{\sum_{j=1}^m ARCDT_j}{m} \quad (\text{Eq. 7-6})$$

In Eq. 7-5; n is the number of points in each region of the urban boundary map; m is the number of central points (Eq. 7-6); $RCDT_{ij}$ is the RCDT that is derived from point i on the urban boundary corresponding to central point j ; $ARCDT_j$ is the Average of RCDTs for points corresponding to central point j ; and $FARCDT$ is the Final Average of $ARCDT_j$ for all central points.

A new urban boundary can then be created using predicted distances from the urban boundary to central points calculated with ARCDTs from each region and the

FARCDT. This research defines two scenarios: (1) FARCDT is applied for all distances across different azimuths for all central points; (2) the ARCDT of each region is applied for the corresponding central point as well as other central points. Thus, only one urban boundary is determined using FARCDT, while the number of urban boundaries determined using ARCDTs are equal to the number of central points. The new predicted urban boundaries created using FARCDT and ARCDTs are then compared with the reference urban boundary map to determine the best match, which can then be used to predict future urban boundaries (Figure 7-2).

7.2.2.3 Calibrating UGBMs using Percent Area Match (PAM) quantity and location

After the end points of predicted distances across different azimuths by DDM and DIM are connected to create a new urban boundary polygon, the agreement between the simulated and the reference urban boundary can be determined using Percent Area Match (PAM) quantity and location metrics (Eq. 7-7 and 7-8). PAM quantity gives the match between the total area under the predicted boundary and the reference boundary (Eq. 7-7). PAM location gives the relative match for the urban area between the reference and predicted maps without considering the overestimate (Figure 7-3); which, in contrast to PAM quantity, also indicates the match in the location of the predicted and reference urban boundaries. PAM location is used to determine how much of the predicted area is located in the right place relative to the reference urban boundary (Eq. 7-8). PAM quantity and location are important for urban planners because it is vital for them to know the spatial location and quantity of area within the urban boundary around the urban area.

If the UGBMs simulates the overall quantity accurately (PAM quantity), then there is a large range for the UGBMs to allocate the location accurately or inaccurately in space (PAM location). Therefore, readers must know the accuracy of the simulation of quantity in order to interpret the other aspects of the assessment. PAM quantity is used as a stop condition to simulate urban boundary change because the quantity of simulated area by UGBMs provides a better match for the quantity of area that is derived from the urban boundary in subsequent time periods, producing a better UGBM. The stop condition for the Null UGBM and the DDM is defined when the total area under the predicted urban boundary becomes greater than the area under the reference urban boundary, or when PAM quantity > 1. Therefore, there is one PAM quantity and location for DIM (rule-based simulation UGBM). On the other hand, there are different PAM quantities and locations for Null UGBM and DDM (rule-based simulation UGBMs) which equal to the number of simulations that are repeated until a stop condition is satisfied.

A PAM ratio for quantity equal to one indicates that the UGBM prediction of the urban area is equal to the reference urban area, a PAM ratio for quantity greater than one means that the UGBM overestimates new urban area and a PAM ratio for quantity less than one indicates that UGBM underestimates the new urban area. Similarly, a PAM ratio for location closer to 1 also indicates a more accurate model.

$$PAM \text{ Quantity} = \frac{APt_2 - AAt_1}{AAt_2 - AAt_1} \quad (\text{Eq. 7-7})$$

$$PAM \text{ Quantity} = \frac{(APt_2 - AAt_1) - \alpha}{AAt_2 - AAt_1} \quad (\text{Eq. 7-8})$$

Where AA_{t_1} = Area within reference urban boundary in time 1; AA_{t_2} = Area within reference urban boundary in time 2; AP_{t_2} = Area within predicted urban boundary in time 2; α = Area over-estimated by AP_{t_2} relative to AA_{t_2} ;

Two PAM quantity values, one closest to and greater than 1.0, and one closest to and less than 1.0, are used to determine the corresponding (1) linear distances from urban boundary for Null UGBM (2) percent level of distance increment for DDM and (3) ARCDT or FARCDT for DIM for predicting one future urban boundary that is an overestimate and another future urban boundary that is an underestimate.

7.2.2.4 Constraints

There are two constraints that we use for the urban growth boundary simulation. First, most of urban boundaries are not fully convex in shape and contain some concavities, so it is not possible to determine a single central point from which one can draw a straight line to the boundary (Figure 7-4a). Thus, several central points may be required to determine the distance from some central location to the urban boundary across all azimuths (Figure 7-4b). Second, there are often different physical or legal obstructions to growth of urban boundaries in cities. Thus, it is necessary to identify obstructed regions and remove them from analysis.

7.3 Implementation of UGBMs

The boundaries of TMA in 1988 and 2000 were obtained from satellite images with a 28.5m resolution, and were overlaid to create one composite map (Figure 7-5). Urban pixels in the image were defined according to Anderson classification level 1 using ArcGIS10 from which urban cells on the edge of the urban area were visually used

to define the urban boundary. Urban boundaries were exported in vector format. Three central points were visually identified as the minimum number of points needed to cover the boundary of the TMA (Figure 7-4b) and a corresponding region was assigned to each central point (Figure 7-5). Eight hundred and seventy one and 783 points were used to create the point vector outlines of the urban boundary in 1988 and 2000 respectively.

7.3.1 Study Area

Tehran is the capital of Iran and is located (Latitude 35° 45' N and Longitude 51° 30' E) in the northern portion of the country. The Tehran Metropolitan Area (TMA) was chosen as our study area (1) because considerable remote sensing and geospatial data needed for delineating urban boundaries exists for the region; and (2) because of the need for an UGBM that can be used for regional planning by the local government. Iran's rapid economic growth from 1980 to 2010 transformed the country to an industrialized nation. TMA has supported a great deal of economic and social development in terms of urban change and the rapid growth of infrastructure. TMA, with a population of over 15 million and a metropolitan area of over 2000 km², is the centre of commercial, financial, cultural and educational activities in Iran. Rapid urban growth has resulted from high population growth and increased rural-urban migration combined with a strong tradition of centralization of government activities focussed in the capital. Consequently, the development and application of UGBMs has particular importance for this region.

7.3.2 Data preparation for Null, DDM and DIM UGBM

For the null UGBM, we used urban boundary of TMA in 1988 as a base map for simulations. The buffer option in ArcGIS10 was used to simulate new urban boundaries

in 2000 based on different increments in linear distance with 50m interval around the urban boundary in 1988. Corresponding urban boundaries with respect to the linear distances are simulated and area of simulated urban boundaries were saved in a excel file and compared with reference urban boundary in 2000 with respect to PAM quantity. The simulations of urban boundaries continue until the PAM quantity greater than 1.0 condition is satisfied as a stop condition.

Using DDM, urban boundary in 2000 was predicted by calculating the distance between the three central points and the 871 points on the 1988 urban boundary across different azimuths (Eq. 7-1 and 7-2). The boundary of each of the three regions was projected by using only the azimuths and distances between points on the boundary corresponding to the central point of the region with distance increments in percent level (Figure 7-5). The corresponding urban boundary with respect to the distance increments is created at each stage and area of produced urban boundary saved in a MS Excel file. We also saved to MS Excel the PAM quantity values which were derived from comparison between our predictions and reference urban boundary in 2000 for different runs until the best over-estimated PAM quantity is satisfied as stop condition.

In order to acquire the best PAM quantity value for our three regions and whole region individually, we defined two scenarios: (1) we determined a single best percent increment in distance for the whole TMA by comparing PAM quantity values between all percent increments from the three central points of our 2000 projection with the reference 2000 urban boundary. (2) We also determined three separate percent increments, one for each of the regions also by comparing PAM quantity values of projection to reference urban boundary in 2000.

For DIM, points on both the 1988 and 2000 urban boundaries and the three central points were used to predict the urban boundary (Eq. 7-1 and 7-2). The same central points were used to calculate the distance between the urban boundaries in 1988 and 2000 in order to maintain the same azimuth between the RCDT and the corresponding distance from central point to boundary.

There are three steps in data preparation for the DIM approach included: (1) The distances between a central point and points on the boundary for each region for both map years are sorted according to azimuth, i.e. from 1° to 360° . (2) Because of considering three independent central points, total numbers of azimuth distances were greater than 360. The distances were averaged to obtain one mean distance per 1° interval, leaving at total of 537 and 486 samples total from the three central points on the 1988 and 2000 urban boundaries respectively. (3) Finally, because the samples were not distributed evenly across the urban boundary, some azimuth degree intervals were left without a distance value. The distance for these azimuth degree intervals was obtained as the average of the two nearest azimuth distances, resulting in a total of 655 and 735 samples on the urban boundary in 1988 and 2000 respectively.

7.4 Result and discussion

7.4.1 Null UGBM

7.4.1.1 Calibration with PAM quantity:

Fifteen urban boundaries were simulated by varying the distances from 50m to 750m with 50m intervals around the TMA boundary in 1988 using buffer option in ArcGIS10. The area of new predicted urban boundary in 2000 is calculated and compared

with area of urban boundary in 2000 using PAM quantity. The best under-estimated and over-estimated PAM quantity was obtained from boundary projection using the null UGBM with 700m and 750m distances around the urban boundary in 1988, respectively (Table 7-1 and 7-2). Figure 7-6 illustrates projected under-estimated and over-estimated urban boundaries in 2000 for the TMA and the reference TMA urban boundary in 1988 and 2000.

7.4.1.2 Forecasting Urban Boundary

For forecasting, 700m and 750m distances around the urban boundary in 2000 are used in the buffer option of ArcGIS10 to produce under-estimated and over-estimated urban boundary in 2012, respectively. Table 7-3 shows the total area of TMA calculated using the corresponding projected urban boundaries in 2012. The over-estimated and under-estimated projected urban boundaries for 2012 with using the best PAM quantity are illustrated in Figure 7-7.

7.4.2 Distance Dependent Method (DDM)

7.4.2.1 Calibration with PAM quantity: Region 1 (western TMA) experienced the least, while Region 2 (northern TMA) experienced the greatest urban growth from 1988 to 2000 (Table 7-1; Figure 7-5). The best fit percent increment in distance for the under-estimated and the over-estimated respectively were: 13% and 14% for the whole region (Figure 7-8a, b and c), 11% and 12% for region 1 (Figure 7-8c), 17% and 18 % for region 2 (Figure 7-8a), and 8% and 9% for region 3 (Figure 7-8b). The best under-estimated and over-estimated PAM quantity between our 2000 projection and the reference 2000 urban boundary are summarized in Table 7-4. The PAM quantity for

regions 1, 2, and 3 obtained from 1) projections using two best match percent increments for each of the corresponding regions (multi-region model), are closer to 1 than those obtained from 2) projections using the two best percent increments for the whole region (whole-region model; Table 7-4). The best match percent increment also varied across the three regions as predicted by the multi-region model (Table 7-4), whereas percent increment growth is assumed to be the same across the three regions in the whole-region model. Further, while the two best match percent increments for each of the regions from the multi-region model provided one underestimate and one overestimate, the two best match percent increments from the whole-region model provided two overestimates for region 1 and 3, and two underestimates for region 2 (Table 7-4). These results suggest that projecting urban boundary from multiple regions is more accurate than projecting urban boundary from a single whole region.

The variation in PAM quantity across different percent increments was lowest in region 2 and greatest in region 3 (Table 7-5). As the variation in PAM quantity increases, the difference between the over-estimated and under-estimated also increases, suggesting that a greater variation in PAM quantity indicates a model that is more sensitive to percent increment and hence is likely to provide a less accurate prediction of urban boundary. Thus, the urban boundary projection for region 2 is more sensitive to percent increment and less accurate than region 3 (Table 7-5). This variation in the relative sensitivity of different regions further demonstrates the importance of predicting changes in urban boundary separately for each region, rather than the region as a whole.

7.4.2.2 Forecasting Urban Boundary: The over-estimated and under-estimated urban boundaries projected for 2012 using the best PAM quantity (13% and 14%)

increment in distances with the whole-region model are illustrated in Figure 7-9a, b and c. For the multiple-region model, the over-estimated and under-estimated urban boundaries projected for 2012 (using 11%, 17% and 8% increments in distances for the under-estimated and 12%, 18% and 9% increment in distances for the over-estimated) for region 1, 2 and 3 (Figure 7-9a, b and c). Table 7-6 shows the total area within each region calculated using the corresponding projected urban boundaries in 2012.

7.4.3 Distance Independent Method (DIM)

We also used the DIM approach to obtain predictions for the whole TMA and each of the individual TMA regions. The urban boundary of the whole TMA was projected using ARCDTs from the three regions as well as the FARCDT (final average of the three ARCDTs). The urban boundaries of the three TMA regions were projected using ARCDTs from all of the regions and the FARCDT. The three regional areas obtained using their corresponding ARCDTs (ARCDT_{1,2,3}) were also added together to produce another whole region estimate for the TMA. Table 7-9 shows the different ARCDTs obtained from each of the three regions as well as the FARCDT (average of the three ARCDTs).

7.4.3.1 Calibration with PAM: For the whole TMA, the PAM quantity between the reference urban boundary in 2000 and the predicted urban boundary using ARCDT3 (ARCDT from region 3) provided the under-estimated value closest to 1, while urban boundaries using ARCDT1, ARCDT2, FARCDT and ARCDT_{1,2,3} all provided over-estimated values (Table 7-8). The best over-estimated PAM quantity was obtained from boundary projection using ARCDT_{1,2,3} (Table 7-8). Figure 7-10 illustrates relative

position of projected urban boundaries in 2000 for the whole TMA (obtained using ARCDT1, ARCDT2, ARCDT3, FARCDT and ARCDT1,2,3) and the reference TMA urban boundary in 2000 and 1988. It is clear from Table 7-8 and Figure 7-10 that the most accurate urban boundary projection is obtained by using ARCDT1,2,3 when modeling the whole TMA.

For individual TMA regions; ARCDT3 gave the only under-estimated PAM quantity value, while FARCDT gave the best over-estimated for region 1 (Table 7-9); while ARCDT1, ARCDT2, ARCDT3 and FARCDT all gave under-estimates for region 2, ARCDT2 gave the PAM quantity value closest to 1 (Table 7-9); and all ARCDTs and FARCDT gave over-estimates for region 3 with ARCDT3 providing the best PAM quantity value (Table 7-9). These results suggest when projecting urban boundary for individual regions, using the corresponding ARCDT for each region is more accurate than using ARCDTs from other regions or the FARCDT.

7.4.2.2 Forecasting Urban Boundary: Figure 7-11 illustrates relative position of projected urban boundaries in 2012 obtained using the best match ARCDTs and FARCDT (ARCDT3, ARCDT1,2,3 and FARCDT) and the reference TMA urban boundary in 1988 and 2000. Table 7-10 shows the total predicted area of the whole TMA in 2012, and table 7-11 shows the predicted area within each region in 2012 calculated using the corresponding projected urban boundaries.

7.4.4 Comparison of DDM UGBM, DIM UGBM and Null UGBM

We compared DDM and DIM (rule-based simulation UGBMs) with each other as well as with the null UGBM. There are differences in the way that the data are used to

parameterize null UGBM and rule-based simulation UGBMs. The rule-based simulation UGBMs employ vector predictor variables (radial distances at the specified azimuths) as only input for DDM, and as input and output for DIM, to simulate urban boundary while the null UGBM employs only urban boundaries in initial and subsequent time as input for simulation and assessment in vector format, respectively. The rule-based simulation UGBMs use mathematical models to simulate and predict urban boundary while null UGBMs use buffer option as a tool for urban boundary simulation and prediction. Both rule-based and null UGBMs indicate smooth shape in prediction of urban boundary.

The PAM quantity and location assessment articulates components of agreement and disagreement based on a philosophy of urban boundary change map comparison that separates explicitly the information concerning the quantity of urban boundary change from the information concerning the location of urban boundary. We obtained total PAM quantity values for DDM and DIM by averaging under-estimated PAM quantity values for the multiple-region model and region 1, 2 and 3, respectively (Table 7-4 and 7-9). The PAM quantity of under-estimated null UGBM is also considered as total PAM quantity for the null UGBM (Table 7-12). Comparing the PAM quantity value for the urban projection in 2000 from the rule-based simulation UGBM and Null UGBM obtained in this study (Tables 7-12) allows us to assess the accuracy of UGBMs in projecting the change in quantity of area between urban boundaries and location of urban boundary. Although DDM and Null UGBM provide the best prediction for quantity, they give the least accurate prediction for location (Tables 7-12). In contrast, DIM UGBM provides the most accurate prediction for location, and the least accurate prediction in quantity. The lower accuracy of Null UGBM in predicting location may be due to the simple fact that

Null UGBM consider to project new urban boundary using the same increment of distances around urban boundary in the initial time. For DDM, the reference distances between central points and points on urban boundary in initial time across different azimuths increase based on different increments in percentage while DIM uses different RCDTs across different azimuths to project a new urban boundary.

7.5 Conclusion

The output from the two rule-based simulation UGBMs (DDM and DIM) are described and compared with a null UGBM in this chapter. Both UGBMs employ a radial growth of the boundary at specified azimuths as inputs, measured using multiple central points within a given urban area, to simulate change in urban boundary location. While the DDM projects using a single urban boundary for projection, the DIM uses urban boundary in both initial and subsequent time periods to make this projection. Our objective was to determine which of these models were the most appropriate for informing urban planners regarding: (1) the feasibility of setting UGBs in a particular location for a specific period of time, as well as (2) where and how future infrastructure efforts need to be focused. We used each model to predict the urban boundary of the TMA, and compared the outputs using PAM quantity and location. It is necessary to understand the agreement between the urban boundary maps in terms of both the total quantity of area simulated as well as the location of the area being simulated. If the correspondence in terms of location is high, then the agreement in terms of pattern must also be high. However, it is possible to have substantial disagreement in location but high agreement in quantity.

UGBs limit land development beyond a politically-designated area. The purpose of delineating the urban boundary is to guide and regulate the location and intensity of land development for given period of time. Thus, it is necessary to determine how fast the boundary of a particular city will expand. While the total amount or area of expansion can be predicted with traditional UGMs, the location of growth simulated by these models may not correspond to an easily identifiable boundary. UGBMs provide a vector map displaying the particular location of an urban boundary at a specific time in the future. Thus, projections from UGBMs, particularly a DIM UGBM, can be used to identify the feasibility of drawing an UGB at a particular distance from the current urban boundary for a given period of time. The parameters that UGBMs consider have large influence on the quantity of simulated urban boundary change and on the accuracy of the simulation. The largest potential for improvement in UGBMs accuracy is improvement in the way the UGBMs simulates the quantity and location of urban boundary change.

Identifying and delineating boundaries around areas of rapid urban growth, particularly in large cities with complex urban boundaries like the TMA, are especially important because of the high risk to social-cohesion and environmental quality in these areas. It is particularly important to consider the demand for the total amount and the location of social, economic and physical infrastructure resources when setting UGBs for large cities. In other words, it is necessary to plan UGBs in such a way as to match the total demand at particular locations for employment opportunities, housing, public facilities such as schools and hospitals, parks, shopping malls, energy (electricity, gas), with the spatial availability of these resources. It is also necessary to determine the location on an UGB where future growth pressure will be greatest in order to determine

where to concentrate local environmental risk reduction measures, i.e. where to build more waste treatment plants, create more green infrastructure etc.). Because the DIM UGBM provided the most accurate prediction for the location of future urban boundary, it can be used to pinpoint specific locations where such social, economic and environmental infrastructure needs to be placed. Further, due to its greater precision in predicting quantity, output from a rule-based UGBM using DDM or null UGBM could be combined with output from a DIM UGBM in order to determine the total amount of infrastructure that will need to be allocated to particular areas near the UGB.

7.6 References

- Acevedo, M. F., Callicott, J. B., Monticino, M., Lyons, D., Palomino, J., Rosales, J., Delgado, L., Ablan, M., Davila, J., Tonella, G., Ramirez, H., & Vilanova, E., (2007). Models of natural and human dynamics in forest landscapes: Cross-site and cross-cultural synthesis. *Geoforum*, 39, 846-866.
- Al-Hathloul, S., Mughal, M.A., (2004). Urban growth management - the Saudi experience. *Habitat Int.*, 28(4), 609-623.
- Alkheder, S, and Shan, J., (2005). Urban growth simulation using remote sensing imagery and neural networks. Third International Symposium Remote Sensing and Data Fusion Over Urban Areas (URBAN 2005) and the 5th International Symposium on Remote Sensing of Urban Areas (URS 2005), March 14- 16, 2005, Tempe, Arizona.
- American Planning Association, (2002). *Growing Smart Guidebook*. Chapter 6 – Regional Planning, Retrieved February 16, 2010 from <http://www.planning.org/growingsmart/guidebook/six02.htm>.
- Anderson, H. A., (1999). Use and Implementation of Urban Growth Boundaries, An Analysis Prepared by the Center for Regional and Neighborhood Action.
- Batisani, N., Yarnal, B., (2009), Urban expansion in Centre County, Pennsylvania: Spatial dynamics and landscape transformations, *Applied Geography*, 29, 235-249.
- Batty, M., (2003). Agent-based pedestrian modeling, WP 61, Center for Advanced Spatial Analysis, London. Available at http://www.casa.ucl.ac.uk/working_papers/paper61.pdf.
- Bengston, D. N., Youn, Y., (2006). Urban containment policies and the protection of natural area: the case of Seoul's greenbelt. *Ecol. Soc.*, 11(1), No. 3.
- Berger, T., Schreinemachers, P. (2006). Creating agents and landscapes for multi agent systems from random samples. *Ecol Soc* 11(2):19.
- Bonabeau, E. (2002). Agent-based modeling: methods and techniques for simulating human systems. *Proceeding of the National Academy of Sciences* 99: 7280–7287.
- Calthorpe, P., Fulton, W., (2001). *The regional city: Planning for the end of sprawl*. Island Press, Washington D.C., pp. 304.
- Clarke, K. C., Hoppen, S. and Gaydos, L., (1997). A self-modifying cellular automaton model of historical urbanization in the San Francisco Bay area. *Environment and Planning B: Planning and Design*, 24, pp. 247–261.
- Clarke, K. C., Gaydos L., (1998). Loose coupling a cellular automaton model and GIS: Long-term growth prediction for San Francisco and Washington/Baltimore. *Int. J. Geogr. Inf. Syst.*, 12 (7), 699-714.
- Coiacetto, E., (2007). Residential sub-market targeting by developers in Brisbane. *Urban Pol. and Res.* 25 (2), 257-274.
- Dewan, A. M., Yamaguchi, Y., (2009), Land use and land cover change in Greater Dhaka, Bangladesh: Using remote sensing to promote sustainable urbanization, *Applied Geography*, 29, 390-401.
- Evans, T., Kelley, H., (2007). The influence of landowner and topographic heterogeneity on the pattern of land cover change in South-central Indiana. *Geoforum*, 39, 819–832.

- Gordon, D. L. A., Vipond, S., (2005). Gross density and new urbanism. *J. Amer. Plann. Assoc.*, 71 (2), 41-54.
- Gunn, S. C., (2007). Green belts: A review of the region's responses to a changing housing agenda. *Environ. Plann. B.* 50 (5), 595-616.
- Han, H., Lai, S., Dang, A., Tan, Z., Wu, C., (2009). Effectiveness of urban construction boundaries in Beijing: An assessment. *Journal of Zhejiang University Science A*, 10 (9), 1285-1295.
- He, C., Okada, N., Zhangd, Q., Shi, P., Zhang, J., (2006), Modeling urban expansion scenarios by coupling cellular automata model and system dynamic model in Beijing, China, *Applied Geography*, 26, 323–345.
- Jaeker W. G., Plantinga A. J., (2007). How have land-use regulations affected property values in Oregon? OSU Extension.
- Jantz, C. A. and Goetz, S. J. (2005). Analysis of scale dependencies in an urban land-use-change model, *International Journal of Geographical Information Science*, Vol. 19, No. 2, 217–241.
- Knaap, G. J., Hopkins, L. D., (2001). The inventory approach to urban growth boundaries. *J. Am. Plann. Assoc.* 67 (3), 314-326.
- Le, Q. B., Park, S. J., Vlek, P. L. G., Cremers, A. B. (2008). Land-use dynamic simulator (LUDAS): a multi-agent system model for simulating spatio-temporal dynamics of coupled Landscape Ecol human-landscape system. I. Structure and theoretical specification. *Ecol Informatics* 3:135–153.
- Matthews, R., Gilbert, N., Roach, A., Polhill, J., Gotts, N. (2007). Agent-based land-use models: a review of applications. *Landscape Ecol*, 22:1447–1459.
- Nelson C. Arthur and Moore, T. (1993). Assessing urban growth management, The case of Portland, Oregon, the USA largest urban growth boundary. *Land use policy*.
- Parker, D. C., Brown, D., Polhill, J., Deadman, P.J., Manson, S. M. (2008). Illustrating a new 'conceptual design pattern' for agent-based models of land use via five case studies-the Mr. Potatohead framework. In: Lo'pez Paredes A, Herna'ndez Iglesias C (eds) *Agent-based modelling in natural resource management*. Pearson Education, Upper Saddle River, p. p. 23–51.
- Phillips, J., Goodstein, E., (2000). Growth Management and Housing Prices: The Case of Portland, Oregon. *Contemporary Economic Policy*. 18 (3), July 2000. Available at SSRN: <http://ssrn.com/abstract=234341>.
- Pijanowski, B. C., Brown, D. G., Shellito, B. A., Manik, G. A., (2002). Using neural networks and GIS to forecast land use changes: a land transformation model. *Comput. Environ. Urban* 26 (6), 553-575.
- Pijanowski, B. C., Pithadia, S., Shellito, B. A., Alexandridis, K., (2005). Calibrating a neural network-based urban change model for two metropolitan areas of Upper Midwest of the United States. *Int. J. Geogr. Inf. Syst.*, 19 (2), 197-215.
- Pijanowski, B. C., Alexandridis, K. T., Muller, D., (2006). Modeling urbanization patterns in two diverse regions of the world. *Journal of Land Use Science*, 1 (2-4), 83-109.
- Pijanowski, B.C., Tayyebi, A., Delavar, M. R., Yazdanpanah, M. J., (2010). Urban expansion simulation using geographic information systems and artificial neural networks, *Int. J. Environ. Res.* 3 (4), 493-502.

- Robinson, D. T., Brown, D. G., Parker, D. C., Schreinemachers, P., Janssen, M. A., Huigen, M., Wittmer, H., Gotts, N., Promburom, P., Irwin, E., Berger, T., Gatzweiler, F., Barnaud, C. (2007). Comparison of empirical methods for building agent based models in land use science. *J Land Use Sci* 2:31–55.
- Sawyer, R. K. (2003). Artificial societies: multi agent systems and the micro-macro link in sociological theory. *Sociol Methods Res* 31:325–363.
- Serra, P., Pons, X., Sauri, D., (2009), Land-cover and land-use change in a Mediterranean landscape: A spatial analysis of driving forces integrating biophysical and human factors, *Applied Geography*, 28, 189-209.
- Shalaby, A., Tateishi, R., (2007), Remote sensing and GIS for mapping and monitoring land cover and land-use changes in the Northwestern coastal zone of Egypt, *Applied Geography*, 27, 28-41.
- Staley, S., Mildner, G., (1999). Urban growth boundaries and housing affordability. Reason Public Policy Institute. Los Angeles.
- Tayyebi, A., Delavar, M. R., Saeedi, S., Amini, J., (2008a). Monitoring the Urban Expansion by Multi-Temporal GIS Maps, Application of Remote Sensing and Imagery (TS 5B), Integrating Generations, FIG Working Week 2008 and FIG/UN-HABITAT Seminar, Stockholm Sweden, June 14–19, 2008.
- Tayyebi, A., Delavar, M. R., Saeedi, S., Amini, J., Alinia, H., (2008b). Monitoring Land Use Change by Multi-Temporal Landsat Remote Sensing Imagery. The International Archives of the Photogrammetry, Remote Sensing and Spatial Information Sciences. Vol. XXXVII. Part B7. Beijing 2008, China, pp. 1037-1043.
- Tayyebi, A., Delavar, M. R., Pijanowski, B. C., Yazdanpanah, M. J. (2009). Accuracy Assessment in Urban Expansion Model, Spatial Data Quality, From Process to Decisions, Edited by R. Devillers and H. Goodchild, Taylor and Francis, CRC Press, Canada, pp. 107-115.
- Tayyebi, A., Delavar, M. R., Pijanowski, B. C., Yazdanpanah, M. J., Saeedi, S. and Tayyebi, A. H. (2010). A Spatial Logistic Regression Model for Simulating Land Use Patterns, A Case Study of the Shiraz Metropolitan Area of Iran, *Advances in Earth Observation of Global Change*, Edited by Emilio Chuvieco, Jonathan Li and Xiaojun Yang, Springer press.
- Verburg, P.H., Soepbaer, W., Veldkamp, A., Limpiada, R., Espaldon, V., Mastura, S., (2002). Modeling the spatial dynamics of regional land use: the CLUE S Model. *Environ. Manage.* 30 (2), 391-405.
- Verburg, P. H., (2006). Simulating feedbacks in land use and land cover change models. *Landscape Ecol.* 21 (8), 1171-1183.
- Wassmer, R. W., Baass, M. C., (2006). Does a more centralized urban form raise housing prices? *J. Policy Anal. Manag.* 25 (2), 439-462.
- White, R. and Engelen, G., (2000). High resolution integrated modeling of the spatial dynamics of urban and regional systems. *Computers, Environment and Urban Systems*, 24, pp. 383–400.
- Yeh, A. G. O. and Li, X., (2002). A cellular automata model to simulate development density for urban planning. *Environment and Planning B: Planning and Design*, 29, pp. 431–450.

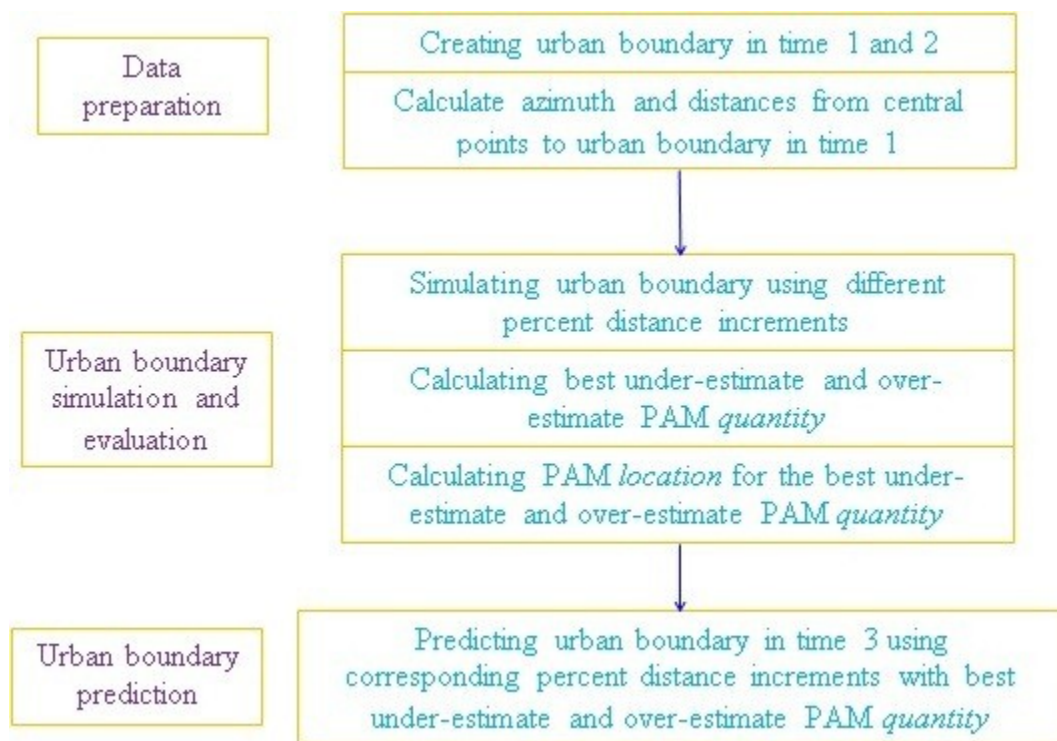


Figure 7-1: Conceptual scheme of DDM

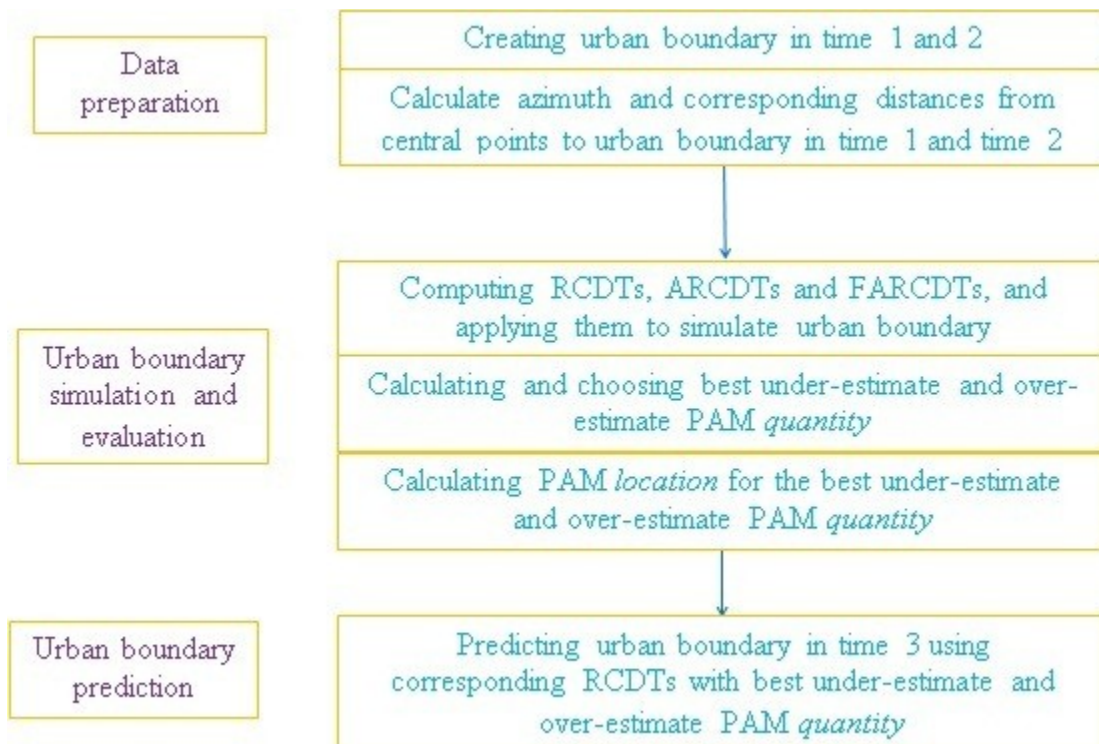


Figure 7-2: Conceptual scheme of DIM

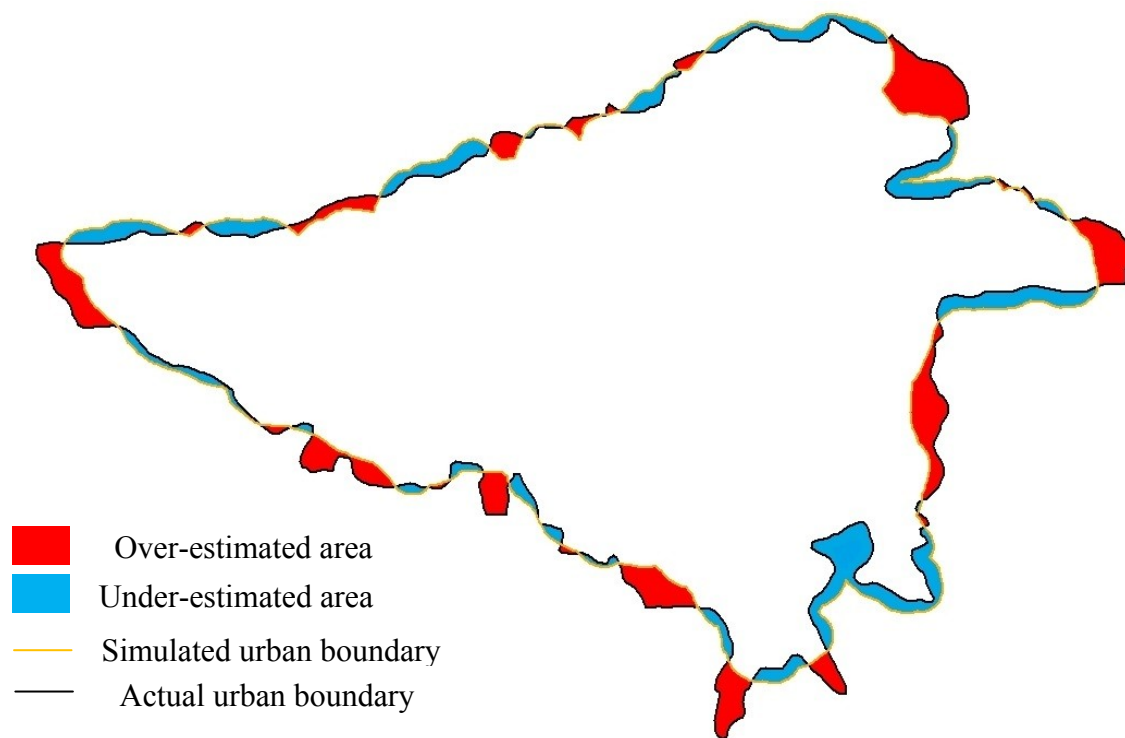
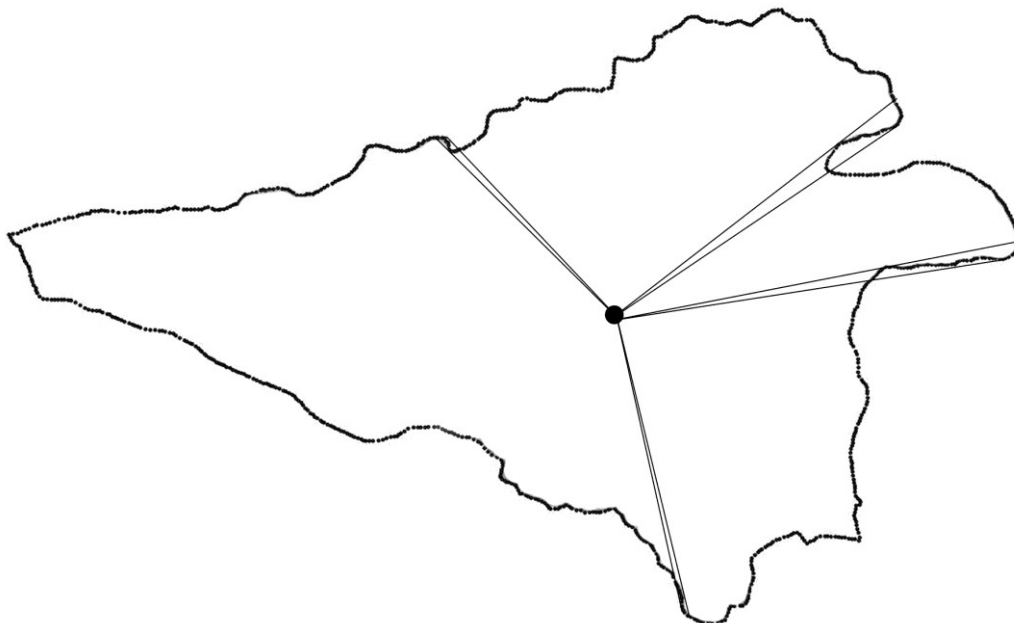
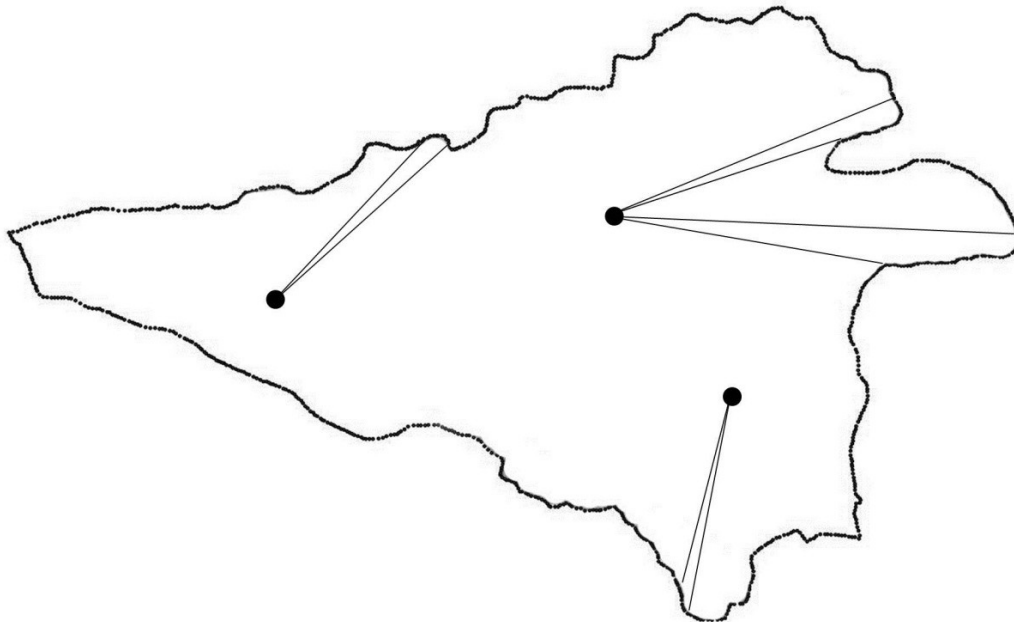


Figure 7-3: Simulated under-estimate and over-estimated areas by UGBMs



a) Problem of simulating urban boundary with a single central point



b) Importance of using three central points for urban boundary simulation
Figure 7-4: Restrictions for urban boundary simulation

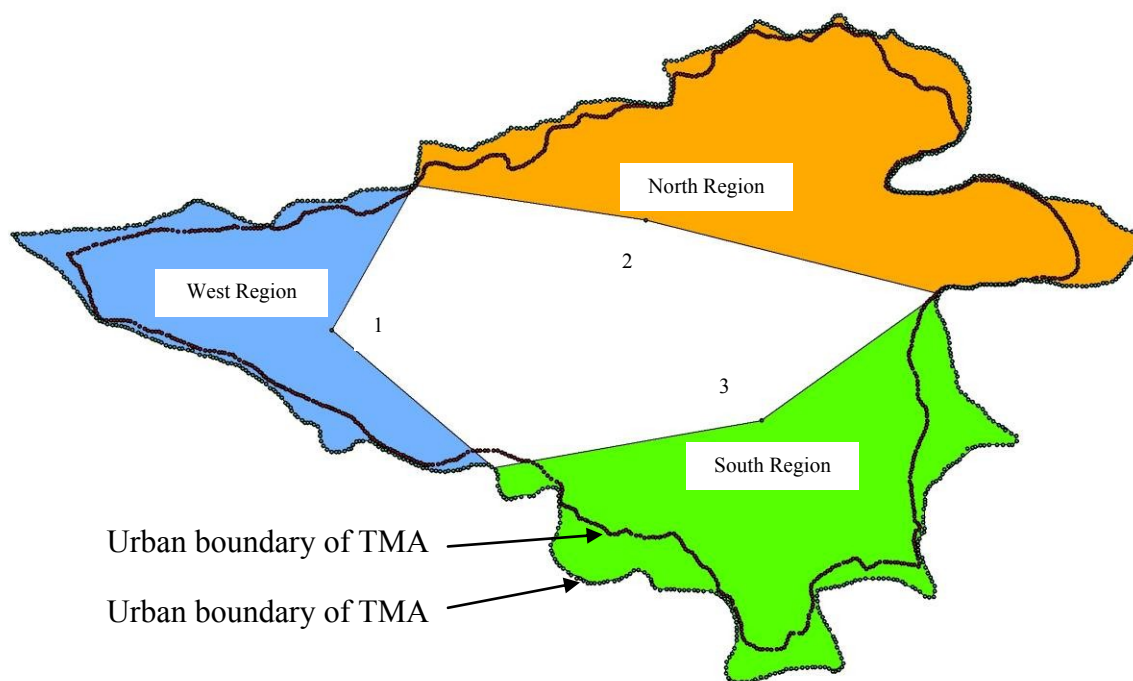


Figure 7-5: Location of three central points and corresponding regions of TMA in 1988 and 2000

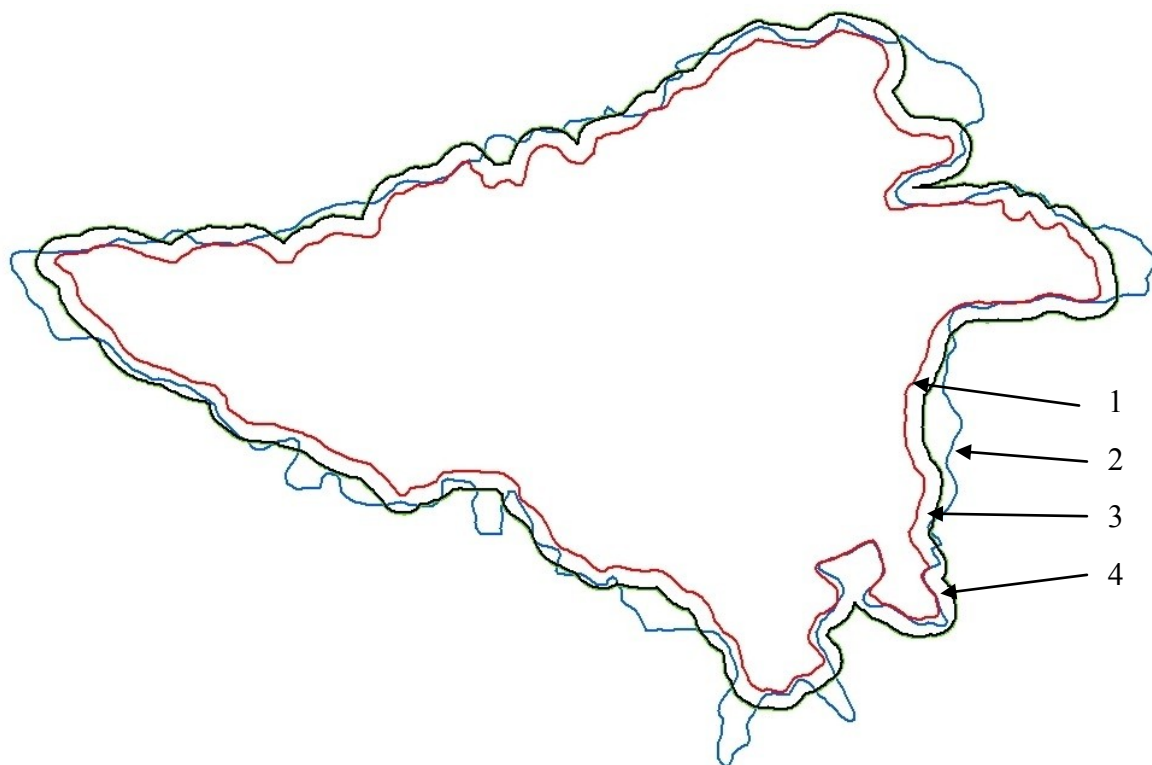


Figure 7-6: Comparing predicted UB from Null UGBM in TMA with reference UB in 2000: (1) Reference UB of TMA in 1988; (2) Reference UB of TMA in 2000; (3) Under-estimate predicted UB of TMA using Null UGBM in 2000 including 700m buffer (Black color); (4) Over-estimate of predicted UB of TMA using Null UGBM in 2000 including 750m buffer (Green color)

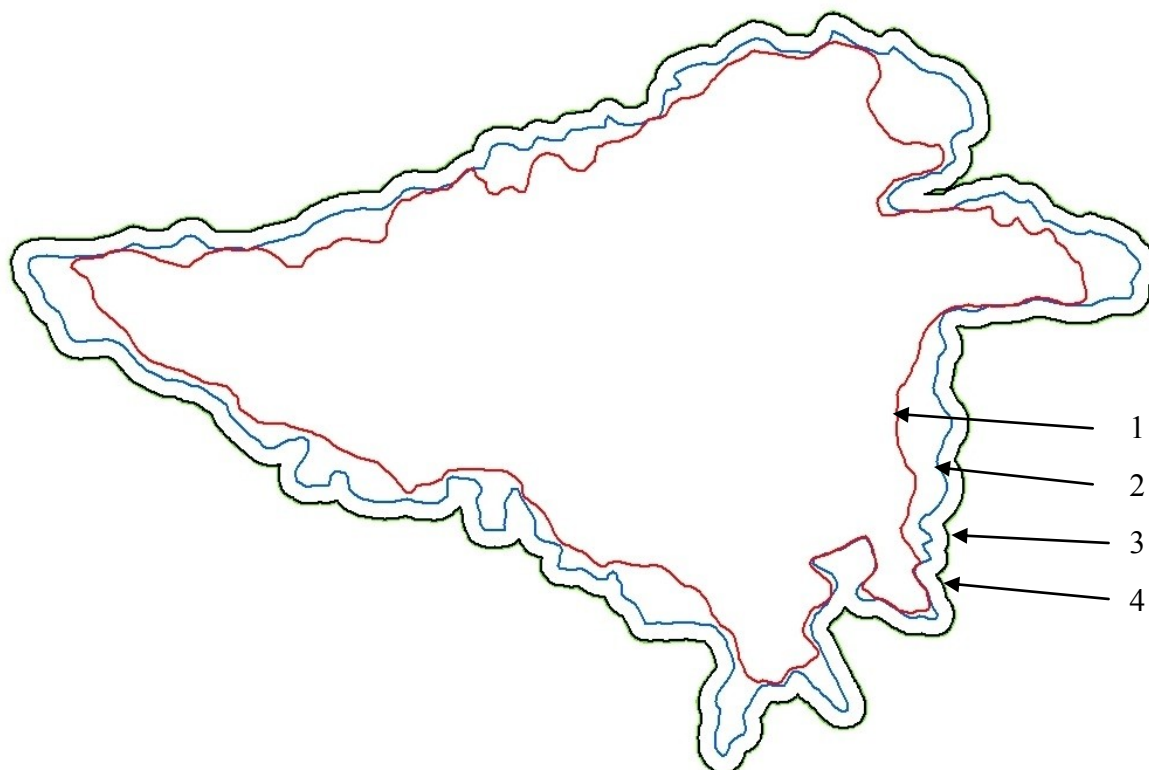
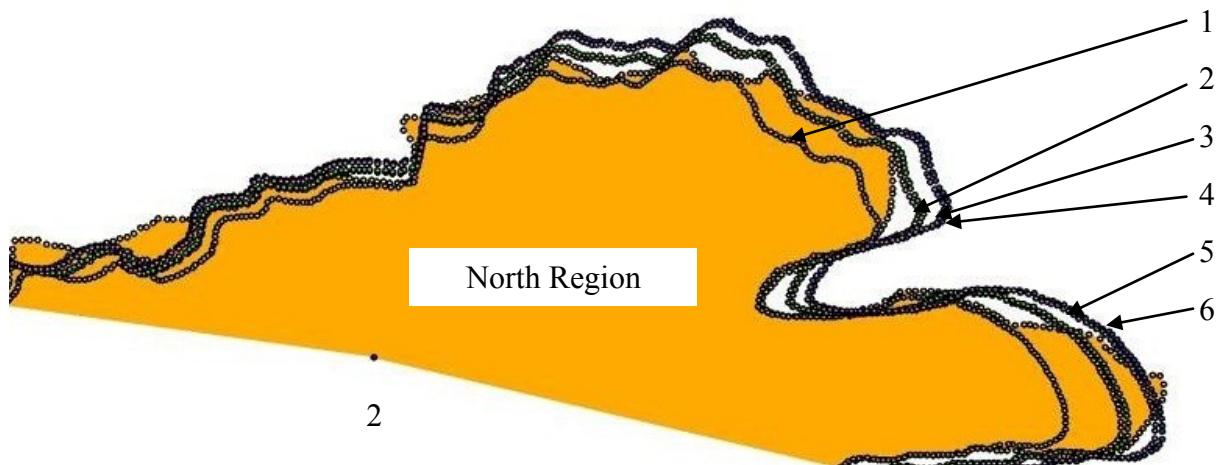
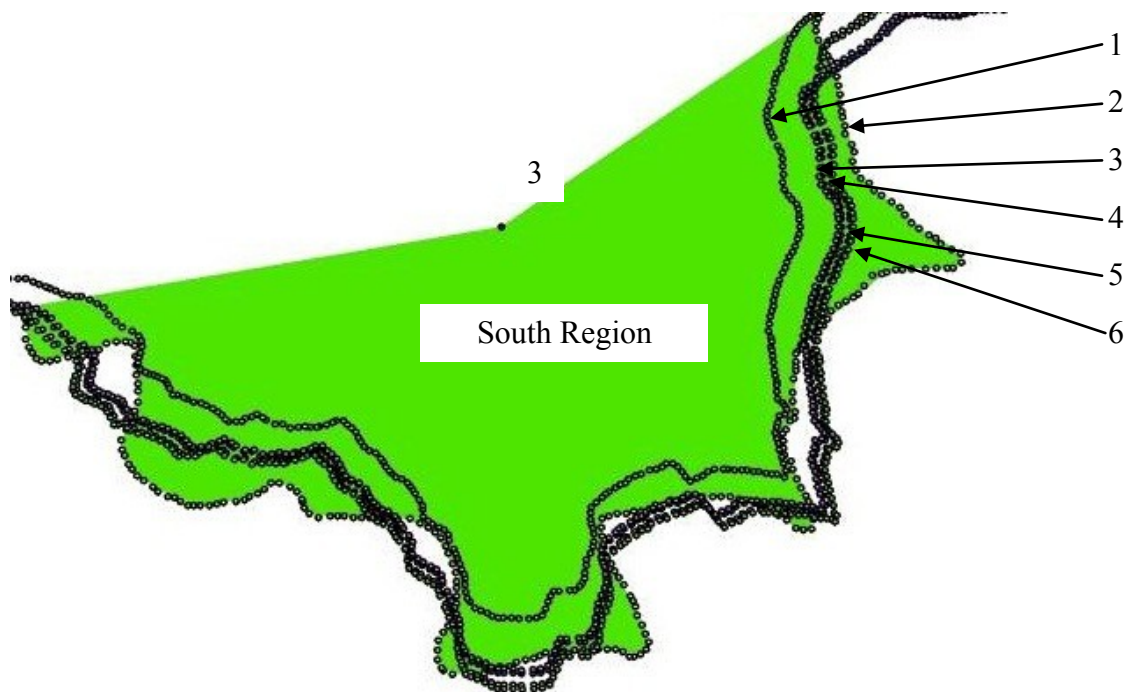


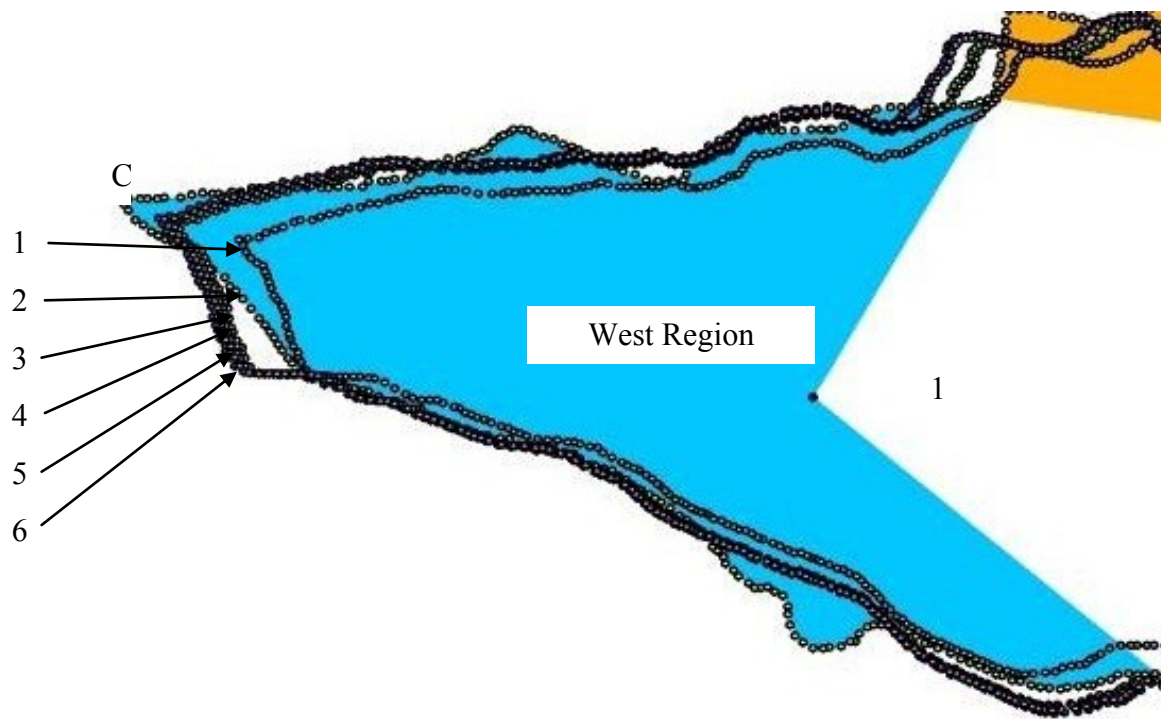
Figure 7-7: The predicted change in UB of TMA from Null UGBM in 2012: (1) Reference UB of TMA in 1988; (2) Reference UB of TMA in 2000; (3) Under-estimate predicted UB of TMA using Null UGBM in 2012 including 700m buffer (Black Color); (4) Over-estimate of predicted UB of TMA using Null UGBM in 2012 including 750m buffer (Green Color)



a)North region of TMA

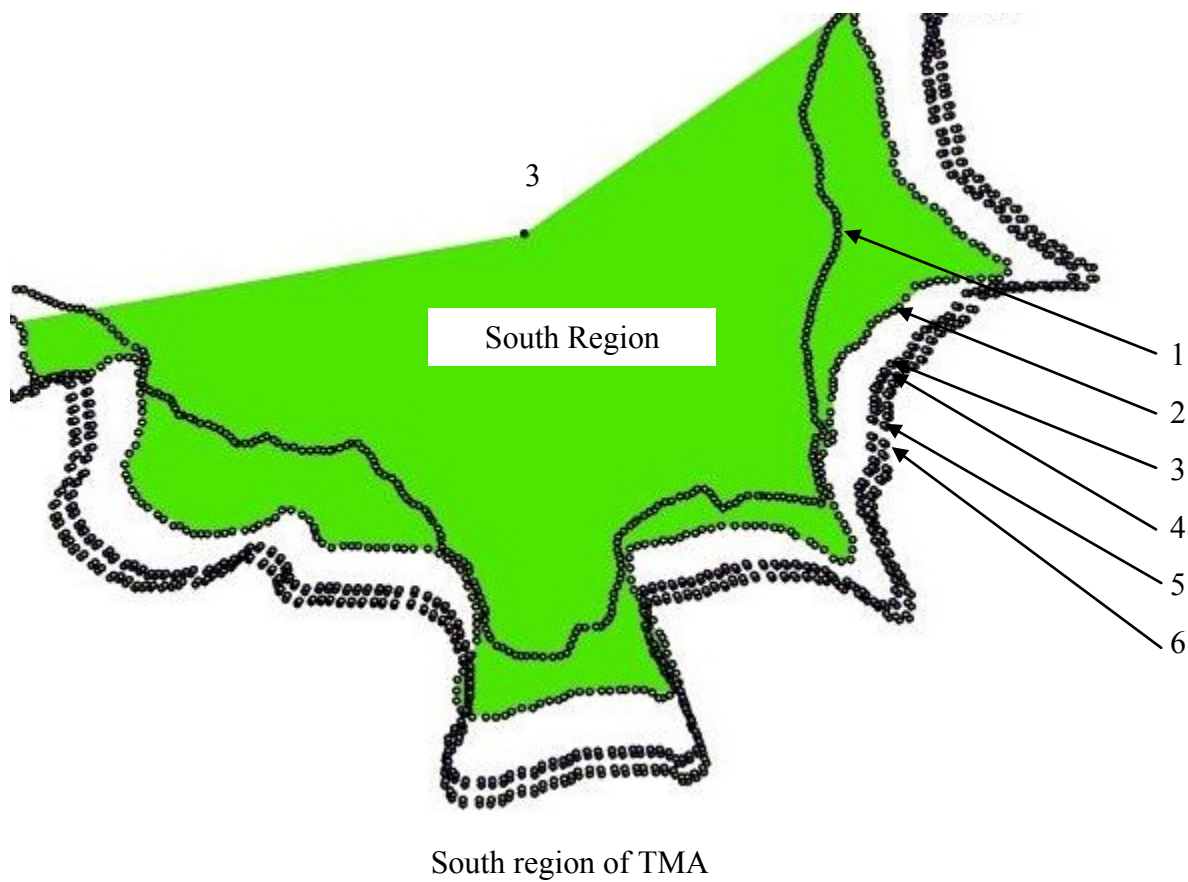
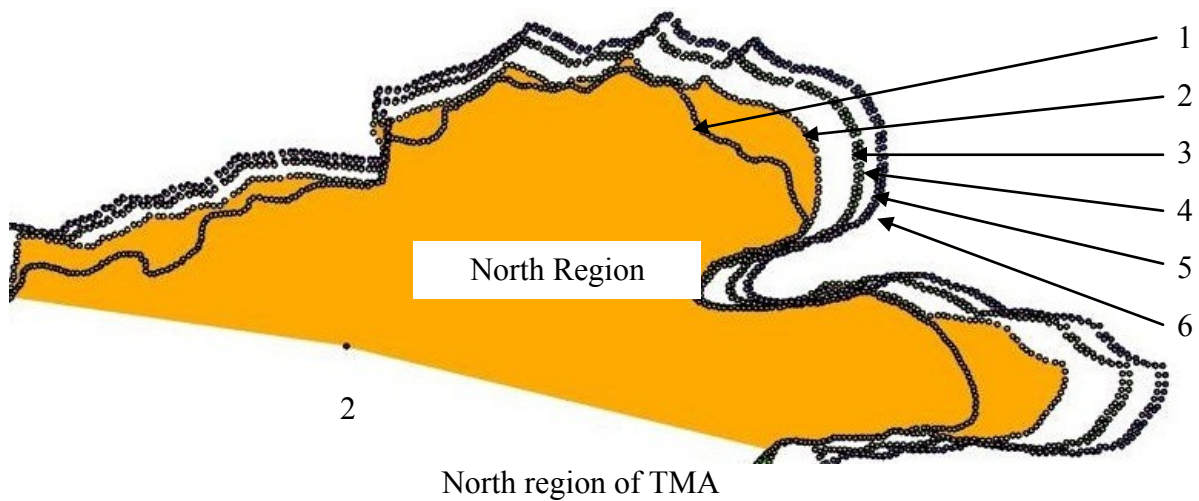


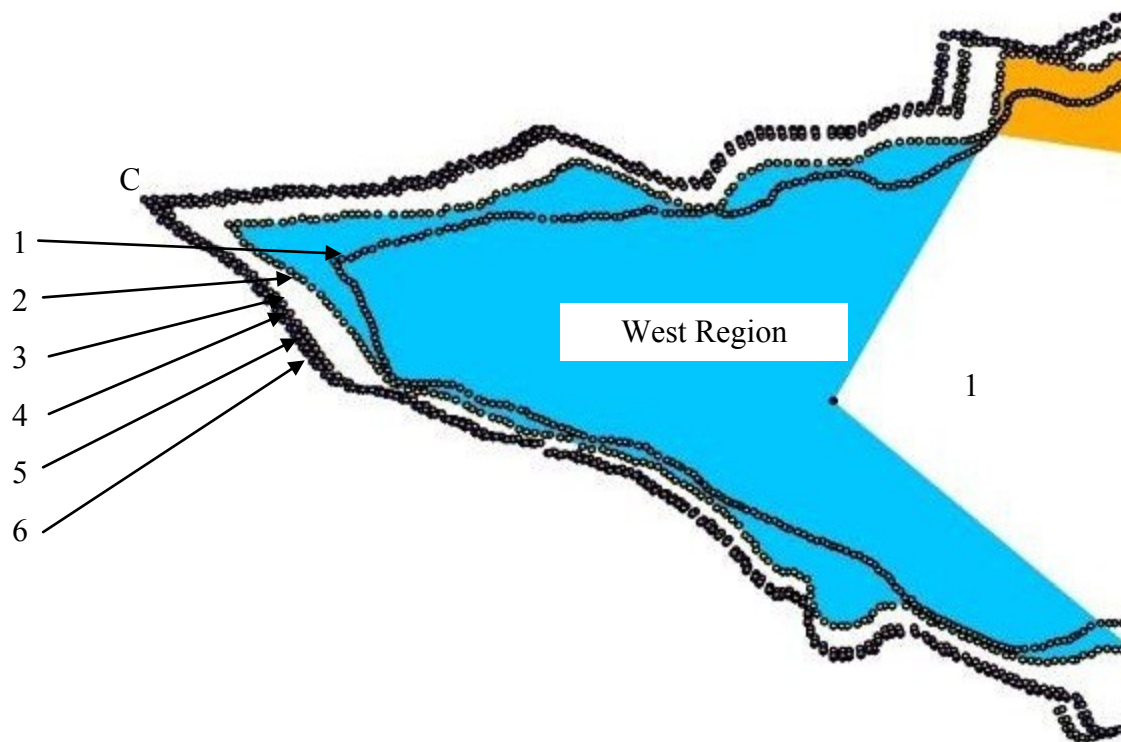
b)South region of TMA



c) West region of TMA

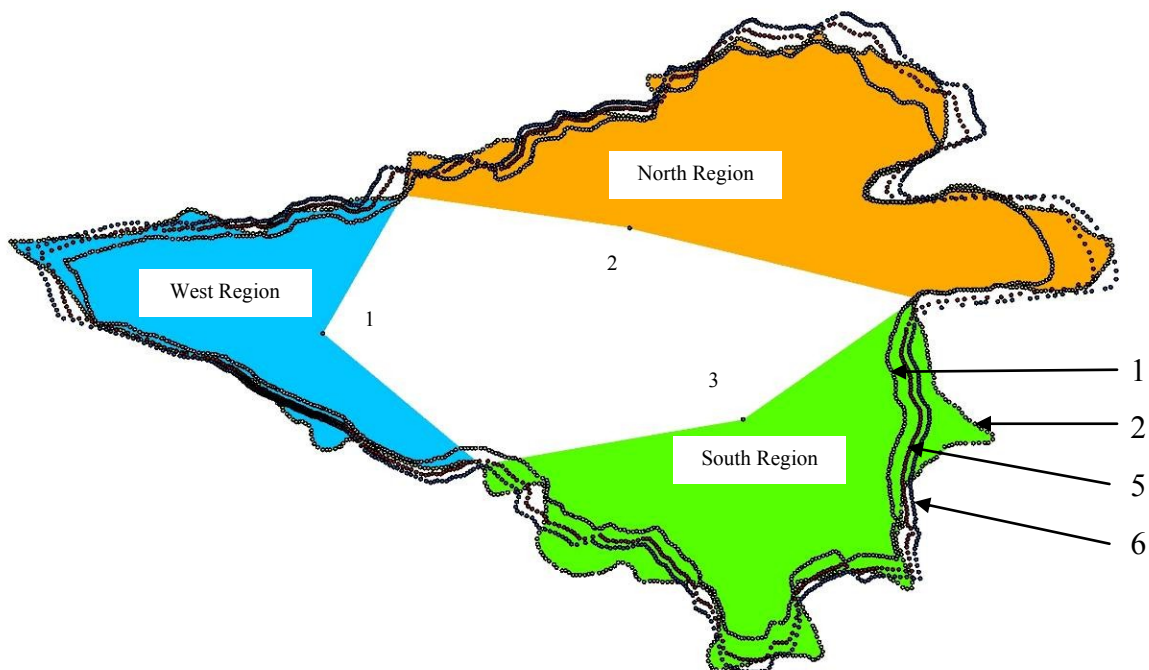
Figure 7-8: Comparing predicted UB from DDM in TMA with reference UB in 2000: (1) Reference UB of TMA in 1988; (2) Reference UB of TMA in 2000; (3 and 4) Under-estimate and over-estimate of predicted UB of TMA using Multiple-region Model in 2000; (5 and 6) Under-estimate and over-estimate of predicted UB of TMA using Whole-region Model in 2000



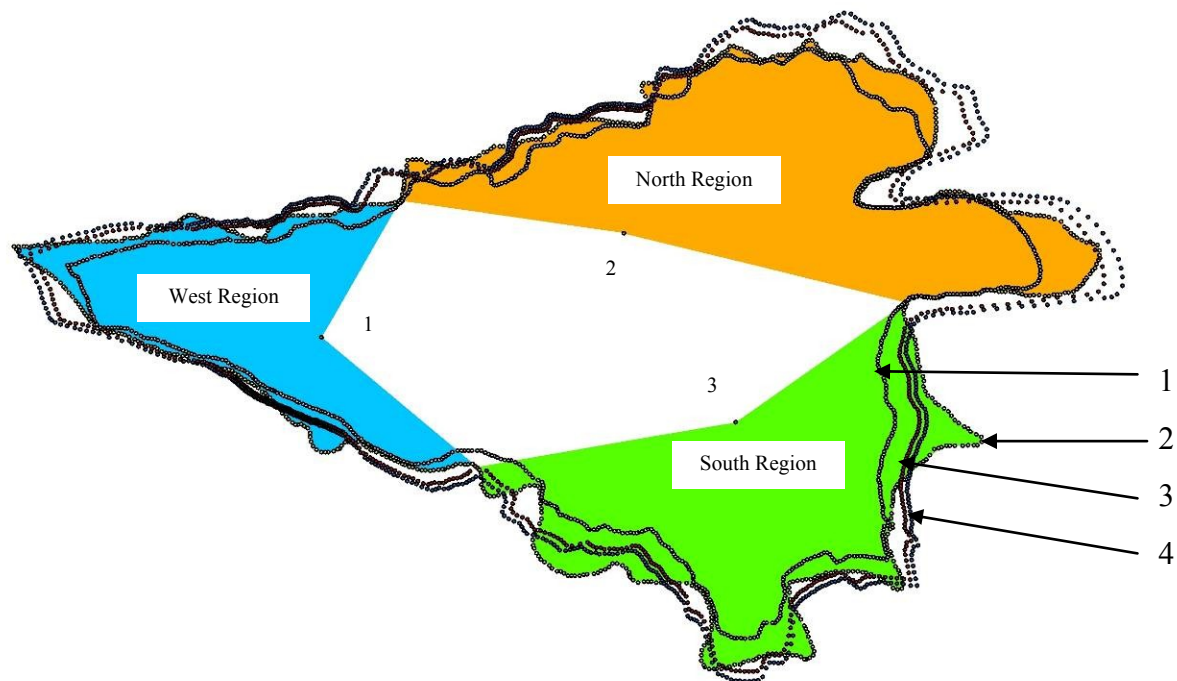


West region of TMA

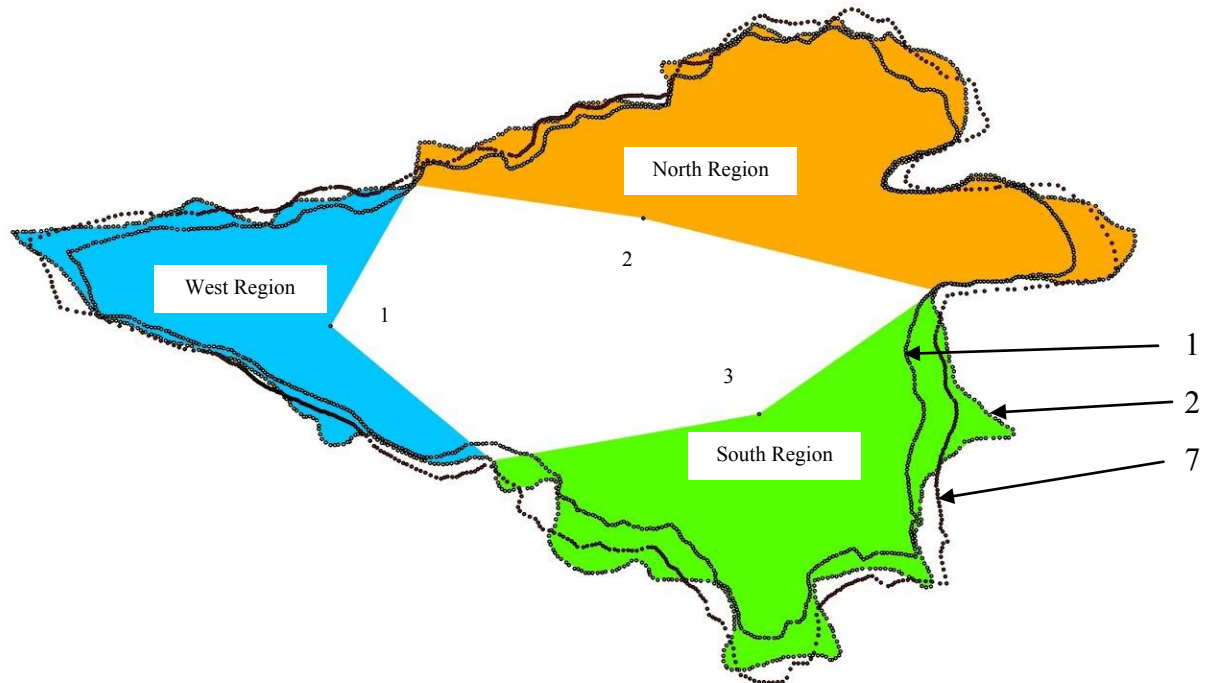
Figure 7-9: The predicted change in UB of TMA from DDM in 2012: (1) Reference UB of TMA in 1988; (2) Reference UB of TMA in 2000; (3 and 4) Under-estimate and over-estimate of predicted UB of TMA using Multiple-region Model in 2012; (5 and 6) Under-estimate and over-estimate of predicted UB of TMA using Whole-region Model in 2012



a) Application of ARCDT3 and FARCDT for urban boundary prediction of TMA

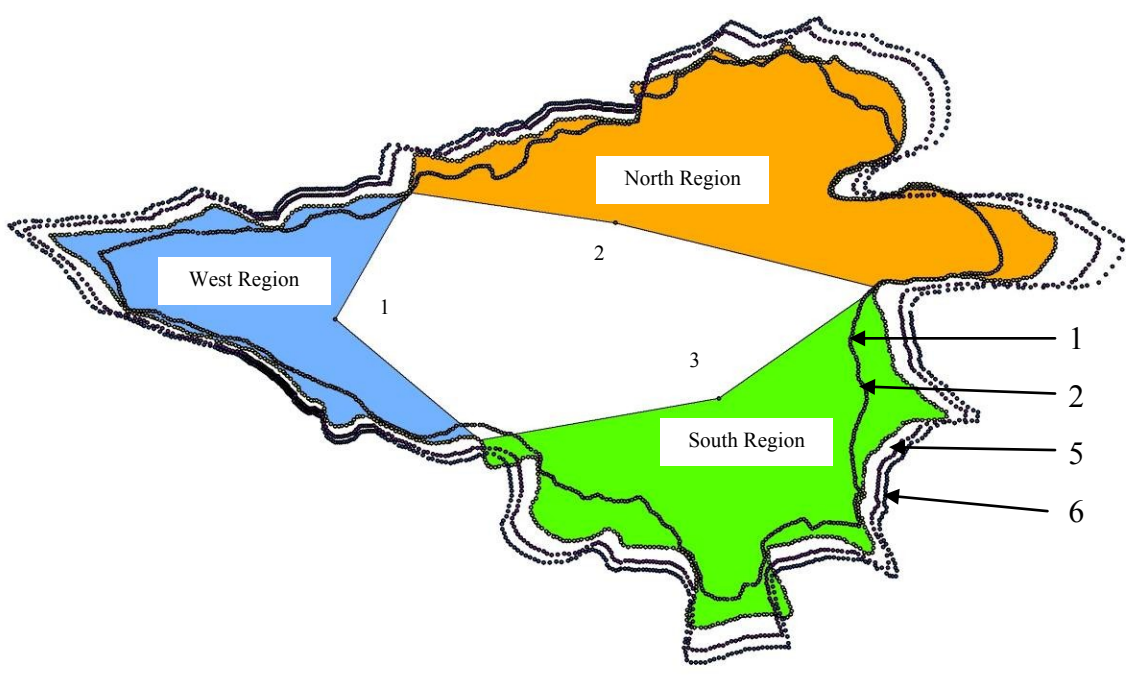


b) Application of ARCDT1 and ARCDT2 for urban boundary prediction of TMA

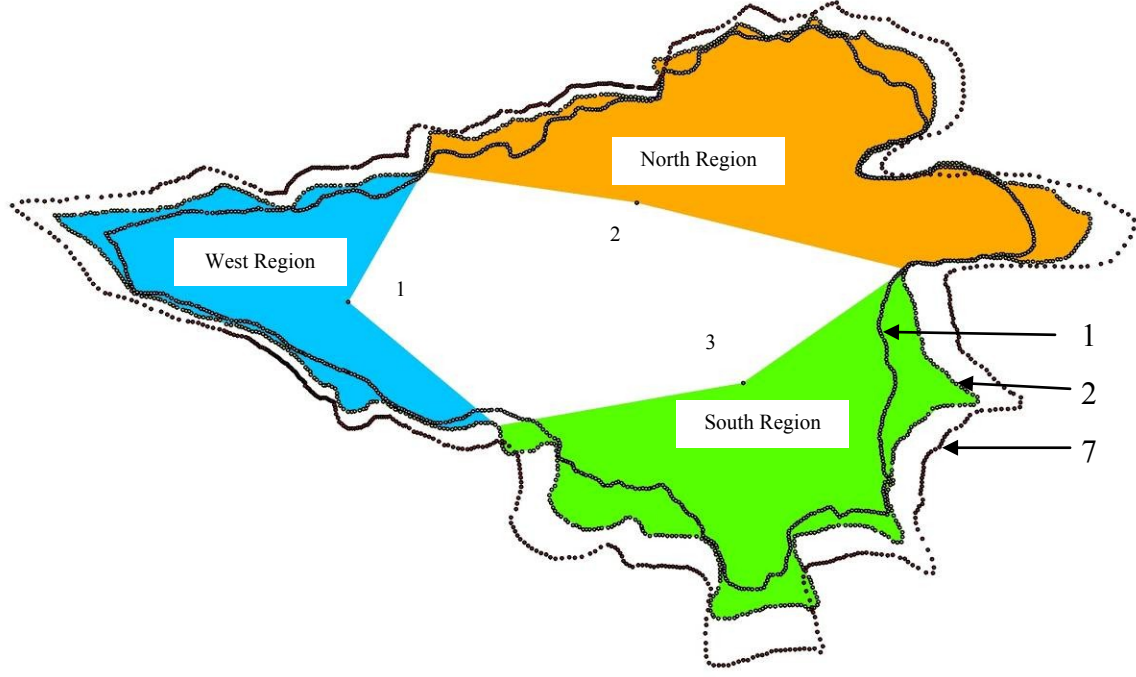


c) Application of ARCDT1, ARCDT2 and ARCDT3 for urban boundary prediction of TMA

Figure 7-10: Comparing predicted UB of TMA (from DIM) with reference UB in 2000:
 (1) UB of TMA in 1988; (2) UB of TMA in 2000; (3) Predicted UB of TMA with ARCDT1; (4) Predicted UB of TMA with ARCDT2; (5) Predicted UB of TMA with ARCDT3; (6) Predicted UB of TMA with FARCDT and (7) Predicted UB of TMA with best ARCDT for each region



a) Application of ARCDT3 and FARCDT for urban boundary prediction of TMA



b) Application of ARCDT1,2,3 for urban boundary prediction of TMA

Figure 7-11: UGB prediction of TMA with DIM in 2012: (1) UB of TMA in 1988; (2) UB of TMA in 2000; (3) Predicted UB of TMA with ARCDT1; (4) Predicted UB of TMA with ARCDT2; (5) Predicted UB of TMA with ARCDT3; (6) Predicted UB of TMA with FARCDT and (7) Predicted UB of TMA with best ARCDT for each region.

Table 7-1: Reference area in 1988 and 2000 for the whole TMA and three regions of TMA

Region	Reference Area of TMA in 1988 (km ²)	Reference Area of TMA in 2000 (km ²)	Change in area from 1988 to 2000 (km ²)
Whole region	539.597150517	636.309856.774	96.712706260
1	80.622465362	99.947659553	19.325194191
2	114.039414876	156.570058350	42.530643474
3	157.085164418	184.632064579	27.546900161

Table 7-2: Comparing the PAM quantity values of predicted urban boundaries using null UGBMs across the distances

Distance for creating buffer	Predicted change in area (km ²) 1988 - 2000	Reference change in area (km ²) 1988 - 2000	PAM Quantity	Status
700	94.7010819672	96.7127062574	0.9792	Under-estimate
750	101.3259023458	96.7127062574	1.0477	Over-estimate

Table 7-3: Predicted area of TMA using null UGBMs in 2012

Distance for creating buffer	Area of TMA in 2012 (km ²)	Predicted change in area (km ²) from 2000 to 2012	Status
700	703.068962044	113.0208141924	Under-estimate
750	710.669804970	120.6216571184	Over-estimate

Table 7-4: Best PAM quantity value for under and over estimate of DDM

	Region	Level of increment	PAM quantity	Status
Multiple-region Model	1	11	0.9683	Under-estimate
		12	1.0613	Over-estimate
	2	17	0.9891	Under-estimate
		18	1.0522	Over-estimate
	3	8	0.9489	Under-estimate
		9	1.0726	Over-estimate
Whole-region Model	1	13	1.1543	Over-estimate
		14	1.2473	Over-estimate
	2	13	0.7367	Under-estimate
		14	0.7998	Under-estimate
	3	13	1.5674	Over-estimate
		14	1.6911	Over-estimate

Table 7-5: Range of change in PAM quantity values in multiple and whole region model

	Region	Range of change
Whole-region Model	Whole region	1.56
Multiple-region Model	1	1.84
	2	1.18
	3	2.51

Table 7-6: Area of TMA for under and over DDM estimates in 2012 from the Whole and Multiple region Models

	Region	Level of increment	Status	Area of TMA in 2012 (km ²)	Predicted change in area (km ²) from 2000 to 2012
Whole-region Model	Whole region	13	Under-estimate	756.835838936	120.525982161
		14	Over-estimate	766.555161891	130.245305116
Multiple-region Model	1	11	Under-estimate	123.1455113361	23.1978517833
		12	Over-estimate	125.3743441439	25.4266845912
	2	17	Under-estimate	214.3287528728	57.7586945229
		18	Over-estimate	218.0081492449	61.4380908950
	3	8	Under-estimate	215.3548401261	30.7227755471
		9	Over-estimate	219.3613559268	34.7292913478
	Whole region	Total of regions 1, 2 and 3	Under-estimate	746.6356484199	110.3257916450
			Over-estimate	756.2756861595	119.9658293846

Table 7-7: ARCDT of regions 1, 2 and 3, and FARCDT for the whole TMA.

Region	Samples	Summation	ARCDT or FARCDT
1	255	39.0898	ARCDT1 = 0.1532
2	205	40.6388	ARCDT2 = 0.1982
3	179	17.4652	ARCDT3 = 0.0975
Whole region	639	97.2086	FARCDT = 0.1521

Table 7-8: PAM quantity between the 2000 projection (using ARCDTs from each region and FARCDT) and the reference 2000 boundary for the whole TMA using DIM

ARCDT	Predicted area (km ²) in 2000	Predicted change in area (km ²) 1988 - 2000	Reference change in area (km ²) 1988 - 2000	PAM quantity
ARCDT1	652.994738866	113.3975883485	96.7127062574	1.1725
ARCDT2	688.483222180	148.8860716625	96.7127062574	1.5394
ARCDT3	610.329876797	70.7327262795	96.7127062574	0.7313
FARCDT	652.085990393	112.4888398755	96.7127062574	1.1631
ARCDT1,2,3	645.0042546737	105.4071041563	96.7127062574	1.0899

Table 7-9: PAM quantity between the 2000 projection (using regional ARCDT values and FARCDT) to the reference area in 2000 for regions 1, 2 and 3 using DIM

Region	ARCDT	Predicted area (m ²) in 2000	Predicted change in area (m ²) 1988 - 2000	Reference change in area (m ²) 1988 - 2000	PAM quantity
1	ARCDT1	104723103.6837	24100638.3221	19325194.1912	1.2471
	ARCDT2	113044443.3660	32421978.0044	19325194.1912	1.6777
	ARCDT3	94848026.5267	14225561.1652	19325194.1912	0.7361
	FARCDT	104511257.7869	23888792.4253	19325194.1912	1.2361
2	ARCDT1	144637625.9464	30598211.0704	42530643.4739	0.7194
	ARCDT2	156130589.5222	42091174.6462	42530643.4739	0.9897
	ARCDT3	130998728.0724	16959313.1964	42530643.4739	0.3988
	FARCDT	144345036.3784	30305621.5024	42530643.4739	0.7126
3	ARCDT1	206910908.9127	49825744.4945	27546900.1608	1.8088
	ARCDT2	223352132.4448	66266968.0266	27546900.1608	2.4056
	ARCDT3	187399825.6996	30314661.2814	27546900.1608	1.1005
	FARCDT	206492345.8094	49407181.3912	27546900.1608	1.7936

Table 7-10: Predicted area of whole TMA using DIM

ARCDT	Predicted area (m ²) in 2012	Change in area (m ²) from 2000 to 2012
ARCDT1	776552458.7535	140242601.9786
ARCDT2	821177895.0795	184868038.3046
ARCDT3	723009829.5600	86699972.7851
FARCDT	775410766.6220	139100909.8471
ARCDT1,2,3	770107817.3148	133797960.5399

Table 7-11: Predicted area of individual TMA regions using DIM

Region	ARCDT	Predicted area (km ²) in 2012	Change in area (km ²) from 2000 to 2012
1	ARCDT1	132.7660943217	32.8184347689
	ARCDT2	143.3157412494	43.3680816967
	ARCDT3	120.2466465660	20.2989870133
	FARCDT	132.4975198478	32.5498602950
2	ARCDT1	205.3805625839	48.8105042340
	ARCDT2	221.7001841873	65.1301258374
	ARCDT3	186.0137864774	29.4437281276
	FARCDT	204.9650952419	48.3950368921
3	ARCDT1	243.0397479352	58.4076833562
	ARCDT2	262.3517834608	77.7197188818
	ARCDT3	220.1218226741	35.4897580951
	FARCDT	242.5480992754	57.9160346964

Table 7-12: Comparing the PAM quantity and location values of rule-based simulation UGBMs versus Null UGBM

UGBMs	Total PAM Quantity	PAM Location
DIM	0.94	0.82
DDM	0.98	0.77
Null	0.97	0.62

CHAPTER 8: CONCLUSIONS AND FUTURE RESEARCH

Humans have altered the land for variety of reasons (e.g. to provide food, fiber, housing, energy, etc. for humans). The rates and extent of land use land cover (LULC) change (LUCC) are significant which can cause changes in ecosystem structure and function across a variety of spatial and temporal scales. Uncontrolled LUCC by humans can have negative impacts on biodiversity (e.g. habitat loss), climate change (e.g. global warming) and the hydrology (e.g. water quality). Sustainability is a major goal of society as it is important to maintain ecosystem services now and for the future. To achieve a sustainable land use system, we need to minimize the negative environmental impacts of LUCC; this will require a deep understanding of the interaction of all components of the land use system. Agricultural expansion typically resulting in deforestation and urbanization resulting from people moving to cities from rural areas are examples of global LUCC that need to be understood and require policies implemented that minimize negative impacts to the environment and to human well-being.

8.1 Major conclusions of dissertation

In chapter 4, ANN, CART and MARS were parameterized with identical data from different areas of the world, one undergoing extensive agricultural expansion (East Africa), another where forests are re-growing (western Michigan, USA), and a third where urbanization is prominent (the Milwaukee Metropolitan Area, USA) to model

binary LUCC. Independent training data and testing data were used to calibrate and validate each model, respectively. Comparisons of simulated maps from LTM, MARS and CART were made using ROC and PCM goodness-of-fit metrics. The three models obtained over 80% and 60% goodness-of-fit for ROC and PCM in the three study areas, respectively. Although all approaches obtained similar accuracies, the ANN-based LTM provided a slightly better goodness-of-fit than MARS and CART across testing data for all three study sites.

LUCC models that can simulate multiple LUCC are rare. In chapter 5, LTM-MC, CART and MARS performance were compared for MC for two diverse regions in the US: southeastern Wisconsin (SEWI; for 10 years) and west-central Michigan (MRW; for 20 years). Three models were developed to simulate three land use changes (agriculture, urban and forest change in SEWI and MRW) using 16 and 17 independent variables in SEWI and MRW, respectively. Comparisons of three models were made using ROC and PCM. The new coding scheme and model structure of the MC-based LTM was accurate, stable and straightforward to implement. MARS, which consider dependent variables in a single group, perform relatively poorly for LUCC simulation; however, LTM-MC and CART perform better than MARS which consider dependent variables in a series of binary classes and LTM was slightly better than CART in both study areas. POLYMARS, which is an extension of MARS that allows for multiple responses (Kooperberg et al. 1997), can be used for MC in future efforts.

Planners could use models that estimate future UGBs based on those factors that drive urban growth. Unfortunately, few models have been developed that simulate the UGBs. In chapter 6, we developed a model to simulate UGBs by integrating ANN and

GIS. PAM quantity and location goodness of fit metrics were used to assess the agreement between simulated and observed urban boundaries. Results show that ANN-UGBM can predict UGBs with urban area with 80 – 84% accuracy. The model predicts urban boundaries in all cardinal directions equally well. The use of UGBs in planning around the world and describing how this model can be used to assist planners in developing future UGBs given the need to understand those factors that contribute toward urban boundary change.

Uncoordinated and scattered development near cities and towns heavily burden local governments with high financial costs due to the lower densities at which they must provide services. In chapter 7, we used the two rule-based models, DDM and DIM, to project the urban boundary of the Tehran Metropolitan Area in 2012 using data from 1988 to 2000. DDM employs a single urban boundary in the initial time step to predict the urban boundary in any subsequent time according to the increment of distances across different azimuths. Similarly, the DIM uses the change in distance between two boundaries, one in the initial time step and one in subsequent time step, across different azimuths, to predict the future urban boundary. We compare these rule-based simulation UGBMs to a null UGBM developed from the same data but lacking in specificity of predictive variables. Results indicate that rule-based UGBMs have a better goodness of fit compared to a null UGBM using PAM quantity and location goodness of fit metrics. UGBMs can be used to assist planners in developing future UGBs.

8.2 Future directions

Current research using LTM is dual-faceted. While some researchers are using LTM to couple with other models for application (e.g. climate and hydrology; Pijanowski et al. 2007), others are still investigating simple properties of LTM and making major refinements (e.g. Tayyebi et al. 2012). There are still some ideas about the LTM that need to be explored. One challenge is the understanding of LTM forecasting and back-casting projections since ANNs hides the details of interpretations. Furthermore, the current structure of the LTM only allows us to evaluate LUCC for one time interval rather than evaluating change in a time-step manner such as is permitted by Markov-chain techniques. A computational issue of LTM in calibration runs is another concept that should be examined in the near future. This would include calibration, and the many parameters (e.g. weight and bias) inside the model, such the control parameters of LTM. Additional research is needed to assess the LTM's ability to predict change at various spatial and temporal scales and with the use of different drivers. With LTM's first decade behind us, many of the restrictions faced in the beginning use of LTM have now been overcome. One of the original goals of the LTM work was to scale the model upward to global scales (Tayyebi et al. 2012). With a new generation of technology, we could generate high-resolution LULC maps for future (100 years later) and past (100 years before) using LTM-HPC at a global scale with the release of data on our own website.

8.3 References

- Kooperberg, C., S. Bose and C. J. Stone. (1997). Polychotomous Regression. *Journal of the American Statistical Association*, 92, 117-127.
- Pijanowski, B., D. K. Ray, A. D. Kendall, J. M. Duckles, and D. W. Hyndman. (2007). Using back-cast land-use change and groundwater travel time models to generate land-use legacy maps for watershed management. *Ecology 884 and Society* 12 (2):25.[online] URL: <http://www.ecologyandsociety.org/vol12/iss2/art25/>.
- Pijanowski, B. C., Tayyebi, A., Delavar, M. R., and Yazdanpanah, M. J. (2009). Urban expansion simulation using geographic information systems and artificial neural networks. *International Journal of Environmental Research*, 3(4), 493-502.
- Tayyebi, A., Pekin, B. K., Pijanowski, B. C., Plourde, J. D., Doucette, J., Braun, D. (2012). Hierarchical modeling of urban growth across the conterminous USA: Developing meso-scale quantity drivers for the Land Transformation Model. *Journal 972 of Land Use Science*. DOI: 10.1080/1747423X.2012.675364.

VITA

VITA

First Name: Amin
Surname: Tayyebi
E-Mail: amin.tayyebi@gmail.com
Address: West Lafayette, IN 47906

EDUCATION HISTORY

Ph.D Degree: (Sep 2010- May 2013)

Graduate Research Assistant, Purdue University, Department of Forestry and Natural Resources, West Lafayette, IN 47907, USA

Thesis: “Simulating land use land cover change using data mining and machine learning algorithm cross the globe”

Major: Geographical Information Systems (GIS)

GPA: 3.96/4

Chair: Bryan Christopher Pijanowski, Prof., Dept. of Forestry and Natural Resources, Purdue University, West Lafayette, IN 47907, USA, Email: bpijanow@purdue.edu

Co-Chair: Jeffrey D. Holland, Prof., Dept. of Entomology, Purdue University, West Lafayette, IN 47907, USA, Email: jdhollan@purdue.edu

Co-Chair: Guofan Shao, Associate Prof., Dept. of Forestry and Natural Resources, Purdue University, West Lafayette, IN 47907, USA, Email: shao@purdue.edu

Co-Chair: Songlin Fei, Assist Prof., Dept. of Forestry and Natural Resources, Purdue University, West Lafayette, IN 47907, USA, Email: sfei@purdue.edu

Masters Degree: (Sep 2007- Feb 2010)

University of Tehran, Surveying and Geomatics Engineering Department, Geographical Information Systems, Tehran, Iran

Thesis: “Spatio-Temporal land use land cover change simulation in GIS”

Major: Geographical Information Systems (GIS)

GPA: 3.85/4

Bachelor Degree: (Sep 2003- Sep 2007)

University of Tehran, Surveying and Geomatics Engineering Department, Tehran, Iran

GPA: 3.5/4

RESEARCH INTEREST

- ✦ Using data mining, machine learning and statistical approaches to simulate (forward or backward in time) land use land cover change (such as Artificial Neural Network, Cellular Automata, Logistic Regression, Classification and Regression Tree, Multivariate Adaptive Regression Splines)
- ✦ Calibration, validation and accuracy assessment of land use land cover change models
- ✦ Error propagation and uncertainty assessment in statistical models

- ✦ Developing Automatic Vehicle Location System (AVLS) for Transportation System in GIS environment
- ✦ Developing Spatial Decision Support Systems (SDSS) for Urban Management in GIS environment
- ✦ Web GIS, Mobile GIS and SQL database
- ✦ Photogrammetry (Reconstruct 3D scene from 2D images), Remote Sensing (Satellite images, Image Processing), Geodesy and Surveying (Route Design, GPS, Total Station, SDRmap, Route Finding)

AWARDS AND HONORS

- ✦ 1th Ranked Student in Master entrance exam in Iran among 843 participants (06/2007)

REVIEWER OF JOURNAL

- ✦ Journal of Landscape and Urban Planning, Editor in chief is Dr. Paul Gobster (<http://ees.elsevier.com/land>)
- ✦ Cities Journal, Editor in chief is Prof. Ali Modarres (<http://ees.elsevier.com/jcit>)

PUBLICATIONS

CONFERENCE AND SYMPOSIUM

- ✦ Monitoring the Urban Expansion by Multi-Temporal GIS Maps. (2008). Tayyebi*, A., Delavar, M. R., Saeedi, S. and Amini, J. Application of Remote Sensing and Imagery (TS 5B), Integrating Generations, FIG Working Week 2008 and FIG/UN-HABITAT Seminar, Stockholm Sweden, June 14–19, 2008.
- ✦ Monitoring Land Use Change by Multi-Temporal Landsat Remote Sensing Imagery. (2008). Tayyebi*, A., Delavar, M. R., Saeedi, S., Amini, J. and Alinia, H. The International Archives of the Photogrammetry, Remote Sensing and Spatial Information Sciences. Vol. XXXVII. Part B7. Beijing 2008, China, pp. 1037-1043.
- ✦ Spatial Multi Criteria Evaluation for Landfill Sites Management. (2009). Tayyebi*, A., Mousavi, M. A., Rajabi and A. H. Tayyebi. The 6th International Symposium on Digital Earth. Chengdu, China, September 8-15, 2009.

JOURNAL

- ✦ Urban Expansion Simulation Using Geospatial Information System and Artificial Neural Networks, (2009). Pijanowski, B. C., Tayyebi*, A., Delavar, M. R. and Yazdanpanah, M. J. *International Journal of Environmental Research*, 3 (4), 493-502.
- ✦ An Urban Growth Boundary Model Using Neural Networks, GIS and Radial Parameterization: An Application to Tehran, Iran, (2011). Tayyebi*, A., Pijanowski, B. C., Tayyebi, A. H. *Landscape and Urban Planning*, 100, 35-44.

- ✦ Two rule-based urban growth boundary models applied to the Tehran metropolitan area, Iran, (2011). Tayyebi, A*, Pijanowski, B. C., Pekin, B. *Applied Geography*, 31(3), 908-918.
- ✦ Hierarchical modeling of urban growth across the conterminous USA: developing meso-scale quantity drivers for the Land Transformation Model, (2012). Tayyebi, A.*, Pekin B. K., Pijanowski B. C., Plourde J. D., Doucette J., Braun, D. *Journal of Land Use Science*. <http://dx.doi.org/10.1080/1747423X.2012.675364>.
- ✦ Error propagation and uncertainty assessment in Land Use Change Models: Application of Artificial Neural Network and Spatial Logistic Regression, (Under Review). Tayyebi, A. H., A. Tayyebi*, and N. Khanna. *Computers, Environment and Urban Systems*.
- ✦ Simulating urban growth at a national scale and with a fine resolution: Configuring the GIS bases Land Transformation Model to run in a High Performance Computing environment (Under review). Pijanowski B. C., Tayyebi, A.*, Doucette J., Braun, D., *Environmental Modeling & Software*.
- ✦ Using CART, MARS and ANNs to Model Land Use Land Cover Change: Application of Data Mining Tools to Three Diverse Areas in USA and Africa Undergoing Land Transformation, (Under Review). Tayyebi, A.*, Pijanowski B. C. *Applied Soft Computing*.
- ✦ Simulating Multiple Land Use Land Cover Change Classes using the Artificial Neural Network Model-based Land Transformation Model (LTM) and Two Data Mining Tools, (Under Review). Tayyebi, A.*, Pijanowski B. C. *International Journal of GIS*.

CHAPTER BOOKS

- ✦ Accuracy Assessment in Urban Expansion Model. (2009). Tayyebi*, A., Delavar, M. R., Pijanowski, B. C., Yazdanpanah, M. J. *Spatial Data Quality, From Process to Decisions*, Edited by R. Devillers and H. Goodchild, Taylor and Francis, CRC Press, Canada, pp. 107-115.
- ✦ Spatial variability of errors in Urban Expansion Model: Implications for error propagation. (2009). Tayyebi*, A., Delavar, M. R., Pijanowski, B. C., Yazdanpanah, M. J. *Spatial Data Quality, From Process to Decisions*, Edited by R. Devillers and H. Goodchild, Taylor and Francis, CRC Press, Canada, pp. 134-135.
- ✦ A Spatial Logistic Regression Model for Simulating Land Use Patterns, A Case Study of the Shiraz Metropolitan Area of Iran. (2010). Tayyebi*, A., Delavar, M. R., Pijanowski, B. C., Yazdanpanah, M. J., Saeedi, S. and Tayyebi, A. H. *Advances in Earth Observation of Global Change*, Edited by Emilio Chuvieco, Jonathan Li and Xiaojun Yang. Springer press.
- ✦ Uncertainty Framework in Land Use Change Models: An Application of Data, Model Parameter and Model Outcome Uncertainty in Land Transformation Model. (2011). Tayyebi, A. H., S. Homayouni, J. Shan, M. J. Yazdanpanah, B. C. Pijanowski and A. Tayyebi*. 7th International Symposium on Spatial Data Quality. Coimbra, Portugal, October 12-14, 2011.
- ✦ Multi-Scale Analysis Approach of Simulating Urban Growth Pattern using a Land Use Change Model. (2011). Tayyebi, A. H., S. Homayouni, J. Shan, M. J. Yazdanpanah, B. C.

Pijanowski and A. Tayyebi*. 7th International Symposium on Spatial Data Quality. Coimbra, Portugal, October 12-14, 2011.

- ✚ Model Parameter Uncertainty Assessment in Land Transformation Model. (2011). Tayyebi, A. H., S. Homayouni, J. Shan, M. J. Yazdanpanah, B. C. Pijanowski and A. Tayyebi*. 7th International Symposium on Spatial Data Quality. Coimbra, Portugal, October 12-14, 2011.

SYMPOSIUM AND CONFERENCE PRESENTATION (Oral)

- ✚ A Decade of LTM as Land Use Land Cover Change Model: Lessons Learned from Applications of Using the LTM, (2012). Tayyebi, A.*, Pijanowski, B. C., 27th Annual Landscape Ecology Symposium, Informing Decisions in a Changing World, Newport, RI, April 8-12, 2012.
- ✚ Comparing single and multiple transitions modeling with the Land Transformation Model for two diverse areas undergoing land use change, (2012). Tayyebi, A.*, Pijanowski, B. C., 27th Annual Landscape Ecology Symposium, Informing Decisions in a Changing World, Newport, RI, April 8-12, 2012.

SOFTWARE AND PROGRAMMING SKILLS

PLATFORMS:

- ✚ Windows Vista/XP/2000/98/NT, DOS

PROGRAMMING LANGUAGES:

- ✚ C#, C++, Mobile Programming (J2ME), Web Programming (ASP.net and HTML)
- ✚ Matlab, SAS and R for statistical analysis

SOFTWARE SKILLS:

- ✚ GIS software such as ArcGIS10 ESRI software (Arcmap, ArcScene, ArcGlobe and ArcCatalog), Python and Land Development Desktop
- ✚ Remote Sensing software such as ENVI, ER Mapper, ERDAS Imagine, SDRMAP and PCI Geomatica
- ✚ Microsoft Office (Word, Excel and Access) and SQL
- ✚ AutoCAD and Microstation
- ✚ Google Earth, Idrisi and SPSS
- ✚ HTML, GML and XML